FERTILITY PRESERVATION: FROM NEXT-GENERATION TECHNOLOGIES TO CLINICAL PRACTICE

EDITED BY: Yuting Fan and Sherman Silber
PUBLISHED IN: Frontiers in Endocrinology

frontiers Research Topics

frontiers

ISSN 1664-8714
ISBN 978-2-83250-857-2
DOI 10.3389/978-2-83250-857-2

About Frontiers

Frontiers is more than just an open-access publisher of scholarly articles: it is a pioneering approach to the world of academia, radically improving the way scholarly research is managed. The grand vision of Frontiers is a world where all people have an equal opportunity to seek, share and generate knowledge. Frontiers provides immediate and permanent online open access to all its publications, but this alone is not enough to realize our grand goals.

Frontiers Journal Series

The Frontiers Journal Series is a multi-tier and interdisciplinary set of open-access, online journals, promising a paradigm shift from the current review, selection and dissemination processes in academic publishing. All Frontiers journals are driven by researchers for researchers; therefore, they constitute a service to the scholarly community. At the same time, the Frontiers Journal Series operates on a revolutionary invention, the tiered publishing system, initially addressing specific communities of scholars, and gradually climbing up to broader public understanding, thus serving the interests of the lay society, too.

Dedication to Quality

Each Frontiers article is a landmark of the highest quality, thanks to genuinely collaborative interactions between authors and review editors, who include some of the world's best academicians. Research must be certified by peers before entering a stream of knowledge that may eventually reach the public - and shape society; therefore, Frontiers only applies the most rigorous and unbiased reviews.
Frontiers revolutionizes research publishing by freely delivering the most outstanding research, evaluated with no bias from both the academic and social point of view. By applying the most advanced information technologies, Frontiers is catapulting scholarly publishing into a new generation.

What are Frontiers Research Topics?

Frontiers Research Topics are very popular trademarks of the Frontiers Journals Series: they are collections of at least ten articles, all centered on a particular subject. With their unique mix of varied contributions from Original Research to Review Articles, Frontiers Research Topics unify the most influential researchers, the latest key findings and historical advances in a hot research area! Find out more on how to host your own Frontiers Research Topic or contribute to one as an author by contacting the Frontiers Editorial Office: frontiersin.org/about/contact

FERTILITY PRESERVATION: FROM NEXT-GENERATION TECHNOLOGIES TO CLINICAL PRACTICE

Topic Editors:
Yuting Fan, Boston IVF, United States
Sherman Silber, Infertility Center of St. Louis, United States

Citation: Fan, Y., Silber, S., eds. (2022). Fertility Preservation: From Next-generation Technologies to Clinical Practice. Lausanne: Frontiers Media SA.
doi: 10.3389/978-2-83250-857-2

Table of Contents

frontiers in Endocrinology

ORIGINAL RESEARCH
published: 04 March 2022
doi: 10.3389/fendo.2022.842037

Clinical Outcomes of *In Vitro* Maturation After Oocyte Retrieval With Gynecological Surgery for Refractory Polycystic Ovary Syndrome: A Retrospective Cohort Study

Wen Zhang[1,2,3,4,5†], *Tingting Liang*[6†], *Bing Han*[1,2,3,4,5], *Rui Yang*[1,2,3,4,5], *Shuo Yang*[1,2,3,4,5], *Yan Yang*[1,2,3,4,5], *Jiajia Zhang*[1,2,3,4,5], *Xiaoying Zheng*[1,2,3,4,5], *Jie Yan*[1,2,3,4,5], *Caihong Ma*[1,2,3,4,5], *Xueling Song*[1,2,3,4,5*†] and *Jie Qiao*[1,2,3,4,5*]

[1] Center for Reproductive Medicine, Department of Obstetrics and Gynecology, Peking University Third Hospital, Beijing, China, [2] National Clinical Research Center for Obstetrics and Gynecology (Peking University Third Hospital), Beijing, China, [3] Key Laboratory of Assisted Reproduction, Ministry of Education (Peking University), Beijing, China, [4] Beijing Key Laboratory of Reproductive Endocrinology and Assisted Reproductive Technology, Beijing, China, [5] Research Units of Comprehensive Diagnosis and Treatment of Oocyte Maturation Arrest, Chinese Academy of Medical Sciences, Beijing, China, [6] Department of Obstetrics and Gynecology, The Second Hospital of Shanxi Medical University, Taiyuan City, China

Objective: To explore the clinical outcomes of unstimulated *in vitro* maturation (IVM) after oocyte retrieval with gynecological surgery (IVM-surgery) for refractory polycystic ovary syndrome (PCOS) and analyze the influencing factors.

Methods: Patients with refractory PCOS who underwent unstimulated IVM-surgery from June 2014 to September 2018 were included in this retrospective cohort study. Matured IVM oocytes were freshly fertilized and subsequently frozen at the blastocyst stage. Frozen-thawed embryo transfer was then conducted according to the desire of patients. Oocytes and embryological outcomes, reproductive outcomes were evaluated. Influencing factors of oocytes and embryological outcomes were analyzed by univariate analysis and multivariate analysis. Receiver operating characteristic curves were used to evaluate the predict value of serum hormone levels for oocytes and embryological outcomes.

Results: A total of 93 patients with refractory PCOS who underwent unstimulated IVM-surgery were included in this study.13 patients (13/85, 15.3%) had spontaneous pregnancy and live birth after surgery. 34 patients (34/93, 36.6%) obtained blastocysts and received embryo transfer, of which 13 patients (13/34, 38.2%) eventually achieved live birth by IVM. Higher anti-Mullerian hormone, antral follicle count and basal serum luteinizing hormone (LH) levels were strongly correlated with higher number of oocytes retrieved (P = 0.004, 0.004, 0.040, respectively). Higher basal serum follicle-stimulating

OPEN ACCESS

Edited by:
Yuting Fan,
Boston IVF, United States

Reviewed by:
Lianghui Diao,
Shenzhen Zhongshan Urology Hospital, China
Cuilian Zhang,
Henan Provincial People's Hospital, China

***Correspondence:**
Jie Qiao
jie.qiao@263.net
Xueling Song
sxldxx@263.net

[†]*These authors have contributed equally to this work and share first authorship*

Specialty section:
This article was submitted to Reproduction, a section of the journal Frontiers in Endocrinology

Received: *23 December 2021*
Accepted: *11 February 2022*
Published: *04 March 2022*

Citation:
Zhang W, Liang T, Han B, Yang R, Yang S, Yang Y, Zhang J, Zheng X, Yan J, Ma C, Song X and Qiao J (2022) Clinical Outcomes of In Vitro Maturation After Oocyte Retrieval With Gynecological Surgery for Refractory Polycystic Ovary Syndrome: A Retrospective Cohort Study. Front. Endocrinol. 13:842037. doi: 10.3389/fendo.2022.842037

hormone (FSH) and LH were significantly associated with higher oocyte maturation rate (P = 0.001 and P = 0.004, respectively) and blastocyst formation (P = 0.036 and P = 0.003, respectively). There was a significant linear correlation between basal serum FSH and LH (r = 0.500, P <0.001). What is more, basal serum FSH and LH had predictive value for oocytes and embryological outcomes.

Conclusion: Unstimulated IVM-surgery provided the opportunity for both spontaneous pregnancy and assisted reproductive technology. Basal FSH and LH were significantly associated with oocyte maturation rate and blastocyst formation of unstimulated IVM-surgery.

Keywords: *in vitro* maturation, IVM-surgery, polycystic ovary syndrome, FSH, LH

INTRODUCTION

Polycystic ovary syndrome (PCOS) is a highly prevalent disorder effecting reproductive-aged women worldwide, which is characterized by clinical or biochemical hyperandrogenism, ovulatory dysfunction and polycystic ovarian morphology (1). The first line treatment for PCOS is clomiphene citrate, which has an ovulation rate of 80%, but 20% of patients are still resistant to clomiphene citrate. Patients who are refractory to at least 3 clomiphene citrate treatment cycles can be diagnosed as refractory PCOS (2). Transvaginal retrieval of immature oocytes has been used for refractory PCOS patients and showed some therapeutic effects (3).

In vitro maturation (IVM) has been used as a technique that has led to the birth of thousands of healthy babies worldwide (4). IVM involves the retrieval of immature oocytes followed by *in vitro* culture to obtain mature oocytes, which has mainly been applied for women with PCOS to avoid the risk of ovarian hyperstimulation syndrome (5) and fertility preservation strategy for women with cancer (6). Compared to conventional *in vitro* fertilization (IVF) treatment, IVM has fewer complications due to the lower hormonal side effects, which is less costly and simpler to perform.

Currently, retrieval of immature oocytes and subsequent IVM in combination with gynecological surgery (IVM-surgery) for benign gynecological diseases is poorly studied. Oocyte retrieval for IVM does not require synchronization with the menstrual cycle or lengthy pretreatment (7), which provides a possibility to perform IVM simultaneously with gynecological surgery. For instance, some patients may undergo a hysteroscopic examination or laparoscopic surgery, transvaginal retrieval of immature oocytes during endoscopic gynecological procedures could be considered. On one hand, IVM-surgery for patients who will undergo subsequent IVF could avoid the additional procedures of ovarian stimulation and oocyte retrieval, which will reduce surgery associated complications, cost and extra time requirements. On the other hand, for patients who wish to have spontaneous pregnancy, IVM-surgery could restore normal pelvic anatomy, create conditions for spontaneous pregnancy and furthermore allow for fertility preservation (8).

Our center of reproductive medicine previously had conducted the first prospective cohort study to evaluate the effectiveness and safety of unstimulated IVM associated with laparoscopy/hysteroscopy procedures. The previous study included a total of 158 women with refractory PCOS who underwent IVM-surgery. Matured IVM oocytes obtained from these women were either freshly fertilized and subsequently frozen at the blastocyst stage (fresh oocyte group, n = 46) or the oocytes were frozen (frozen oocyte group, n = 112) for fertility preservation followed by later thawing for insemination and cleavage embryo transfer (ET) (n = 33). In the fresh oocyte group, the clinical pregnancy rate and live birth rate per ET cycle were 69.2% and 53.8%, respectively. In the frozen oocyte group, the clinical pregnancy rate and live birth rate per ET cycle were 28.6% and 19.1%, respectively. The previous study concluded that IVM-surgery on unstimulated ovaries is a novel option that can be considered for fertility preservation for women requiring gynecological surgery. However, the sample size of previous studies was small. Due to the poor fertility outcome of frozen oocyte group, we did not continue the corresponding study, but focused on the IVM population. The previous study only included 46 patients of which matured IVM oocytes were freshly fertilized and subsequently frozen at the blastocyst stage. We subsequently expanded the sample size to recruit more patients with refractory PCOS who were willing to undergo unstimulated IVM-surgery. Therefore, this study retrospectively analyzed the clinical outcomes of these patients and analyzed the influencing factors.

MATERIALS AND METHODS

Study Design and Patients

This was a retrospective cohort study of patients with refractory PCOS who underwent laparoscopic and/or hysteroscopic surgery for benign indications at the Reproductive Centre of the Peking University Third Hospital from June 2014 to September 2018. This study was conducted based on a finished prospective cohort study (Clinical Trials ID: chictr-ONC-17011861). The study was approved by the Ethics Committee of Peking University (2014S2004).

The inclusion criteria were as follows: (1) infertile women with refractory PCOS who has undergone laparoscopy/hysteroscopy and conducted IVM during the surgery. PCOS was diagnosed according to the Rotterdam ESHRE/ASRM consensus criteria (2004); (2) age ≤ 38 years old; (3) basal

serum follicle-stimulating hormone (FSH) < 10 IU/L. Exclusion criteria were: (1) with previous ovarian surgery, pelvic mass of unclear origin, bilateral ovarian cyst or clinical suspicion of endometrial hyperplasia; (2) with other endocrine severe diseases, immune diseases, and tumors. After retrieval of immature oocytes, *in vitro* culture was conducted to obtain mature oocytes and then matured IVM oocytes were freshly fertilized and subsequently frozen at the blastocyst stage. The recruited patients were followed up until March 2020.

Transvaginal Oocyte Retrieval and Gynecological Surgery

No stimulation with gonadotropin and no human Chorionic Gonadotropin (hCG) trigger treatment before immature follicle aspiration was conducted. Immature follicle aspiration was carried out by an experienced operator before gynecological surgery. All visible follicles (2-10mm) were aspirated with 19-gauge single-lumen aspiration needles (K-OPS-7035-REH-ET; Cook, Queensland, Australia) under a suction pressure of 80 mmHg. Laparoscopic ovarian drilling was the most common surgical procedure performed during this study. Each patient received only once laparoscopic ovarian drilling. For patients with anti-mullerian hormone (AMH) < 5 ng/ml, laparoscopic ovarian drilling is not considered. As this study was conducted based on a finished prospective cohort study, detailed information can be found in XL Song's study (8).

IVM Culture Protocol, Oocyte Fertilization, Embryo Culture and Blastocyst Vitrification

The cumulus–oocyte complexes (COCs) were examined under a stereomicroscope (Nikon, SMZ1000, Japan), which were then transferred into IVM oocyte medium (Sage IVM media kit; Origio, Denmark) supplemented with 0.075 IU/ml of FSH and 0.075 IU/ml of luteinizing hormone (LH) (Menopur; Ferring Reproductive Health, Kiel, Germany) for maturation. Maturity of COCs was then evaluated after IVM culture for 28–32 h. Immature oocytes were further cultured for an additional 10–14 h. Only oocytes with extrusion of the first polar body were considered to be mature (metaphase II (MII) stage oocytes). Mature oocytes were inseminated by intra-cytoplasmic sperm injection, which is done routinely for IVM in our lab, but not because of male factors. All embryos were cultured in GM medium (G-M, Life Global, CT, USA) supplemented with 10% synthetic serum substitute (SSS; Irvine Scientific, Santa Ansa, CA, USA). Quality of embryos was evaluated according to the Istanbul Consensus Workshop on Embryo Assessment criteria (9). Day-3 embryos were further cultured to develop into the blastocyst for cryopreservation. Blastocysts were evaluated according to the Gardner morphological grading system.

Frozen-Thawed Embryo Transfer

Blastocyst vitrification and thawing procedure were reported previously (10). Oral oestradiol valerate (Progynova, 6 mg, daily; Schering, Berlin, Germany) was initiated on the second day of the menstrual cycle. Progesterone withdrawal bleeding was administrated for anovulatory women to identify the menstrual cycle phase. Progesterone intravaginal gel (Crinone 8% 90 mg, daily; Merck Serono, USA) combined with oral dydrogesterone was administered for 7 days when the endometrial thickness reached 8mm. After 7 days of progesterone treatment, one blastocyst was transferred into the uterine. Detailed information can be found in XL Song's study (8).

Clinical Data and Definitions

The basic characteristics of the participants, such as age, body mass index (BMI), infertility type, infertility duration, insulin resistance, AMH, basal serum FSH, luteinizing hormone (LH), testosterone levels on the 3rd menstruation day, antral follicle count (AFC) and free androgen index (FAI) (total testosterone×100/sex hormone binding globulin) were evaluated. Insulin resistance was defined as index of homeostasis model assessment of insulin resistance (HOMA-IR)> 2.5. HOMA-IR = fasting blood glucose (mmol/L) × fasting insulin level (mIU/L)/22.5. Oocytes, embryological outcomes and reproductive outcomes of IVM-surgery were also evaluated. Oocyte maturation rate was defined as the number of MII oocytes divided by all the cultured oocytes. Live birth was defined as the birth of at least one living child, irrespective of the duration of gestation. Patients were considered lost to follow-up when we cannot reach them in any way.

Statistical Analysis

Characteristics were presented as mean ± standard deviation (SD) or median (interquartile range, IQR) for continuous variables, and percentages for categorical variables. Comparisons between ratios were performed using the Chi-square test or Fisher exact test. Continuous variables were analyzed by t-test or nonparametric tests. Logistic regression models were used to estimate the effect of serum hormone levels on oocytes and embryological outcomes. Associations between two parameters were evaluated by Spearman's test and scatter plots were drawn. Receiver operating characteristic curves (ROC) were made to determine the relationship between serum hormone levels and oocytes and embryological outcomes. Cut-off values of number of oocytes retrieved and oocyte maturation rate for predicting blastocysts formation was determined by ROC curve and its clinical practical value. Statistical significance was set at a probability (P) value < 0.05. Analysis was performed using statistical package for social science (SPSS) software, version 25.0 (IBM, Armonk, New York, USA).

RESULTS

Characteristics and Oocytes Outcomes of Refractory PCOS Patients Who Underwent IVM-Surgery

A total of 93 patients with refractory PCOS who underwent unstimulated IVM-surgery were included in this study. Baseline characteristics, surgical indications as well as oocytes and embryological outcomes are presented in **Table 1**.

TABLE 1 | Characteristics of the study participants who underwent IVM-surgery.

Baseline characteristics, n = 93	
Age (years), mean ± SD	28.6 ± 3.1
BMI (kg/m^2), mean ± SD	24.8 ± 3.2
Primary infertility, %	73.1%
Infertility duration > 60 months, %	26.9%
HOMA-IR, %	
HOMA-IR > 2.5, %	51.6%
HOMA-IR ≤ 2.5, %	48.4%
FSH (mIU/ml), mean ± SD	5.6 ± 1.6
LH (mIU/ml), mean ± SD	9.2 ± 5.3
AMH (ng/ml), mean ± SD	12.7 ± 5.6
Testosterone (nmol/L), median (IQR)	1.7 (1.0, 2.3)
FAI, median (IQR)	7.1 (4.1, 13.0)
Antral follicle count, mean ± SD	19.7 ± 8.7
PCOS type, %	
with hyperandrogenism, %	61.3%
without hyperandrogenism, %	38.7%
Clomiphene citrate treatment cycles, mean ± SD	3.3 ± 0.6
Indications for surgery, n = 93	
LOD for clomiphene citrate resistance, n (%)	54 (58.1%)
Tubal pathology, n (%)	29 (31.2%)
Ovarian cyst, n (%)	4 (4.3%)
(Teratoma n = 2, endometrioma n = 2)	
Uterine pathology, n (%)	6 (6.5%)
(Leiomyoma n = 1, uterine septum n = 2, intrauterine adhesions n = 1, endometrial polyps n = 2)	
Oocytes and embryological outcomes of IVM-surgery cycles, n = 93	
Oocytes retrieved, median (IQR)	12 (8, 19)
Matured oocyte rate, median (IQR)	41.5% (27.3%, 56.0%)
Blastocyst formation, %	45.2%

IVM, in vitro maturation; BMI, body mass index.
HOMA-IR, index of homeostasis model assessment of insulin resistance.
FAI, free androgen index; LOD, laparoscopic ovarian drilling.
IQR, interquartile range; SD, standard deviation.

Reproductive Outcomes of Patients With IVM-Surgery

Of the 93 patients with refractory PCOS who underwent unstimulated IVM-surgery, 8 patients (8/93, 8.6%) were lost to follow-up. Reproductive outcomes of 85 patients were shown in **Figure 1**. After IVM-surgery, 47 patients met the criteria for natural conception after surgery and attempted to be pregnant without assisted reproductive technology, of which 13 patients (13/85, 15.3%) had a live birth. On the other hand, among the 93 patients, 42 patients (42/93, 45.2%) obtained blastocysts, 34 patients received embryo transfer, and 13 patients (13/34, 38.2%) eventually achieved live birth, as shown in **Figure 1**. Due to the limited sample size, we did not explore the influencing factors of natural conception and live birth through IVM.

Factors Influencing the Number of Oocytes Retrieved During IVM-Surgery for Refractory PCOS Patients

We divided the patients into two groups according to the number of oocytes retrieved, with a threshold of 15. There were statistically significant differences in serum AMH, AFC and basal serum LH levels between the two groups, as shown in **Table 2**. Multivariate analysis results further confirmed the correlation between serum hormone level, AFC and number of oocytes retrieved (**Table 3**). AMH, AFC and LH levels were higher in patients with number of oocytes retrieved > 15 oocytes when compared to patients with fewer oocytes (P = 0.004, 0.004, 0.040, respectively). However, there were no statistically significant differences in other indicators between the two groups.

Factors Influencing Oocyte Maturation Rate During IVM-Surgery for Refractory PCOS Patients

We divided the patients into two groups according to oocyte maturation rate, with a threshold of 50%. There were statistically significant differences in basal serum FSH and basal serum LH levels between the two groups, as shown in **Table 4**. Multivariate analysis results further confirmed the above results (**Table 3**). FSH and LH levels were higher in patients with oocyte maturation rate > 50% (P = 0.001 and P = 0.004, respectively). Besides, Spearman's test demonstrated that there was a significant linear correlation between basal serum FSH and LH (r = 0.500, P < 0.001) (**Figure 2**). Furthermore, the predictive value of basal serum FSH and LH on oocyte maturation rate was analyzed by ROC curve. The areas under the ROC curve (AUC) of FSH and LH were 0.688 and 0.610 (P = 0.004 and P = 0.089, respectively), respectively. Therefore, serum basal FSH showed predictive value for oocyte maturation rate (**Figure 3A**).

Factors Influencing Blastocysts Formation During IVM-Surgery for Refractory PCOS Patients

As for blastocysts formation, there were also statistically significant differences in basal serum FSH and basal serum LH levels between the two groups, as shown in **Table 5**. Multivariate analysis results also confirmed the above results (**Table 3**). FSH and LH levels were higher in patients with blastocysts formation (P = 0.036 and P = 0.003, respectively). Besides, AUC of FSH and LH for predicting blastocysts formation were 0.646 and 0.654, respectively, with P = 0.020 and P = 0.014, respectively. Therefore, both serum basal FSH and LH showed predictive value for blastocysts formation (**Figure 3B**).

DISCUSSION

In the present study, patients with refractory PCOS undergoing unstimulated IVM-surgery were included. IVM-surgery offered the opportunity for both spontaneous pregnancy and assisted reproductive technology. Total of 26 patients (26/85, 30.6%) finally achieved live birth after IVM-surgery by spontaneous pregnancy or by IVM. For refractory PCOS patients undergoing IVM-surgery, higher AMH, AFC and LH levels were strongly correlated with higher number of oocytes retrieved. Higher basal FSH and LH were significantly associated with higher oocyte maturation rate and blastocyst formation, what is more,

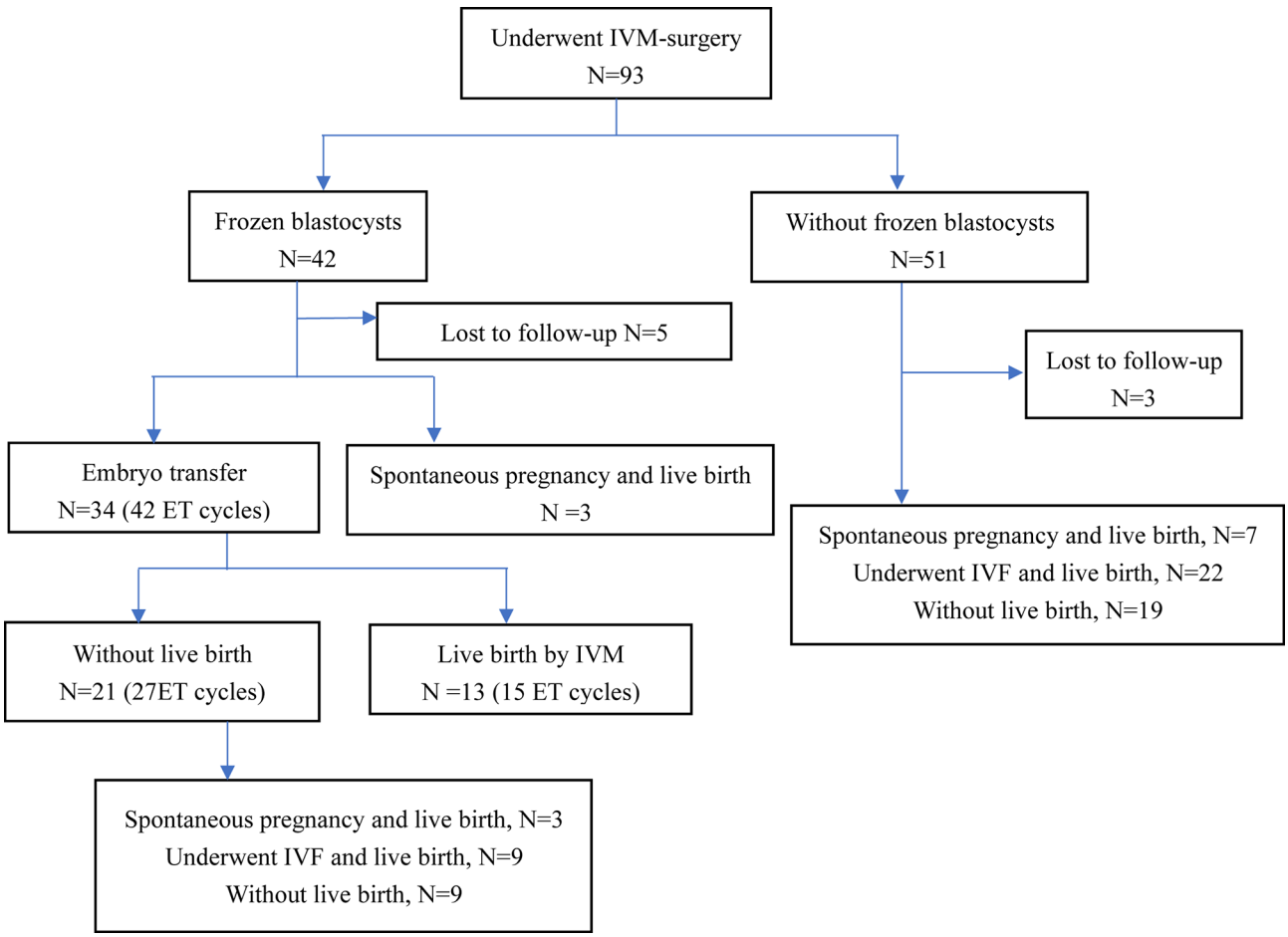

FIGURE 1 | Reproductive outcomes of patients with IVM-surgery. ET, embryo transfer; IVM, *in vitro* maturation; IVF, *in vitro* fertilization.

basal FSH and LH had predictive value for oocytes and embryological outcomes.

Our study did demonstrate the effectiveness of IVM for refractory PCOS patients, with 45.2% (42/93) of patients obtaining blastocysts, 81.0% (34/42) of which underwent embryo transfer and 38.2% (13/34) finally had live births through IVM. IVM is not appropriate for normally ovulating patients with dominant follicles, because dominant follicles can inhibit the growth of other follicles and promote atresia, leading to adverse outcomes for IVM (8). All patients included in this

TABLE 2 | Factors influencing the number of oocytes retrieved during IVM-surgery.

	Number of Oocytes retrieved		P value*
	≤15 n = 61	>15 n = 32	
Age (years), mean ± SD	28.6 ± 3.0	28.6 ± 3.3	0.978
BMI (kg/m^2), mean ± SD	24.5 ± 3.4	25.5 ± 2.6	0.160
Primary infertility, %	70.5%	78.1%	0.430
Infertility duration > 60 months, %	23.0%	34.4%	0.238
Insulin resistance, %	46.2%	60.9%	0.263
FSH (mIU/ml), mean ± SD	5.5 ± 1.5	5.8 ± 1.8	0.320
LH (mIU/ml), median (IQR)	8.7 (3.5,12.7)	9.3 (6.2, 12.9)	0.035
AMH (ng/ml), median (IQR)	10.6 (7.0,17.0)	15.9 (11.2,18.2)	0.001
Testosterone (nmol/L), median (IQR)	1.8 (0.8,2.4)	1.9 (1.4,2.3)	0.415
FAI, median (IQR)	6.5 (4.0,12.7)	7.1 (4.2,17.0)	0.538
Antral follicle count, mean ± SD	17.5 ± 7.8	23.7 ± 9.1	0.001

**P value of univariate analysis. IVM, in vitro maturation; BMI, body mass index; SD, standard deviation; FAI, free androgen index; IQR, interquartile range.*

TABLE 3 | Multivariate analysis of factors influencing oocytes and embryological outcomes.

	OR	95%CI	P value*
Oocytes retrieved			
Basal LH	2.684	1.047, 6.878	0.040
Basal AMH	5.623	1.763, 17.936	0.004
Antral follicle count	1.087	1.027, 1.151	0.004
Matured oocyte rate			
Basal FSH	8.070	2.421, 26.893	0.001
Basal LH	4.044	1.562, 10.469	0.004
Available blastocysts formation			
Basal FSH	2.765	1.068, 7.160	0.036
Basal LH	3.945	1.583, 9.833	0.003

**Adjusted by age and BMI.*

study had refractory PCOS, and these patients basically had no dominant follicle growth, which met IVM requirements. Song XL's study also confirmed that for IVM-surgery, 41.3% (19/46) of patients obtaining blastocysts, 68.4% (13/19) of which underwent embryo transfer and 53.8% (7/13) finally had live births through IVM. Thus, IVM-surgery for refractory PCOS is feasible.

IVM-surgery not only provided patients with the opportunity to have a pregnancy through assisted reproductive technology, but also provided them with the opportunity to have spontaneous pregnancy. Patients included in this study were infertile patients with refractory PCOS, thus these patients would continue to be infertile and unable to obtain a spontaneous pregnancy without the intervention of IVM-surgery. With treatment of IVM-surgery, 13 patients (13/85, 15.3%) had spontaneous pregnancy and live birth after surgery, which proved that IVM-surgery provided conditions for spontaneous pregnancy. Effect of IVM-surgery on spontaneous pregnancy could be explained as follows. On one hand, the procedure itself could remove the pathological factors affecting infertility. On the other hand, the procedure of laparoscopic ovarian drilling and aspiration of transvaginal oocyte retrieval reduced the number of theca cells, which decreased the production of androgen (11). What was more, transvaginal oocyte retrieval reduced ovarian punctures and did not require electrocautery, which led to less trauma to the ovarian tissue and protected the ovarian reserve. All these created conditions for spontaneous pregnancy.

As for the IVM technology, the technique is not widely used because there are still many unresolved issues, such as the oocyte retrieval protocol, the composition of the culture medium, and the culture time, which are still uncertain. In the present study, we also explored the factors influencing the oocytes and embryological outcomes.

Basal AMH, AFC and LH showed strong correlation with the number of oocytes retrieved. AMH is specifically expressed in granulosa cells of small growing follicles, which is important indicators reflecting ovarian reserve (12). It has been proposed as a surrogate for antral follicle count in the diagnosis of PCOS. Previous studies have noted that there was a linear relationship between AMH and oocyte yield after ovarian stimulation (13, 14). Therefore, AMH is of value in predicting oocyte yield for IVM. AFC is also an important indicator of ovarian reserve, which is the number of antral follicles detected by transvaginal ultrasound before oocyte retrieval. Therefore, theoretically, the AFC is a direct parameter of the number of oocytes obtained. The present study showed that AFC was strongly correlated with the number of oocytes retrieved, which was also consistent with the results of previous studies (15, 16). LH showed positive correlations with AMH in the PCOS patients (17), which may be the reason why LH was found to correlate with the number of oocytes obtained in our study.

Basal FSH was closely related to oocyte maturation rate and blastocyst formation in present study. FSH stimulates the growth

TABLE 4 | Factors influencing oocyte maturation rate during IVM-surgery.

	Matured oocyte rate		P value*
	≤50% n = 53	>50% n = 37	
Age (years), mean ± SD	29.1 ± 3.1	28.1 ± 3.1	0.138
BMI (kg/m^2), mean ± SD	24.8 ± 3.2	25.0 ± 3.2	0.673
Primary infertility, %	67.9%	78.4%	0.276
Infertility duration > 60 months, %	28.3%	24.3%	0.675
Insulin resistance, %	50.0%	57.7%	0.554
FSH (mIU/ml), mean ± SD	5.2 ± 1.5	6.1 ± 1.6	0.008
LH (mIU/ml), median (IQR)	7.6 (3.5,11.9)	10.4 (5.8,16.4)	0.036
AMH (ng/ml), median (IQR)	12.8 (7.4,16.8)	11.4 (8.5,19.3)	0.971
Testosterone (nmol/L), median (IQR)	1.8 (1.2,2.3)	1.9 (0.9,2.4)	0.621
FAI, median (IQR)	6.3 (3.8,12.0)	8.8 (4.2,15.1)	0.347
Antral follicle count, mean ± SD	20.3 ± 9.6	18.2 ± 7.3	0.269

**P value of univariate analysis; IVM, in vitro maturation; BMI, body mass index; SD, standard deviation; FAI, free androgen index; IQR, interquartile range.*

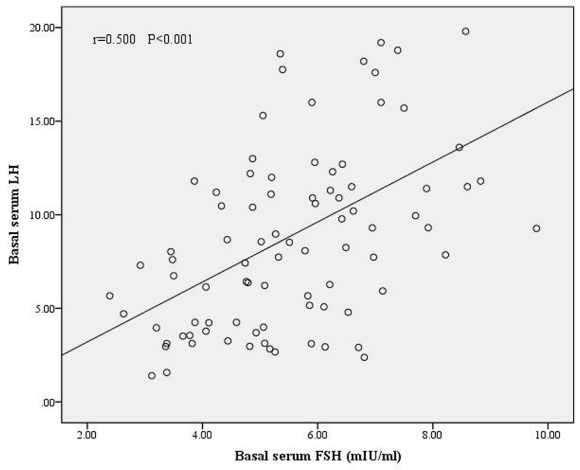

FIGURE 2 | Correlation between basal serum FSH and LH. There was a significant linear correlation between FSH and LH (r = 0.500, $P < 0.001$).

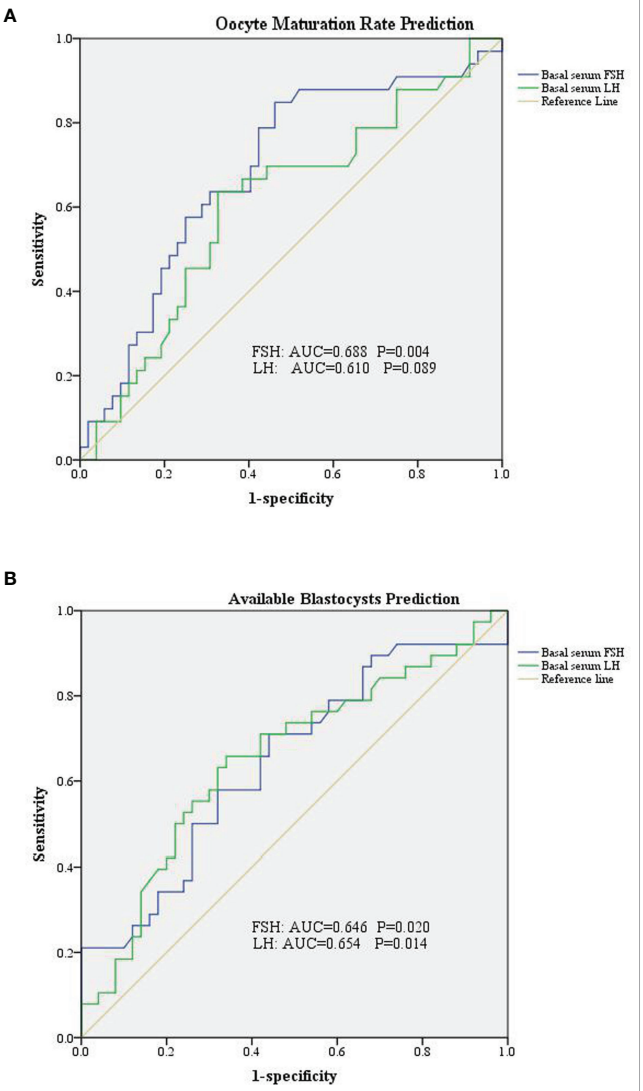

FIGURE 3 | Receiver operating characteristic curve of basal serum FSH and LH in prediction of oocytes and embryological outcomes. **(A)** Basal serum FSH has predictive value for oocyte maturation rate. **(B)** Both basal serum FSH and basal serum LH has predictive value for available blastocysts.

and maturation of immature oocytes into mature (Graafian) secondary follicles before ovulation (18). For PCOS patients, low levels of FSH makes it difficult to reach the "threshold" required for follicle maturation, which is an important cause of follicle arrest (19). Therefore, FSH pretreatment before IVM or addition of FSH to the culture system of IVM, theoretically, could promote follicular growth and maturation and thus improve the oocytes and embryological outcomes. In our study, median of matured oocyte rate in IVM was 41.5%, which was lower than the previous study in which Walls et al. reported that matured oocyte rate was as high as 73.0% (5). The reason for the low rate of matured oocyte rate in our study was that we did not use any gonadotrophins stimulation before transvaginal oocyte retrieval procedure, however Walls et al. administered gonadotrophins for 3–6 days before IVM (FSH priming). Anderiesz et al. demonstrated that the addition of recombinant FSH alone into the culture system increased the maturation of human oocytes compared to the maturation of oocytes with no hormones (20). Further, Jesús Cadenas noted that FSH improved oocyte nuclear maturation at concentrations above 70 IU/L suggesting a threshold for FSH during IVM of *in vitro* collected human oocytes from small antral follicles (21). Our study also found similar conclusions: compared with those with lower basal serum FSH, those with higher basal FSH had higher oocyte maturation rate and higher probability of blastocyst acquisition. Meanwhile, FSH showed certain predictive value for oocytes and embryological outcomes. These studies suggested that FSH pretreatment before transvaginal retrieval of immature oocytes or culture medium supplemented with FSH could improve IVM oocytes and embryological outcomes. Therefore, in subsequent clinical practice, we could give appropriate FSH stimulation before IVM-surgery.

Basal LH also showed close relationship with oocyte maturation rate and blastocyst formation. Patients with PCOS often have increased pulsatile release of pituitary gonadotropins, as evidenced by abnormally elevated LH (22). LH has a role in promoting ovulation and oocyte maturation in humans. Child TJ reported a maturation rate of 80.3% for IVM outcomes with natural cycle in patients with PCOS (23), which was much higher than the data in our study (41.5%), which may be due to the fact that Child TJ's study used a modified natural cycle protocol for IVM using hCG to induce ovulation 3-5 days prior to ovulation retrieval, whereas all patients in our study did not have hCG trigger therapy prior to ovulation retrieval. However, recent evidence suggested that IVM culture systems plus LH were not associated with oocyte maturation. C. Accardo et al. demonstrated that LH alone had no effect on the developmental of potential of bovine oocytes (24), which neither improved

TABLE 5 | Factors influencing available blastocysts formation during IVM-surgery.

	Available blastocyst formation		P value*
	Yes n = 42	No n = 51	
Age (years), mean ± SD	28.1 ± 2.9	29.1 ± 3.2	0.127
BMI (kg/m^2), mean ± SD	24.9 ± 3.1	24.8 ± 3.2	0.779
Primary infertility, %	76.2%	70.6%	0.544
Infertility duration > 60 months, %	28.6%	25.5%	0.739
Insulin resistance, %	50.0%	53.1%	0.806
FSH (mIU/ml), mean ± SD	6.1 ± 1.8	5.2 ± 1.4	0.012
LH (mIU/ml), median (IQR)	11.1 (7.5,15.6)	6.1 (3.5,10.9)	0.010
AMH (ng/ml), median (IQR)	14.4 (9.2,17.7)	12.5 (7.1,17.4)	0.512
Testosterone (nmol/L), median (IQR)	2.1 (1.2,2.4)	1.7 (1.0,2.5)	0.318
FAI, median (IQR)	7.1 (4.0,13.8)	6.5 (3.9,12.8)	0.799
Antral follicle count, mean ± SD	21.5 ± 9.6	18.1 ± 7.7	0.066

**P value of univariate analysis; IVM, in vitro maturation; BMI, body mass index; SD, standard deviation; FAI, free androgen index; IQR, interquartile range.*

matured oocyte rate nor blastocyst formation, however recombinant FSH alone or in combination with recombinant LH may have stimulatory effects on the progression of the meiotic cycle (24). It can be explained by the phenomenon that cumulus and granulosa cells of medium-sized (2–6 mm) follicles express FSH receptors but could hardly express LH receptors (25). Rubens Fadini et al. noted that hCG could promote in vivo meiotic resumption and progression to the MII stage in oocytes of follicles of a diameter of 10–12 mm (26). Therefore, LH could hardly affect the growth and development of small follicles. In this study, the follicles obtained from patients with refractory PCOS were all small follicles, so theoretically, basal serum LH did not affect the development of follicles. However, our study found that LH was significantly correlated with oocyte maturation rate and blastocysts formation, which may be related to several reasons. On one hand, this study showed the significant linear correlation between LH and FSH in included patients, therefore due to the linear correlation between FSH and LH, the effect of FSH on oocyte maturation and blastocysts formation could lead to the significant correlation between LH and oocyte maturation and blastocysts formation. In other words, although theoretically basal serum LH did not affect the development of small follicles as we have discussed above, the direct impact of FSH on follicles and linear correlation between LH and FSH led to the phenomenon that LH was significantly correlated with oocyte maturation rate and blastocysts formation. One the other hand, another possible reason was that the level of LH represented the severity of PCOS, which itself affected follicular growth and development through other pathways, and therefore showed a significant correlation between LH and oocyte maturation rate and blastocysts formation. And whether LH could affect follicular growth and development through other unexplored ways needs to be confirmed by further studies.

Both FSH and LH play important roles in follicular growth, development and maturation. Previous studies have also demonstrated that FSH combined with LH can improve follicle and embryo outcomes for IVM. C Accardo compared the effects of four different IVM culture medium on sheep oocytes (IVM culture medium with recombinant FSH (r-FSH) alone, recombinant LH (r-LH) alone, r-FSH and r-LH simultaneously and without gonadotropin), which discovered the highest maturation rate was reached in the r-FSH/r-LH group (91.9%) (24). Anderiesz et al. demonstrated that although r-FSH combination with r-LH did not significantly increase matured oocyte rate, it could improve human embryonic developmental competence (20). Fadini R assessed and compared the clinical efficiency of four different priming approaches for normo-ovulatory women: no priming, hCG (10,000 IU), FSH (150 IU/d for 3 days from day 3), and FSH/hCG (26). They found that FSH/hCG priming generated the highest amount of MII oocytes and clinical pregnancy rates were much higher in the FSH/hCG treated women compared with all the other treatments. We speculated that FSH combined with LH can affect follicles of different stages and sizes. FSH promotes follicle growth and LH promotes maturation of grown follicles, thus jointly improves oocytes and embryological outcomes. Therefore, for refractory PCOS patients, appropriate FSH stimulation before IVM-surgery can be applied without LH stimulation simultaneously because of the absence of LH receptor in small follicles from refractory PCOS patients, however, whether LH should be added after FSH stimulation depends on the size and stage of follicles.

There were some advantages and disadvantages of this study. To the best of our knowledge, this study was the largest to date in exploring unstimulated IVM-surgery. The study confirmed the feasibility of unstimulated IVM-surgery. More importantly, the clinical practice significance of IVM-surgery is that it opens up new options for assisted reproduction, which is a novel option that can be considered for fertility preservation for women requiring gynecological surgery, without affecting the effect of surgery. After the IVM-surgery, the patient has both the chance of spontaneous pregnancy and the choice of assisted reproduction, and when the patient chooses assisted reproduction after IVM-surgery, they already have had a transplantable blastocyst. What is more, this study found the factors affecting oocytes and embryological outcomes. These significant findings suggested that appropriate gonadotropins stimulation could be given before IVM-surgery in subsequent assisted reproductive clinical practices. The disadvantage of this study was that due to the limited sample size, the influencing factors of live birth in IVM-surgery could not be further explored. Subsequent studies could further explore the influencing factors of live birth in IVM-surgery and the effectiveness of gonadotropins stimulation before IVM-surgery.

CONCLUSION

Unstimulated IVM-surgery provided the opportunity for both spontaneous pregnancy and assisted reproductive technology. Basal FSH and basal LH were significantly associated with oocyte maturation rate and blastocyst formation of unstimulated IVM-surgery.

DATA AVAILABILITY STATEMENT

The raw data supporting the conclusions of this article will be made available by the authors, without undue reservation.

ETHICS STATEMENT

The studies involving human participants were reviewed and approved by Ethics Committee of Peking University. Written informed consent for participation was not required for this study in accordance with the national legislation and the institutional requirements.

AUTHOR CONTRIBUTIONS

CM, XS, JY, and JQ contributed to conception and design of the study. RY, SY, YY, JZ, XZ, JY, and XS were involved in data acquisition. WZ, TL, and BH organized the database. WZ and TL performed the statistical analysis. WZ wrote the first draft of the manuscript. TL and BH wrote sections of the manuscript. All authors contributed to the article and approved the submitted version.

FUNDING

This study was supported by the National Natural Science Foundation of China (No.81521002), the major consulting research project of the Chinese Academy of Engineering (No. 2020-XZ-22), and the CAMS Innovation Fund for Medical Sciences (2019-I2M-5-001).

REFERENCES

1. Lizneva D, Suturina L, Walker W, Brakta S, Gavrilova-Jordan L, Azziz R. Criteria, Prevalence, and Phenotypes of Polycystic Ovary Syndrome. *Fertil Steril* (2016) 106(1):6–15. doi: 10.1016/j.fertnstert.2016.05.003
2. Ghomian N, Khosravi A, Mousavifar N. A Randomized Clinical Trial on Comparing the Cycle Characteristics of Two Different Initiation Days of Letrozole Treatment in Clomiphene Citrate Resistant PCOS Patients in IUI Cycles. *Int J Fertil Steril* (2015) 9(1):17–26. doi: 10.22074/ijfs.2015
3. Chen ZJ, Li Y, Zhao LX, Jiang JJ, Tang R, Sheng Y, et al. Treatment of Polycystic Ovarian Syndrome With Anovulatory Infertility by Ultrasound-Guided Immature Follicle Aspiration. *Zhonghua fu chan ke za zhi* (2005) 40 (5):295–8. doi: 10.3760/j.issn:0529-567x.2005.05.003
4. Chian RC, Xu CL, Huang JY, Ata B. Obstetric Outcomes and Congenital Abnormalities in Infants Conceived With Oocytes Matured In Vitro. *Facts Views Vision ObGyn* (2014) 6(1):15–8.
5. Walls ML, Hunter T, Ryan JP, Keelan JA, Nathan E, Hart RJ. *In Vitro* Maturation as an Alternative to Standard *In Vitro* Fertilization for Patients Diagnosed With Polycystic Ovaries: A Comparative Analysis of Fresh, Frozen and Cumulative Cycle Outcomes. *Hum Reprod (Oxford England)* (2015) 30 (1):88–96. doi: 10.1093/humrep/deu248
6. Berwanger AL, Finet A, El Hachem H, le Parco S, Hesters L, Grynberg M. New Trends in Female Fertility Preservation: *In Vitro* Maturation of Oocytes. *Future Oncol (London England)* (2012) 8(12):1567–73. doi: 10.2217/fon.12.144
7. Creux H, Monnier P, Son WY, Tulandi T, Buckett W. Immature Oocyte Retrieval and In Vitro Oocyte Maturation at Different Phases of the Menstrual Cycle in Women With Cancer Who Require Urgent Gonadotoxic Treatment. *Fertil Steril* (2017) 107(1):198–204. doi: 10.1016/j.fertnstert.2016.09.041
8. Song XL, Lu CL, Zheng XY, Nisenblat V, Zhen XM, Yang R, et al. Enhancing the Scope of *In Vitro* Maturation for Fertility Preservation: Transvaginal Retrieval of Immature Oocytes During Endoscopic Gynaecological Procedures. *Hum Reprod (Oxford England)* (2020) 35(4):837–46. doi: 10.1093/humrep/dez273
9. Balaban B, Brison D, Calderon G, Catt J, Conaghan J, Cowan L, et al. The Istanbul Consensus Workshop on Embryo Assessment: Proceedings of an Expert Meeting. *Hum Reprod (Oxford England)* (2011) 26(6):1270–83. doi: 10.1093/humrep/der037
10. Zheng X, Wang L, Zhen X, Lian Y, Liu P, Qiao J. Effect of Hcg Priming on Embryonic Development of Immature Oocytes Collected From Unstimulated Women With Polycystic Ovarian Syndrome. *Reprod Biol Endocrinol: RB&E* (2012) 10:40. doi: 10.1186/1477-7827-10-40
11. Fernandez H, Morin-Surruca M, Torre A, Faivre E, Deffieux X, Gervaise A. Ovarian Drilling for Surgical Treatment of Polycystic Ovarian Syndrome: A Comprehensive Review. *Reprod Biomed Online* (2011) 22(6):556–68. doi: 10.1016/j.rbmo.2011.03.013
12. Dewailly D, Andersen CY, Balen A, Broekmans F, Dilaver N, Fanchin R, et al. The Physiology and Clinical Utility of Anti-Mullerian Hormone in Women. *Hum Reprod Update* (2014) 20(3):370–85. doi: 10.1093/humupd/dmt062
13. Nelson SM, Yates RW, Fleming R. Serum Anti-Müllerian Hormone and FSH: Prediction of Live Birth and Extremes of Response in Stimulated Cycles–Implications for Individualization of Therapy. *Hum Reprod (Oxford England)* (2007) 22(9):2414–21. doi: 10.1093/humrep/dem204
14. La Marca A, Sighinolfi G, Radi D, Argento C, Baraldi E, Artenisio AC, et al. Anti-Mullerian Hormone (AMH) as a Predictive Marker in Assisted Reproductive Technology (ART). *Hum Reprod Update* (2010) 16(2):113–30. doi: 10.1093/humupd/dmp036
15. Filippi F, Martinelli F, Paffoni A, Reschini M, Raspagliesi F, Somigliana E. Fertility Preservation in Women With Malignancies: The Accuracy of Antral Follicle Count Collected Randomly During the Menstrual Cycle in Predicting the Number of Oocytes Retrieved. *J Assist Reprod Genet* (2019) 36: (3):569–78. doi: 10.1007/s10815-018-1377-0
16. Guzman L, Ortega-Hrepich C, Polyzos NP, Anckaert E, Verheyen G, Coucke W, et al. A Prediction Model to Select PCOS Patients Suitable for IVM Treatment Based on Anti-Mullerian Hormone and Antral Follicle Count. *Hum Reprod (Oxford England)* (2013) 28(5):1261–6. doi: 10.1093/humrep/det034
17. Cui Y, Shi Y, Cui L, Han T, Gao X, Chen ZJ. Age-Specific Serum Antimüllerian Hormone Levels in Women With and Without Polycystic Ovary Syndrome. *Fertil Steril* (2014) 102(1):230–6.e2. doi: 10.1016/j.fertnstert.2014.03.032
18. Holesh JE, Bass AN, Lord M. *Physiology, Ovulation*. StatPearls. Treasure Island (FL: StatPearls Publishing Copyright © 2021, StatPearls Publishing LLC (2021).
19. Coyle C, Campbell RE. Pathological Pulses in PCOS. *Mol Cell Endocrinol* (2019) 498:110561. doi: 10.1016/j.mce.2019.110561
20. Anderiesz C, Ferraretti A, Magli C, Fiorentino A, Fortini D, Gianaroli L, et al. Effect of Recombinant Human Gonadotrophins on Human, Bovine and Murine Oocyte Meiosis, Fertilization and Embryonic Development In Vitro.

Hum Reprod (Oxford England) (2000) 15(5):1140–8. doi: 10.1093/humrep/15.5.1140
21. Cadenas J, Nikiforov D, Pors SE, Zuniga LA, Wakimoto Y, Ghezelayagh Z, et al. A Threshold Concentration of FSH Is Needed During IVM of Ex Vivo Collected Human Oocytes. *J Assist Reprod Genet* (2021) 38(6):1341–8. doi: 10.1007/s10815-021-02244-8
22. Baskind NE, Balen AH. Hypothalamic-Pituitary, Ovarian and Adrenal Contributions to Polycystic Ovary Syndrome. *Best Pract Res Clin Obstet Gynaecol* (2016) 37:80–97. doi: 10.1016/j.bpobgyn.2016.03.005
23. Child TJ, Abdul-Jalil AK, Gulekli B, Tan SL. *In Vitro* Maturation and Fertilization of Oocytes From Unstimulated Normal Ovaries, Polycystic Ovaries, and Women With Polycystic Ovary Syndrome. *Fertil Steril* (2001) 76(5):936–42. doi: 10.1016/S0015-0282(01)02853-9
24. Accardo C, Dattena M, Pilichi S, Mara L, Chessa B, Cappai P. Effect of Recombinant Human FSH and LH on In Vitro Maturation of Sheep Oocytes; Embryo Development and Viability. *Anim Reprod Sci* (2004) 81(1-2):77–86. doi: 10.1016/j.anireprosci.2003.10.004
25. van Tol HT, van Eijk MJ, Mummery CL, van den Hurk R, Bevers MM. Influence of FSH and Hcg on the Resumption of Meiosis of Bovine Oocytes Surrounded by Cumulus Cells Connected to Membrana Granulosa. *Mol Reprod Dev* (1996) 45(2):218–24. doi: 10.1002/(SICI)1098-2795(199610)45:2<218::AID-MRD15>3.0.CO;2-X
26. Fadini R, Mignini Renzini M, Dal Canto M, Epis A, Crippa M, Caliari I, et al. Oocyte In Vitro Maturation in Normo-Ovulatory Women. *Fertil Steril* (2013) 99(5):1162–9. doi: 10.1016/j.fertnstert.2013.01.138

Conflict of Interest: The authors declare that the research was conducted in the absence of any commercial or financial relationships that could be construed as a potential conflict of interest.

frontiers | Frontiers in Endocrinology

ORIGINAL RESEARCH
published: 03 June 2022
doi: 10.3389/fendo.2022.886678

Human Ovarian Follicles Xenografted in Immunoisolating Capsules Survive Long Term Implantation in Mice

*Margaret A. Brunette[1], Hadrian M. Kinnear[2,3], Prianka H. Hashim[4], Colleen L. Flanagan[1], James R. Day[1], Marilia Cascalho[5,6], Vasantha Padmanabhan[4,7] and Ariella Shikanov[1,2,4]**

[1] Department of Biomedical Engineering, University of Michigan, Ann Arbor, MI, United States, [2] Program in Cellular and Molecular Biology, University of Michigan, Ann Arbor, MI, United States, [3] Medical Scientist Training Program, University of Michigan, Ann Arbor, MI, United States, [4] Department of Obstetrics and Gynecology, University of Michigan, Ann Arbor, MI, United States, [5] Department of Surgery, University of Michigan, Ann Arbor, MI, United States, [6] Department of Microbiology & Immunology, University of Michigan, Ann Arbor, MI, United States, [7] Department of Pediatrics & Communicable Diseases, University of Michigan, Ann Arbor, MI, United States

Female pediatric cancer survivors often develop Premature Ovarian Insufficiency (POI) owing to gonadotoxic effects of anticancer treatments. Here we investigate the use of a cell-based therapy consisting of human ovarian cortex encapsulated in a poly-ethylene glycol (PEG)-based hydrogel that replicates the physiological cyclic and pulsatile hormonal patterns of healthy reproductive-aged women. Human ovarian tissue from four donors was analyzed for follicle density, with averages ranging between 360 and 4414 follicles/mm^3. Follicles in the encapsulated and implanted cryopreserved human ovarian tissues survived up to three months, with average follicle densities ranging between 2 and 89 follicles/mm^3 at retrieval. We conclude that encapsulation of human ovarian cortex in PEG-based hydrogels did not decrease follicle survival after implantation in mice and was similar to non-encapsulated grafts. Furthermore, this approach offers the means to replace the endocrine function of the ovary tissue in patients with POI.

Keywords: human ovaries, immunoisolation, poly (ethylene glycol), xenografts, hydrogels

OPEN ACCESS

Edited by:
Yuting Fan,
Boston IVF, United States

Reviewed by:
Jingjie Li,
The Sixth Affiliated Hospital of Sun Yat-sen University, China
Rossella Vicenti,
University of Bologna, Italy

***Correspondence:**
Ariella Shikanov
shikanov@umich.edu

Specialty section:
This article was submitted to Reproduction, a section of the journal Frontiers in Endocrinology

Received: *28 February 2022*
Accepted: *15 April 2022*
Published: *03 June 2022*

Citation:
Brunette MA, Kinnear HM, Hashim PH, Flanagan CL, Day JR, Cascalho M, Padmanabhan V and Shikanov A (2022) Human Ovarian Follicles Xenografted in Immunoisolating Capsules Survive Long Term Implantation in Mice. Front. Endocrinol. 13:886678. doi: 10.3389/fendo.2022.886678

1 INTRODUCTION

Over 500,000 survivors of pediatric cancers live in the United States today (1). Due to advances in anticancer therapy, the 5-year survival rate for pediatric cancer patients reached nearly 85% in 2016, which is a significant increase from 50% in the 1970s (1, 2). This population will continue to grow as the incidence rate of pediatric cancers continues to increase, with an estimated 10,500 new diagnoses in 2021 for children aged 0-14 (1). Unfortunately, chemotherapy and radiation can have detrimental effects on male and female gonads, which may result in delayed or completely absent pubertal development (3). The delay or absence of pubertal development negatively impacts patient quality of life and carries long-term health risks associated with decreased bone strength and endocrinopathies (4). The standard of care for puberty induction in adolescent girls with premature ovarian insufficiency (POI) is hormone replacement therapy (HRT), which was developed to treat postmenopausal symptoms in mature women and does not recapitulate physiologic cyclic and pulsatile hormonal patterns found in healthy, reproductive aged women (5, 6). HRT delivers

constant doses of estrogen and progesterone, reconstituting ovarian function only partially (7), and precluding ovarian-body homeostasis. Furthermore, the long-term safety and efficacy of HRT to induce puberty has yet to be established (8).

To address the lack of available treatments to induce physiological puberty in adolescent girls with POI, we have developed an immunoisolating hydrogel-based capsule for implantation of donor ovarian tissue without the need for immunosuppression (9–11). Multiple biomaterials have been investigated for supporting follicle growth *in vitro* and *in vivo*, including alginate (12–14), alginate-matrigel (15), fibrin (12, 16), fibrin-alginate (12, 17, 18), and poly(ethylene glycol) (PEG) (19, 20). Here we utilize a system comprised of ovarian tissue surrounded by a degradable PEG hydrogel that promotes follicle growth and expansion. The degradable PEG hydrogel core is surrounded by a non-degradable PEG shell that prevents infiltration of immune cells while allowing diffusion of oxygen, nutrients, and hormones. Our previous studies with these PEG capsules and murine ovarian tissue grafts demonstrated that (1) follicles survive and undergo folliculogenesis for at least 60 days, (2) the capsule prevents immune cell infiltration, and (3) the estrus cycle is restored after encapsulated allogenic tissue is implanted in ovariectomized mice (10).

It remains unknown whether the immunoisolating capsule can support the survival of human ovarian tissue *in vivo*, a key step towards translating this technology to clinical use. Despite many similarities with murine physiology, human ovarian tissue carries some significant morphological differences. Human ovarian tissue is heterogenous with respect to stromal tissue structure, stromal cell and follicle distribution. The majority of primordial follicles are found in the cortex surrounded by a dense stromal tissue, while more mature follicles are found closer to the medulla. In contrast, murine ovarian tissue is more homogeneous, with densely packed follicles present throughout the entire ovary and surrounded by significantly looser stroma (21). Furthermore, follicle density varies between different donors, the right and left ovary from the same donor, and different locations in the cortex from the same ovary (22). Lastly, murine and human primordial follicles are approximately the same size (~30μm), but the terminal diameter of pre-ovulatory follicles in mice is only ~400μm, while human follicles reach a much larger terminal diameter ranging from 2,000 to 20,000μm (23). Keeping these differences in mind, the main objective of this study was to investigate whether follicles in human ovarian tissues survive the encapsulation process and maintain viability after implantation. We encapsulated human ovarian tissue from donors in a dual-layered PEG capsule and implanted these capsules subcutaneously into non-obese diabetic/severe combined immunodeficient gamma (NSG) mice and evaluated follicle survival in fresh and cryopreserved human ovarian tissue that was either encapsulated or non-encapsulated.

2 MATERIALS AND METHODS

2.1 Collection of Human Ovarian Tissue

Organ procurement for research purposes followed standardized protocols in place at the International Institute for the Advancement of Medicine (IIAM) and the associated Organ Procurement Organization (OPO) involved in the harvest. For this study ovaries were procured from four deceased donors (age range: 18-26 years) by the IIAM, see **Table 1** for additional donor information. Before cross-clamp, the organs were perfused with either Belzer University of Wisconsin® Cold Storage Solution (Bridge of Life, SC, USA), Custodiol® HTK (Histidine-Tryptophan-Ketoglutarate) Solution (Essential Pharmaceuticals, NC, USA), or SPS-1 Static Preservation Solution (Organ Recovery Systems, IL, USA). Organs were placed in perfusion solution and shipped on ice. De-identified donor information is summarized in **Table 1**, including age, weight, height, BMI, and cross-clamp time (time at which the organ is cut from blood/oxygen supply). Cold ischemic time (CIT) was calculated as the time interval between cross-clamp time of the donor (and subsequent cessation of arterial blood flow to the ovaries) in the operation room and start time of the tissue harvest subsequent to arrival at the laboratory.

TABLE 1 | Donor information.

Donor No.	1	2	3	4
Age (years)	26	18	18	23
Height (cm)	157	160	163	165
Weight (kg)	60.2	70.3	52.8	67.9
BMI	24.4	27.5	20.0	25.0
Ethnicity	Black or African American	Black or African American	White	White
Cause of Death	Anoxia	Anoxia	Head trauma	Head trauma
Storage Solution	UW	UW	HTK	UW
Right Ovary Size (cm)	4x2x1	3x1x0.5	4x3x1.2	4x2.5x1.7
Left Ovary Size (cm)	4x2x1	3x1.5x0.5	NA	3.5x2x1.2
Cardiac arrest/downtime	YES 30 minutes	NO	NO	YES 10 minutes
Cross-clamp Date and Time*	7/24/2019 16:27	10/14/2019 6:03	1/9/2019 17:22	12/19/2019 15:46
Cold Ischemic Time (hours)**	9.8	18.8	7.9	5.1

UW, University of Wisconsin Solution; HTK, Histidine-Tryptophan-Ketoglutarate Solution.
**Time at which the organ is cut from blood/oxygen supply.*
***Time between cross-clamp and the beginning of tissue processing.*

2.2 Ethical Approval Process

The IIAM procures tissue and organs for non-clinical research from Organ Procurement Organizations (OPOs), which comply with state Uniform Anatomical Gift Acts (UAGA) and are certified and regulated by the Centers for Medicare and Medicaid Services (CMS). These OPOs are members of the Organ Procurement and Transplantation Network (OPTN) and the United Network for Organ Sharing (UNOS) and operate under a set of standards established by the Association of Organ Procurement Organizations (AOPO) and UNOS. Informed, written consent from the deceased donor's family was obtained for the tissue used in this publication. A biomaterial transfer agreement is in place between IIAM and the authors that restricts the use of the tissue for pre-clinical research that does not involve the fertilization of gametes. The use of deceased donor ovarian tissue in this research is categorized as 'not regulated', per 45 CFR 46.102 and the 'Common Rule', as it does not involve human subjects and complies with the University of Michigan's IRB requirements as such.

2.3 Tissue processing

All tissue processing was done aseptically in a biosafety cabinet. After receiving donor tissue the ovaries were separated from other reproductive tissues (i.e. the uterus, fallopian tubes) (**Figures 1A, B**). The ovaries were decortified using a custom cutting guide (Reprolife Japan, Tokyo) to remove 1 mm thick cortex pieces that were approximately 10mmx10mm squares (**Figures 1C**, **2A**). The squares were then cut into approximately 1mm wide strips, 10mm in length and 1mm thick (**Figures 1D**, **2A**) using a McIlwain Tissue Chopper (The Mickle Laboratory Engineering Co. Ltd., Surrey, UK) and aseptically transferred into holding media (Quinn's Advantage Medium with HEPES (QAMH), 10% Quinn's Advantage Serum Protein Substitute (SPS), CooperSurgical, Måløv, Denmark). The tissue was divided into three groups: 1) Encapsulation of fresh tissue pieces followed by immediate implantation in mice; 2) Fixation using Bouin's fixative (Ricca Chemical, USA) or 4% paraformaldehyde (PFA) (AlfaAesar, USA), and stored overnight at 4°C; 3) Cryopreservation using either slow freezing or vitrification methods.

2.4 Cryopreservation

2.4.1 Slow Freezing:

The methods as described by Xu et al. were used for slow freezing (24). Briefly, strips of cortical tissue approximately 1mm x 10mm x 1mm were placed into cryovials (Nunc, Roskilde, Denmark) filled with pre-cooled cryoprotectant media (QAMH, 10% SPS, 0.75M

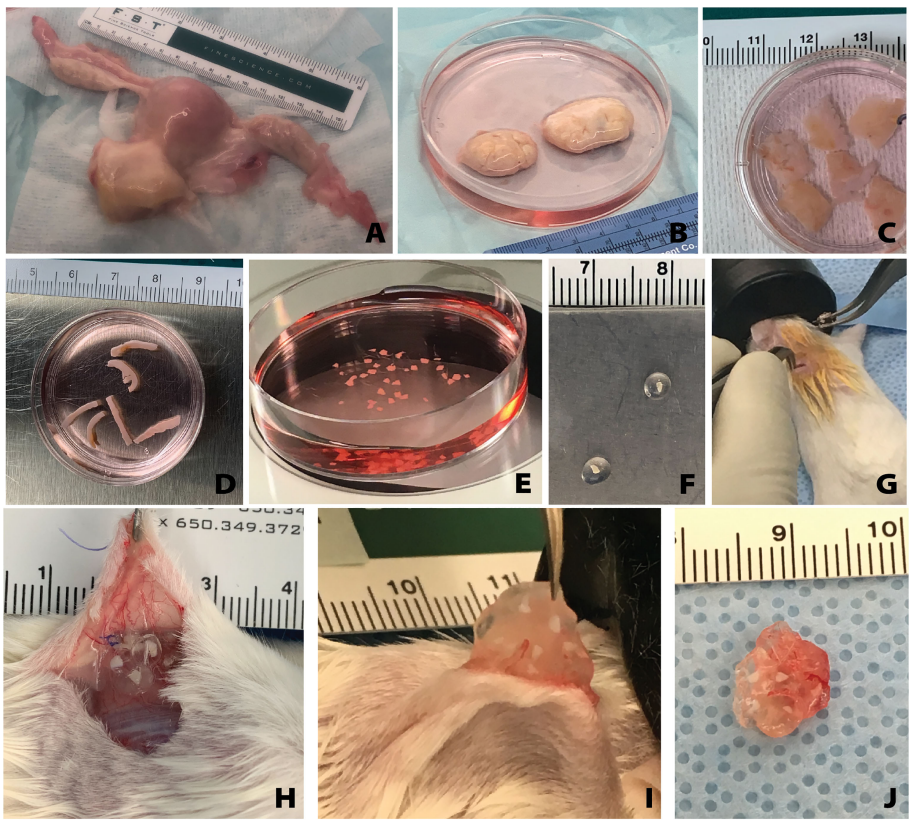

FIGURE 1 | Overview of human tissue processing and implantation. Tissue received from UNOS donors **(A)** was processed to isolate the ovaries **(B)**. Ovarian cortex tissue approximately 10mm x 10mm x 1mm is removed **(C)**, then cut to approximately 1mm x 10mm x 1mm **(D)**, and finally cut to approximately 1mm x 1mm x 1mm **(E)**. The small tissues are encapsulated in the hydrogel capsule **(F)** and implanted subcutaneously **(G)**. Removal of the capsules from the subcutaneous space **(H)** was conducted at various time points. The capsules were removed from the mice **(I, J)** and then fixed for histological processing and staining.

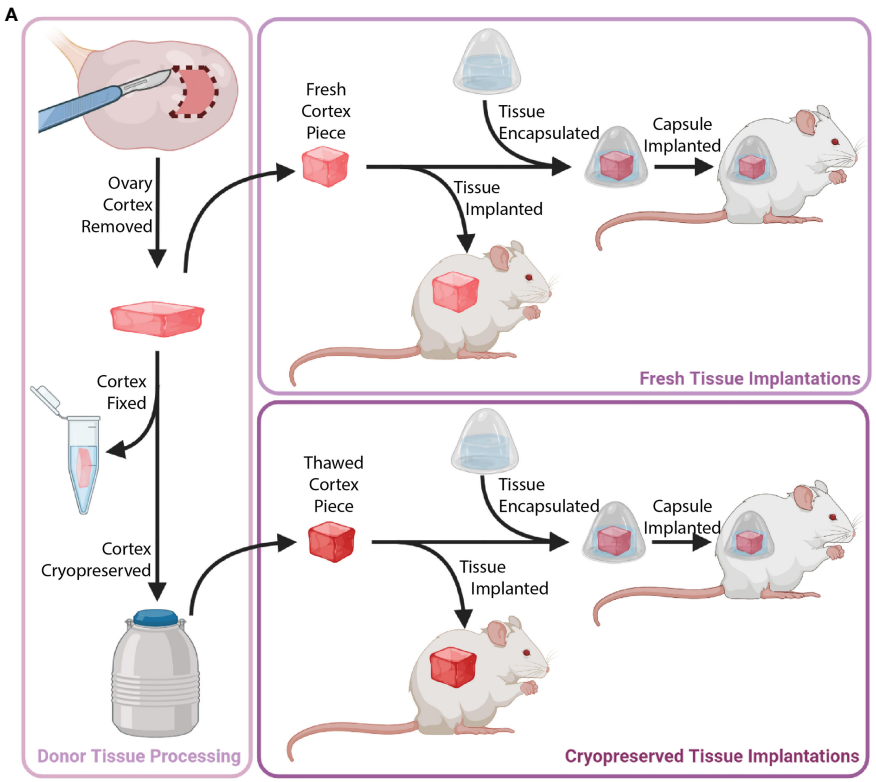

B

	3 days	1 week	2 weeks	1 month	2 month	3 months
# Capsules (donor)	50 (2,4)	50 (2,4)	30 (4)	70 (1,2,3,4)	20 (3)	20 (3)
# Strips (donor)	5 (2,4)	5 (2,4)	3 (4)	7 (1,2,3,4)	2 (3)	2 (3)

FIGURE 2 | Description of implanted tissue groups. Tissue processing was conducted as shown in part **(A)**. Cortical tissue strips were cut into squares either as fresh tissue (Donors 1 and 2) or post-cryopreservation (Donors 3 and 4). Capsules and control tissue were implanted in mice. The total number of capsules/strips at each time point are shown in part **(B)**.

dimethyl sulfoxide (DMSO) (Sigma Aldrich, St. Louis, USA), 0.75M ethylene glycol (Sigma Aldrich, St. Louis, USA), 0.1M sucrose (Sigma Aldrich, St. Louis, USA), and equilibrated at 4°C for at least 30 minutes. After equilibration, cryovials were loaded into the Cryologic Freeze Control System (Cryologic, Victoria, Australia). Vials were then frozen *via* the following protocol: samples were (1) cooled from 4°C to -9°C at a rate of -2°C/min (2) equilibrated for 6 min at -9°C (3) seeded manually using large swabs cooled by submersion in liquid nitrogen (4) held for 4 min at -9°C (5) cooled to -40°C at a rate of -0.3°C/min and (6) plunged into liquid nitrogen and stored in a cryogenic storage dewar until thawed for use.

2.4.2 Vitrification

The methods as described by Kagawa et al. were used for vitrification, with minor changes to the timing (25). Briefly, strips of tissue approximately 1mm x 10mm x 1mm were first transferred to an equilibration solution (7.5% ethylene glycol, 7.5% DMSO, and 20% SPS) for 25 minutes and then transferred to a vitrification solution (20% ethylene glycol, 20% DMSO, 0.5M sucrose, and 20% SPS) until the tissue sank to the bottom of the vial, indicating saturation with the solution. Each strip was placed on a 25 µm thick copper cryostrip (Lyon Industries, South Carolina, USA), which was then submerged in liquid nitrogen for approximately 30 seconds. Strips were transferred into a cryovial (Nunc, Roskilde, Denmark) filled with and submerged in liquid nitrogen. Samples were stored in liquid nitrogen until thawed for use.

2.5 Thawing Tissue

2.5.1 Slow Frozen Tissues:

The process described by Xu et al. was followed with minimal changes (24). Briefly, vials with ovarian tissue were removed from liquid nitrogen and placed in a 37°C bath. Once the cryoprotectant media in the vial had thawed, the tissue was removed from the vial and put into Thaw Solution One (1M DMSO, 0.1M Sucrose, 10% SPS in QAMH) for ten minutes. Tissue was then incubated sequentially in Thaw Solution Two

(0.5M DMSO, 0.1M Sucrose, 10% SPS in QAMH), Three (0.1M Sucrose, 10% SPS in QAMH), and Four (10% SPS in QAMH) for ten minutes each. All thaw solutions were maintained at room temperature during this process. Tissue strips were cut into cubes measuring approximately 1mm3 while still in Thaw Solution Four.

2.5.2 Vitrified Tissues

The process described by Lee et al. was followed, with minor modifications (26). The cryovials with ovarian cortex strips were removed from liquid nitrogen. The copper supports with tissue were immediately transferred into Thaw Solution One (1mg/mL Human Serum Albumin (HSA) (MilliporeSigma, MA, USA) and 1M sucrose in QAMH). Copper supports were removed, and the tissue was incubated at 37°C for three minutes. Tissue was transferred to Thaw Solution Two (1mg/mL HSA and 0.5M sucrose in QAMH) for 5 minutes at room temperature. Tissue was then transferred to Thaw Solution Three (1mg/mL HSA in QAMH), brought up to 37°C, and cut into cubes measuring approximately 1mm3.

2.6 Encapsulation

The pieces of ovarian cortical tissue (1mm^3) (**Figure 2A**) were maintained in the final thaw solution media (Solution 4 for slow freezing, Solution 3 for vitrification) at 37°C until encapsulation (**Figure 1E**). The PEG core was prepared by cross-linking 8-arm PEG-VS (40 kDa, Jenkem Technology, Beijing, China) (5% w/v) with plasmin sensitive peptide (Ac-GCYK↓NSGCYK↓NSCG, MW 1525.69 g/mol, > 90% Purity, Genscript, ↓ indicates the cleavage site of the peptide). The PEG shell was prepared with 4-arm PEG-VS (20 kDa, Jenkem Technology) (5% w/v), Irgacure 2959 (Ciba, Switzerland, MW = 224.3) (0.4% w/v), and N-vinyl-2-pyrrolidone (Sigma-Aldrich, St. Louis, USA) (0.1% v/v).

The tissue was then placed in a 4µL droplet of degradable PEG core pre-cursor solution. After five minutes of crosslinking the core was transferred into 10µL of non-degradable PEG shell pre-cursor solution. The shell was cross-linked *via* UV light at constant intensity (4.4mW/cm^2, 6 minutes). Encapsulated tissue (**Figures 1F**, **2A**) was maintained in Leibovitz L-15 media (Gibco, USA) at 37°C until implantation.

2.7 Subcutaneous Implantation

Animal experiments for this work were performed in accordance with the protocol approved by the Institutional Animal Care and Use Committee (IACUC) at the University of Michigan (PRO00007716 & PRO00009635). The IACUC guidelines for survival surgery in rodents and the IACUC Policy on Analgesic Use in Animals Undergoing Surgery were followed for all procedures.

Female NSG mice (strain 005557, The Jackson Laboratory, Bar Harbor, ME, USA) 6-8 weeks old were anesthetized using isoflurane (2-3%) *via* inhalation. Mice were given preemptive analgesics (Carprofen, RIMADYL, Zoetis, USA, 5mg/kg body) *via* subcutaneous injection. An incision was made in the medial/dorsal skin. Nine to ten PEG capsules, along with an equivalent amount of non-encapsulated tissue (as a control), were inserted into the dorsal subcutaneous space in the mouse (**Figures 1G**, **2B**). The control graft was inserted subcutaneously and sutured using 5/0 absorbable sutures (AD surgical) to the subcutaneous tissue to ensure graft recovery. Using 5/0 absorbable sutures the incision was closed, with special attention paid to avoid suturing capsules/control tissue. Mice recovered in a clean cage and were monitored post-operatively for 7-10 days.

2.8 Implant Removal

Mice were anesthetized using isoflurane as described above. An incision was made in the medial/dorsal skin, avoiding implanted grafts. The encapsulated and control grafts were removed (**Figures 1H–J**), placed in either Bouin's fixative or 4% PFA overnight at 4°C, washed, and stored in 70% ethanol or PBS, depending on respective fixative.

2.9 Histology

All samples were processed at the Histology Core in the Dental School at the University of Michigan. The paraffin embedded tissue blocks were serially sectioned at a thickness of 5µm and stained with hematoxylin and eosin.

2.10 Follicle Counting

Slides were viewed using a brightfield microscope (Leica DM 1000, Germany) at 20 or 40x magnification. Encapsulated tissue and control non-encapsulated grafts were analyzed for follicle density. Every 16th section was analyzed for follicles for all groups. For slow frozen encapsulated tissue groups between 6 and 17 sections were analyzed per mouse (n=3 mice per time point). For slow frozen non-encapsulated control tissue between 5 and 14 sections were analyzed per mouse (n=3 mice per time point). In the slow frozen groups, each data point represents the follicle density calculated from all capsules retrieved from each mouse. For vitrified encapsulated tissue groups between 4 and 10 sections were analyzed per mouse (n=2 mice per time point). For vitrified non-encapsulated control tissue between 5 and 8 sections were analyzed per mouse (n=2 mice per time point). In the vitrified groups, each data point represents the follicle density calculated from all capsules retrieved from each mouse. For fresh fixed tissue, between 8 and 12 sections were analyzed per donor where each data point represents the follicle density calculated from a single analyzed section. Follicles were counted manually and follicle stage was identified using standard morphological guidelines (27). All primordial and primary follicles were counted for each analyzed section. Preantral and antral were counted only after comparing the location of the follicle in the tissue and follicle size in preceding and subsequent sections to avoid "double-counting". Density measurements were calculated using an estimated area (1mm^2 per section) based on the approximate geometry of the sample, and the estimated tissue section thickness. The follicle density values reported in this study are all normalized to the same volume.

2.11 Statistical Analysis

Statistical analysis was performed using GraphPad Prism software. A 1-way ANOVA was used for fresh tissue analysis comparing follicle density between donors. Tukey's comparison test was used for implanted tissue analysis to a evaluate

differences in follicle density across two variables (time and encapsulation). The results were considered statistically significant when $p < 0.05$.

3 RESULTS

3.1 Fresh Donor Tissue Prior to Processing Reveals Donor Heterogeneity

First, we analyzed the follicle density in ovarian cortex from each donor to benchmark a starting point for the grafts. In this study we used ovarian tissue from 4 young healthy deceased donors, ranging from 18 to 26 years old. Inherently, human ovarian cortex varies greatly between donors and location in the ovary. As expected, all donor tissues displayed a high degree of heterogeneity between different strips and various locations in the same cortical strip from the same donor as well as across different donors. The average follicle density in ovarian tissue from Donor 1, 26 years old and BMI of 24.4, was 361 ± 304 follicles/mm^3 (average ± standard deviation). The average follicle density in the ovarian cortex of Donor 2, 18 years old and BMI 27.5, was 1528 ± 528 follicles/mm^3. Donor 3, 18 years old and BMI of 20, had an average follicle density of 4414 ± 521 follicles/mm^3. Donor 4, 25 years old and BMI of 24.9, had an average follicle density of 464 ± 152 follicles/mm^3 (**Figures 3A, B**). Donor 3 had the greatest follicle density, 4414 ± 521 follicles/mm^3 ($p<0.0001$) compared to the other three donors. The follicle density of Donor 2 was greater compared to the lower follicle densities of Donors 1 and 4 ($p <0.0001$). The follicle densities of Donors 1 and 4 were relatively similar and not significantly different. Histological images from each donor showed multiple primordial and primary follicles (**Figures 3C–N**). The cortical stroma had regions of densely packed primordial follicles with oocytes surrounded by a single layer of flat squamous granulosa cells (**Figure 3E iii.**, **Figure 3K i.**, **Figure 3N i.**). In addition to primordial follicles, primary and small preantral follicles were also identified in the ovarian tissue from all donors. Primary follicles showed the characteristic oocyte surrounded by a single layer of cuboidal granulosa cells (**Figure 3E i.**, **Figure 3H iv. Figure 3K ii.**), while preantral follicles had a few layers of granulosa cells surrounding the oocyte (**Figure 3H ii.**).

3.2 Follicles in Encapsulated Fresh Ovarian Cortical Tissues Survive for At Least One Month After Implantation in NSG Mice

Grafting of non-encapsulated human ovarian tissue is a gold standard for restoration of fertility in human patients and animal models ((28)). However, whether encapsulated human ovarian allograft survives encapsulation and implantation has yet to be demonstrated. Here, we investigated whether the encapsulation of fresh ovarian cortical tissue in a hydrogel decreases follicle survival and longevity after implantation in mice, and compared to non-encapsulated fresh tissue. Immediately after receiving and processing ovaries from Donors 1 and 2, we encapsulated and implanted ovarian cortical tissues in mice with nine to ten capsules per animal for time periods of 3 days (n=2 mice), 1 week (n=2), and 1 month (n=3) (**Figures 4D–F** respectively). A non-encapsulated cortical strip measuring 1mm x 10mm x 1mm was implanted in each mouse and served as a control (**Figures 4A–C**). Recovery of the capsules from the subcutaneous space was reasonably straightforward as the capsules typically clumped together (**Figure 1J**). Eight to ten capsules were recovered in six out of seven mice (no capsules were recovered from one animal, possibly due to degradation). Non-encapsulated control tissue was recovered in all seven mice. Eight to twenty-six sections for each implant type (encapsulated or non-encapsulated) were analyzed using bright field microscopy to assess follicle survival. Multiple follicles at different stages ranging from primordial to antral were present in retrieved encapsulated tissue from all time points up to a month post implantation within the same capsule (**Figure 4F**). Nuclear staining of the encapsulated tissue retrieved after 3 days and 1 week identified the presence of multiple stromal cells around the follicles. The encapsulated tissue had multiple surviving follicles after 1 month, however qualitative analysis showed a decrease in number of stromal cells. Overall, we concluded that follicle survival in human ovarian cortex was not decreased by the encapsulation process and was similar to the non-encapsulated controls.

3.3 Slow Frozen, Short-Term Implanted Tissues Tolerate Encapsulation and Survive to the Same Extent as Non-Encapsulated Tissue Following Implantation

The next objective was to determine whether encapsulation of cryopreserved ovarian tissue using the slow freezing approach, similar to the current clinical practice recommended for fertility preservation in pediatric patients, negatively affected follicle survival. Ovarian cortical strips from Donor 4 that had previously been slow frozen, were thawed and encapsulated. Multiple capsules and all non-encapsulated tissues were recovered in all 20 mice. There was no statistically significant difference in follicle density between encapsulated and non-encapsulated grafts at any time point (**Figure 5A**). For the 1-day time point, the follicle density was 24 ± 21 follicles/mm^3 (average ± standard deviation) in the non-encapsulated graft and 90 ± 60 in the encapsulated tissue. For the 3-days' time point, the average follicle density was 30 ± 21 and 73 ± 35, for the 1-week time point, the average follicle density was 28 ± 23 and 80 ± 43, for the 2-weeks' time point, the average follicle density was 25 ± 18 and 89 ± 51 for the 1-month time point, the average follicle density was 39 ± 22 and 81 ± 109, respectively. The difference in follicle density was not statistically significant between different time points, nor was it different when comparing between encapsulated and non-encapsulated groups at each time point. These findings suggest that after slow freezing (1) human ovarian follicles tolerate encapsulation in the dual-layered PEG hydrogel capsule and (2) encapsulated human ovarian tissue survives to the same extent as non-encapsulated tissues when implanted in mice.

A

Donor No.	Age (years)	BMI (kg/m2)
1	26	24
2	18	27
3	18	20
4	23	25

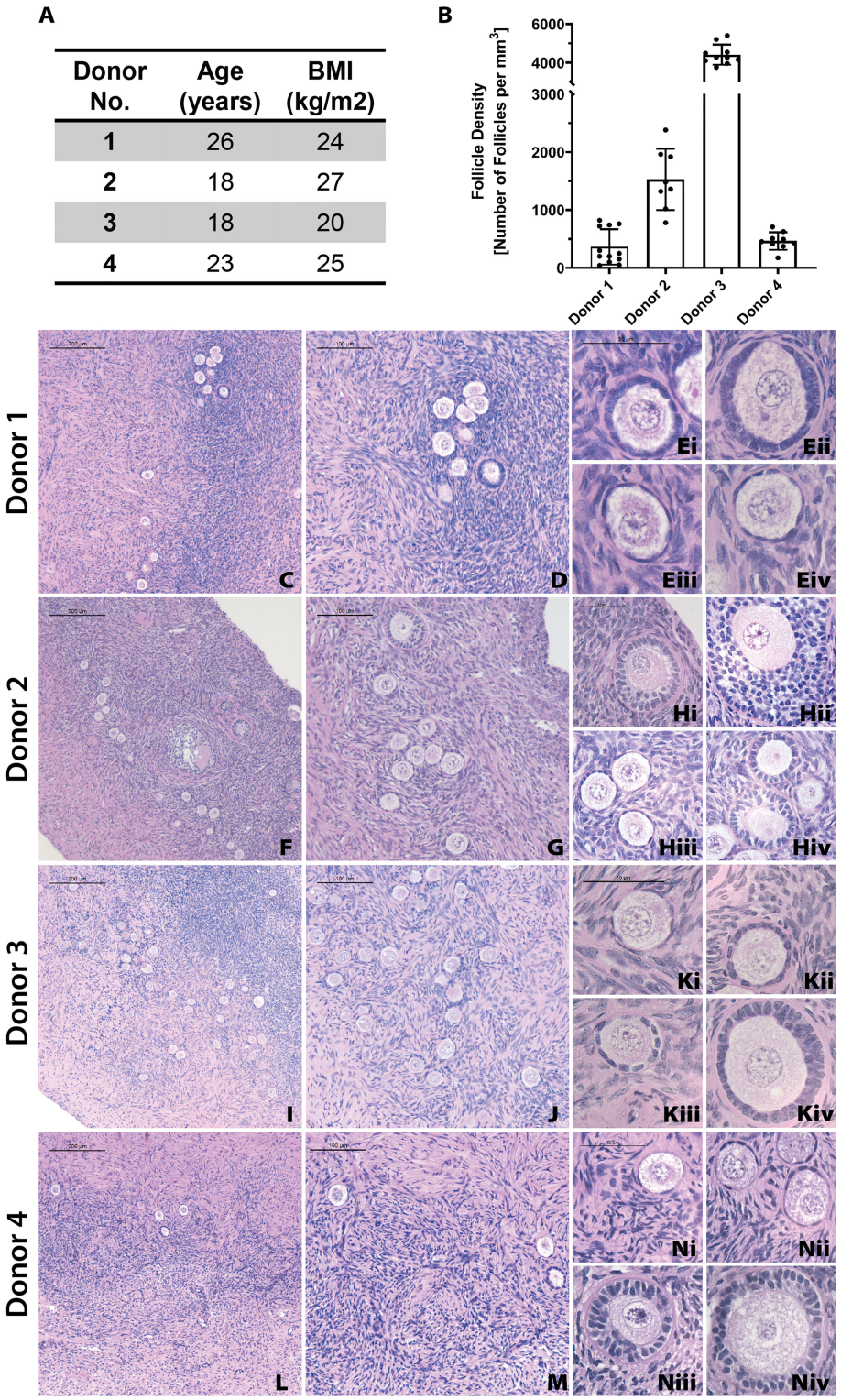

FIGURE 3 | Donor metrics and initial histology. The donor tissues used in this study were selected from a bank from donors with various ages and BMI values **(A)**. Follicle density values were calculated for each donor from fresh/fixed tissues **(B)**. The large differences in average follicle density between donors is supported by histological images **(C–N)**. Representative images from Donor 1 **(C–E)**, Donor 2 **(F–H)**, Donor 3 **(I–K)**, and Donor 4 **(L–N)** show stark differences in follicle distribution at low magnification **(C, F, I, L)**. Increased magnification shows the presence of primordial **(E iii., K i., N i)**, primary **(E i., H iv., K ii.)**, and secondary **(H ii.)** follicles. Scale bars represent 200μm for **C**, **F**, **I**, and **L**. Scale bars represent 100 μm for **D**, **G**, **J**, and **M**. Scale bars represent 50μm for all others.

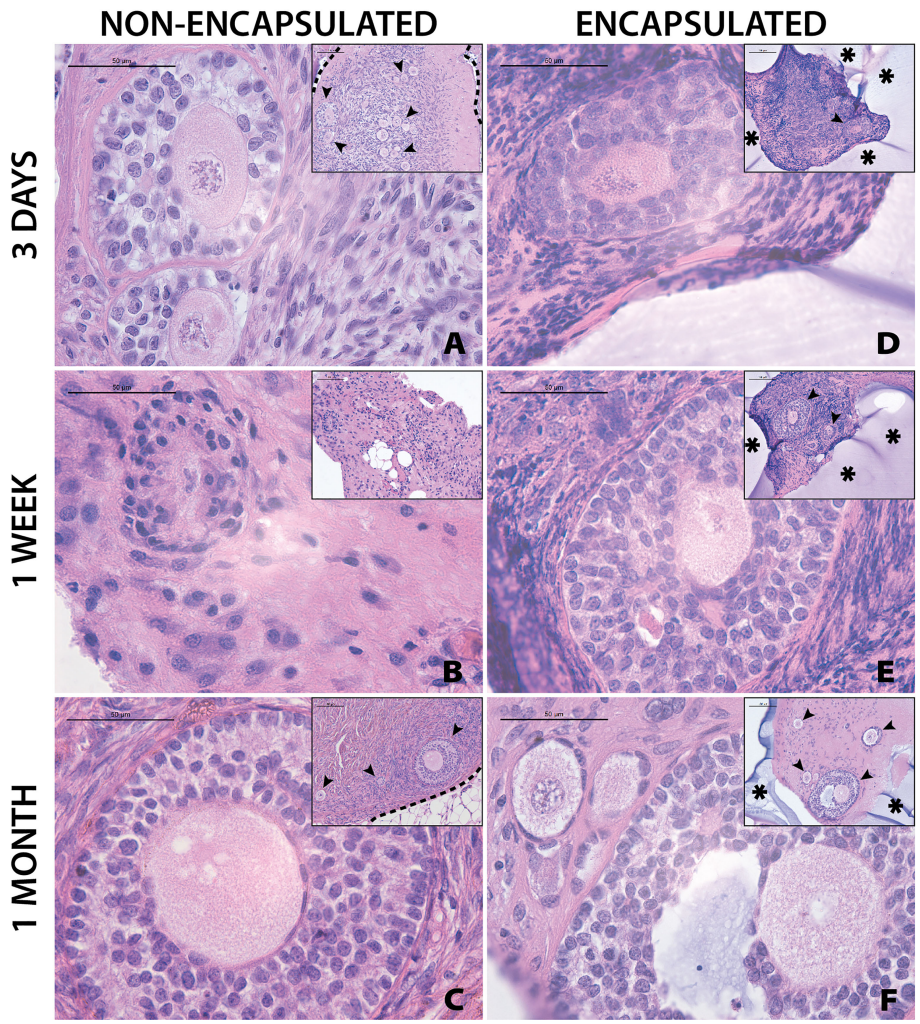

FIGURE 4 | Follicles in fresh tissue survive up to one month. Representative images from non-encapsulated fresh tissue samples **(A–C)** and encapsulated fresh tissue samples **(D–F)** are shown here. These samples were removed from mice at various time points of 3 days **(A, D)**, 1 week **(B, E)**, and 1 month **(C, F)**. Scale bars represent 100μm for inserts and 50μm for all others. Black arrow heads (➤) indicate follicles, asterisks (⁎) indicate the PEG capsule, and dashed black lines (—) indicate the human ovarian tissue border with surrounding murine tissue after implantation.

Although follicle numbers were not significantly different between groups, we also wanted to probe whether there were any differences between groups in terms of the quality of the stromal compartment. Qualitative histological analysis of tissue fixed immediately post-thawing (**Figure 5B**) and tissue fixed after implantation showed similar distribution of stromal cells (marked with hematoxylin). Furthermore, similar stromal cell densities were evident across time points, as well as between encapsulated (**Figures 5H–L**) and non-encapsulated groups (**Figures 5C–G**) at the same time points, except for the 1-month encapsulated tissue (**Figure 5L**). The 1-month encapsulated tissue had less cellular staining around the follicles and more fibrous portions of the extracellular matrix (stained pink with eosin). Furthermore, the types of follicles seen in encapsulated and non-encapsulate groups at various time points were comparable, with primordial and primary follicles being the most prevalent. Taken together, these observations support the hypothesis that follicles can survive slow freezing before encapsulation and survive up to one month *in vivo*.

3.4 Vitrified, Long-Term Implanted Tissues Tolerate Encapsulation and Survive Up to Three Months *In Vivo*

The final objective of this study was to investigate whether the two clinically available cryopreservation methods, slow freezing and vitrification specifically, have different outcomes of follicle survival in grafted tissue following encapsulation and implantation. Vitrified tissue from Donor 3 was encapsulated and implanted in mice for 2 and 3 months. Non-encapsulated, $1mm^3$ grafts served as controls. Two months after implantation the average follicle density was 17 follicles/mm^3 in the non-encapsulated grafts and 2 follicles/mm^3 in the encapsulated

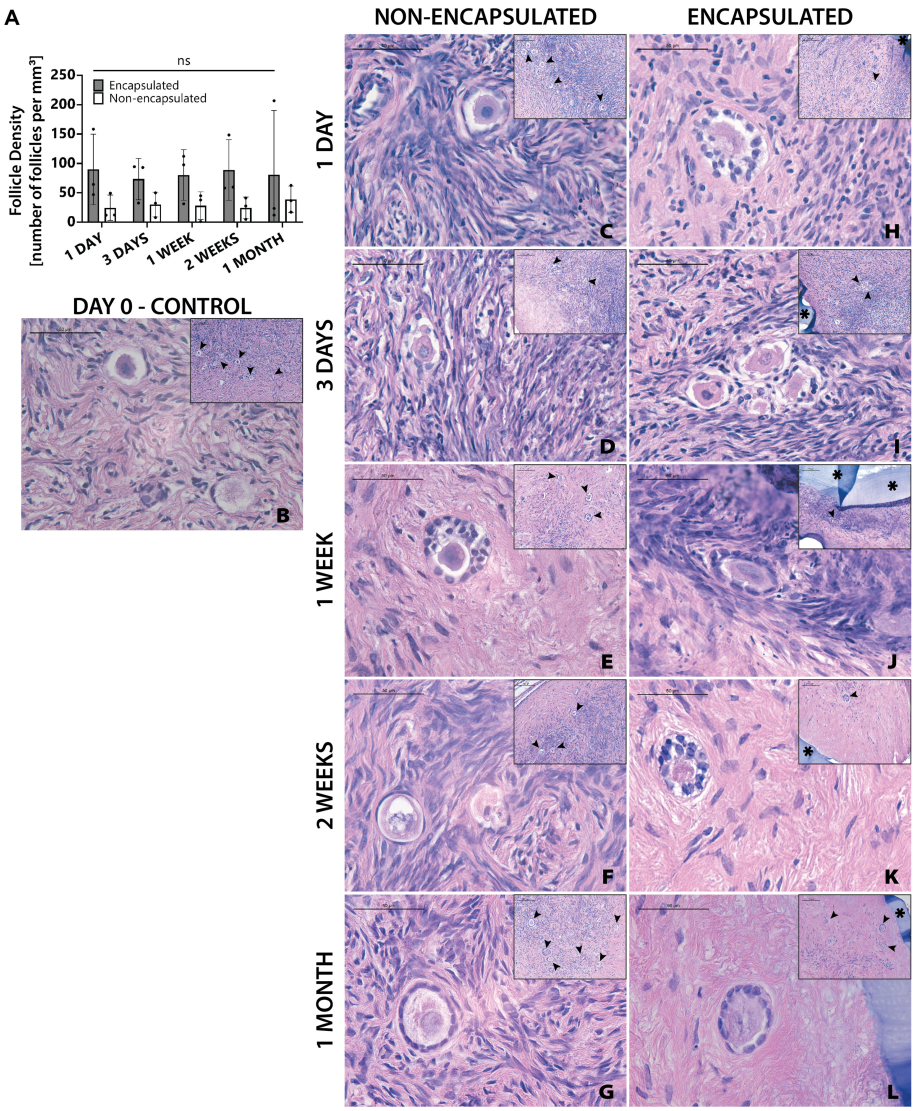

FIGURE 5 | Follicles in slow frozen tissue survive up to one month. Follicle density values **(A)** are determined from histological images **(C–L)**. Non-implanted thawed/fixed tissue **(B)** is a control for non-encapsulated groups **(C–G)** and encapsulated groups **(F–L)**. These samples were removed from mice at various time points of 1 day **(C, H)**, 3 days **(D, I)**, 1 week **(E, J)**, 2 weeks **(F, K)**, and 1 month **(G, L)**. Scale bars represent 100μm for inserts and 50μm for all others. Black arrow heads (➢) indicate follicles, asterisks (•) indicate the PEG capsule, and dashed black lines (—) indicate the human ovarian tissue border with surrounding murine tissue after implantation.

tissue. For the 3-month time point, the average follicle density was 57 follicles/mm^3 in the non-encapsulated graft and 22 follicles/mm^3 in the encapsulated tissue (**Figure 6A**). Vitrified tissue had greater cell density in the stroma (**Figure 6B**) than frozen tissue before implantation (**Figure 5B**). Encouragingly, follicles in implanted tissues survived up to three months post-implantation, but the surrounding stroma had lower cell density compared to tissue prior to implantation (**Figures 6C–F**); the decrease in stroma cell density was observed in all implanted groups, similarly to the one-month time point for encapsulated slow frozen tissue (**Figure 5L**) In comparison to other slow frozen tissue, vitrified groups similarly have a follicle pool comprised predominantly of primordial and primary follicles. Based on our findings, we concluded that follicles and ovarian stromal cells tolerate vitrification before encapsulation, and survive up to three months *in vivo*.

4 DISCUSSION

Previously, using PEG-based immunoisolating capsules we have demonstrated that the capsule protected murine ovarian allografts in immune competent and sensitized murine hosts and promoted folliculogenesis up to antral stages after single and

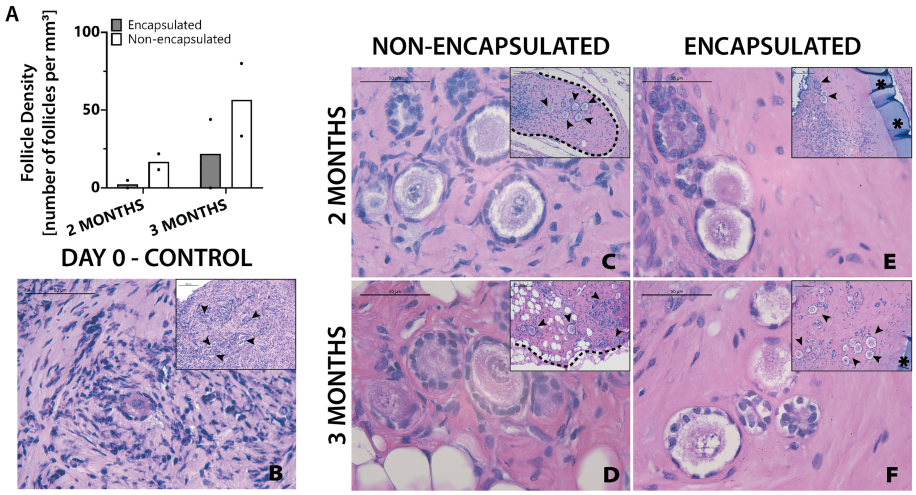

FIGURE 6 | Follicles in vitrified tissue survive up to three months. Follicle density values **(A)** are determined from histological images **(C–F)**. Non-implanted thawed/fixed tissue **(B)** is a control for non-encapsulated groups **(C, D)** and encapsulated groups **(E, F)**. These samples were removed from mice at various time points of 2 months **(C, E)** and 3 months **(D, F)**. Scale bars represent 100μm for inserts and 50μm for all others. Black arrow heads (➤) indicate follicles, asterisks (•) indicate the PEG capsule, and dashed black lines (—) indicate the human ovarian tissue border with surrounding murine tissue after implantation.

repeated implantations (10). Despite mice and humans having similar hypothalamus-pituitary-gonad axis regulation, circulating cytokines and hormones, and developmental stages of follicular differentiation, existence of other physiological and anatomical differences between human and murine ovarian tissues necessitates further investigation to determine translatability of the use of immunoisolating capsules from mouse to human tissues. One example of the challenges working with human tissue is that human primordial follicles are spread heterogeneously in the stroma of ovarian cortex and require normalization of the follicle counts in each graft. The heterogeneity of human tissue introduced significant variance into our quantification of follicle density. To control for this, encapsulated tissues and corresponding non-encapsulated tissue originating from the same donor were included within same groups to minimize the impact of inherent heterogeneity between donors. Tissue pieces placed in the encapsulated groups and non-encapsulated groups were randomized to minimize skewing of results due to heterogeneity present in a single ovary. Even with these adaptations it is uncertain if differences seen are an artifact of tissue heterogeneity or are a result of tissue treatment; persistence of a large variability resulting in largely qualitative methods of analysis. One option to minimize the effect of heterogeneity on follicle density analysis is to significantly increase the number of human donors and recipient mice. Another option is to use cryopreserved tissues that would have undergone a thorough characterization prior to xenografting, allowing for donors with similar follicle densities to be used in the same study.

Ovarian tissue cryopreservation (OTC) enables preservation of many thousands of primordial follicles all at once without the need of ovarian stimulation and can be performed at any age from early prepubertal years to late thirties. Slow freezing and vitrification of ovarian tissues are the two most studied methods of cryopreservation. The majority of clinical data, such as the rates of live births (29–31), the efficiency and safety of OTC in terms of follicle survival and patients' outcomes after transplantation, is available for slow freezing methods, which was considered experimental for a few decades and was recently clinically approved (32). Slow freezing in general uses a low amount of cryoprotective agents to reduce cell toxicity. This method utilizes standardized equipment and detailed cooling protocols such that there is decreased variability between operators, as well as between batches. On the downside, slow freezing poses the risk of intracellular ice crystal formation, which can be minimized by manual seeding at the media/air interface (33, 34). Vitrification, another cryopreservation method, is currently only approved for embryo and egg cryopreservation (35). It utilizes greater concentrations of cryoprotectants that prevent ice crystal formation. Vitrification does not require standardized equipment, which results in some variability between operators and batches. So far, this method has been clinically approved for oocyte and embryo cryopreservation but is still considered experimental for OTC. Possibly, in the future, it may become clinically approved for OTC as well.

Both cryopreservation methods have been shown to have negligible impact on follicle count as compared to fresh tissue (36) and ensure the survival of primordial follicles, which are critical for the application described in this study; dormant primordial follicles in the implanted encapsulated tissue functions as the ovarian reserve, determining the quality and the lifespan of the encapsulated tissue. Additionally, OTC allows important screening for disease or infection and analysis of the follicle density in the donor tissue that would not be possible with fresh tissue. While some reports show that vitrification results in

(1) decreased primordial follicle DNA damage and (2) better outcomes for stromal tissue (37), others indicate that slow freezing is superior for (1) preserving primordial follicles, (2) preventing DNA damage, and (3) promoting follicular cell proliferation (26). Comparison of the survival of slow frozen and vitrified tissues with fresh tissues used as controls showed fresh tissues to have more mature (i.e. secondary/antral) follicles, as expected. More mature follicles contain oocytes that are more metabolically active and antral follicles contain the cumulus-oocyte complex, resulting in decreased cryoprotectant agent penetration and therefore increased probability of ice crystal formation (38). Our observation that the stroma in slow frozen tissues (**Figure 5**) is less fibrous as compared to vitrified tissues (**Figure 6**) is somewhat unexpected since the literature indicates that vitrification typically has better stromal cell survival (37). The most likely explanation for these differing results is that there was more variability between operators during the vitrification process. Notably, an important finding from the present study is that follicles can survive the process of cryopreservation and survive for at least 30 days *in vivo*, regardless of cryopreservation method.

Encapsulation may slow down the diffusion of nutrients, yet it is necessary to prevent rejection of the grafts. Our comparison of tissues that underwent the encapsulation process to tissues that did not, found that the follicle densities of non-encapsulated tissues were not higher than the follicle densities in encapsulated tissues. Qualitative examination of the implants also indicates minimal differences between encapsulated and non-encapsulated tissues at early time points, but larger differences begin to appear starting around one month. The main change observed is a decrease in stromal cell density in encapsulated tissues. This trend is emphasized by greater areas of fibrous stromal extracellular matrix, the mostly eosin-stained matrix without visible nuclei. The relative similarities between short term implants and subsequent differences in long term implants indicate that the process of encapsulation is not harmful to human tissues. It is hypothesized that as time goes on the rate of diffusion of nutrients is inadequate to support these tissues.

In conclusion, we have shown that an immunoisolating dual PEG capsule supported follicle survival in human ovarian xenografts up to 90 days *in vivo*. The process of encapsulation did not decrease follicle density compared with non-encapsulated grafts. Cryopreservation of ovarian cortical strips allowed for thorough analysis of follicular density to ensure graft longevity. Moving forward towards clinical translation of this technology, a greater scale of characterization of the donor tissue and optimization of the PEG shell to increase diffusion and increase stromal cell survival at later time points, should be done.

DATA AVAILABILITY STATEMENT

The raw data supporting the conclusions of this article will be made available by the authors, without undue reservation.

ETHICS STATEMENT

The animal study was reviewed and approved by Institutional Animal Care and Use Committee at the University of Michigan.

AUTHOR CONTRIBUTIONS

Study design: MB, AS. Murine experiments: MB, HK, JD. Histological sample preparation: MB, PH. Follicle counting and figure compilation: MB. Wrote original manuscript draft: MB, CF, VP, AS. Manuscript review & editing: MB, HK, PH, CF, JD, MC, VP, AS. All authors contributed to the article and approved the submitted version.

FUNDING

National Institutes of Health grant R01HD104173, R01EB022033 (MB, CF, JD, MC, AS). National Institutes of Health grant T32DE007057 (MB). National Institutes of Health grant R01HD09823 (HK, PH, AS). National Institutes of Health grant F30HD100163 (HK). Chan Zuckerberg Initiative (CF, MC, VP, AS).

ACKNOWLEDGMENTS

The authors would like to thank Dr. Evan Farkash and Jenna Barnes for their help in histological sample preparation and analysis. Figures were created with BioRender.

REFERENCES

1. Jones RM, Pattwell SS. Future Considerations for Pediatric Cancer Survivorship: Translational Perspectives From Developmental Neuroscience. *Dev Cognit Neurosci* (2019) 38:100657. doi: 10.1016/j.dcn.2019.100657
2. Siegel RL, Miller KD, Fuchs HE, Jemal A. Cancer Statistics, 2021. *CA Cancer J Clin* (2021) 71:7–33. doi: 10.3322/caac.21654
3. Akasha AM, Woodruff TK. *Oncofertility: Preservation of Ovarian Function After a Cancer Diagnosis. 3rd ed*. PCK Leung and EY Adashi, editors. London: Elsevier Inc (2019) p. 501–8. doi: 10.1016/B978-0-12-813209-8.00031-5
4. International Programme on Chemical Safety. "Endocrinology and Endocrine Toxicology". In: T Damstra, S Barlow, A Bergman, R Kavlock and G van der Kraak, editors. *Global Assessment of the State-Of-the-Science of Endocrine Disruptors*. Geneva: World Health Organization (2002). p. 11–32.
5. Pierson RA. "Human Folliculogenesis Revisited: The Menstrual Cycle Visualized by Ultrasonography". In: PCK Leung and EY Adashi, editors. *The Ovary*. London: Elsevier Inc (2019). p. 51–69. doi: 10.1016/b978-0-12-813209-8.00003-0
6. McCartney CR, Marshall JC. "Neuroendocrinology of Reproduction". In: *Yen & Jaffe's Reproductive Endocrinology: Physiology, Pathophysiology, and Clinical Management*. Philadelphia: Elsevier Inc (2019). p. 1–24.e8. doi: 10.1016/B978-0-323-47912-7.00001-9
7. Langer RD. The Evidence Base for HRT: What can We Believe? *Climacteric* (2017) 20:91–6. doi: 10.1080/13697137.2017.1280251

8. Christin-Maitre S. Use of Hormone Replacement in Females With Endocrine Disorders. *Horm Res Paediatr* (2017) 87:215–23. doi: 10.1159/000457125
9. Day JR, David A, Cichon AL, Kulkarni T, Cascalho M, Shikanov A. Immunoisolating Poly(Ethylene Glycol) Based Capsules Support Ovarian Tissue Survival to Restore Endocrine Function. *J BioMed Mater Res Part A* (2018) 106:1381–9. doi: 10.1002/jbm.a.36338
10. Day JR, David A, Barbosa MG de M, Brunette MA, Cascalho M, Shikanov A. Encapsulation of Ovarian Allograft Precludes Immune Rejection and Promotes Restoration of Endocrine Function in Immune-Competent Ovariectomized Mice. *Sci Rep* (2019) 9:16614. doi: 10.1038/s41598-019-53075-8
11. Day JR, David A, Kim J, Farkash EA, Cascalho M, Milašinović N, et al. The Impact of Functional Groups of Poly(Ethylene Glycol) Macromers on the Physical Properties of Photo-Polymerized Hydrogels and the Local Inflammatory Response in the Host. *Acta Biomater* (2018) 67:42–52. doi: 10.1016/j.actbio.2017.12.007
12. Xu J, Lawson MS, Yeoman RR, Molskness TA, Ting AY, Stouffer RL, et al. Fibrin Promotes Development and Function of Macaque Primary Follicles During Encapsulated Three-Dimensional Culture. *Hum Reprod* (2013) 28:2187–200. doi: 10.1093/humrep/det093
13. Pangas SA, Saudye H, Shea LD, Woodruff TK. Novel Approach for the Three-Dimensional Culture of Granulosa Cell-Oocyte Complexes. *Tissue Eng* (2003) 9:1013–21. doi: 10.1089/107632703322495655
14. Rios PD, Kniazeva E, Lee HC, Xiao S, Oakes RS, Saito E, et al. Retrievable Hydrogels for Ovarian Follicle Transplantation and Oocyte Collection. *Biotechnol Bioeng* (2018) 115:2075–86. doi: 10.1002/bit.26721
15. Vanacker J, Luyckx V, Dolmans MM, Des Rieux A, Jaeger J, Van Langendonckt A, et al. Transplantation of an Alginate-Matrigel Matrix Containing Isolated Ovarian Cells: First Step in Developing a Biodegradable Scaffold to Transplant Isolated Preantral Follicles and Ovarian Cells. *Biomaterials* (2012) 33:6079–85. doi: 10.1016/j.biomaterials.2012.05.015
16. Shikanov A, Zhang Z, Xu M, Smith RM, Rajan A, Woodruff TK, et al. Fibrin Encapsulation and Vascular Endothelial Growth Factor Delivery Promotes Ovarian Graft Survival in Mice. *Tissue Eng - Part A* (2011) 17:3095–104. doi: 10.1089/ten.tea.2011.0204
17. Kniazeva E, Hardy AN, Boukaidi SA, Woodruff TK, Jeruss JS, Shea LD. Primordial Follicle Transplantation Within Designer Biomaterial Grafts Produce Live Births in a Mouse Infertility Model. *Sci Rep* (2015) 5:1–11. doi: 10.1038/srep17709
18. Shikanov A, Xu M, Woodruff TK, Shea LD. Interpenetrating Fibrin-Alginate Matrices for *In Vitro* Ovarian Follicle Development. *Biomaterials* (2009) 30:5476–85. doi: 10.1016/j.biomaterials.2009.06.054
19. Shikanov A, Smith RM, Xu M, Woodruff TK, Shea LD. Hydrogel Network Design Using Multifunctional Macromers to Coordinate Tissue Maturation in Ovarian Follicle Culture. *Biomaterials* (2011) 32:2524–31. doi: 10.1016/j.biomaterials.2010.12.027
20. Tomaszewski CE, Constance E, Lemke MM, Zhou H, Padmanabhan V, Arnold KB, et al. Adipose-Derived Stem Cell-Secreted Factors Promote Early Stage Follicle Development in a Biomimetic Matrix. *Biomater Sci* (2019) 7:571–80. doi: 10.1039/c8bm01253a
21. Myers M, Britt KL, Wreford NGM, Ebling FJP, Kerr JB. Methods for Quantifying Follicular Numbers Within the Mouse Ovary. *Reproduction* (2004) 127:569–80. doi: 10.1530/rep.1.00095
22. Schmidt KLT, Byskov AG, Andersen AN, Müller J, Andersen CY. Density and Distribution of Primordial Follicles in Single Pieces of Cortex From 21 Patients and in Individual Pieces of Cortex From Three Entire Human Ovaries. *Hum Reprod* (2003) 18:1158–64. doi: 10.1093/humrep/deg246
23. Griffin J, Emery BR, Huang I, Peterson CM, Carrell DT. Comparative Analysis of Follicle Morphology and Oocyte Diameter in Four Mammalian Species (Mouse, Hamster, Pig, and Human). *J Exp Clin Assist Reprod* (2006) 3:2. doi: 10.1186/1743-1050-3-2
24. Xu M, Banc A, Woodruff TK, Shea LD. Secondary Follicle Growth and Oocyte Maturation by Culture in Alginate Hydrogel Following Cryopreservation of the Ovary or Individual Follicles. *Biotechnol Bioeng* (2009) 103:378–86. doi: 10.1002/bit.22250
25. Kagawa N, Kuwayama M, Nakata K, Vajta G, Silber S, Manabe N, et al. Production of the First Offspring From Oocytes Derived From Fresh and Cryopreserved Pre-Antral Follicles of Adult Mice. *Reprod BioMed Online* (2007) 14:693–9. doi: 10.1016/S1472-6483(10)60670-0
26. Lee S, Ryu K, Kim B, Kang D, Kim YY, Kim T. Comparison Between Slow Freezing and Vitrification for Human Ovarian Tissue Cryopreservation and Xenotransplantation. *Int J Mol Sci* (2019) 20:3346. doi: 10.3390/ijms20133346
27. Gougeon A. Dynamics of Follicular Growth in the Human: A Model From Preliminary Results. *Hum Reprod* (1986) 1:81–7. doi: 10.1093/oxfordjournals.humrep.a136365
28. Duncan FE, Zelinski M, Gunn AH, Pahnke JE, O'Neill CL, Songsasen N, et al. Ovarian Tissue Transport to Expand Access to Fertility Preservation: From Animals to Clinical Practice. *Reproduction* (2016) 152:R201–10. doi: 10.1530/REP-15-0598
29. Donnez J, Dolmans M-M. Transplantation of Ovarian Tissue. *Best Pract Res Clin Obstet Gynaecol* (2014) 28:1188–97. doi: 10.1016/j.bpobgyn.2014.09.003
30. Stoop D, Cobo A, Silber S. Fertility Preservation for Age-Related Fertility Decline. *Lancet* (2014) 384:1311–9. doi: 10.1016/s0140-6736(14)61261-7
31. Gellert SE, Pors SE, Kristensen SG, Bay-Bjørn AM, Ernst E, Yding Andersen C. Transplantation of Frozen-Thawed Ovarian Tissue: An Update on Worldwide Activity Published in Peer-Reviewed Papers and on the Danish Cohort. *J Assist Reprod Genet* (2018) 35:561–70. doi: 10.1007/s10815-018-1144-2
32. Nahata L, Woodruff TK, Quinn GP, Meacham LR, Chen D, Appiah LC, et al. Ovarian Tissue Cryopreservation as Standard of Care: What Does This Mean for Pediatric Populations? *J Assist Reprod Genet* (2020) 37:1323–6. doi: 10.1007/s10815-020-01794-7
33. Huang H, Zhao G, Zhang Y, Xu J, Toth TL, He X. Predehydration and Ice Seeding in the Presence of Trehalose Enable Cell Cryopreservation. *ACS Biomater Sci Eng* (2017) 3:1758–68. doi: 10.1021/acsbiomaterials.7b00201
34. Isachenko V, Isachenko E, Reinsberg J, Montag M, Braun F, van der Ven H. Cryopreservation of Human Ovarian Tissue: Effect of Spontaneous and Initiated Ice Formation. *Reprod BioMed Online* (2008) 16:336–45. doi: 10.1016/S1472-6483(10)60593-7
35. The Practice Committees of the American Society for Reproductive Medicine and the Society for Assisted Reproductive Technology. Mature Oocyte Cryopreservation: A Guideline. *Fertil Steril* (2013) 99:37–43. doi: 10.1016/j.fertnstert.2012.09.028
36. Fan Y, Flanagan CL, Brunette MA, Jones AS, Baker BM, Silber SJ, et al. Fresh and Cryopreserved Ovarian Tissue From Deceased Young Donors Yields Viable Follicles. *F&S Sci* (2021) 2:248–58. doi: 10.1016/j.xfss.2021.06.003
37. Shi Q, Xie Y, Wang Y, Li S. Vitrification Versus Slow Freezing for Human Ovarian Tissue Cryopreservation: A Systematic Review and Meta-Anlaysis. *Sci Rep* (2017) 7:1–9. doi: 10.1038/s41598-017-09005-7
38. Leonel ECR M, Lucci C, A. Amorim C. "Cryopreservation of Preantral Follicles". In: *Cryopreservation Biotechnology in Biomedical and Biological Sciences*. London: IntechOpen (2018). p. 71–89. doi: 10.5772/intechopen.79538

Conflict of Interest: The authors declare that the research was conducted in the absence of any commercial or financial relationships that could be construed as a potential conflict of interest.

The handling editor YF declared a past collaboration with the author AS.

frontiers | Frontiers in Endocrinology

SYSTEMATIC REVIEW
published: 10 June 2022
doi: 10.3389/fendo.2022.918899

A Systematic Review of Ovarian Tissue Transplantation Outcomes by Ovarian Tissue Processing Size for Cryopreservation

Ashley A. Diaz[1,2], *Hana Kubo*[1,2], *Nicole Handa*[1,2], *Maria Hanna*[1,2] *and Monica M. Laronda*[1,2]*

[1] Stanley Manne Children's Research Institute, Ann & Robert H. Lurie Children's Hospital of Chicago, Chicago, IL, United States, [2] Feinberg School of Medicine, Northwestern University, Chicago, IL, United States

OPEN ACCESS

Edited by:
Yuting Fan,
Boston IVF, United States

Reviewed by:
Mary B. Zelinski,
Oregon Health & Science University, United States
Matthias W Beckmann,
University Hospital Erlangen, Germany
Giuliano Marchetti Bedoschi,
University of São Paulo, Brazil
Xiangyan Ruan,
Capital Medical University, China
Nalini Mahajan,
Independent researcher, New Delhi, India

***Correspondence:**
Monica M. Laronda
mlaronda@luriechildrens.org

Specialty section:
This article was submitted to Reproduction, a section of the journal Frontiers in Endocrinology

Received: 12 April 2022
Accepted: 10 May 2022
Published: 10 June 2022

Citation:
Diaz AA, Kubo H, Handa N, Hanna M and Laronda MM (2022) A Systematic Review of Ovarian Tissue Transplantation Outcomes by Ovarian Tissue Processing Size for Cryopreservation. Front. Endocrinol. 13:918899. doi: 10.3389/fendo.2022.918899

Ovarian tissue cryopreservation (OTC) is the only pre-treatment option currently available to preserve fertility for prepubescent girls and patients who cannot undergo ovarian stimulation. Currently, there is no standardized method of processing ovarian tissue for cryopreservation, despite evidence that fragmentation of ovaries may trigger primordial follicle activation. Because fragmentation may influence ovarian transplant function, the purpose of this systematic review was (1) to identify the processing sizes and dimensions of ovarian tissue within sites around the world, and (2) to examine the reported outcomes of ovarian tissue transplantation including, reported duration of hormone restoration, pregnancy, and live birth. A total of 2,252 abstracts were screened against the inclusion criteria. In this systematic review, 103 studies were included for analysis of tissue processing size and 21 studies were included for analysis of ovarian transplantation outcomes. Only studies where ovarian tissue was cryopreserved (via slow freezing or vitrification) and transplanted orthotopically were included in the review. The size of cryopreserved ovarian tissue was categorized based on dimensions into strips, squares, and fragments. Of the 103 studies, 58 fertility preservation sites were identified that processed ovarian tissue into strips (62%), squares (25.8%), or fragments (31%). Ovarian tissue transplantation was performed in 92 participants that had ovarian tissue cryopreserved into strips (n = 51), squares (n = 37), and fragments (n = 4). All participants had ovarian tissue cryopreserved by slow freezing. The pregnancy rate was 81.3%, 45.5%, 66.7% in the strips, squares, fragment groups, respectively. The live birth rate was 56.3%, 18.2%, 66.7% in the strips, squares, fragment groups, respectively. The mean time from ovarian tissue transplantation to ovarian hormone restoration was 3.88 months, 3.56 months, and 3 months in the strips, squares, and fragments groups, respectively. There was no significant difference between the time of ovarian function' restoration and the size of ovarian tissue. Transplantation of ovarian tissue, regardless of its processing dimensions, restores ovarian hormone activity in the participants that were reported in the literature. More detailed information about the tissue processing size and outcomes post-transplant are required to identify a preferred or more successful processing method.

Systematic Review Registration: [https://www.crd.york.ac.uk], identifier [CRD42020189120].

Keywords: fertility preservation, ovarian tissue cryopreservation, ovarian tissue transplantation, ovarian tissue size, oncofertility

INTRODUCTION

According to the American Cancer Society, 927,910 women and 10,500 children were diagnosed with cancer in 2021 (1). Advancements in cancer treatments, such as chemotherapy and radiation, have led to an increased chance of survival in these patients. Specifically, the 5-year survival rate of women aged 15-39 and children under the age of 14 is 86.7% and 84%, respectively (2). Cancer survivors are interested in methods that would improve their quality of life after treatment (3).

Cancer treatments such as the alkylating agent cyclophosphamide are gonadotoxic and cause irreversible damage to the germ cells by triggering double-stranded DNA breaks leading to apoptosis (4). This extreme decline in germ cells directly impairs ovarian endocrine function, which has systemic effects in the body, such as the increased risk of osteoporosis, high blood pressure, cardiovascular disease, and decline in cognitive function (5). The American Society of Clinical Oncology has recommended that oncologists describe and offer fertility preservation to their patients (6). Fertility preservation methods include ovarian transposition, gonadal shielding during pelvic radiotherapy, egg cryopreservation, embryo cryopreservation, and ovarian tissue cryopreservation (OTC) (7). The latter of these methods is the only option currently available to preserve fertility for prepubescent since they do not produce mature gametes (7, 8). OTC preserves primordial follicles within ovarian cortical microenvironment (7). Four key components are involved in OTC: ovarian surgical procurement, ovarian tissue processing, tissue cryopreservation, and storage. A unique feature of OTC is that in the future, the patient can choose to reimplant the ovarian cortical tissue orthotopically or heterotopically for fertility purposes or to restore ovarian endocrine function (7). Not only has this fertility preservation method been used to benefit cancer patients, but also women who want to postpone fertility and menopause (7). In 1999, the first successful autotransplantation of frozen-thawed ovarian cortical tissue was performed, but it was not until 2006 when Meirow et al. reported the first live birth obtained from OTC (9, 10).

Reported in 2017, ovarian tissue transplantation (OTT) has resulted in over 130 births (11). A recent meta-analysis of three centers has stated a pregnancy rate of about 50% (12). Although a vast majority of participants (95%) have the return of endocrine function post-transplantation, the average duration of endocrine function of ovarian tissue after transplantation is approximately 2-5 years (13). It has been shown that the duration of the ovarian tissue function is correlated to its ovarian reserve (14). Additionally, in xenograft experiments there is a decline in primordial follicles *via* activation and apoptosis in human, bovine, and marmoset 3-days post-transplantation of ovarian tissue (14). A review from Roness et al. has outlined that every step of OTC/OTT from the participant's initial reserve to transplantation site can impact the premature loss of the primordial follicles and impact ovarian tissue function (15). Studies done in mice and humans have shown that fragmentation of ovarian tissue stimulates follicle activation pathways, such as Hippo and PI3K-AKT (16, 17). Fragmenting the ovarian cortex during the tissue processing for OTC may activate primordial follicles and reduce the ovarian reserve. OTC has recently been designated as a nonexperimental procedure by the American Society for Reproductive Medicine (ASRM) (18). However, there is currently no standard method of processing ovarian tissue, which emphasizes the importance of examining if fragmentation impacts the function of transplanted ovarian tissue. In this systematic review, we sought (1) to identify the sizes and processing techniques used to cryopreserve ovarian tissue around the world, and (2) to examine the reported results of different sized ovarian cortical tissue in participants who have undergone OTT on functional longevity, hormone restoration, pregnancy, and live birth. This report examines different dimensions of cryopreserved ovarian cortical tissue on fertility and ovarian function post-transplantation.

MATERIALS AND METHODS

Search Strategy

This systematic review followed the Preferred Reporting Items for Systematic Review and Meta-Analysis Protocols (PRISMA-P) guidelines and statement. This review's protocol is registered on PROSPERO and is available on Centre for Reviews and Dissemination (CRD) website at https://www.crd.york.ac.uk (registration number #: CRD42020189120). All literature searches were conducted on the National Institute of Health (NIH) PubMed database (https://www.ncbi.nlm.nih.gov/pubmed/). We performed all searches until February 2022. The searches had no date restrictions, the document types included were case studies, multi-center studies, and articles that focused on the processing size of ovarian cortical tissue and reproductive outcomes in human patients who have undergone OTT. We included the following keywords in the search: "ovarian tissue cryopreservation", "hormone restoration", "live birth", "success", "output", "size", "fragments", "strips", "cubes", "squares", "slivers", "processing", and "transplantation". A total of 14 searches were conducted. The parameters for the searches were: ((ovarian tissue cryopreservation), (ovarian tissue cryopreservation) AND ((hormone restoration) OR (pregnancy) OR (live birth) OR (success) OR (output)), (((ovarian tissue cryopreservation) AND((hormone restoration) OR (pregnancy) OR (live birth) OR (success) OR (output)) AND ((fragments) OR (strips) OR (squares) OR (cubes) OR (slices) OR

(pieces) OR (slivers))), (((fragments) OR (strips) OR (squares) OR (cubes) OR (slices) OR (pieces) OR (slivers)) AND (Ovarian tissue processing)), ((((fragments) OR (strips) OR (squares) OR (cubes) OR (slices) OR (pieces) OR (slivers)) AND (Ovarian tissue processing)) AND (((Live birth) or (pregnancy) or (hormone restoration)))) AND (ovarian tissue cryopreservation), ((fragments) OR (strips) OR (squares) OR (cubes) OR (slices) OR (pieces) OR (slivers)) AND (Ovarian tissue cryopreservation)), (((fragments) OR (strips) OR (squares) OR (cubes) OR (slices) OR (pieces) OR (slivers)) AND (Ovarian tissue cryopreservation))) AND (((Pregnancy) or (live birth) or (success))), ((ovarian tissue cryopreservation) AND ((squares) OR (strips) OR (cubes) OR (slivers) OR (fragments) OR (pieces)), (((ovarian tissue cryopreservation) AND ((squares) OR (strips) OR (cubes) OR (slivers) OR (fragments) OR (pieces))) AND ((hormone function) OR (ovarian activity)), ((ovarian tissue cryopreservation) AND ((squares) OR (strips) OR (cubes) OR (slivers) OR (fragments) OR (pieces))) AND (restoration), (ovarian tissue cryopreservation) AND ((size) OR (fragments) OR (cubes) OR (strips) OR (slivers) OR (processing)), (ovarian tissue cryopreservation) AND (processing), (ovarian tissue cryopreservation) AND (size), (ovarian tissue cryopreservation) AND ((fragments) OR (strips) OR (cubes) OR (squares) OR (slivers)), respectively. The results were compiled, and duplicated results were removed. Titles and abstracts were manually reviewed to determine articles that met the inclusion/exclusion criteria. We presented a PRISMA flow diagram to layout the identification, screening, eligibility, and included studies for this review.

Inclusion/Exclusion Criteria

In this systematic review, we had two subgroups: ovarian tissue processing for cryopreservation and transplanted frozen/thawed processed ovarian tissue. Studies focused on ovarian tissue processing for cryopreservation were gathered for the processing analysis, and studies that included outcomes of OTT were considered for the outcomes analysis. Only studies that contained participants who have undergone OTC regardless of age, diagnosis, and previous cancer treatment for fertility preservation and hormone restoration purposes were included for the outcomes analysis. Studies were excluded if ovarian tissue was used for other reasons than future fertility or hormone restoration purposes such as for experimental analysis. These included studies underwent further screening which focused on OTT outcomes. For the outcomes analysis, studies which contained participants who have undergone OTC and orthotopic auto transplantation regardless of age, diagnosis, and previous cancer treatment were included. Studies that contained participants who have only undergone OTC without a record of transplantation, non-human studies, ovarian tissue that was cultured/incubated in drugs before transplantation, heterotopic OTT, and OTT using donor ovaries were not included in this analysis.

Study Selection

Duplicated articles were removed from the lists that were generated from the search strategies above. The titles and abstracts of the remaining articles were manually examined by three independent reviewers (AAD, NH, MTH) for inclusion and exclusion criteria based on the criteria of this study, previously mentioned. Reasons for exclusion and inclusion for all articles were recorded in the screening process. To avoid disagreements and bias in the study selection process, a fourth reviewer (HK) screened the title, abstracts, and full text of all articles for inclusion criteria. Articles that met the inclusion criteria were independently examined for data extraction by three reviewers (AAD, NH, MTH).

Data Extraction

Three reviewers (AAD, NH, MTH) assessed the full-length articles that met the inclusion criteria to extract study measures. The reasons for exclusion were recorded for those articles that did not meet the inclusion criteria after full-article examination. Articles that met the inclusion criteria for OTC had the following data extracted: lab name, location of site, country of origin, number of participants, age of participant(s) at OTC, condition of participant(s), previous cancer treatment prior to OTC, date range of which tissue was processed, surgical technique of ovary removal, partial or whole ovary removal, methods used to process ovarian tissue during OTC, techniques used to process tissue, name of the 'size' of cortical ovarian tissue processed, dimensions of tissue pieces (length x width x thickness, mm), number of total tissue processed/cryopreserved, and cryopreservation technique (slow freeze, vitrification). Only articles that cryopreserved human ovarian tissue for future fertility or hormone purposes, explicitly stated methods of processing ovarian tissue, and had clear dimensions (length, width) of OTC tissue were assessed. Additional data were gathered for studies that met inclusion criteria for OTT outcomes analyses including: age of participant(s) at OTT, site of transplantation, number of total ovarian tissue pieces transplanted, beginning of ovarian hormone restoration (months), the longevity of ovarian function (months), the number of participants which underwent transplantation, number of participants that underwent assisted reproductive technology (ART) to conceive (yes/no, number of rounds, number of participants), number of participants that conceived spontaneously (yes/no, number of participants), the number of pregnancies, and the number of live births. Every participant in these studies were treated individually to avoid bias and to effectively assess the ovarian activity outcomes. The extracted data was verified by one reviewer (AAD) for validity and bias.

Characterization of Size

The size of cryopreserved ovarian tissue was characterized into three categories based on dimensions of tissue pieces (length, width): strips, squares, fragments. Processed ovarian tissue were categorized as strips if the length (≥ 5 mm) and width had different measurements. Squares were determined to be ovarian tissue which had the same measurements for length (≥ 5 mm) and width (≥ 5 mm). Fragments were determined to be tissue which had the length and width < 5 mm. Only studies that included clear dimensions of the length and width of the processed ovarian tissue were included in this review.

Outcome Measurements

For the outcomes analysis the following data were evaluated: dimensions of processed ovarian tissue (length, width,

thickness), most common dimensions of ovarian tissue, area of tissue transplanted, pregnancy rate, live birth rate, time to resumption of ovarian function post-transplantation, and longevity of ovarian hormone function. Only articles that contain these data measurements were assessed. The most common dimension of ovarian tissue was defined by the greatest number of participants that have the length and width of the ovarian tissue pieces in common. The average area of tissue transplanted was determined by the average area of the size of ovarian tissue pieces and the average amount of total tissue transplanted. Fertility rate was calculated to be percentage of the number of participants that obtained pregnancy to the number of participants that attempted pregnancy. Live birth rate was calculated to be the percentage of the number of participants who obtained live birth to participants who attempted pregnancy. We defined ovarian function restoration as the time of decline of FSH levels to premenopausal state, an increase in estradiol levels, or to time of resumption of menses, if the study included all these factors the former was noted.

Statistical Analysis

The number of tissues transplanted, and area of tissue transplanted were expressed as mean and range. The following parameters: age at OTC, age at OTT, and time of ovarian restoration from OTT were expressed as mean with standard deviations. To determine the differences between size of ovarian tissue and age at OTC, OTT, and ovarian restoration a One-way ANOVA was performed, $P<0.05$ were considered significantly different. Statistical analyses were performed using GraphPad PRISM.

Risk of Bias

Two authors (AAD, HK) independently evaluated each article included in this systematic review for risk for bias. In this systematic review case reports, multi-center studies, and articles were assessed for quality assessment. For these platforms, the Joanna Briggs Institute Critical appraisal checklist was utilized to examine the clarity on the participant's demographic characteristics, medical history, current clinical condition, intervention or treatment procedure, post-interventions, adverse/unanticipated events. Disagreements or conflicts on risk of bias assessment were resolved by a third reviewer (MML) **(Supplementary Tables 1, 2)**.

RESULTS

Study Selection

Figure 1 represents the PRISMA Flow diagram that was constructed for this systematic review. This diagram shows the screening, identification, eligibility, and inclusion steps conducted for OTC processing and OTT outcomes analyses. Studies that focused on OTC were gathered for OTC processing research; these articles underwent further screening for OTT and for OTT outcomes analysis. A total of 4,874 results were identified in PubMed; after manual removal of duplicate results, a total of 2,252 results were assessed for screening against the OTC inclusion criteria (**Figure 1**).

Of the abstract screened, 367 results met the inclusion criteria for the tissue processing analysis. Two-hundred and sixty-four results were excluded with reasons **(Figure 1)**. A total of 103 studies specifying the methods of processing ovarian tissue for cryopreservation, dimensions of cryopreserved ovarian tissue pieces, and location of the site were identified and included in this review for the outcomes analysis **(Figure 1)**. As previously mentioned, the articles included for processing analysis were further screened against the inclusion criteria for OTT. Twenty-one articles that were used for processing analysis were included for OTT outcomes analysis in this review. A total of 82 articles were excluded from outcomes analysis with reasons **(Figure 1)**. In this systematic review, 103 studies that contained participants that underwent OTC were included **(Supplementary Table 3)**. Additionally, 21 studies described 92 participants who underwent OTC and autologous transplantation **(Supplementary Table 4)**.

Ovarian Tissue Processing Sites

In this review, 58 unique sites published how ovarian tissue was processed for cryopreservation and tissue size categorized into three groups: strips, squares, and fragments (**Table 1**). There were 15, 3, and 10 unique length and width dimensions for strips, squares, and fragments, respectively. A total of 36 sites (62%) from 18 countries processed the ovarian tissue into strips (19–71) (**Table 1**). The most common dimension (length, width) for strips of 10 mm x 5 mm is processed in 19 different sites, with a range of 5-30 mm by 1-20 mm, (length, width). A total of 15 sites (25.8%) process ovarian tissue into squares, with the dimensions of 5 x 5 mm being the most common in 12 different sites and a range of 5-10 mm by 5-10 mm (length, width) (**Table 1**). Ovarian tissue was processed into squares in 15 sites from 11 countries (20, 65, 72–98). In total, 17 different sites (29.3%) from 12 countries process ovarian tissue into dimensions that were categorized into fragments (**Table 1**) (21, 62, 77, 99–122). Fragments with the dimensions of 2 x 2 mm (length, width) were the most common in 5 sites. The fragment dimensions ranged from 0.5-4 by 0.3-3 mm (length, width) (**Table 1**). Reported thicknesses ranged from 1 – 2 mm, and one site reporting a thickness of 5 mm (**Table 1**).

Of the 58 unique OTC processing sites, 8 (13.8%) cut ovarian tissue into different dimensions within the same size categories, 6,1, and 2 sites for strips, squares, and fragments, respectively (**Table 1**). Additionally, 9 sites (15.5%) processed ovarian tissue into different sizes (**Table 2**).

To determine if there is a correlation between age at OTC, participant diagnosis or ovarian tissue procurement method and the chosen size for tissue processing, additional data was extracted from articles where sites reported using multiple tissue processing sizes. Two sites (3.4%) cryopreserved ovarian tissue into all three sizes (**Table 2**.) The Juliane Marie Centre for Women at University Hospital of Copenhagen in Copenhagen, Denmark reported cutting tissue into the following dimensions (1): strips: 5 x 4, 5 x 1 (2), squares: 5 x 5 (3), fragments: 4 x 3, 3 x 3, 3 x 2, 2 x 2 mm^2 (length, width) (**Table 2**). This site processed a 9-year-old Ewing's sarcoma participant's ovarian tissue into 5 x 4

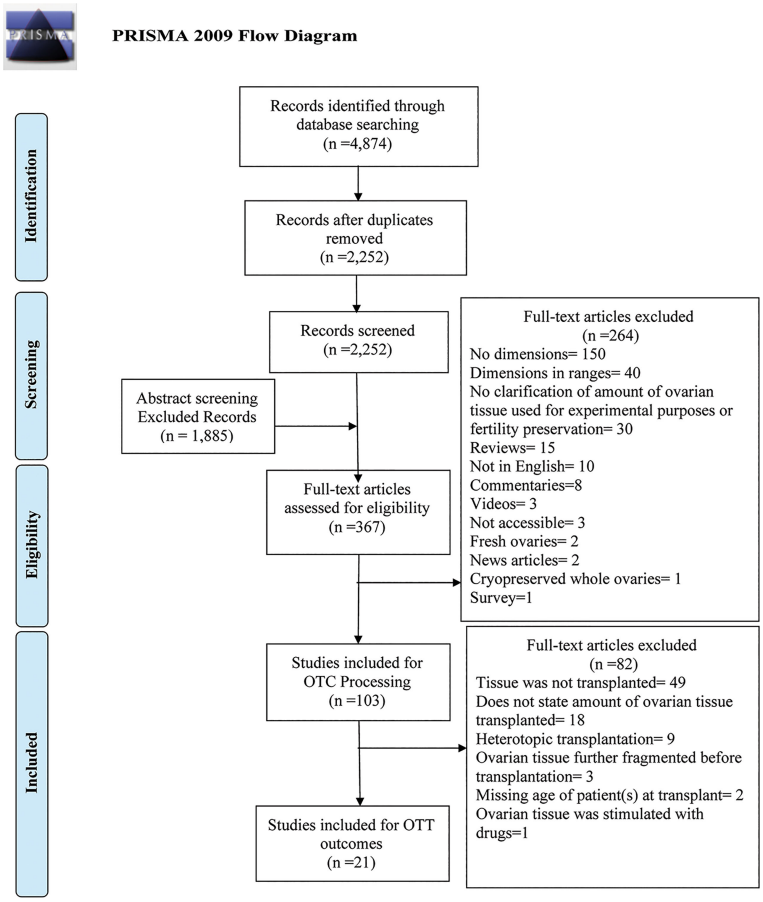

FIGURE 1 | PRISMA Flow diagram for ovarian tissue cryopreservation and transplantation.

mm^2 (64). Six galactosemia participants at this site had one ovary removed for fertility preservation at the ages of 1.7, 0.9, 4.5, 0.3, 2.9, and 11.7 and ovarian tissue was cut into the dimensions: 5 x 5, 4 x 3, 3 x 3, 3 x 2, 2 x 2, and 2 x 2 mm^2, respectively (77). Additionally at this site, 25 leukemia participants had 5 x 1 mm^2 strips cryopreserved (71). The Royal Women's Hospital in Victoria, Australia also reported processing ovarian tissue into multiple different sizes (1): strips: 5 x 1 (2), squares: 5 x 5 (3), fragments: 2 x 2, 3 x 3, 4 x 3 mm^2 (**Table 2**). Over 40 participants at this site had ovarian tissue processed into squares at the mean age of 26 (range 17.8 – 40.7), these participants had wide range of diagnoses (79). Also at this site 17 participants that had a mean age of 27.4 (range 17.8 – 35.9) at OTC had their ovarian tissue processed and cryopreserved into 5 x 1 mm^2 strips (68). The Royal Women's Hospital processed 9 participants (mean age at OTC= 20.6, range 18-31) ovarian tissue into 4 x 2 mm^2 fragments, these participants had various from of diseases (120).

In total 4 sites (6.9%) cut ovarian tissue into strips and fragments. The Cliniques Universitaires Saint-Luc in Brussels, Belgium, reported processing ovarian tissue into strips and fragments with the following dimensions: 12 x 4, 10 x 5, 10 x 4, 10 x 3, and 2 x 2 mm^2 (**Table 2**). At this site, 6 participants with different diagnoses and a mean age of 23.8 (range 21-28) underwent partial or whole oophorectomy had 12 x 4 mm^2 strips cryopreserved (22). A 23-year-old sickle cell anemia participant, at the Cliniques Universitaires Saint-Luc, that underwent a unilateral oophorectomy for fertility preservation had 10 x 5 mm^2 ovarian tissue strips cryopreserved (29). Four participants, with the mean age of 23.5 (range 21-28) at OTC, had their ovarian tissue was cut into 10 x 4 mm^2 strips for cryopreservation (123). A 22-year-old participant at this site had 10 x 3 mm^2 ovarian strips cryopreserved. Additionally at this site, 2 participants (17 and 25 years old at OTC) had fragments cryopreserved in the dimensions of 2 x 2 mm^2 (22). In the Lis Maternity Hospital at Tel Aviv Sourasky Medical Center in Tel Aviv, Israel, 93 participants (average at OTC 15.4, range 0–25) with a wide range of diagnosis at OTC, had 0.5 x 0.3 mm^2 fragments cryopreserved (**Table 2**) (116). Also at this site, an 18 year old participant with Hodgkin's disease had ovarian tissue cut into 10 x 5 mm^2 strips for OTC (43). At University Medical Center Utrecht in Utrecht, The Netherlands, 10 participants with different diagnoses underwent unilateral oophorectomy for fertility preservation and had 10 x 3 strips and 2 x 2 mm^2 fragments cryopreserved (52) (**Table 2**).

TABLE 1 | Ovarian tissue cryopreservation processing sizes across different sites around the world.

Size	Dimensions length x width (mm^2) thickness (*site*)	Sites of OTC processing
Strips	161 x 5 a *(a)*	a. University Paul Sabatier, Toulouse, France.
	30 x 20 a *(b)*	b. Sheba Medical Center, Sackler School of Medicine, Tel-Aviv University, Tel-Aviv, Israel.
	20 x 10 b *(c)*	c. St. Luke's Hospital, St. Louis, Missouri, USA.
	12 x 4 a *(d)*	d. Cliniques Universitaires Saint-Luc, Université Catholique de Louvain, Brussels, Belgium.
	10 x 5 a *(d, e, f, g)*, b *(d, h-p)*, d *(q-u)*, e *(v, w)*	e. Medical University of Vienna, Vienna, Austria.
	10 x 4 b *(d)*	f. University Medical Centre Ljubljana, Ljubljana, Slovenia.
	10 x 3 a *(d, x)*, b *(u)*	g. Institute University Dexeus, Barcelona, Spain.
	10 x 1 a *(y)*	h. Beijing Obstetrics and Gynecology Hospital, Capital Medical University, Beijing, China.
	8 x 5 a *(l, z)*	i. Royan Institute for Reproductive Biomedicine, ACECR, Tehran, Iran.
	8 x 4 b *(h, aa-dd)*	j. Israel and Sackler Faculty of Medicine, Tel Aviv University, Tel Aviv, Ramat Aviv, Israel
	6 x 4 d *(ee)*	k. Leiden University Medical Center, Leiden, the Netherlands.
	5 x 4 b *(ff)*	l. Radboud University Medical Center, Nijmegen, The Netherlands.
	5 x 3 b *(gg)*, d *(ee)*	m. Ankara University Faculty of Medicine, Ankara, Turkey.
	5 x 2 b *(hh)*	n. Christie Hospital, Manchester, UK.
	5 x 1 b *(ii, jj)*, g *(ff)*	o. University of Pennsylvania, Philadelphia, USA.
Squares	12 x 12 b *(kk)*	p. Children's National Hospital, Washington, D.C., USA
	10 x 10 b *(gg)*, c *(c)*, d *(gg, kk)*	q. Hôpital Jean-Verdier, Hôpitaux Universitaires Paris-Seine-Saint-Denis, Assistance Publique, Hôpitaux de Paris, Bondy, France.
	5 x 5 a *(ff)*, b *(ii, ff, mm-rr)*, d *(ff, ss-vv)*,e *(ss)*	r. Lis Maternity Hospital, Tel Aviv Sourasky Medical Center, Tel Aviv, Israel.
Fragments	4 x 3 a *(ff)*	s. Chaim Sheba Medical Center, Tel Hashomer, Israel.
	4 x 2 b *(ii, ww)*, e *(xx)*	t. Cleveland Clinic, Cleveland, Ohio, USA.
	3 x 3 a *(ff)*, b *(yy, zz)*	u. University of Bologna, S Orsola-Malpighi Hospital of Bologna, Italy.
	3 x 2 d *(ss)*	v. New York Medical College, New York, New York, USA.
	3 x 1 f *(aaa)*	w. Naval Medical Center San Diego, San Diego, California, USA
	2 x 2 a *(ff, w, bbb)*, b (*ccc*), e (*d*)	x. University Medical Center Utrecht, Utrecht, The Netherlands.
	2 x 1 a (*zz*), b (*dd*), f (*ddd*)	y. University of Valencia, Valencia, Spain.
	1 x 1 a (*zz, eee*)	z. Centre for Reproductive Medicine, UZ Brussel, Brussels, Belgium.
	0.5 x 0.5 b *(fff)*	aa. Heinrich-Heine-University, Düsseldorf, Germany.
	0.5 x 0.3 a *(r)*	bb. University Women's Hospital Düsseldorf, Düsseldorf, Germany.
		cc. Bern University Hospital, Bern, Switzerland.
		dd. Medical University of Bonn, Bonn, Germany.
		ee. Assistance Publique-Hôpitaux de Paris Saint Louis Hospital, Paris, France.
		ff. The Juliane Marie Centre for Women, University Hospital of Copenhagen, University of Copenhagen, Rigshospitalet-Copenhagen, Denmark.
		gg. Marianna University School of Medicine, Kawasaki City, Japan.
		hh. Shahid Sadoughi University of Medical Sciences, Yazd, Iran.
		ii. Royal Women's Hospital, Parkville, Victoria, Australia.
		jj. Hadassah Hebrew University Hospital, Jerusalem, Israel.
		kk. Rose Ladies Clinic, Tokyo, Japan.
		ll. Monash IVF, Melbourne, Victoria, Australia.
		mm. Ghent University Hospital, Ghent, Belgium.
		nn. University of Torino, S. Anna Hospital, Torino, Italy.
		oo. Seoul National University Bundang Hospital, Seongnam, Korea.
		pp. Oslo University Hospital, Oslo, Norway.
		qq. AVA-PETER Fertility Clinic, Saint-Petersburg, Russia.
		rr. University of Kansas Medical Center, Kansas City, Kansas, USA.
		ss. Erasme Hospital, Université Libre de Bruxelles, Brussels, Belgium.
		tt. Aarhus University, Aarhus, Denmark.
		uu. Eulji University School of Medicine, Seoul, South Korea
		vv. Gameta Hospital, Lodz, Poland.
		ww. Monash Medical Centre, Clayton, Victoria, Australia.
		xx. University of Cologne, Cologne, Germany
		yy. Medical University of Innsbruck, Innsbruck, Austria.

(Continued)

TABLE 1 | Continued

Size	Dimensions length x width (mm^2) thickness (*site*)	Sites of OTC processing
		zz. Erlangen University Hospital, Friedrich-Alexander University of Erlangen-Nuremberg, Erlangen, Germany.
		aaa. Karolinska University Hospital, Stockholm, Sweden.
		bbb. Hospital Center São João, Porto, Portugal.
		ccc. McGill University Health Center, McGill University, Montreal, Quebec, Canada
		ddd. University of Oxford, Oxford, UK.
		eee. Johannes Gutenberg University, Mainz, Germany.
		fff. Département de Biologie de la Reproduction, CHU Montpellier, Univ Montpellier, France.

[a]*thickness no mentioned.*
[b]*thickness of 1 mm.*
[c]*thickness of 1-1.5 mm.*
[d]*thickness of 1-2 mm.*
[e]*thickness of 2 mm.*
[f]*thickness of 5 mm.*

Two additional sites report processing tissue into strips and squares (3.4%). St. Luke's Hospital in St. Louis, Missouri, USA cryopreserves participants' ovarian tissue into 20 x 10 mm^2 strips and 10 x 10 mm^2 squares (20) (**Table 2**). From 1997 to 2007, slow freezing was this site's main method of cryopreservation and therefore cut ovarian tissue into 20 x 10 mm^2 strips (20). This site changed its method of cryopreservation to vitrification in 2007. From 2007 to 2017, participants at this site had 10 x 10 mm^2 squares cryopreserved for fertility preservation (20). In Japan, the Marianna University School of Medicine uses 5 x 3 mm^2 strips and 10 x 10 mm^2 squares for participants with various diagnosis at OTC (17, 73) (**Table 2**).

Of the 58 processing sites 1 site uses both squares and fragments as its size for cryopreserving ovarian tissue. Erasme Hospital in Brussels, Belgium cryopreserves tissue as 5 x 5 mm^2 squares, which has been used for over 200 participants (age range 0-27) with different diagnoses at OTC, and regardless of partial or whole ovary removal (89) (**Table 2**). Additionally, a 13-year-old sickle cell anemia participant at this site had 3 x 2 mm^2 fragments ovarian tissue cryopreserved for fertility preservation (100).

Characteristics of OTT Participants

The clinical metadata for participants that were included in this systematic review is detailed in **Supplementary Table 4**. A total of 92 unique participants who underwent OTT after OTC with the goal of having a biological child or restoring hormones were included in this analysis (21, 22, 25, 34, 37, 44, 57, 59, 61, 64, 66, 78, 84, 91–93, 95, 111, 115, 118, 124). Overall, 51, 37, and 4 participants had their ovarian tissue processed into strips, squares, and fragments, respectively (**Table 3**). The three most predominant

TABLE 2 | Processing sites that cut ovarian tissue into different sizes.

Size of processed ovarian tissue	Site(s)	Dimensions length x width (mm^2)
All three sizes	The Juliane Marie Centre for Women, University Hospital of Copenhagen, University of Copenhagen, Copenhagen, Denmark.	Strips: 5 x 4, 5 x 1 Squares: 5 x 5 Fragments: 4 x 3, 3 x 3, 3 x 2, 2 x 2
	Royal Women's Hospital, Parkville, Victoria, Australia.	Strips: 5 x 1 Squares: 5 x 5 Fragments: 2 x 2, 3 x 3, 4 x 3
Strips and fragments	Cliniques Universitaires Saint-Luc, Université Catholique de Louvain, Brussels, Belgium.	Strips: 12 x 4, 10 x 5, 10 x 4, 10 x 3 Fragments: 2 x 2
	Lis Maternity Hospital, Tel Aviv Sourasky Medical Center, Tel Aviv, Israel.	Strips: 10 x 5 Fragments: 0.5 x 0.3
	University Medical Center Utrecht, Utrecht, The Netherlands.	Strips: 10 x 3 Fragments: 2 x 2
	Medical University of Bonn, Bonn, Germany.	Strips: 8 x 4 Fragments: 2 x 1
Strips and squares	St. Luke's Hospital, St. Louis, Missouri, USA.	Strips: 20 x 10 Squares: 10 x 10
	Marianna University School of Medicine, Kawasaki City, Japan.	Strips: 5 x 3 Squares: 10 x 10
Squares and fragments	Erasme Hospital, Université Libre de Bruxelles, Brussels, Belgium.	Squares: 5 x 5 Fragments: 3 x 2

TABLE 3 | OTC/OTT Participant characteristics for fertility and hormone outcomes (21, 22, 25, 34, 37, 44, 57, 59, 61, 64, 66, 78, 84, 91–93, 95, 111, 115, 118, 124).

Size of processed ovarian tissue	Strips	Squares	Fragments
Range Dimensions of processed ovarian tissue Length x Width (mm^2)	6-10 x 2-5	5 x 5	2-3 x 1-2
Most common dimension Length x Width (mm^2), (n=67)	6 x 4 (n = 28)	5 x 5 (n = 37)	2 x 2 (n = 2)
No. of OTC/OTT participants	51	37	4
Method of cryopreservation	Slow freeze: 50	Slow freeze: 37	Slow freeze: 4
(Slow freeze, Vitrification)	Vitrification: 0	Vitrification: 0	Vitrification: 0
Mean Age at OTC	27.4 ± 6.6, 9-40	29.8 ± 5.31, 15.4-38	22.8 ± 3.3, 18-25
Years ± SD, Range			
Mean Age at OTT	33.1 ± 5.3, 13.6-41.9	33.8± 4.95, 27-43	30.3 ± 1.7, 28-32
Years ± SD, Range			
No. of participants with previous treatment prior to OTC	21	2	1
Average number of tissues transplanted, ± SD, Range (1^{st}, 2^{nd}, 3^{rd})	1^{st}: 11.5 ± 7.8, 2-46 2^{nd}: 11.7 ± 4, 8-16 (n=7)	1^{st}:10.9 ± 2.8, 6-17 2^{nd}: 8.3 ± 4.3, 3-16 (n=10)	1^{st}: 21.8 ± 30.3, 4-67 2^{nd}: 20 (n=1) 3^{rd}: 49 (n=1)
Av. Area of tissue transplanted (mm^2) ± SD, Range, mm^2 (Total, 1^{st}, 2^{nd}, 3^{rd})	Total: 394.58 ± 262.7, 40 – 1152 1^{st}: 334.0 ± 172.5, 40-920 2^{nd}: 385.75 ± 100.7, 216-550 3^{rd}: -	Total: 328.4 ± 128, 150 -750 1^{st}: 271.8 ± 69.9, 150-425 2^{nd}: 207.5 ± 108, 75-400 mm^2 3^{rd}: -	Total: 134.8 ± 139.8, 12-268 1^{st}; 83 ± 123.8, 12-268 2^{nd}: 60 (n=1) 3^{rd}:147 (n=1)

conditions that were present in the total participant population were Hodgkin's lymphoma (23.9%), breast cancer (29.3%), and other conditions (17.4%) (**Figure 2A**). In the strips and fragment participant populations, Hodgkin's lymphoma was the most prevalent diagnosis (**Figures 2B, D**). Additionally, the most prevalent condition for participants whose ovaries were processed into squares was breast cancer (**Figure 2C**). The mean age at OTC was 27.4, 29.8, and 22.8 years for participants whose ovaries were processed into strips, squares, and fragments, respectively (**Figure 3A**). The mean age at the time of OTT was 33.1, 33.8, and 30.3 for strips, squares, and fragments groups, respectively (**Figure 3B**). There was statistically significant difference in the age at the time of OTC (P-value= 0.0390) between all three sizes, but no significant difference between two sizes. Furthermore, there was no statistically significant difference between the age at the time OTT (P-value= 0.4130) in the three different size ovarian tissue pieces, respectively (**Figures 3A, B**). Although all groups had at least one participant with previous cancer treatment before OTC, the strips group had the greatest number of participants in this subgroup (n=21) (**Table 3**). The ovarian tissue was most often processed into

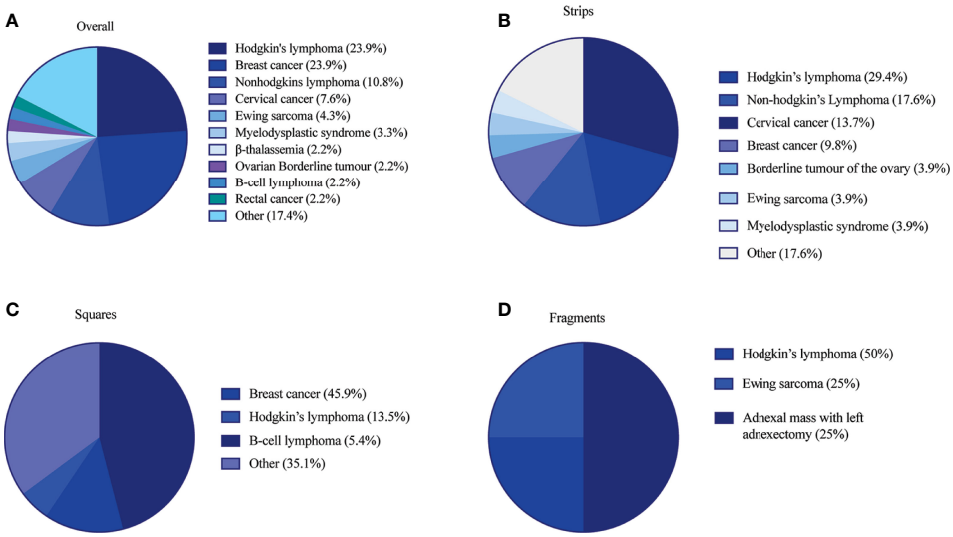

FIGURE 2 | Participant diagnosis at time of OTC in **(A)** overall patient population **(B)** strips **(C)** squares and **(D)** fragments group. Diagnoses in the other category included the following in (1) overall: acute lymphocytic leukemia, adnexal mass with left adnexectomy, aplastic anemia, autoimmune vasculitis, choriocarcinoma, colorectal cancer, endometrial cancer, granulomatosis with polyangiitis, leukemia, neuroendocrine tumor, ovarian cancer, Schwachman-diamond syndrome, sickle cell anemia, synovial sarcoma of the lung and pelvic sarcoma, systemic lupus erythematosus, T-cell lymphoma (2), strips: acute lymphocytic leukemia, aplastic anemia, β-thalassemia, colorectal cancer, endometrial cancer, rectal cancer, Schwachman-diamond syndrome, sickle cell anemia, systemic lupus erythematosus, and (3) squares: autoimmune vasculitis, β-thalassemia, choriocarcinoma, Ewing's sarcoma, granulomatosis with polyangiitis, leukemia, myelodysplastic syndrome, neuroendocrine tumor, non-Hodgkin's lymphoma, ovarian cancer, rectal cancer, synovial sarcoma of the lung and pelvic sarcoma, T-cell lymphoma (21, 22, 25, 34, 37, 44, 57, 59, 61, 64, 66, 78, 84, 91–93, 95, 111, 115, 118, 124).

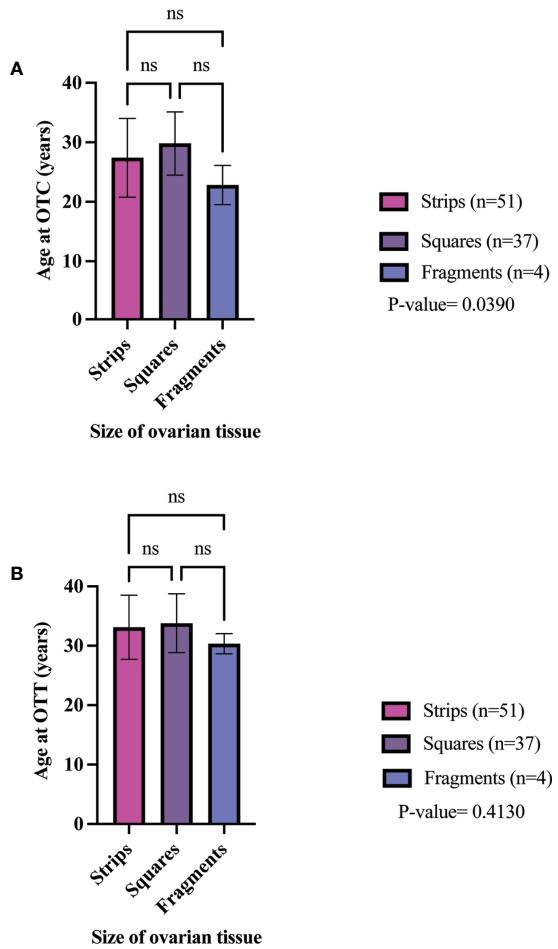

FIGURE 3 | Age of participant at OTC **(A)** and OTT **(B)** in different size cryopreserved and transplanted ovarian tissue. P-values greater than 0.05 were considered not significantly different (ns) (21, 22, 25, 34, 37, 44, 57, 59, 61, 64, 66, 78, 84, 91–93, 95, 111, 115, 118, 124).

the dimensions of 6 x 4 mm^2, 5 x 5 mm^2, and 2 x 2 mm^2 (length x width) in the strips, squares, and fragments groups, respectively prior to OTT (**Table 3**). Eighteen participants underwent a second OTT 7, 10, and 1 strips, squares, and fragments groups, respectively and one participant underwent a third OTT (**Table 3**). A total of 51 participants whose ovarian tissue was processed into strips, 9 into squares, and 3 into fragment were included for analysis because information on hormone restoration and longevity was reported. The average area of tissue per first OTT was 334.0 mm^2, 271.8 mm^2, and 123.8 mm^2 for strips, squares, and fragments groups, respectively. Overall, the total average area of tissue transplanted was 394.58 mm^2, 328.4 mm^2, and 134.8 mm^2 for strips, squares, and fragments groups, respectively (**Table 3**). There was a statistically significant difference between the total and first average area of tissue per OTT in all three size ovarian tissue pieces. (P-value= 0.0432 and 0.0013, respectively) Additionally, there was not a statistically significant difference in total and first average area of tissue per OTT between two groups (**Table 3**; **Figures 4A, B**).

Ovarian Tissue Processing Size and Pregnancy Outcomes

52.2% (48/92) of all participants who were reported to undergo OTT were also monitored for pregnancy attempts using assisted reproductive technologies (ART) or spontaneously (21, 22, 25, 34, 37, 44, 57, 59, 61, 64, 66, 78, 84, 91–93, 95, 111, 115, 118, 124). A total of 16, 11 and 3 participants with strip, square, and fragment ovarian tissue pieces attempted pregnancy (**Table 4**). The pregnancy rates were 81.3, 45.5, and 66.7% for strip, square, and fragment ovarian tissue pieces (21, 22, 25, 34, 37, 44, 57, 59, 61, 64, 66, 78, 84, 91–93, 95, 111, 115, 118, 124).

In the strips group, 6 participants used ART methods, 13 participants used spontaneous methods, and 3 participants used both methods to attempt pregnancy (25, 34, 37, 44, 57, 59, 61, 63, 64). Overall, there were 14 pregnancies in this group; 4 pregnancies resulted from ART, and 10 were obtained spontaneously. Of the three strips participants that used both methods to attempt pregnancy, 2 participants achieved pregnancy with ART and spontaneous methods, and one participant was successful at achieving pregnancy spontaneously (34, 59). In total, 9 strips participants had pregnancies that resulted in a live birth. One participant has a total of two separate live births from both ART and spontaneous pregnancies. The live birth rate for the strips groups was 56.3% and there was a total of 12 live births (2 ART, 10 spontaneous) (**Table 4**). Two strips participants birthed twins (34, 61). Two participants in the strips groups had miscarriages, one participant had a termination of pregnancy, and one participant had an ongoing pregnancy at the end of the study (59, 63). In total, four participants in the strips group who attempted pregnancy had a second transplant (34, 63). Two participants were unsuccessful in obtaining pregnancy with the first transplant, so to increase chances of pregnancy they underwent a second OTT (**Table 4**) (34, 63). The first participant achieved three spontaneous pregnancies that resulted in two separate successful live births and one miscarriage (63). The second participant had a successful spontaneous pregnancy and subsequent live birth (34, 63). Of the two other participants in the strips group that had a second OTTs, one participant got pregnant with the first OTT but resulted in a miscarriage, and the other had a termination of pregnancy (63). These two participants had a successful spontaneous pregnancy and live birth with the second transplant (63).

The square group had a pregnancy rate of 45.5%. These participants obtained pregnancy with ART (n=2) or spontaneously (n=3) (**Table 4**) (78, 84, 91–95). In addition, there were a total of five pregnancies in this group; two were achieved using ART, and three were achieved spontaneously. In total, two participants in the squares group had a termination of pregnancy, and one participant had an ongoing pregnancy at the end of the study (78, 92, 95). The live birth rate for the squares group was 18.2%. In this group, 10 participants had a second transplantation and 8 of these participants were not included for pregnancy outcomes due to unclear pregnancy attempts (**Table 4**) (91, 93). A total of 3 spontaneous pregnancies were

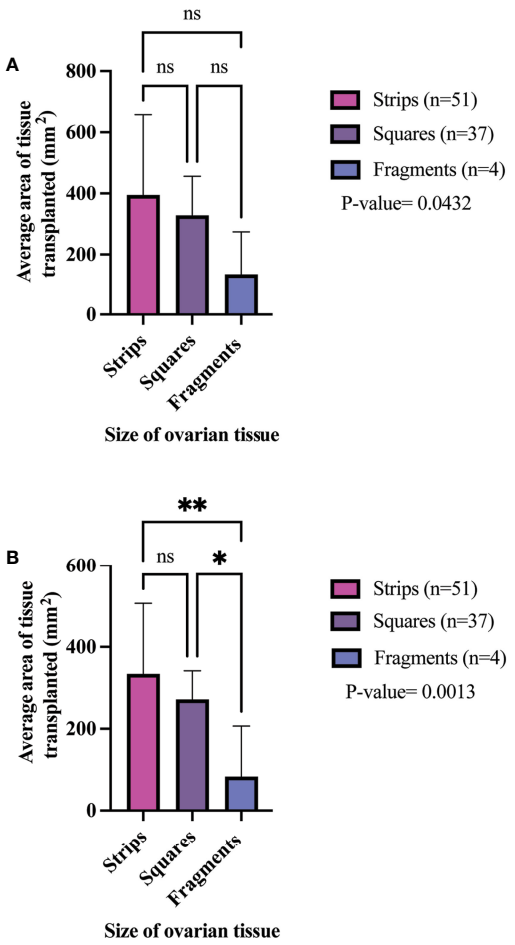

FIGURE 4 | Total average area of tissue transplanted **(A)** and per 1st OTT **(B)** in different size cryopreserved and transplanted ovarian tissue. P-values greater than 0.05 were considered not significantly different (ns) P-values greater than 0.05 were considered not significantly different (ns).P-values less than 0.05 (*) and 0.005(**) were considered significantly different. (21, 22, 25, 34, 37, 44, 57, 59, 61, 64, 66, 78, 84, 91–93, 95, 111, 115, 118, 124).

obtained from these excluded participants (93). Two participants had a total of two separate pregnancies, where in one participant both pregnancies resulted in termination and in the other participant both pregnancies resulted in live birth (93). The third participant that was excluded had a single spontaneous pregnancy which was terminated (93). Two participants were included that underwent a second OTT (**Table 4**) (91, 93). One participant attempted pregnancy spontaneously with first transplantation to increase chances of pregnancy, and then requested a second transplant that resulted in a successful live birth (91). The other participant was unsuccessful at obtaining pregnancy with the first and second OTT (91).

In the fragments group, 3 participants attempted pregnancy spontaneously (**Table 4**) (21, 111, 118). Two of these participants were successful at obtaining pregnancy and live birth (21, 111). In this group, one participant had a total of three separate OTTs (118). This participant attempted pregnancy with the first transplant, however, due to decline ovarian hormone levels the participant had multiple transplants that resulted in a single pregnancy and live birth (118).

OTT Hormone Restoration and Function Longevity

Decreased FSH levels or menstrual cycle resumption and the duration of ovarian hormone production post-transplantation determined ovarian function. Overall, 98% of participants had restoration of ovarian function with first OTT; only one participant in the strips group showed no reestablishment of ovarian activity **(Table 5)** (34). The mean time from OTT to ovarian hormone restoration was 3.88 months (range: 1.6-7.5 months), 3.56 months (range: 1.8-4.6), and 3 months (range:1-5 months) in the strip, square, and fragment groups per first OTT, respectively **(Table 5**; **Figure 5)** (21, 22, 25, 34, 37, 44, 57, 59, 61, 64, 66, 78, 84, 91, 92, 95, 111, 115, 124). There was no statistically significant difference of the mean time from OTT to ovarian restoration in all three sizes (P-value= 0.2104) **(Figure 5)**. In all three groups, over 88% of participants had ovarian activity lasting over six months **(Table 5)**. One participant who had OTT with strips and one with squares had continuous function at 2.4- and 2.8-months post-transplantation, respectively (34, 92). The strips group had the highest percentage of participants with hormone production lasting over one-year post-transplantation with their first OTT (86%) **(Table 5)**. In total, two participants from the strips group had ovarian activity lasting over five years with their first OTT (63). The strips, squares, and fragments groups had 84, 55.6, and 100% of participants with ongoing ovarian function with first OTT, respectively. In total, eight (16%) and four (44.4%) participants had cessation of ovarian function with first OTT in the strips and square groups, respectively (44, 63, 64).In total, 10 participants underwent a second OTT(8 strips and 2 squares) **(Table 5)** (34, 63, 78, 91). In the strips group, 8 participants had an end of ovarian function with the first OTT at a mean of 1.29 years, (range 0.75-3.2 years) post transplantation (34, 63). Additionally, one participant in the strips group that had two OTT did not have restoration of ovarian function with second OTT (63). Participants with ovarian restoration from second OTT, six participants had ongoing function and one participant had an ovarian cessation at one year post second OTT (34, 63). In the squares group, 4 participants had the end of ovarain fuction, two participant had a second OTT **(Table 5)** (84, 91). Of the two participants that did not have a second OTT, ovarian function ceased at 2 and 3.75 years, respectively (mean=2.9 years) (84, 91). Two participants from the squares group underwent a second OTT due to cessation of ovarian function at 1.25 years and 7 months post first OTT (78, 91).However, the second OTT in one participant did not restore ovarian activity (91). The other participant had ongoing ovarian activity lasting over 1.5 years with second OTT (91).

DISCUSSION

There have been several recent systematic reviews of OTC and OTT that have identified the different cryoprotectant protocols

TABLE 4 | Pregnancy and live birth outcome after transplantation per 1st transplant (21, 22, 25, 34, 37, 44, 57, 59, 61, 64, 66, 78, 84, 91–93, 95, 111, 115, 118, 124).

Size of processed ovarian tissue (No. of OTT Participants)	Participants who attempted to become pregnant n, (%)	Pregnancy rate n, (%)	Number of Pregnancies	Live birth rate n, (%)	Number of Live Births
Strips (n = 51)	16[g]/51, (31.4)	13[h]/16, (81.3)	14	9[j]/16, (56.3)	12[k]
Total	6	4	4	2	2
ART	13	11	10[i]	8	10
spontaneous					
Squares (n = 37)	11/37, (29.7)	5/11, (45.5)	5	2/11, (18.2)	2
Total	6	2	2	1	1
ART	5	3	3	1	1
spontaneous					
Fragments (n = 4)	3/4, (75)	2/3, (66.7)	2	2/3, (66.7)	2
Total	0	0	0	0	0
ART	3	2	2	2	2
spontaneous					

[g]*Three participants in the strips category used both ART and spontaneous methods to attempt pregnancy.*
[h]*Two participants in the strips category that used both ART and spontaneous methods to attempt pregnancy obtained pregnancy with both methods, one participant in the strips category that used both ART and spontaneous methods to attempt pregnancy obtained pregnancy only with spontaneous methods.*
[i]*One participant in the strips category that used both ART and spontaneous methods to attempt pregnancy obtained pregnancy only with spontaneous methods, had an ongoing pregnancy.*
[j]*One participant in the strips category obtained a live birth from both ART and spontaneous methods.*
[k] *Two participants in the strips category had twins.*

OTC, fresh and frozen OTT for hormone restoration, ovarian tissue transport prior to OTC, age at OTC, and vitrification versus slow-freezing methods for OTC (13, 125–127).This is the first systematic review that considered the size of ovarian tissue pieces that were processed for OTC and the outcomes of OTT within those size categories. OTT is a technique emerging in the field of reproductive science and has been performed in over 318 patients (128). The ovarian tissue is processed for OTC by thinning the tissue, removing most of the ovarian medulla and isolating the ovarian cortical tissue. The cortex is then cut into pieces to allow for penetration of the cryoprotectant in preparation for cryopreservation (129). In this systematic review, 58 unique sites reported details on the dimensions used for OTC. This analysis identified that ovarian tissue is cut into multiple different sizes. Ten sites located in the U.S., Belgium, Australia, China, Japan, Israel, Germany, Denmark, and Netherlands processed the ovarian tissue in multiple sizes within the same clinical site. There were no correlations found between age at OTC or diagnosis and the size of processed ovarian tissue. There were no indications of a regional preference for ovarian tissue processing size and, furthermore, seven sites cut ovarian tissue into different dimensions within the same size category. These findings highlight that there is no standard size of cryopreserved ovarian tissue. Studies have shown that fragmentation of the ovarian cortex leads to follicle activation (17). This investigation revealed that 36 sites (62% of sites) process ovarian tissue into strips and is the most predominant cryopreserved size. These findings also demonstrate that most sites around the world process the ovarian tissue to have a thickness of 1-2 mm, which coincides with a thickness which has been shown to reduce ice crystal formation and injury, reduce ischemic time, and increase oxygen diffusion once transplanted (130, 131). Transplantation of ovarian tissue has been reported to restore ovarian activity in 95% of transplantations (12, 128). In the results described here, the ovarian function was restored in 98% of participants that underwent OTT.

Fertility clinics in Denmark and Japan utilize fragmentation of ovarian tissue for POI patients to activate dormant follicles and increase fertilization rates (132, 133). Based on this and other evidence from animal models that suggest that disruption of the microenvironment can initiate follicle activation, it was hypothesized that ovarian tissue used in OTT that had been processed into smaller pieces would result in fewer pregnancies

TABLE 5 | Ovarian function outcome after transplantation.

Size of processed ovarian tissue (No. of OTT Participants)	Months from OTT HP mean ± SD, range	HP lasting ≥6 months n, (%)	HP lasting ≥1 year n, (%)	HP lasting ≥ 2 years n, (%)	HP ≥ 5 years n, (%)	Participants with ongoing ovarian function n, (%)	Participants with reported cessation of ovarian function n, (%)
Strips	3.88 ± 0.84, 1.6-7.5	49/51, (96)	45/51,	19/51, (37.3)	2/51, (4)	42/51, (84)	9[q]/51, (17.6)
1st (n = 51)		7/8, (87.5)	(88.2)	4/8, (50)	1/8, (12.5)	6/8, (75)	2[q]/8, (25)
2nd (n = 8)			7/8, (87.5)				
Squares	3.56 ± 1.03,	8/9, (88.9)	4/9, (44.4)	3/9, (33.3)	0/9, (0)	5/9, (55.6)	4/9, (44.4)
1st (n = 9)	1.8-4.6	1/2, (50)	1/2, (50)	0/2, (0)	0/2, (0)	1/2, (50)	1[q]/2, (50)
2nd (n = 2)							
Fragments	3 ± 2,	3/3, (100)	1/3, (33.3)	0/3, (0)	0/3, (0)	3/3, (100)	0/3, (0)
1st (n = 3)	1-5						

[q]*Participant did not have resumption of ovarian activity. HP, hormone production (21, 22, 25, 34, 37, 44, 57, 59, 61, 64, 66, 78, 84, 91, 92, 95, 111, 115, 124).*

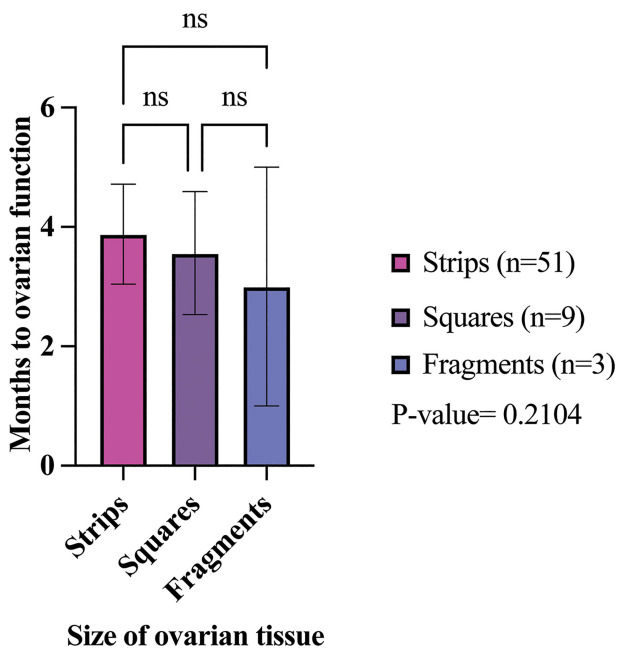

FIGURE 5 | Months to restoration of ovarian activity in different size transplanted ovarian tissues. The average time to ovarian restoration per first OTT was 3.88, 3.56, and 3 months in the strip, square, and fragment groups, respectively. P-values greater than 0.05 were considered not significantly different (ns) (21, 22, 25, 34, 37, 44, 57, 59, 61, 64, 66, 78, 84, 91–93, 95, 111, 115, 118, 124).

and shorter duration of ovarian function, and a shorter time to initiate ovarian function after OTT (16). After transplantation there is up to an 80% loss in ovarian reserve due to factors such as ischemic time (14, 15). The graft size can influence ischemic time, such that smaller graft sizes can have shorter ischemic time than larger graft sizes, leading to earlier ovarian function (15, 134, 135). The resumption of ovarian activity on average did decrease with a smaller processing size (strips 3.88 months, squares 3.56 months, and fragments 3 months). Additionally, the squares group had the highest rate (44.4%) of participants that had a reported cessation of ovarian activity with the first OTT, followed by the strips group (17.6%). Even though more tissue on average was transplanted in the strips than squares group, the strips group had a shorter ovarian tissue lifespan (1.29 years) for the first OTT compared to squares group (2.9 years). While some of these results followed the expected trend, the longevity of ovarian tissue function in the strips group is lower than the reported literature range of 2-5 years due to the lack of follow-ups on participants with OTT in the reviewed reports (128). If further participant follow-up was performed for each study through to cessation of ovarian function, then the longevity of ovarian tissue function would be better understood. While the analysis accounted for the location of the transplant by excluding heterotopic sites, and the reported results only included tissue that was cryopreserved using a slow freezing and not vitrification technique, there are other confounding factors that may contribute to ovarian tissue function after OTT. We also note that there were studies with exciting findings that did not meet our inclusion criteria. For instance, Oktay et al. have implemented the use of extracellular matrix scaffolds, which show promise in extending graft longevity (136).

OTC followed by OTT has resulted in over 140 published live births worldwide and it has been reported to lead to multiple live births from the same OTT procedure (60, 128). This systematic review of reports that contained information on ovarian tissue processing size and OTT outcomes identified an overall pregnancy rate of 81.3%, 45.5%, 66.7% of participants in strips, squares, and fragments groups, respectively. In the strips and fragments groups, the pregnancy rates were higher than the 50% pregnancy rate from OTT reported in the literature (12). This vast difference in pregnancy rate is probably attributed to the fact that authors have not published or described the additional information required for this analysis. The live birth rate was higher in the strips groups (56.3%) compared to squares (18.2%). However, in these two groups, participants (2 squares, 1 strips) had a termination of pregnancy which could have impacted the live birth rate (63, 92, 93, 95). The fragments group had the highest birth rate (66.7%) in all three groups. The small sample size of participants in the fragments group (n=4) compared to the strips (n=51) and squares (n=37) was a contributing factor to these high rates. The participant data utilized for this systematic review was limited by the number of published case studies that contain participants who underwent autologous orthotopic OTT, follow-up time points in studies that discussed OTT outcomes, and contained data on the ovarian tissue sizes. This systematic review relies heavily on the information of case studies, therefore, can introduce an internal validity threat to our reported results. An additional caveat to this study is that authors publishing on OTT might not be reporting unsuccessful OTT cases and have not reported detailed follow-ups of past reported case studies. Evidence is needed to identify and understand factors that could contribute to follicle burnout within the first few months post-OTT, such as impact of tissue fragmentation on preventing ischemia-reperfusion injury and initiating angiogenesis, to develop a unified best practice for ovarian tissue processing (20).

CONCLUSION

This systematic review determined the processing sizes of cryopreserved ovarian tissue in sites across the world and examined ovarian function restoration in different sized ovarian tissue pieces in OTT participants. It is shown in this review that there is no standard for processing ovarian tissue and documentation of ovarian restoration outcomes in participants. Although the time of resumption of ovarian activity was not statistically significant between the different sizes, this could have been due to the small population size of the fragments and squares group. The participant population size used in this systematic review could have been more prominent by changing the rigorous inclusion/exclusion criteria to include studies that did not contain enough information about the participants. However, changing the inclusion/exclusion criteria of this systematic review to

include studies that lacked important participant information would increase bias within the review. This systematic review has shown the importance of documenting information on the participant before OTC, explicit ovarian tissue processing and transplantation methods, and updating participants' ovarian outcomes post-transplantation *via* follow-ups. This call to action of proper documentation and consistent OTT participant follow-ups will allow scientists and clinicians to drive research questions with the goals of improving OTC/OTT and maximizing fertility outcomes.

DATA AVAILABILITY STATEMENT

The original contributions presented in the study are included in the article/**Supplementary Material**. Further inquiries can be directed to the corresponding author.

AUTHOR CONTRIBUTIONS

AD and ML contributed to the study concept, design, and data interpretation. AD contributed to data analysis. HK contributed to the study quality assessment and unbiased reviewer. AD, HK, and ML contributed to manuscript preparation. NH, MH, and AD contributed to data collection. All authors contributed to the article and approved the submitted version.

FUNDING

This works was supported in part by the Children's Research Fund, the Ann & Robert H. Lurie Children's Hospital Faculty Practice Plan award (ML), the Warren and Eloise Batts endowment (ML).

ACKNOWLEDGMENTS

We thank Drs. Francesca Duncan and Erin Rowell for guidance in study design and impact.

SUPPLEMENTARY MATERIAL

The Supplementary Material for this article can be found online at: https://www.frontiersin.org/articles/10.3389/fendo.2022.918899/full#supplementary-material

REFERENCES

1. Siegel RL, Miller KD, Fuchs HE, Jemal A. Cancer Statistics, 2021. *CA: A Cancer J Clin* (2021) 71(1):7–33. doi: 10.3322/caac.21654
2. Miller KD, Fidler-Benaoudia M, Keegan TH, Hipp HS, Jemal A, Siegel RL. Cancer Statistics for Adolescents and Young Adults, 2020. *CA: A Cancer J Clin* (2020) 70(6):443–59. doi: 10.3322/caac.21637
3. Shrestha A, Martin C, Burton M, Walters S, Collins K, Wyld L. Quality of Life Versus Length of Life Considerations in Cancer Patients: A Systematic Literature Review. *Psycho-Oncol* (2019) 28(7):1367–80. doi: 10.1002/pon.5054
4. Bedoschi G, Navarro PA, Oktay K. Chemotherapy-Induced Damage to Ovary: Mechanisms and Clinical Impact. *Future Oncol* (2016) 12(20):2333–44. doi: 10.2217/fon-2016-0176
5. Chahal H, Drake W. The Endocrine System and Ageing. *J Pathol* (2007) 211 (2):173–80. doi: 10.1002/path.2110
6. Lee SJ, Schover LR, Partridge AH, Patrizio P, Wallace WH, Hagerty K, et al. American Society of Clinical Oncology Recommendations on Fertility Preservation in Cancer Patients. *J Clin Oncol* (2006) 24(18):2917–31. doi: 10.1200/JCO.2006.06.5888
7. Kim S, Lee Y, Lee S, Kim T. Ovarian Tissue Cryopreservation and Transplantation in Patients With Cancer. *Obstetrics Gynecol Sci* (2018) 61 (4):431. doi: 10.5468/ogs.2018.61.4.431
8. Wallace WHB, Anderson RA, Irvine DS. Fertility Preservation for Young Patients With Cancer: Who is at Risk and What can be Offered? *Lancet Oncol* (2005) 6(4):209–18. doi: 10.1016/S1470-2045(05)70092-9
9. Marin L, Bedoschi G, Kawahara T, Oktay KH. History, Evolution and Current State of Ovarian Tissue Auto-Transplantation With Cryopreserved Tissue: A Successful Translational Research Journey From 1999 to 2020. *Reprod Sci* (2020) 27(4):955–62. doi: 10.1007/s43032-019-00066-9
10. Meirow D, Levron J, Eldar-Geva T, Hardan I, Fridman E, Zalel Y, et al. Pregnancy After Transplantation of Cryopreserved Ovarian Tissue in a Patient With Ovarian Failure After Chemotherapy. *N Engl J Med* (2005) 353 (3):318–21. doi: 10.1056/NEJMc055237
11. Donnez J, Dolmans MM. Fertility Preservation in Women. *N Engl J Med* (2017) 377(17):1657–65. doi: 10.1056/NEJMra1614676
12. Shapira M, Dolmans MM, Silber S, Meirow D. Evaluation of Ovarian Tissue Transplantation: Results From Three Clinical Centers. *Fertil Steril* (2020) 114(2):388–97. doi: 10.1016/j.fertnstert.2020.03.037
13. Corkum KS, Rhee DS, Wafford QE, Demeestere I, Dasgupta R, Baertschiger R, et al. Fertility and Hormone Preservation and Restoration for Female Children and Adolescents Receiving Gonadotoxic Cancer Treatments: A Systematic Review. *J Pediatr Surg* (2019) 54(11):2200–9. doi: 10.1016/j.jpedsurg.2018.12.021
14. Gavish Z, Spector I, Peer G, Schlatt S, Wistuba J, Roness H, et al. Follicle Activation is a Significant and Immediate Cause of Follicle Loss After Ovarian Tissue Transplantation. *J Assisted Reprod Genet* (2018) 35(1):61–9. doi: 10.1007/s10815-017-1079-z
15. Roness H, Meirow D. FERTILITY PRESERVATION: Follicle Reserve Loss in Ovarian Tissue Transplantation. *Reproduction* (2019) 158(5):F35–44. doi: 10.1530/REP-19-0097
16. Nagamatsu G, Shimamoto S, Hamazaki N, Nishimura Y, Hayashi K. Mechanical Stress Accompanied With Nuclear Rotation is Involved in the Dormant State of Mouse Oocytes. *Sci Advances* (2019) 5(6):eaav9960. doi: 10.1126/sciadv.aav9960
17. Kawamura K, Cheng Y, Suzuki N, Deguchi M, Sato Y, Takae S, et al. Hippo Signaling Disruption and Akt Stimulation of Ovarian Follicles for Infertility Treatment. *Proc Natl Acad Sci* (2013) 110(43):17474–9. doi: 10.1073/pnas.1312830110
18. Fertility Preservation in Patients Undergoing Gonadotoxic Therapy or Gonadectomy: A Committee Opinion. *Fertility Sterility* (2019) 112 (6):1022–33. doi: 10.1016/j.fertnstert.2019.09.013
19. Meirow D, Ra'anani H, Shapira M, Brenghausen M, Derech Chaim S, Aviel-Ronen S, et al. Transplantations of Frozen-Thawed Ovarian Tissue Demonstrate High Reproductive Performance and the Need to Revise Restrictive Criteria. *Fertil Steril* (2016) 106(2):467–74. doi: 10.1016/j.fertnstert.2016.04.031
20. Silber SJ, DeRosa M, Goldsmith S, Fan Y, Castleman L, Melnick J. Cryopreservation and Transplantation of Ovarian Tissue: Results From One Center in the USA. *J Assist Reprod Genet* (2018) 35(12):2205–13. doi: 10.1007/s10815-018-1315-1
21. Donnez J, Dolmans MM, Demylle D, Jadoul P, Pirard C, Squifflet J, et al. Livebirth After Orthotopic Transplantation of Cryopreserved Ovarian Tissue. *Lancet* (2004) 364(9443):1405–10. doi: 10.1016/S0140-6736(04)17222-X
22. Donnez J, Squifflet J, Van Eyck AS, Demylle D, Jadoul P, Van Langendonckt A, et al. Restoration of Ovarian Function in Orthotopically Transplanted Cryopreserved Ovarian Tissue: A Pilot Experience. *Reprod BioMed Online* (2008) 16(5):694–704. doi: 10.1016/S1472-6483(10)60484-1

23. Mayerhofer K, Ott J, Nouri K, Stoegbauer L, Fischer EM, Lipovac M, et al. Laparoscopic Ovarian Tissue Harvesting for Cryopreservation: An Effective and Safe Procedure for Fertility Preservation. *Eur J Obstet Gynecol Reprod Biol* (2010) 152(1):68–72. doi: 10.1016/j.ejogrb.2010.05.034
24. Ott J, Nouri K, Stögbauer L, Fischer EM, Lipovac M, Promberger R, et al. Ovarian Tissue Cryopreservation for non-Malignant Indications. *Arch Gynecol Obstet.* (2010) 281(4):735–9. doi: 10.1007/s00404-009-1224-8
25. Ruan X, Du J, Korell M, Kong W, Lu D, Jin F, et al. Case Report of the First Successful Cryopreserved Ovarian Tissue Retransplantation in China. *Climacteric* (2018) 21(6):613–6. doi: 10.1080/13697137.2018.1514005
26. González C, Devesa M, Boada M, Coroleu B, Veiga A, Barri PN. Combined Strategy for Fertility Preservation in an Oncologic Patient: Vitrification of *In Vitro* Matured Oocytes and Ovarian Tissue Freezing. *J Assist Reprod Genet* (2011) 28(12):1147–9. doi: 10.1007/s10815-011-9628-3
27. Virant-Klun I, Vogler A. *In Vitro* Maturation of Oocytes From Excised Ovarian Tissue in a Patient With Autoimmune Ovarian Insufficiency Possibly Associated With Epstein-Barr Virus Infection. *Reprod Biol Endocrinol* (2018) 16(1):33. doi: 10.1186/s12958-018-0350-1
28. Philippart C, Masciangelo R, Camboni A, Donnez J, Dolmans MM. Basal Lamina Characterization in Frozen-Thawed and Long-Term Grafted Human Prepubertal Ovarian Tissue. *Reprod BioMed Online* (2021) 42 (5):859–69. doi: 10.1016/j.rbmo.2021.02.012
29. Dolmans MM, Jadoul P, Gilliaux S, Amorim CA, Luyckx V, Squifflet J, et al. A Review of 15 Years of Ovarian Tissue Bank Activities. *J Assist Reprod Genet* (2013) 30(3):305–14. doi: 10.1007/s10815-013-9952-x
30. Abir R, Ben-Aharon I, Garor R, Yaniv I, Ash S, Stemmer SM, et al. Cryopreservation of *In Vitro* Matured Oocytes in Addition to Ovarian Tissue Freezing for Fertility Preservation in Paediatric Female Cancer Patients Before and After Cancer Therapy. *Hum Reprod* (2016) 31(4):750–62. doi: 10.1093/humrep/dew007
31. Abtahi NS, Ebrahimi B, Fathi R, Khodaverdi S, Mehdizadeh Kashi A, Valojerdi MR. An Introduction to The Royan Human Ovarian Tissue Bank. *Int J Fertil Steril* (2016) 10(2):261–3. doi: 10.22074/ijfs.2016.4918
32. Jenninga E, Louwe LA, Peters AA, Nortier JW, Hilders CG. Timing of Fertility Preservation Procedures in a Cohort of Female Patients With Cancer. *Eur J Obstet Gynecol Reprod Biol* (2012) 160(2):170–3. doi: 10.1016/j.ejogrb.2011.11.011
33. Hoekman EJ, Smit VT, Fleming TP, Louwe LA, Fleuren GJ, Hilders CG. Searching for Metastases in Ovarian Tissue Before Autotransplantation: A Tailor-Made Approach. *Fertil Steril* (2015) 103(2):469–77. doi: 10.1016/j.fertnstert.2014.11.001
34. Hoekman EJ, Louwe LA, Rooijers M, Westerlaken LAJ, Klijn NF, Pilgram GSK, et al. Ovarian Tissue Cryopreservation: Low Usage Rates and High Live-Birth Rate After Transplantation. *Acta Obstetricia Gynecologica Scandinavica* (2020) 99(2):213–21. doi: 10.1111/aogs.13735
35. Jenninga E, Hilders CG, Louwe LA, Peters AA. Female Fertility Preservation: Practical and Ethical Considerations of an Underused Procedure. *Cancer J* (2008) 14(5):333–9. doi: 10.1097/PPO.0b013e31818860ac
36. Bastings L, Liebenthron J, Westphal JR, Beerendonk CC, van der Ven H, Meinecke B, et al. Efficacy of Ovarian Tissue Cryopreservation in a Major European Center. *J Assist Reprod Genet* (2014) 31(8):1003–12. doi: 10.1007/s10815-014-0239-7
37. Sonmezer M, Ozkavukcu S, Sukur YE, Kankaya D, Arslan O. First Pregnancy and Live Birth in Turkey Following Frozen-Thawed Ovarian Tissue Transplantation in a Patient With Acute Lymphoblastic Leukemia Who Underwent Cord Blood Transplantation. *J Assist Reprod Genet* (2020) 37 (8):2033–43. doi: 10.1007/s10815-020-01850-2
38. Radford JA, Lieberman BA, Brison DR, Smith AR, Critchlow JD, Russell SA, et al. Orthotopic Reimplantation of Cryopreserved Ovarian Cortical Strips After High-Dose Chemotherapy for Hodgkin's Lymphoma. *Lancet* (2001) 357(9263):1172–5. doi: 10.1016/S0140-6736(00)04335-X
39. Gracia CR, Chang J, Kondapalli L, Prewitt M, Carlson CA, Mattei P, et al. Ovarian Tissue Cryopreservation for Fertility Preservation in Cancer Patients: Successful Establishment and Feasibility of a Multidisciplinary Collaboration. *J Assist Reprod Genet* (2012) 29(6):495–502. doi: 10.1007/s10815-012-9753-7
40. Hanfling SN, Parikh T, Mayhew A, Robinson E, Graham J, Gomez-Lobo V, et al. Case Report: Two Cases of Mature Oocytes Found in Prepubertal Girls During Ovarian Tissue Cryopreservation. *F S Rep* (2021) 2(3):296–9. doi: 10.1016/j.xfre.2021.03.007
41. Sermondade N, Sonigo C, Sifer C, Valtat S, Ziol M, Eustache F, et al. Serum Antimüllerian Hormone Is Associated With the Number of Oocytes Matured In Vitro and With Primordial Follicle Density in Candidates for Fertility Preservation. *Fertil Steril* (2019) 111(2):357–62. doi: 10.1016/j.fertnstert.2018.10.018
42. Shai D, Aviel-Ronen S, Spector I, Raanani H, Shapira M, Gat I, et al. Ovaries of Patients Recently Treated With Alkylating Agent Chemotherapy Indicate the Presence of Acute Follicle Activation, Elucidating its Role Among Other Proposed Mechanisms of Follicle Loss. *Fertil Steril* (2021) 115(5):1239–49. doi: 10.1016/j.fertnstert.2020.11.040
43. Azem F, Hasson J, Cohen T, Shwartz T, Mey-Raz N, Almog B, et al. Retrieval of Immature Oocytes After Chemotherapy for Hodgkin's Disease and Prolonged Ovarian Down-Regulation With Gonadotropin-Releasing Hormone Agonist. *Fertil Steril* (2009) 92(2):828.e1–2. doi: 10.1016/j.fertnstert.2009.04.052
44. Fabbri R, Pasquinelli G, Magnani V, Macciocca M, Vicenti R, Parazza I, et al. Autotransplantation of Cryopreserved Ovarian Tissue in Oncological Patients: Recovery of Ovarian Function. *Future Oncol* (2014) 10(4):549–61. doi: 10.2217/fon.13.234
45. Meirow D, Baum M, Yaron R, Levron J, Hardan I, Schiff E, et al. Ovarian Tissue Cryopreservation in Hematologic Malignancy: Ten Years' Experience. *Leuk Lymphoma* (2007) 48(8):1569–76. doi: 10.1080/10428190701471957
46. Meirow D, Hardan I, Dor J, Fridman E, Elizur S, Ra'anani H, et al. Searching for Evidence of Disease and Malignant Cell Contamination in Ovarian Tissue Stored From Hematologic Cancer Patients. *Hum Reprod* (2008) 23 (5):1007–13. doi: 10.1093/humrep/den055
47. Hickman LC, Uy-Kroh MJ, Chiesa-Vottero A, Desai N, Flyckt R. Ovarian Tissue Cryopreservation for Benign Gynecologic Disease: A Case of Ovarian Torsion and Review of the Literature. *J Minim Invasive Gynecol* (2016) 23 (3):446–9. doi: 10.1016/j.jmig.2015.12.011
48. Oktay K, Oktem O. Ovarian Cryopreservation and Transplantation for Fertility Preservation for Medical Indications: Report of an Ongoing Experience. *Fertil Steril* (2010) 93(3):762–8. doi: 10.1016/j.fertnstert.2008.10.006
49. Schermerhorn SMV, Rosen MP, Blevins EM, Byrd KA, Rabban JT, Marsh P, et al. Regional Air Transportation of Ovarian Tissue for Cryopreservation in a Prepubertal Female With Cancer. *Pediatr Blood Cancer* (2021) 68(9): e29107. doi: 10.1002/pbc.29107
50. Dolmans MM, Donnez J, Camboni A, Demylle D, Amorim C, Van Langendonckt A, et al. IVF Outcome in Patients With Orthotopically Transplanted Ovarian Tissue. *Hum Reprod* (2009) 24(11):2778–87. doi: 10.1093/humrep/dep289
51. Fabbri R, Vicenti R, Macciocca M, Pasquinelli G, Lima M, Parazza I, et al. Cryopreservation of Ovarian Tissue in Pediatric Patients. *Obstet Gynecol Int* (2012) 2012:910698. doi: 10.1155/2012/910698
52. Janse F, Donnez J, Anckaert E, De Jong FH, Fauser BCJM, Dolmans M-M. Limited Value of Ovarian Function Markers Following Orthotopic Transplantation of Ovarian Tissue After Gonadotoxic Treatment. (2011) 96(4):1136–44. doi: 10.1210/jc.2010-2188
53. Policiano C, Subirá J, Aguilar A, Monzó S, Iniesta I, Rubio Rubio JM. Impact of ABVD Chemotherapy on Ovarian Reserve After Fertility Preservation in Reproductive-Aged Women With Hodgkin Lymphoma. *J Assist Reprod Genet* (2020) 37(7):1755–61. doi: 10.1007/s10815-020-01844-0
54. Delattre S, Segers I, Van Moer E, Drakopoulos P, Mateizel I, Enghels L, et al. Combining Fertility Preservation Procedures to Spread the Eggs Across Different Baskets: A Feasibility Study. *Hum Reprod* (2020) 35(11):2524–36. doi: 10.1093/humrep/deaa193
55. Peek R, Schleedoorn M, Smeets D, van de Zande G, Groenman F, Braat D, et al. Ovarian Follicles of Young Patients With Turner's Syndrome Contain Normal Oocytes But Monosomic 45,X Granulosa Cells. *Hum Reprod* (2019) 34(9):1686–96. doi: 10.1093/humrep/dez135
56. Li Y, Ruan X, Liebenthron J, Montag M, Zhou Q, Kong W, et al. Ovarian Tissue Cryopreservation for Patients With Premature Ovary Insufficiency Caused by Cancer Treatment: Optimal Protocol. *Climacteric* (2019) 22 (4):383–9. doi: 10.1080/13697137.2018.1554644
57. Ruan X, Cheng J, Korell M, Du J, Kong W, Lu D, et al. Ovarian Tissue Cryopreservation and Transplantation Prevents Iatrogenic Premature

Ovarian Insufficiency: First 10 Cases in China. *Climacteric* (2020) 23(6):574–80. doi: 10.1080/13697137.2020.1767569
58. Du J, Ruan X, Jin F, Li Y, Cheng J, Gu M, et al. Abnormalities of Early Folliculogenesis and Serum Anti-Müllerian Hormone in Chinese Patients With Polycystic Ovary Syndrome. *J Ovarian Res* (2021) 14(1):36. doi: 10.1186/s13048-021-00786-0
59. Ruan X, Du J, Lu D, Duan W, Jin F, Kong W, et al. First Pregnancy in China After Ovarian Tissue Transplantation to Prevent Premature Ovarian Insufficiency. *Climacteric* (2021) 24(6):624–8. doi: 10.1080/13697137.2021.1956453
60. Liebenthron J, Montag M, Reinsberg J, Köster M, Isachenko V, van der Ven K, et al. Overnight Ovarian Tissue Transportation for Centralized Cryobanking: A Feasible Option. *Reprod BioMed Online* (2019) 38(5):740–9. doi: 10.1016/j.rbmo.2019.01.006
61. Chehab G, Krüssel J, Fehm T, Fischer-Betz R, Schneider M, Germeyer A, et al. Successful Conception in a 34-Year-Old Lupus Patient Following Spontaneous Pregnancy After Autotransplantation of Cryopreserved Ovarian Tissue. *Lupus* (2019) 28(5):675–80. doi: 10.1177/0961203319839482
62. Van der Ven H, Liebenthron J, Beckmann M, Toth B, Korell M, Krüssel J, et al. Ninety-Five Orthotopic Transplantations in 74 Women of Ovarian Tissue After Cytotoxic Treatment in a Fertility Preservation Network: Tissue Activity, Pregnancy and Delivery Rates. *Hum Reprod* (2016) 31(9):2031–41. doi: 10.1093/humrep/dew165
63. Poirot C, Fortin A, Lacorte JM, Akakpo JP, Genestie C, Vernant JP, et al. Impact of Cancer Chemotherapy Before Ovarian Cortex Cryopreservation on Ovarian Tissue Transplantation. *Hum Reprod* (2019) 34(6):1083–94. doi: 10.1093/humrep/dez047
64. Ernst E, Kjærsgaard M, Birkebæk NH, Clausen N, Andersen CY. Case Report: Stimulation of Puberty in a Girl With Chemo- and Radiation Therapy Induced Ovarian Failure by Transplantation of a Small Part of Her Frozen/Thawed Ovarian Tissue. *Eur J Cancer* (2013) 49(4):911–4. doi: 10.1016/j.ejca.2012.09.028
65. Takae S, Furuta S, Keino D, Shiraishi E, Iwahata Y, Oyama K, et al. Surgical Management of Unilateral Oophorectomy for Ovarian Tissue Cryopreservation in High-Risk Children and Adolescents With Varied Backgrounds. *Pediatr Surg Int* (2021) 37(8):1021–9. doi: 10.1007/s00383-021-04900-7
66. Poirot C, Brugieres L, Yakouben K, Prades-Borio M, Marzouk F, de Lambert G, et al. Ovarian Tissue Cryopreservation for Fertility Preservation in 418 Girls and Adolescents Up to 15 Years of Age Facing Highly Gonadotoxic Treatment. Twenty Years of Experience at a Single Center. *Acta Obstet Gynecol Scand* (2019) 98(5):630–7. doi: 10.1111/aogs.13616
67. Mohsenzadeh M, Khalili MA, Tabibnejad N, Yari N, Agha-Rahimi A, Karimi-Zarchi M. Embryo Cryopreservation Following In-Vitro Maturation for Fertility Preservation in a Woman With Mullerian Adenosarcoma: A Case Report. *J Hum Reprod Sci* (2017) 10:138–41. doi: 10.4103/jhrs.JHRS_93_16
68. Gook D, Hale L, Polyakov A, Manley T, Rozen G, Stern K. Experience With Transplantation of Human Cryopreserved Ovarian Tissue to a Sub-Peritoneal Abdominal Site. *Hum Reprod* (2021) 36(9):2473–83. doi: 10.1093/humrep/deab167
69. Karavani G, Schachter-Safrai N, Chill HH, Mordechai Daniel T, Bauman D, Revel A. Single-Incision Laparoscopic Surgery for Ovarian Tissue Cryopreservation. *J Minim Invasive Gynecol* (2018) 25(3):474–9. doi: 10.1016/j.jmig.2017.10.007
70. Karavani G, Schachter-Safrai N, Revel A, Mordechai-Daniel T, Bauman D, Imbar T. In Vitro Maturation Rates in Young Premenarche Patients. *Fertil Steril* (2019) 112(2):315–22. doi: 10.1016/j.fertnstert.2019.03.026
71. Greve T, Clasen-Linde E, Andersen MT, Andersen MK, Sørensen SD, Rosendahl M, et al. Cryopreserved Ovarian Cortex From Patients With Leukemia in Complete Remission Contains No Apparent Viable Malignant Cells. *Blood* (2012) 120(22):4311–6. doi: 10.1182/blood-2012-01-403022
72. Kikuchi I, Kagawa N, Silber S, Kuwayama M, Takehara Y, Aono F, et al. Oophorectomy for Fertility Preservation *via* Reduced-Port Laparoscopic Surgery. *Surg Innov* (2013) 20(3):219–24. doi: 10.1177/1553350612449074
73. Takae S, Sugishita Y, Yoshioka N, Hoshina M, Horage Y, Sato Y, et al. The Role of Menstrual Cycle Phase and AMH Levels in Breast Cancer Patients Whose Ovarian Tissue Was Cryopreserved for Oncofertility Treatment. *J Assist Reprod Genet* (2015) 32(2):305–12. doi: 10.1007/s10815-014-0392-z
74. Kawamura K, Ishizuka B, Hsueh AJW. Drug-Free *in-Vitro* Activation of Follicles for Infertility Treatment in Poor Ovarian Response Patients With Decreased Ovarian Reserve. *Reprod BioMed Online* (2020) 40(2):245–53. doi: 10.1016/j.rbmo.2019.09.007
75. Meng L, Kawamura K, Yoshioka N, Tamura M, Furuyama S, Nakajima M, et al. Learning Curve of Surgeons Performing Laparoscopic Ovarian Tissue Transplantation in Women With Premature Ovarian Insufficiency: A Statistical Process Control Analysis. *J Minim Invasive Gynecol* (2022) 29(4):559–66. doi: 10.1016/j.jmig.2021.12.014
76. Rosendahl M, Loft A, Byskov AG, Ziebe S, Schmidt KT, Andersen AN, et al. Biochemical Pregnancy After Fertilization of an Oocyte Aspirated From a Heterotopic Autotransplant of Cryopreserved Ovarian Tissue: Case Report. *Hum Reprod* (2006) 21(8):2006–9. doi: 10.1093/humrep/del140
77. Mamsen LS, Kelsey TW, Ernst E, Macklon KT, Lund AM, Andersen CY. Cryopreservation of Ovarian Tissue May Be Considered in Young Girls With Galactosemia. *J Assist Reprod Genet* (2018) 35(7):1209–17. doi: 10.1007/s10815-018-1209-2
78. Burmeister L, Kovacs GT, Osianlis T. First Australian Pregnancy After Ovarian Tissue Cryopreservation and Subsequent Autotransplantation. *Med J Aust* (2013) 198(3):158–9. doi: 10.5694/mja12.11768
79. Rozen G, Avagliano S, Agresta F, Gook D, Polyakov A, Stern C. Ovarian Tissue Grafting: Lessons Learnt From Our Experience With 55 Grafts. *Reprod Med Biol* (2021) 20(3):277–88. doi: 10.1002/rmb2.12380
80. De Roo C, Lierman S, Tilleman K, De Sutter P. *In-Vitro* Fragmentation of Ovarian Tissue Activates Primordial Follicles Through the Hippo Pathway. *Hum Reprod Open* (2020) 2020(4):hoaa048. doi: 10.1093/hropen/hoaa048
81. El Issaoui M, Giorgione V, Mamsen LS, Rechnitzer C, Birkebæk N, Clausen N, et al. Effect of First Line Cancer Treatment on the Ovarian Reserve and Follicular Density in Girls Under the Age of 18 Years. *Fertil Steril* (2016) 106(7):1757–62.e1. doi: 10.1016/j.fertnstert.2016.09.001
82. Greve T, Schmidt KT, Kristensen SG, Ernst E, Andersen CY. Evaluation of the Ovarian Reserve in Women Transplanted With Frozen and Thawed Ovarian Cortical Tissue. *Fertil Steril* (2012) 97(6):1394–8.e1. doi: 10.1016/j.fertnstert.2012.02.036
83. Schmidt KL, Andersen CY, Loft A, Byskov AG, Ernst E, Andersen AN. Follow-Up of Ovarian Function Post-Chemotherapy Following Ovarian Cryopreservation and Transplantation. *Hum Reprod* (2005) 20(12):3539–46. doi: 10.1093/humrep/dei250
84. Revelli A, Marchino G, Dolfin E, Molinari E, Delle Piane L, Salvagno F, et al. Live Birth After Orthotopic Grafting of Autologous Cryopreserved Ovarian Tissue and Spontaneous Conception in Italy. *Fertil Steril* (2013) 99(1):227–30. doi: 10.1016/j.fertnstert.2012.09.029
85. Lee JR, Lee D, Park S, Paik EC, Kim SK, Jee BC, et al. Successful in Vitro Fertilization and Embryo Transfer After Transplantation of Cryopreserved Ovarian Tissue: Report of the First Korean Case. *J Korean Med Sci* (2018) 33(21):e156. doi: 10.3346/jkms.2018.33.e15
86. Tanbo T, Greggains G, Storeng R, Busund B, Langebrekke A, Fedorcsak P. Autotransplantation of Cryopreserved Ovarian Tissue After Treatment for Malignant Disease - The First Norwegian Results. *Acta Obstet Gynecol Scand* (2015) 94(9):937–41. doi: 10.1111/aogs.12700
87. Bystrova O, Lapina E, Kalugina A, Lisyanskaya A, Tapilskaya N, Manikhas G. Heterotopic Transplantation of Cryopreserved Ovarian Tissue in Cancer Patients: A Case Series. *Gynecol Endocrinol* (2019) 35(12):1043–9. doi: 10.1080/09513590.2019.1648413
88. Kim SS. Assessment of Long Term Endocrine Function After Transplantation of Frozen-Thawed Human Ovarian Tissue to the Heterotopic Site: 10 Year Longitudinal Follow-Up Study. *J Assist Reprod Genet* (2012) 29(6):489–93. doi: 10.1007/s10815-012-9757-3
89. Imbert R, Moffa F, Tsepelidis S, Simon P, Delbaere A, Devreker F, et al. Safety and Usefulness of Cryopreservation of Ovarian Tissue to Preserve Fertility: A 12-Year Retrospective Analysis. *Hum Reprod* (2014) 29(9):1931–40. doi: 10.1093/humrep/deu158
90. Fasano G, Dechène J, Antonacci R, Biramane J, Vannin AS, Van Langendonckt A, et al. Outcomes of Immature Oocytes Collected From Ovarian Tissue for Cryopreservation in Adult and Prepubertal Patients. *Reprod BioMed Online* (2017) 34(6):575–82. doi: 10.1016/j.rbmo.2017.03.007
91. Andersen CY, Rosendahl M, Byskov AG, Loft A, Ottosen C, Dueholm M, et al. Two Successful Pregnancies Following Autotransplantation of Frozen/Thawed Ovarian Tissue. *Hum Reprod* (2008) 23(10):2266–72. doi: 10.1093/humrep/den244

92. Greve T, Ernst E, Markholt S, Schmidt KT, Andersen CY. Legal Termination of a Pregnancy Resulting From Transplanted Cryopreserved Ovarian Tissue. *Acta Obstet Gynecol Scand* (2010) 89(12):1589–91. doi: 10.3109/00016349.2010.512074
93. Dueholm Hjorth IM, Kristensen SG, Dueholm M, Humaidan P. Reproductive Outcomes After In Vitro Fertilization Treatment in a Cohort of Danish Women Transplanted With Cryopreserved Ovarian Tissue. *Fertil Steril* (2020) 114(2):379–87. doi: 10.1016/j.fertnstert.2020.03.035
94. Tryde Schmidt KL, Yding Andersen C, Starup J, Loft A, Byskov AG, Nyboe Andersen A. Orthotopic Autotransplantation of Cryopreserved Ovarian Tissue to a Woman Cured of Cancer - Follicular Growth, Steroid Production and Oocyte Retrieval. *Reprod BioMed Online* (2004) 8(4):448–53. doi: 10.1016/S1472-6483(10)60929-7
95. Ernst EH, Offersen BV, Andersen CY, Ernst E. Legal Termination of a Pregnancy Resulting From Transplanted Cryopreserved Ovarian Tissue Due to Cancer Recurrence. *J Assist Reprod Genet* (2013) 30(7):975–8. doi: 10.1007/s10815-013-0026-x
96. Kim SS, Hwang IT, Lee HC. Heterotopic Autotransplantation of Cryobanked Human Ovarian Tissue as a Strategy to Restore Ovarian Function. *Fertil Steril* (2004) 82(4):930–2. doi: 10.1016/j.fertnstert.2004.02.137
97. Radwan P, Abramik A, Wilczyński J, Radwan M. Successful Autotransplantation of Cryopreserved Ovarian Tissue With Recovery of the Ovarian Function. *Ginekol Pol* (2016) 87(3):235–40. doi: 10.17772/gp/61981
98. Demeestere I, Simon P, Buxant F, Robin V, Fernandez SA, Centner J, et al. Ovarian Function and Spontaneous Pregnancy After Combined Heterotopic and Orthotopic Cryopreserved Ovarian Tissue Transplantation in a Patient Previously Treated With Bone Marrow Transplantation: Case Report. *Hum Reprod* (2006) 21(8):2010–4. doi: 10.1093/humrep/del092
99. Donnez J, Dolmans MM, Demylle D, Jadoul P, Pirard C, Squifflet J, et al. Restoration of Ovarian Function After Orthotopic (Intraovarian and Periovarian) Transplantation of Cryopreserved Ovarian Tissue in a Woman Treated by Bone Marrow Transplantation for Sickle Cell Anaemia: Case Report. *Hum Reprod* (2006) 21(1):183–8. doi: 10.1093/humrep/dei268
100. Demeestere I, Simon P, Dedeken L, Moffa F, Tsépélidis S, Brachet C, et al. Live Birth After Autograft of Ovarian Tissue Cryopreserved During Childhood. *Hum Reprod* (2015) 30(9):2107–9. doi: 10.1093/humrep/dev128
101. Donnez J, Squifflet J, Jadoul P, Demylle D, Cheron AC, Van Langendonckt A, et al. Pregnancy and Live Birth After Autotransplantation of Frozen-Thawed Ovarian Tissue in a Patient With Metastatic Disease Undergoing Chemotherapy and Hematopoietic Stem Cell Transplantation. *Fertil Steril* (2011) 95(5):1787.e1–4. doi: 10.1016/j.fertnstert.2010.11.041
102. Huang JY, Tulandi T, Holzer H, Tan SL, Chian RC. Combining Ovarian Tissue Cryobanking With Retrieval of Immature Oocytes Followed by *In Vitro* Maturation and Vitrification: An Additional Strategy of Fertility Preservation. *Fertil Steril* (2008) 89(3):567–72. doi: 10.1016/j.fertnstert.2007.03.090
103. Huang JY, Tulandi T, Holzer H, Lau NM, Macdonald S, Tan SL, et al. Cryopreservation of Ovarian Tissue and *In Vitro* Matured Oocytes in a Female With Mosaic Turner Syndrome: Case Report. *Hum Reprod* (2008) 23(2):336–9. doi: 10.1093/humrep/dem307
104. Elizur SE, Tulandi T, Meterissian S, Huang JY, Levin D, Tan SL. Fertility Preservation for Young Women With Rectal Cancer–a Combined Approach From One Referral Center. *J Gastrointest Surg* (2009) 13(6):1111–5. doi: 10.1007/s11605-009-0829-3
105. Cheng J, Ruan X, Zhou Q, Li Y, Du J, Jin F, et al. Long-Time Low-Temperature Transportation of Human Ovarian Tissue Before Cryopreservation. *Reprod BioMed Online* (2021) 43(2):172–83. doi: 10.1016/j.rbmo.2021.05.006
106. Isachenko E, Rahimi G, Isachenko V, Nawroth F. *In-Vitro* Maturation of Germinal-Vesicle Oocytes and Cryopreservation in Metaphase I/II: A Possible Additional Option to Preserve Fertility During Ovarian Tissue Cryopreservation. *Reprod BioMed Online* (2004) 8(5):553–7. doi: 10.1016/S1472-6483(10)61102-9
107. Maltaris T, Koelbl H, Fischl F, Seufert R, Schmidt M, Kohl J, et al. Xenotransplantation of Human Ovarian Tissue Pieces in Gonadotropin-Stimulated SCID Mice: The Effect of Ovariectomy. *Anticancer Res* (2006) 26(6b):4171–6.
108. Maltaris T, Dragonas C, Hoffmann I, Mueller A, Beckmann MW, Dittrich R. Simple Prediction of the Survival of Follicles in Cryopreserved Human Ovarian Tissue. *J Reprod Dev* (2006) 52(4):577–82. doi: 10.1262/jrd.18012
109. Maltaris T, Beckmann MW, Binder H, Mueller A, Hoffmann I, Koelbl H, et al. The Effect of a GnRH Agonist on Cryopreserved Human Ovarian Grafts in Severe Combined Immunodeficient Mice. *Reproduction* (2007) 133(2):503–9. doi: 10.1530/REP-06-0061
110. Dittrich R, Mueller A, Binder H, Oppelt PG, Renner SP, Goecke T, et al. First Retransplantation of Cryopreserved Ovarian Tissue Following Cancer Therapy in Germany. *Dtsch Arztebl Int* (2008) 105(15):274–8. doi: 10.3238/arztebl.2008.0274
111. Dittrich R, Lotz L, Keck G, Hoffmann I, Mueller A, Beckmann MW, et al. Live Birth After Ovarian Tissue Autotransplantation Following Overnight Transportation Before Cryopreservation. *Fertil Steril* (2012) 97(2):387–90. doi: 10.1016/j.fertnstert.2011.11.047
112. Lotz L, Liebenthron J, Nichols-Burns SM, Montag M, Hoffmann I, Beckmann MW, et al. Spontaneous Antral Follicle Formation and Metaphase II Oocyte From a non-Stimulated Prepubertal Ovarian Tissue Xenotransplant. *Reprod Biol Endocrinol* (2014) 12:41. doi: 10.1186/1477-7827-12-41
113. Dittrich R, Hackl J, Lotz L, Hoffmann I, Beckmann MW. Pregnancies and Live Births After 20 Transplantations of Cryopreserved Ovarian Tissue in a Single Center. *Fertil Steril* (2015) 103(2):462–8. doi: 10.1016/j.fertnstert.2014.10.045
114. Raffel N, Lotz L, Hoffmann I, Liebenthron J, Söder S, Beckmann MW, et al. Repetitive Maturation of Oocytes From Non-Stimulated Xenografted Ovarian Tissue From a Prepubertal Patient Indicating the Independence of Human Ovarian Tissue. *Geburtshilfe Frauenheilkd* (2017) 77(12):1304–11. doi: 10.1055/s-0043-122601
115. Póvoa A, Xavier P, Calejo L, Soares S, Sousa M, Silva J, et al. First Transplantation of Cryopreserved Ovarian Tissue in Portugal, Stored for 10 Years: An Unexpected Indication. *Reprod BioMed Online* (2016) 32(3):334–6. doi: 10.1016/j.rbmo.2015.12.002
116. Fouks Y, Hamilton E, Cohen Y, Hasson J, Kalma Y, Azem F. *In-Vitro* Maturation of Oocytes Recovered During Cryopreservation of Pre-Pubertal Girls Undergoing Fertility Preservation. *Reprod BioMed Online* (2020) 41(5):869–73. doi: 10.1016/j.rbmo.2020.07.015
117. Walker CA, Bjarkadottir BD, Fatum M, Lane S, Williams SA. Variation in Follicle Health and Development in Cultured Cryopreserved Ovarian Cortical Tissue: A Study of Ovarian Tissue From Patients Undergoing Fertility Preservation. *Hum Fertil (Camb).* (2021) 24(3):188–98. doi: 10.1080/14647273.2019.1616118
118. Rodriguez-Wallberg KA, Karlström PO, Rezapour M, Castellanos E, Hreinsson J, Rasmussen C, et al. Full-Term Newborn After Repeated Ovarian Tissue Transplants in a Patient Treated for Ewing Sarcoma by Sterilizing Pelvic Irradiation and Chemotherapy. *Acta Obstet Gynecol Scand* (2015) 94(3):324–8. doi: 10.1111/aogs.12568
119. Stern CJ, Gook D, Hale LG, Agresta F, Oldham J, Rozen G, et al. First Reported Clinical Pregnancy Following Heterotopic Grafting of Cryopreserved Ovarian Tissue in a Woman After a Bilateral Oophorectomy. *Hum Reprod* (2013) 28(11):2996–9. doi: 10.1093/humrep/det360
120. Gook DA, Edgar DH, Borg J, Archer J, McBain JC. Diagnostic Assessment of the Developmental Potential of Human Cryopreserved Ovarian Tissue From Multiple Patients Using Xenografting. *Hum Reprod* (2005) 20(1):72–8. doi: 10.1093/humrep/deh550
121. Seshadri T, Gook D, Lade S, Spencer A, Grigg A, Tiedemann K, et al. Lack of Evidence of Disease Contamination in Ovarian Tissue Harvested for Cryopreservation From Patients With Hodgkin Lymphoma and Analysis of Factors Predictive of Oocyte Yield. *Br J Cancer* (2006) 94(7):1007–10. doi: 10.1038/sj.bjc.6603050
122. Stern CJ, Toledo MG, Hale LG, Gook DA, Edgar DH. The First Australian Experience of Heterotopic Grafting of Cryopreserved Ovarian Tissue: Evidence of Establishment of Normal Ovarian Function. *Aust N Z J Obstet Gynaecol* (2011) 51(3):268–75. doi: 10.1111/j.1479-828X.2011.01289.x
123. Dolmans MM, Marinescu C, Saussoy P, Van Langendonckt A, Amorim C, Donnez J. Reimplantation of Cryopreserved Ovarian Tissue From Patients

With Acute Lymphoblastic Leukemia is Potentially Unsafe. *Blood* (2010) 116 (16):2908–14. doi: 10.1182/blood-2010-01-265751
124. Schmidt KL, Ernst E, Byskov AG, Nyboe Andersen A, Yding Andersen C. Survival of Primordial Follicles Following Prolonged Transportation of Ovarian Tissue Prior to Cryopreservation. *Hum Reprod* (2003) 18 (12):2654–9. doi: 10.1093/humrep/deg500
125. Khattak H, Malhas R, Craciunas L, Afifi Y, Amorim CA, Fishel S, et al. Fresh and Cryopreserved Ovarian Tissue Transplantation for Preserving Reproductive and Endocrine Function: A Systematic Review and Individual Patient Data Meta-Analysis. *Hum Reprod Update* (2022) 28 (3):400–16. doi: 10.1093/humupd/dmac015
126. Shi Q, Xie Y, Wang Y, Li S. Vitrification Versus Slow Freezing for Human Ovarian Tissue Cryopreservation: A Systematic Review and Meta-Anlaysis. *Sci Rep* (2017) 7(1):8538. doi: 10.1038/s41598-017-09005-7
127. Vilela JMV, Dolmans MM, Amorim CA. Ovarian Tissue Transportation: A Systematic Review. *Reprod BioMed Online* (2021) 42(2):351–65. doi: 10.1016/j.rbmo.2020.11.001
128. Gellert SE, Pors SE, Kristensen SG, Bay-Bjørn AM, Ernst E, Yding Andersen C. Transplantation of Frozen-Thawed Ovarian Tissue: An Update on Worldwide Activity Published in Peer-Reviewed Papers and on the Danish Cohort. *J Assisted Reprod Genet* (2018) 35(4):561–70. doi: 10.1007/s10815-018-1144-2
129. Newton H, Fisher J, Arnold JR, Pegg DE, Faddy MJ, Gosden RG. Permeation of Human Ovarian Tissue With Cryoprotective Agents in Preparation for Cryopreservation. *Hum Reprod* (1998) 13(2):376–80. doi: 10.1093/humrep/13.2.376
130. Gavish Z, Ben-Haim M, Arav A. Cryopreservation of Whole Murine and Porcine Livers. *Rejuvenation Res* (2008) 11(4):765–72. doi: 10.1089/rej.2008.0706
131. Oktay K, Karlikaya G, Aydin B. Ovarian Cryopreservation and Transplantation: Basic Aspects. *Mol Cell Endocrinology* (2000) 169(1-2):105–8. doi: 10.1016/S0303-7207(00)00361-0
132. Suzuki N, Yoshioka N, Takae S, Sugishita Y, Tamura M, Hashimoto S, et al. Successful Fertility Preservation Following Ovarian Tissue Vitrification in Patients With Primary Ovarian Insufficiency. *Hum Reprod* (2015) 30 (3):608–15. doi: 10.1093/humrep/deu353
133. Lunding SA, Pors SE, Kristensen SG, Landersoe SK, Jeppesen JV, Flachs EM, et al. Biopsying, Fragmentation and Autotransplantation of Fresh Ovarian Cortical Tissue in Infertile Women With Diminished Ovarian Reserve. *Hum Reprod* (2019) 34(10):1924–36. doi: 10.1093/humrep/dez152
134. Cleary M, Snow M, Paris M, Shaw J, Cox SL, Jenkin G. Cryopreservation of Mouse Ovarian Tissue Following Prolonged Exposure to an Ischemic Environment. *Cryobiology* (2001) 42(2):121–33. doi: 10.1006/cryo.2001.2315
135. Kim SS, Yang HW, Kang HG, Lee HH, Lee HC, Ko DS, et al. Quantitative Assessment of Ischemic Tissue Damage in Ovarian Cortical Tissue With or Without Antioxidant (Ascorbic Acid) Treatment. *Fertility Sterility* (2004) 82 (3):679–85. doi: 10.1016/j.fertnstert.2004.05.022
136. Oktay K, Marin L, Bedoschi G, Pacheco F, Sugishita Y, Kawahara T, et al. Ovarian Transplantation With Robotic Surgery and a Neovascularizing Human Extracellular Matrix Scaffold: A Case Series in Comparison to Meta-Analytic Data. *Fertil Steril* (2022) 117(1):181–92. doi: 10.1016/j.fertnstert.2021.08.034

Conflict of Interest: ML is an Advisor for Dimension Inx, LLC.

The remaining authors declare that the research was conducted in the absence of any commercial or financial relationships that could be construed as a potential conflict of interest.

Publisher's Note: All claims expressed in this article are solely those of the authors and do not necessarily represent those of their affiliated organizations, or those of the publisher, the editors and the reviewers. Any product that may be evaluated in this article, or claim that may be made by its manufacturer, is not guaranteed or endorsed by the publisher.

frontiers | Frontiers in Endocrinology

ORIGINAL RESEARCH
published: 20 June 2022
doi: 10.3389/fendo.2022.896357

Noninvasive Chromosome Screening for Evaluating the Clinical Outcomes of Patients With Recurrent Pregnancy Loss or Repeated Implantation Failure

Haitao Xi[1,2], Lin Qiu[2], Yaxin Yao[3], Lanzi Luo[1], Liucai Sui[2], Yanghua Fu[2], Qiuyi Weng[2], Jing Wang[3], Junzhao Zhao[2] and Yingzheng Zhao[1]**

[1] Department of Pharmaceutics, School of Pharmaceutical Sciences, Wenzhou Medical University, Wenzhou, China, [2] Department of Obstetrics and Gynecology, Reproductive Medicine Center, The Second Affiliated Hospital of Wenzhou Medical University, Wenzhou, China, [3] Department of Clinical Research, Yikon Genomics, Suzhou, China

OPEN ACCESS

Edited by:
Yuting Fan,
Boston IVF, United States

Reviewed by:
Marion Martins,
Boston IVF, United States
William Kutteh,
University of Tennessee Health Science Center (UTHSC), United States
Alan Decherney,
Clinical Center (NIH), United States

***Correspondence:**
Junzhao Zhao
z.joyce08@163.com
Yingzheng Zhao
pharmtds@163.com

Specialty section:
This article was submitted to Reproduction, a section of the journal Frontiers in Endocrinology

Received: 15 March 2022
Accepted: 16 May 2022
Published: 20 June 2022

Citation:
Xi H, Qiu L, Yao Y, Luo L, Sui L, Fu Y, Weng Q, Wang J, Zhao J and Zhao Y (2022) Noninvasive Chromosome Screening for Evaluating the Clinical Outcomes of Patients With Recurrent Pregnancy Loss or Repeated Implantation Failure. Front. Endocrinol. 13:896357. doi: 10.3389/fendo.2022.896357

This retrospective cohort study explores whether noninvasive chromosome screening (NICS) for aneuploidy can improve the clinical outcomes of patients with recurrent pregnancy loss (RPL) or repeated implantation failure (RIF) in assisted reproductive technology. A total of 273 women with a history of RPL or RIF between 2018 and 2021 were included in this study. We collected data of all oocyte retrieval cycles and single blastocyst resuscitation transfer cycles. For the patients experiencing RPL, NICS reduced the miscarriages rate per frozen embryo transfer (FET), improved the ongoing pregnancies rate and live birth rate: 17.9% vs 42.6%, adjusted OR 0.39, 95% CI 0.16–0.95; 40.7% vs 25.0%, adjusted OR 2.00, 95% CI 1.04–3.82; 38.9% vs 20.6%, adjusted OR 2.53, 95% CI 1.28–5.02, respectively. For the patients experiencing RIF, the pregnancy rates per FET in the NICS group were significantly higher than those in the non-NICS group (46.9% vs. 28.7%, adjusted OR 2.82, 95% CI 1.20–6.66). This study demonstrated that the selection of euploid embryos through NICS can reduce the miscarriage rate of patients experiencing RPL and improve the clinical pregnancy rate of patients experiencing RIF. Our data suggested NICS could be considered as a possibly useful screening test in clinical practice.

Keywords: noninvasive chromosome screening, repeated implantation failure, recurrent pregnancy loss, assisted reproductive technology, clinical outcomes

INTRODUCTION

In vitro fertilization-embryo transfer (IVF-ET) is an effective method to treat infertility widely performed worldwide (1). Nevertheless, chromosomal abnormalities often exist in early human embryos, leading to embryo implantation failure and pregnancy loss during IVF treatment (2, 3), especially in patients with a history of recurrent pregnancy loss (RPL) and repeated implantation

failure (RIF) (4–6). RPL is defined as the loss of ≥2 pregnancies, which is confirmed at least by either serum or urine b-hCG, i.e. including non-visualized pregnancy losses (biochemical pregnancy losses and/or resolved and treated pregnancies of unknown location) (7), whereas RIF is the failure of ≥3 implantations (8). Sahoo et al. (9) reported that chromosome abnormalities were detected in 3,975 of 7,396 (53.7%) cases of miscarriage tissues. Besides, Kort et al. (6) analyzed 10,711 cases of blastocysts retrospectively and found that the incidence of embryo aneuploidy was significantly higher in patients experiencing RIF than in the control group.

Currently, the most commonly used embryo selection method is morphological evaluation. However, the chromosomes of embryos cannot be identified *via* morphology (2, 3). Among blastocysts with good morphology, only 42% of embryos had normal chromosomes. Among these, only 30% of ICM graded A Embryos, the chromosomes, were normal (10). Therefore, in some special populations [such as women with recurrent miscarriage and repeated implantation failure (RIF)], embryos are usually evaluated through pre-implantation genetic testing for aneuploidy (PGT-A) (11–13). A retrospective study showed that the live birth and clinical pregnancy rate were improved through the PGT-A in women with RPL (14). The authors included 1,389 blastocysts derived from PGT-A cycles in IVF patients with advanced maternal age, those with RIF, those with recurrent miscarriage, and oocyte donors. Compared to that in the control group without PGT-A, the live birth rates of the four groups were improved (15). However, specific equipment and extensive expertise are required for the biopsy procedure, restraining the utility of PGT-A in assisted reproduction. Moreover, the embryos were screened for chromosomal ploidy before transferring to the uterus (16, 17), and the long-term impact of biopsy is an important concern for undetermined health risks, such as adrenal development and response to cold stress (18), epigenetic reprogramming (19), and neurological conditions (20). Notably, implantation rates were lower with increased biopsied trophectoderm (TE) cell numbers and sizes than with appropriate cell numbers and sizes (21, 22).

Stigliani et al. (23) first observed genomic DNA contents in embryo culture medium. Since then, multiple studies have been published using culture medium or blastocoelic fluid for analyzing chromosomal ploidy (24–31). Xu et al. (27) first reported a noninvasive chromosome screening (NICS) assay based on a Multiple Annealing and Looping-Based Amplification Cycle-Next Generation Sequencing (NGS) strategy using spent blastocyst culture medium, which was validated in 42 IVF and resulted in five live births among seven women. Fang et al. (29) obtained an ongoing pregnancy rate of 58% and reported 27 normal live births in a pilot clinical study using NICS. Nevertheless, the clinical application of NICS has been evaluated only in small-scale trials.

Here, we designed a retrospective cohort study including 273 patients experiencing RPL or RIF to confirm the clinical value of NICS. To the best of our knowledge, this is the first large-scale validation study of NICS in the patients experiencing RPL or RIF.

MATERIALS AND METHODS

Study Participants and Data Collection

We initially included 303 women with a history of RPL (≥2 pregnancies) (7) or RIF (≥3implantations) (8), exclusion criteria were APS, diabetes, hypothyroidism or other severe complications, from July 2018 to May 2021, according to the records of the Reproductive Centre at the Second Affiliated Hospital of Wenzhou Medical University. However, 10 women that abandoned embryo transfer and 20 women with chromosomal rearrangements, abnormal uterine cavity morphology, endometrial lesions, endometrial injury, intrauterine effusion, or untreated hydrosalpinx were excluded from the study. The final cohort comprised 273 women, from which we collected data of all oocyte retrieval cycles and single blastocyst resuscitation transfer cycles.

The variables analyzed in the study were: age at retrieval, the history of pregnancies, live births, and miscarriages, body mass index (BMI), hormone levels, the number of oocyte retrieval cycles, oocytes, cleavages, and D5 or D6 blastocysts, and blastocyst morphology (expansion, inner cell mass, and trophectoderm). After consulting patients, we divided them into two groups. Patients experiencing RPL or RIF who received the noninvasive chromosome screening for aneuploidy were included in the NICS group, while those who underwent conventional morphology embryo transfer during the same period were included in the non-NICS group. The euploid embryos were transferred to the NICS group. The study design is illustrated in **Figure 1**.

Oocyte Retrieval and Embryo Culture

This study was performed at the first IVF/Intracytoplasmic Sperm Injection (ICSI) cycles after injection of 3.75 mg triptorelin for prolonged pituitary downregulation in the follicular phase of the menstrual cycle. Ovarian stimulation with exogenous gonadotropins promoted the growth of follicles. When two or more leading follicles reached 18 mm, ovulation was induced with 10,000 IU human chorionic gonadotropin (hCG). Oocyte retrieval was performed at 35 h post-hCG administration. Cumulus-enclosed oocytes were separated from the follicular fluid, placed in a medium, and incubated at 37°C incubated d Cumulus-encl$_2$ atmosphere for 2 h. Routine IVF or ICSI was performed based on sperm quality. The embryos were placed in droplets of G-1 PLUS medium (Vitrolife, Göteborg Sweden) in AMP-30D incubators (Bioz, Los Altos, CA, USA) in a 6.0% CO_2 and 5% O_2 balance N_2 atmosphere at 37°C.

Blastocyst Culture and Transfer

D3 embryos were placed in 30-μL droplets of G-2 PLUS medium (Vitrolife) supplemented with washed and pre-gassed mineral oil (Sage, Atlanta, GA, USA) and cultured to the blastocyst stage in AMP-30D incubators (Bioz) in a 6.0% CO_2 and 5% O_2 balance N_2 atmosphere at 37°C. At 2 d of culture, the development and quality of blastocysts were evaluated according to the blastocyst scoring system, including expansion (1–6), inner cell mass (A, B, C), and trophectoderm (A, B, C). Blastocysts were categorized

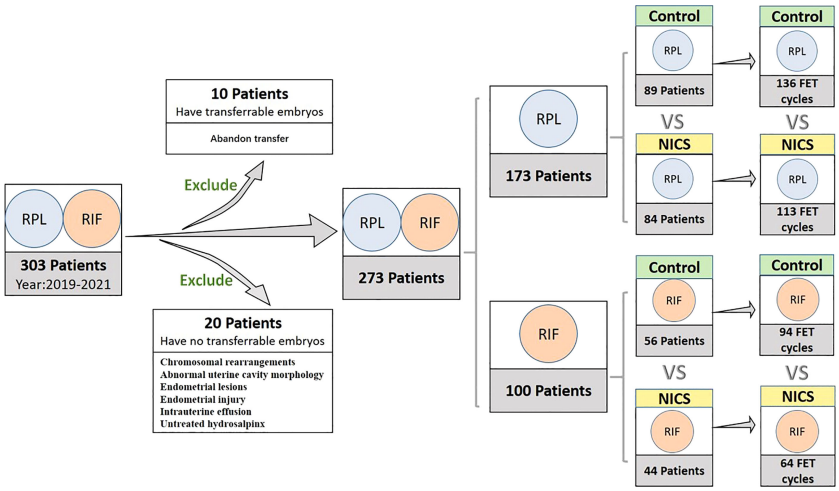

FIGURE 1 | Inclusion and classification of patient selection in this study. NICS, noninvasive chromosome screening; RPL, recurrent pregnancy loss; RIF, repeated implantation failure; Control, blastocyst morphology (non-NICS).

into good, fair, or poor quality based on the simplified SART embryo scoring system (30). The grade is good when the ICM/TE is AA, AB, or BA; the grade is fair when the ICM/TE is BB or AC; the grade is poor when the ICM/TE is CA, BC, or CB. All blastocysts were previously frozen and thawed by vitrification using the Cryotop Safety kit (Kitazato, Fuji-shi, Shizuoka, Japan), according to the manufacturer's instructions. A single blastocyst was selected for transfer to each patient based on morphology (nonintervention group) or NICS results (intervention group).

Sample Collection for NICS Assay

To prevent medium cross-contamination, different Pasteur pipettes were used for each embryo. Approximately 30 µL of blastocyst medium from each embryo was transferred into RNase-DNase-free PCR tubes containing 5 µL of cell lysis buffer (Yikon Genomics, Suzhou, China). the same amount of blastocyst culture medium was collected to be used as a negative control. All collected samples were flash-frozen in liquid nitrogen and stored at -80°C until subjected to the NICS assay.

Whole-Genome Amplification and NGS Data Analysis

Whole-genome amplification was performed using culture media, followed by library preparation using ChromInst (Yikon Genomics; EK100100724 NICS Inst Library Preparation Kit). NGS was performed on an Illumina MiSeq platform that yielded approximately 2 million sequence reads from each sample. The high-quality reads were extracted and mapped to the human hg19 genome. After removing duplication reads, the read numbers were counted along the whole genome with a bin size of 1 Mb and normalized by the GC content, as well as a reference dataset to represent the relative copy number. The copy number of each bin was then segmented by circular binary segmentation (CBS) algorithms to merge bins with similar trends and calculate the final copy numbers.

Assessment of Outcome Variables

Our primary outcomes included the clinical pregnancy rates, miscarriage rates, and ongoing pregnancy rates. The clinical pregnancy rate was defined as the number of cycles with gestational sacs visualized on transvaginal ultrasonography divided by the total number of transplant cycles. The miscarriage rate was calculated as the number of pregnancy failures after a gestational sac was documented by transvaginal ultrasonography divided by the total number of clinical pregnancies. The ongoing pregnancy rate was the number of cycles of any pregnancy that went beyond 12 weeks of gestation, divided by the total number of transplant cycles. Ectopic pregnancy was considered a clinical pregnancy and not a miscarriage.

Statistical Analysis

Descriptive data for continuous variables are presented as means ± standard deviation, whereas categoric data as numbers and percentages. The Student's *t*-test or Mann–Whitney test were used to identify significant differences in parametric and non-parametric data, respectively. The chi-square test or Fisher exact test were used for categoric variables in each group. Multiple logistic regression analysis was conducted to compare the outcomes of NICS and non-NICS groups after controlling the covariables at $p < 0.10$ and covariables considered clinically influential.

All analyses were conducted using the statistical software BMI SPSS, Version 25. A P-value < 0.05 was considered denoting statistical significance.

Ethics Approval and Consent to Participate

This study was approved by the Institutional Review Board (IRB) of the Second Affiliated Hospital of Wenzhou Medical University (number: 2021-K-13-01). Informed consent was obtained in accordance with the institutional guidelines before embryo analysis.

RESULTS

Variable Analysis

Of the 303 women initially included in the study, 10 that abandoned embryo transfer and 20 that had no transferrable embryos were excluded from the final cohort. Finally, blastocysts were transferred to 273 women during 407 transfer cycles (**Figure 1**).

Of the 173 patients with a history of RPL, were enrolled in the study, of which 84 were for the NICS group and 89 were included as the non-NICS group. In total, 113 FET cycles were performed for the patients in the NICS group, and 136 high-quality blastocysts were obtained from 89 patients (**Table 1**). Of the 100 patients with a history of RIF, 44 were for the NICS group and 56 for the non-NICS group. In total, 64 FET cycles were performed for the patients in the NICS group, and 94 high-quality blastocysts were obtained from the non-NICS group (**Table 2**).

Data variables analyzed in this study were age at retrieval, the history of pregnancies, live births, and miscarriages, BMI, hormone levels, the number of oocyte retrieval cycles, oocytes, cleavages, and D5 or D6 blastocysts, and blastocyst morphology (expansion, inner cell mass, and trophectoderm) were comparable by Student's t-test or Mann–Whitney *U* test, each as appropriate (**Tables 1**, **2**).

Our analysis showed no significant differences in age, BMI, and hormone levels between the NICS and non-NICS groups in patients experiencing RPL or RIF. The number of previous miscarriages in the NICS group of patients experiencing RPL or RIF was significantly higher than in the non-NICS group. Besides, infertility duration showed statistical significance (p = 0.001, p = 0.004) in the NICS group and non-NICS group, no matter which feature the patients were in. The number of miscarriages and infertility duration affected clinical outcomes. Thus, they were included in the multiple logistic regression analysis.

Blastocyst Morphological Assessments and NICS Results

The blastocyst transplantation was based on morphology and NICS results. Blastocysts were evaluated based on their development and quality using the Gardner scores system and divided into three categories: good (AA/BA/AB), fair (BB/AC), and poor (CA/BC/CB) (32). As shown in **Tables 1**, **2**, no significant differences were observed between the NICS group and the control group of patients experiencing RIF. Of the patients experiencing RPL, the non-NICS group was lower than the NICS group (37.2% vs. 24.3%) in the poor category; however, there was no significant difference between the other two categories.

TABLE 1 | Baseline demographics of patients experiencing recurrent pregnancy loss (RPL) after embryo selection by noninvasive chromosome screening (NICS) versus blastocyst morphology (Non-NICS).

Variable	NICS	Non-NICS	*p*-value
Number of patients	84	89	
Female age (y)	32.4 ± 3.8	33.4 ± 4.7	0.109
Female body mass index (kg m^{-2})	22.1 ± 2.8	22.4 ± 3.1	0.371
Male age (y)	34.7 ± 4.1	35.2 ± 4.7	0.381
Male body mass index (kg m^{-2})	24.0 ± 3.0	24.5 ± 3.2	0.293
Infertility duration (y)	1.4 ± 0.7	2.1 ± 2.2	0.001
Number of prior miscarriages	2.9 ± 1.3	2.5 ± 1.1	0.023
Number of previous embryo transfers	0.63 ± 1.0	2.2 ± 1.8	<0.001
Number of prior live births	5 (6.0%)	1 (1.1%)	0.108
Prolactin (ng m^{-1})	20.0 ± 44.9	21.4 ± 45.9	0.831
Testosterone	0.5 ± 0.3	0.9 ± 4.3	0.415
Progesterone	0.7 ± 0.5	0.6 ± 0.6	0.357
Follicle-stimulating hormone	6.8 ± 2.1	7.5 ± 4.2	0.158
Luteinizing hormone	4.8 ± 3.7	5.8 ± 9.6	0.349
Estradiol	62.7 ± 58.1	66.7 ± 71.88	0.673
Number of COH cycles	87	105	
Number of COH cycles per patient	1.04	1.18	0.007
Gonadotropin days ($\bar{x}$ ± SD)	10.2 ± 2.1	10.5 ± 2.9	0.416
Gonadotropin dosage (×75 IU, $\bar{x}$ ± SD)	2,065.3 ± 768.1	1,956.3 ± 856.9	0.359
Number of retrieval oocytes ($\bar{x}$ ± SD)	12.8 ± 7.0	12.8 ± 7.3	0.977
Number of cleaving zygotes ($\bar{x}$ ± SD)	8.9 ± 4.7	9.5 ± 6.0	0.441
Number of blastocysts	4.7 ± 3.3	4.4 ± 3.1	0.513
Number of FET cycles	113	136	
Embryos at day 5	80 (70.8%)	114 (83.8%)	0.014
Embryos at day 6	33 (29.2%)	22 (16.2%)	
Blastocyst quality, Good (AA/BA/AB)	36 (31.9%)	45 (33.1%)	0.837
Blastocyst quality, Fair (BB/AC)	35 (31.0%)	58 (42.6%)	0.058
Blastocyst quality, Poor (CA/BC/CB)	42 (37.2%)	33 (24.3%)	0.027
Number of embryos	371		
Aneuploidy rate	195/371(52.56%)		

COH, controlled ovarian hyperstimulation; SD, standard deviation; FET, frozen-thawed embryo transfer. A total of 371 embryos were examined in the RPL group for aneuploidy.

TABLE 2 | Baseline demographics of patients experiencing repeated implantation failure (RIF) after embryo selection by noninvasive chromosome screening (NICS) versus blastocyst morphology (Non-NICS).

Variable	NICS	Non-NICS	*p*-value
Number of patients	44	56	
Female age (y)	32.1 ± 4.7	33.3 ± 4.3	0.143
Female body mass index (kg m^{-2})	21.0 ± 2.5	21.7 ± 2.4	0.101
Male age (y)	34.2 ± 5.2	34.9 ± 4.9	0.407
Male body mass index (kg m^{-2})	24.2 ± 3.4	23.8 ± 3.4	0.498
Infertility duration (y)	3.5 ± 2.9	5.2 ± 3.0	0.004
Number of prior miscarriages	1.9 ± 1.2	0.8 ± 1.1	<0.001
Number of previous embryo transfers	4.4 ± 1.3	4.2 ± 1.3	0.379
Number of prior live births	1/44 (2.3%)	0	
Prolactin (ng m^{-1})	26.2 ± 76.4	15.1 ± 9.9	0.231
Testosterone	0.5 ± 0.2	0.5 ± 0.3	0.973
Progesterone	0.8 ± 1.0	0.6 ± 0.3	0.287
Follicle-stimulating hormone	7.8 ± 2.4	7.5 ± 3.5	0.608
Luteinizing hormone	5.2 ± 2.2	4.5 ± 2.7	0.108
Estradiol	50.4 ± 25.8	51.2 ± 41.70	0.913
Number of COH cycles	44	70	
Number of COH cycles per patient	1	1.3	<0.001
Gonadotropin days ($\bar{x}$ ± SD)	10.0 ± 2.4	11.0 ± 2.4	0.03
Gonadotropin dosage (×75 IU, $\bar{x}$ ± SD)	1,838.4 ± 748.3	2,192.1 ± 872.7	0.028
Number of retrieval oocytes ($\bar{x}$ ± SD)	13.9 ± 7.5	13.0 ± 7.5	0.551
Number of cleaving zygotes ($\bar{x}$ ± SD)	10.8 ± 6.1	9.7 ± 5.4	0.319
Number of blastocysts ($\bar{x}$ ± SD)	5.3 ± 2.8	4.2 ± 3.2	0.059
Number of FET cycles	64	94	
Embryos at day 5	48 (75.0%)	64 (68.1%)	0.24
Embryos at day 6	16 (25.0%)	30 (31.9%)	
Blastocyst quality, Good (AA/BA/AB)	11 (17.2%)	22 (23.4%)	0.345
Blastocyst quality, Fair (BB/AC)	31 (48.4%)	34 (36.2%)	0.124
Blastocyst quality, Poor (CA/BC/CB)	22 (34.4%)	38 (40.4%)	0.442
Number of embryos	189		
Aneuploidy rate	107/189 (56.61%)		

COH, controlled ovarian hyperstimulation; SD, standard deviation; FET, frozen-thawed embryo transfer. A total of 189 embryos were examined in the RIF group for aneuploidy.

In the NICS assay, we sequenced approximately 2 million reads on each culture medium sample. The read numbers were counted along the 24 chromosomes with a bin size of 1 Mb and normalized by the mean of the corresponding bin in all samples. Examples of the results of NICS were demonstrated in **Additional File 1**.

Comparison of Clinical Outcomes Between NICS and Non-NICS Groups for Patients Experiencing RPL or RIF

For the patients experiencing RPL, the miscarriage rate per FET was significantly lower in the NICS group than in the non-NICS group (17.9% vs. 42.6%, adjusted OR 0.39, 95% CI 0.16–0.95), whereas the ongoing pregnancy rate (40.7% vs. 25.0%, adjusted OR 2.0, 95% CI 1.04–3.82) and live birth rate (38.9% vs. 20.6%, adjusted OR 2.53, 95% CI 1.28–5.02) were significantly higher in the NICS group compared to the non-NICS group (**Figure 2**; **Table 3**). Nevertheless, no differences were identified in pregnancy rates per patient between the NICS and non-NICS groups (49.6% vs. 44.9%, adjusted OR 1.13, 95% CI 0.61–2.07; **Table 3**).

For the patients experiencing RIF, the pregnancy rates per FET were significantly higher in the NICS group than in the non-NICS group (46.9% vs. 28.7%, adjusted OR 2.82 95% CI 1.20–6.66. **Figure 3**; **Table 4**), whereas the live birth rate and ongoing pregnancy rate per FET and per patient were no significant difference in the NICS group than in the non-NICS group. Nevertheless, no differences were identified in the miscarriage rate per clinical pregnancy between the NICS and non-NICS groups (23.3% vs. 25.9%, adjusted OR 1.35, 95% CI 0.34–5.42; **Table 4**).

DISCUSSION

To our knowledge, this is the first large-scale study to confirm the effectiveness of NICS as a diagnostic test for the outcomes of IVF in women with a history of RPL or RIF. We demonstrated that the miscarriage rate was significantly lower in women with RPL (n = 173), whereas the pregnancy rate was significantly higher in the NICS group than in the non-NICS group of women with RIF (n = 100). To confirm that the improvement of clinical outcomes in the NICS group was related to the genetic testing alone despite the other factors, we included the variables at $p < 0.10$ and related to the clinical outcome in the adjusted models. Our results strongly supported the high clinical value of NICS in women with RPL before embryo transfer since it significantly increased the live birth rate per transfer cycle through the multiple logistic

TABLE 3 | Comparison of clinical outcomes patients experiencing recurrent pregnancy loss (RPL).

	NICS	Non-NICS	Adjusted odds ratio (95% CI), *p*-value
Number of transferred cycles	113	136	
Clinical pregnancies rate (%)	56/113 (49.6%)	61/136 (44.9%)	1.13 (0.61–2.07), 0.697
Miscarriages rate (%)	10/56 (17.9%)	26/61 (42.6%)	0.39 (0.16–0.95), 0.038
Ectopic pregnancies	0	1/61 (1.6%)	
Ongoing pregnancies rate (%)	46/113 (40.7%)	34/136 (25.0%)	2.0 (1.04–3.82), 0.037
Live birth rate (%)	44/113 (38.9%)	28/136 (20.6%)	2.53 (1.28–5.02), 0.008

NICS group, embryo selection by noninvasive chromosome screening; control group, blastocyst morphology.
**Adjusted for female age, infertility duration, number of prior miscarriages, number of previous embryo transfers, number of COH cycles, embryo morphology, and Day 5/6 blastocysts.*

regression analysis (38.9% vs. 20.6%, adjusted OR 2.53, 95% CI 1.28-5.02). The pregnancy rates per FET in the NICS group were significantly higher than in the non-NICS control group (46.9% vs. 28.7%, adjusted OR 2.82, 95% CI 1.20–6.66) for the patients experiencing RIF. Similarly, Fang et al. obtained an ongoing pregnancy rate of 58% and reported 27 normal live births in patients experiencing RPL or RIF after transferring 50 embryos identified as euploid by NICS (29).

In this study, women with RPL had a history of ≥2 miscarriages, spontaneous abortion, and/or biochemical pregnancy, as described in the ESHRE guideline (7, 31). The definition of RPL differs among organizations. For instance, the Royal College of Obstetricians and Gynecologists and the European Society of Human Reproduction and Embryology support that a miscarriage includes all pregnancy ≥3 losses up to 24 weeks of gestation, whereas the American Society for Reproductive Medicine does not provide a time limit and ≥2 miscarriages of pregnancy, excludes biochemical pregnancy (32). The rate of chromosome abnormality decreases with the developmental stage: 70–80% in clinical miscarriages (33), 4% in stillbirths, and 0.3% in newborn babies (34). The selection of euploid embryos can reduce the rate of miscarriages, which are probably caused by chromosome abnormalities (35).

Women with RIF had a history of ≥3 failed implantations of 4–6 high-score blastomeres or >3 high-score blastocysts (8). A retrospective analysis of 10,711 blastocysts showed that the incidence of blastocyst aneuploidy in patients experiencing RIF is significantly higher than that in the control group, and embryo aneuploidy is a primary reason for implantation failure (6). A clinical study suggested that transplanting euploid embryos may help patients experiencing RIF to achieve pregnancy (36). A multi-center, prospective, pilot study showed that screening for embryo ploidy improved the live birth rate per embryo transfer procedure in both RPL (52.4% vs 21.6%) and RIF group (62.5% vs 31.7%), which indicated PGT-A has an advantage reducing the number of embryo transfer cycles (37).

Chromosome aneuploidy is common in embryos following IVF, even in younger women, and is a major failure factor. Although morphology is correlated with euploidy, it can only increase euploidy by a few percentage points at most when used to select replacement embryos. Embryos with good morphology may have chromosomal abnormalities (10). Routine embryo screening for aneuploidy requires intensive biopsy procedures, which are costly and time-consuming. The accuracy of NICS has been verified in many studies, and a 58% clinical pregnancy success rate has been reported for patients experiencing RIF and RPL (29). Recently, the utility of niPGT-A is challenged in the article by Hanson et al. (38). Here, we also found that NICS

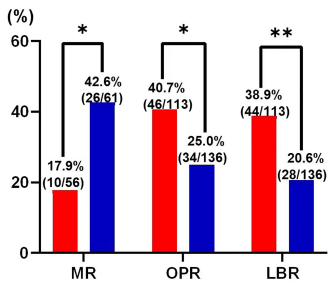

FIGURE 2 | Pregnancy outcomes of patients with recurrent pregnancy loss (RPR) after embryo selection by noninvasive chromosome screening (NICS) versus blastocyst morphology (control). MR, miscarriages rate; OPR, ongoing pregnancy rate; LBR, live birth rate. *$p < 0.05$, **$p < 0.01$.

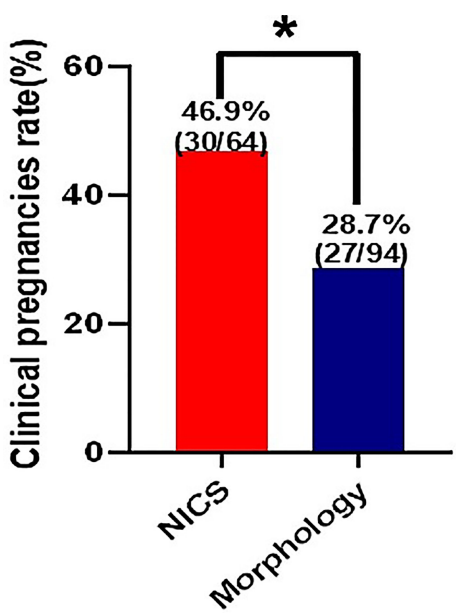

FIGURE 3 | Clinical pregnancy rate of patients with repeated implantation failure (RIF) after embryo selection by noninvasive chromosome screening (NICS) versus blastocyst morphology (control). *$p < 0.05$.

TABLE 4 | Comparison of clinical outcomes patients experiencing recurrent implantation failure.

	NICS	Non-NICS	Adjusted odds ratio (95% CI), *p*-value
Number of transferred cycles	64	94	
Clinical pregnancies rate (%)	30/64 (46.9%)	27/94 (28.7%)	2.82 (1.20–6.66), 0.018
Miscarriages rate (%)	7/30 (23.3%)	7/27 (25.9%)	1.35 (0.34–5.42), 0.671
Ectopic pregnancies	3/30 (10%)	0	
Ongoing pregnancies rate (%)	20/64 (31.3%)	20/94 (21.3%)	2.19 (0.88–5.47), 0.094
Live birth rate (%)	19/64 (29.7%)	20/94 (21.3%)	1.96 (0.78–4.92), 0.154

NICS group, embryo selection by noninvasive chromosome screening; control group, blastocyst morphology.
**Adjusted for female age, infertility duration, number of prior miscarriages, number of COH cycles, gonadotropin days, gonadotropin dosage, number of blastocysts embryo morphology and Day 5/6 blastocysts.*

allowed the selection of embryos, increasing the live birth rates in women with RPL and improving the clinical pregnancy rates in women with RIF based on many patients, which is meaningful to both clinicians and basic scientists on NICS assay. Chen et al. (39) assessed the performance by comparing with the CNV from the whole embryo assay as the gold standard. The differences of sensitivity, specificity, NPV, and PPV between TE-PGT and NICS were not statistically significant. Our center is participating in a multi-unit clinical trial for women ≥35 years of age to further validate the clinical value of NICS since a more comprehensive application requires advanced technology such as modified WGA and sequencing protocols and novel diagnostic algorithms. The validation of NICS in different populations and the accumulation of detectable sample sizes may help markedly reduce the detection cost per embryo.

There are limitations in our study: 1) as a retrospective study, patients in the NICS groups had different clinical prognoses than those in the non-NICS groups, introducing bias in the study results, and 2) the loss and cycle cancelation caused by euploid selection after NICS was not calculated since only women with a good prognosis reach the blastocyst stage and have an euploid embryo to transfer.

Our large-scale retrospective study demonstrated noninvasive chromosome screening for aneuploidy improved the clinical outcomes for patients experiencing RPL or RIF. NICS could be considered as a possibly useful screening test in clinical practice.

DATA AVAILABILITY STATEMENT

Data of this project can be accessed after an approval application to the China National Genebank (CNGB, https://db.cngb.org/cnsa/). Please refer to https://db.cngb.org/ for detailed data, accession number CNP0002817.

ETHICS STATEMENT

The studies involving human participants were reviewed and approved by the Institutional Review Board (IRB) of the Second Affiliated Hospital of Wenzhou Medical University. The patients/participants provided their written informed consent to participate in this study.

AUTHOR CONTRIBUTIONS

HX conceived of the presented idea and the experiments, developed the theory, performed the computations and wrote manuscript; LQ developed the theory, analyzed data and wrote manuscript; YY and LL carried out the experiment and investigation; LS helped to perform the analysis with constructive discussions.; YF and QW collected and analyzed data; JW assisted with the experiments; JZ and YZ administrated the whole project. All authors discussed the results and contributed to the final manuscript.

FUNDING

This study was supported by the Research Fund for Lin He's Academician Workstation of New Medicine and Clinical Translation at the Second Affiliated Hospital of Wenzhou Medical University (grant no. 18331105) and the National Key Research and Development Program (grant no. 2018YFC1003103).

ACKNOWLEDGMENTS

The authors would like to thank Shiping Bo and Shujie Ma for their assistance in NGS data analysis as well as Tuan Li and Yangyun Zou for statistical analysis.

SUPPLEMENTARY MATERIAL

The Supplementary Material for this article can be found online at: https://www.frontiersin.org/articles/10.3389/fendo.2022.896357/full#supplementary-material

REFERENCES

1. Gardner DK, Schoolcraft WB. Culture and Transfer of Human Blastocysts. *Curr Opin Obstet Gynecol* (1999) 11:307–11. doi: 10.1097/00001703-199906000-00013
2. Alfarawati S, Fragouli E, Colls P, Stevens J, Gutiérrez-Mateo C, Schoolcraft WB, et al. The Relationship Between Blastocyst Morphology, Chromosomal Abnormality, and Embryo Gender. *Fertil Steril* (2011) 95:520–4. doi: 10.1016/j.fertnstert.2010.04.003
3. Capalbo A, Rienzi L, Cimadomo D, Maggiulli R, Elliott T, Wright G, et al. Correlation Between Standard Blastocyst Morphology, Euploidy and Implantation: An Observational Study in Two Centers Involving 956 Screened Blastocysts. *Hum Reprod* (2014) 29:1173–81. doi: 10.1093/humrep/deu033
4. Dai R, Xi Q, Wang R, Zhang H, Jiang Y, Li L, et al. Chromosomal Copy Number Variations in Products of Conception From Spontaneous Abortion by Next-Generation Sequencing Technology. *Med (Baltim)* (2019) 98:e18041. doi: 10.1097/MD.0000000000018041
5. Elkarhat Z, Kindil Z, Zarouf L, Razoki L, Aboulfaraj J, Elbakay C, et al. Chromosomal Abnormalities in Couples With Recurrent Spontaneous Miscarriage: A 21-Year Retrospective Study, a Report of a Novel Insertion, and a Literature Review. *J Assist Reprod Genet* (2019) 36:499–507. doi: 10.1007/s10815-018-1373-4
6. Kort JD, McCoy RC, Demko Z, Lathi RB. Are Blastocyst Aneuploidy Rates Different Between Fertile and Infertile Populations? *J Assist Reprod Genet* (2018) 35:403–8. doi: 10.1007/s10815-017-1060-x
7. The European Society of Human Reproduction and Embryology. Definitions of Infertility and Recurrent Pregnancy Loss: A Committee Opinion. *Fertil Steril* (2020) 113:533–5. doi: 10.1016/j.fertnstert.2019.11.025
8. Coughlan C, Ledger W, Wang Q, Liu F, Demirol A, Gurgan T, et al. Recurrent Implantation Failure: Definition and Management. *Reprod Biomed Online* (2014) 28:14–38. doi: 10.1016/j.rbmo.2013.08.011
9. Sahoo T, Dzidic N, Strecker MN, Commander S, Travis MK, Doherty C, et al. Comprehensive Genetic Analysis of Pregnancy Loss by Chromosomal Microarrays: Outcomes, Benefits, and Challenges. *Genet Med* (2017) 19:83–9. doi: 10.1038/gim.2016.69
10. Munné S, Wells D, Cohen J. Technology Requirements for Preimplantation Genetic Diagnosis to Improve Assisted Reproduction Outcomes. *Fertil Steril* (2010) 94:408–30. doi: 10.1016/j.fertnstert.2009.02.091
11. Greco E, Bono S, Ruberti A, Lobascio AM, Greco P, Biricik A, et al. Comparative Genomic Hybridization Selection of Blastocysts for Repeated Implantation Failure Treatment: A Pilot Study. *BioMed Res Int* (2014) 2014:1–10. doi: 10.1155/2014/457913
12. Lei C-X, Ye J-F, Sui Y-L, Zhang Y-P, Sun X-X. Retrospective Cohort Study of Preimplantation Genetic Testing for Aneuploidy With Comprehensive Chromosome Screening Versus Nonpreimplantation Genetic Testing in Normal Karyotype, Secondary Infertility Patients With Recurrent Pregnancy Loss. *Reprod Dev Med* (2019) 3:205. doi: 10.4103/2096-2924.274544
13. Cozzolino M, Diaz-Gimeno P, Pellicer A, Garrido N. Evaluation of the Endometrial Receptivity Assay and the Preimplantation Genetic Test for Aneuploidy in Overcoming Recurrent Implantation Failure. *J Assist Reprod Genet* (2020) 37:2989–97. doi: 10.1007/s10815-020-01948-7
14. Bhatt SJ, Marchetto NM, Roy J, Morelli SS, McGovern PG. Pregnancy Outcomes Following *In Vitro* Fertilization Frozen Embryo Transfer (IVF-FET) With or Without Preimplantation Genetic Testing for Aneuploidy (PGT-A) in Women With Recurrent Pregnancy Loss (RPL): A SART-CORS Study. *Hum Reprod* (2021) 36:2339–44. doi: 10.1093/humrep/deab117
15. Lee C-I, Wu C-H, Pai Y-P, Chang Y-J, Chen C-I, Lee T-H, et al. Performance of Preimplantation Genetic Testing for Aneuploidy in IVF Cycles for Patients With Advanced Maternal Age, Repeat Implantation Failure, and Idiopathic Recurrent Miscarriage. *Taiwan J Obstet Gynecol* (2019) 58:239–43. doi: 10.1016/j.tjog.2019.01.013
16. Grati FR, Gallazzi G, Branca L, Maggi F, Simoni G, Yaron Y. An Evidence-Based Scoring System for Prioritizing Mosaic Aneuploid Embryos Following Preimplantation Genetic Screening. *Reprod BioMed Online* (2018) 36:442–9. doi: 10.1016/j.rbmo.2018.01.005
17. Hodes-Wertz B, Grifo J, Ghadir S, Kaplan B, Laskin CA, Glassner M, et al. Idiopathic Recurrent Miscarriage Is Caused Mostly by Aneuploid Embryos. *Fertil Steril* (2012) 98:675–80. doi: 10.1016/j.fertnstert.2012.05.025
18. Zeng Y, Lv Z, Gu L, Wang L, Zhou Z, Zhu H, et al. Preimplantation Genetic Diagnosis (PGD) Influences Adrenal Development and Response to Cold Stress in Resulting Mice. *Cell Tissue Res* (2013) 354:729–41. doi: 10.1007/s00441-013-1728-1
19. Zhao H-C, Zhao Y, Li M, Yan J, Li L, Li R, et al. Aberrant Epigenetic Modification in Murine Brain Tissues of Offspring From Preimplantation Genetic Diagnosis Blastomere Biopsies. *Biol Reprod* (2013) 89:117. doi: 10.1095/biolreprod.113.109926
20. Middelburg KJ, Heineman MJ, Haadsma ML, Bos AF, Kok JH, Hadders-Algra M. Neurological Condition of Infants Born After *In Vitro* Fertilization With Preimplantation Genetic Screening. *Pediatr Res* (2010) 67:430–4. doi: 10.1203/PDR.0b013e3181d2273e
21. Zhang S, Luo K, Cheng D, Tan Y, Lu C, He H, et al. Number of Biopsied Trophectoderm Cells Is Likely to Affect the Implantation Potential of Blastocysts With Poor Trophectoderm Quality. *Fertil Steril* (2016) 105:1222–27.e4. doi: 10.1016/j.fertnstert.2016.01.011
22. Guzman L, Nuñez D, López R, Inoue N, Portella J, Vizcarra F, et al. The Number of Biopsied Trophectoderm Cells may Affect Pregnancy Outcomes. *J Assist Reprod Genet* (2019) 36:145–51. doi: 10.1007/s10815-018-1331-1
23. Stigliani S, Anserini P, Venturini PL, Scaruffi P. Mitochondrial DNA Content in Embryo Culture Medium Is Significantly Associated With Human Embryo Fragmentation. *Hum Reprod* (2013) 28:2652–60. doi: 10.1093/humrep/det314
24. Yeung QSY, Zhang YX, Chung JPW, Lui WT, Kwok YKY, Gui B, et al. A Prospective Study of non-Invasive Preimplantation Genetic Testing for Aneuploidies (NiPGT-A) Using Next-Generation Sequencing (NGS) on Spent Culture Media (SCM). *J Assist Reprod Genet* (2019) 36:1609–21. doi: 10.1007/s10815-019-01517-7
25. Shamonki MI, Jin H, Haimowitz Z, Liu L. Proof of Concept: Preimplantation Genetic Screening Without Embryo Biopsy Through Analysis of Cell-Free DNA in Spent Embryo Culture Media. *Fertil Steril* (2016) 106:1312–8. doi: 10.1016/j.fertnstert.2016.07.1112
26. Rubio C, Navarro-Sánchez L, García-Pascual CM, Ocali O, Cimadomo D, Venier W, et al. Multicenter Prospective Study of Concordance Between Embryonic Cell-Free DNA and Trophectoderm Biopsies From 1301 Human Blastocysts. *Am J Obstet Gynecol* (2020) 223:751.e1–1.e13. doi: 10.1016/j.ajog.2020.04.035
27. Xu J, Fang R, Chen L, Chen D, Xiao J-P, Yang W, et al. Noninvasive Chromosome Screening of Human Embryos by Genome Sequencing of Embryo Culture Medium for *In Vitro* Fertilization. *Proc Natl Acad Sci U S A* (2016) 113:11907–12. doi: 10.1073/pnas.1613294113
28. Huang L, Bogale B, Tang Y, Lu S, Xie XS, Racowsky C. Noninvasive Preimplantation Genetic Testing for Aneuploidy in Spent Medium may be More Reliable Than Trophectoderm Biopsy. *Proc Natl Acad Sci U S A* (2019) 116:14105–12. doi: 10.1073/pnas.1907472116
29. Fang R, Yang W, Zhao X, Xiong F, Guo C, Xiao J, et al. Chromosome Screening Using Culture Medium of Embryos Fertilized *In Vitro*: A Pilot Clinical Study. *J Transl Med* (2019) 17:73. doi: 10.1186/s12967-019-1827-1
30. Munné S, Kaplan B, Frattarelli JL, Child T, Nakhuda G, Shamma FN, et al. Preimplantation Genetic Testing for Aneuploidy Versus Morphology as Selection Criteria for Single Frozen-Thawed Embryo Transfer in Good-Prognosis Patients: A Multicenter Randomized Clinical Trial. *Fertil Steril* (2019) 112:1071–9.e7. doi: 10.1016/j.fertnstert.2019.07.1346
31. The ESHRE Guideline Group on RPL, Bender Atik R, Christiansen OB, Elson J, Kolte AM, Lewis S, et al. ESHRE Guideline: Recurrent Pregnancy Loss. *Hum Reprod Open* (2018) 2018:hoy004. doi: 10.1093/hropen/hoy004
32. Practice Committee of the American Society for Reproductive Medicine. Evaluation and Treatment of Recurrent Pregnancy Loss: A Committee Opinion. *Fertil Steril* (2012) 98:1103–11. doi: 10.1016/j.fertnstert.2012.06.048
33. Ogasawara M, Aoki K, Okada S, Suzumori K. Embryonic Karyotype of Abortuses in Relation to the Number of Previous Miscarriages. *Fertil Steril* (2000) 73:300–4. doi: 10.1016/S0015-0282(99)00495-1
34. Nagaoka SI, Hassold TJ, Hunt PA. Human Aneuploidy: Mechanisms and New Insights Into an Age-Old Problem. *Nat Rev Genet* (2012) 13:493–504. doi: 10.1038/nrg3245

35. Forman EJ, Hong KH, Franasiak JM, Scott RT. Obstetrical and Neonatal Outcomes From the BEST Trial: Single Embryo Transfer With Aneuploidy Screening Improves Outcomes After *In Vitro* Fertilization Without Compromising Delivery Rates. *Am J Obstet Gynecol* (2014) 210:157.e1–6. doi: 10.1016/j.ajog.2013.10.016
36. McCoy RC, Demko ZP, Ryan A, Banjevic M, Hill M, Sigurjonsson S, et al. Evidence of Selection Against Complex Mitotic-Origin Aneuploidy During Preimplantation Development. *PLoS Genet* (2015) 11:e1005601. doi: 10.1371/journal.pgen.1005601
37. Sato T, Sugiura-Ogasawara M, Ozawa F, Yamamoto T, Kato T, Kurahashi H, et al. Preimplantation Genetic Testing for Aneuploidy: A Comparison of Live Birth Rates in Patients With Recurrent Pregnancy Loss Due to Embryonic Aneuploidy or Recurrent Implantation Failure. *Hum Reprod* (2019) 34:2340–8. doi: 10.1093/humrep/dez229
38. Hanson BM, Tao X, Hong KH, Comito CE, Pangasnan R, Seli E, et al. Noninvasive Preimplantation Genetic Testing for Aneuploidy Exhibits High Rates of Deoxyribonucleic Acid Amplification Failure and Poor Correlation With Results Obtained Using Trophectoderm Biopsy. *Fertil Steril* (2021) 115 (6):1461–70. doi: 10.1016/j.fertnstert.2021.01.028
39. Chen L, Sun Q, Xu J, Fu H, Liu Y, Yao Y, et al. A Non-Invasive Chromosome Screening Strategy for Prioritizing *In Vitro* Fertilization Embryos for Implantation. *Front Cell Dev Biol* (2021) 9:708322. doi: 10.3389/fcell.2021.708322

Conflict of Interest: The authors declare that the research was conducted in the absence of any commercial or financial relationships that could be construed as a potential conflict of interest.

Publisher's Note: All claims expressed in this article are solely those of the authors and do not necessarily represent those of their affiliated organizations, or those of the publisher, the editors and the reviewers. Any product that may be evaluated in this article, or claim that may be made by its manufacturer, is not guaranteed or endorsed by the publisher.

frontiers | Frontiers in Endocrinology

ORIGINAL RESEARCH
published: 29 June 2022
doi: 10.3389/fendo.2022.930786

Analysis of Fertility Preservation by Ovarian Tissue Cryopreservation in Pediatric Children in China

Xiangyan Ruan[1], Jiaojiao Cheng[1], Juan Du[1], Fengyu Jin[1], Muqing Gu[1], Yanglu Li[1], Rui Ju[1], Yurui Wu[2], Huanmin Wang[3], Wei Yang[3], Haiyan Cheng[3], Long Li[4], Wenpei Bai[5], Weimin Kong[6], Xin Yang[7], Shulan Lv[8], Yuejiao Wang[1], Yu Yang[1], Xin Xu[1], Lingling Jiang[1], Yanqiu Li[1] and Alfred O. Mueck[1,9]*

[1] Department of Gynecological Endocrinology, Beijing Obstetrics and Gynecology Hospital, Capital Medical University, Beijing Maternal and Child Health Care Hospital, Beijing, China, [2] Department of Thoracic Surgery and Surgical Oncology, Children's Hospital, Capital Institute of Pediatrics, Beijing, China, [3] Department of Surgical Oncology, Beijing Children's Hospital, Capital Medical University, National Center for Children's Health, Beijing, China, [4] Department of Pediatric Surgery, Children's Hospital, Capital Institute of Pediatrics, Beijing, China, [5] Department of Obstetrics and Gynecology, Beijing Shijitan Hospital, Capital Medical University, Beijing, China, [6] Department of Gynecological Oncology, Beijing Obstetrics and Gynecology Hospital, Capital Medical University, Beijing Maternal and Child Health Care Hospital, Beijing, China, [7] Department of Obstetrics and Gynecology, Peking University People's Hospital, Beijing, China, [8] Department of Gynecology and Obstetrics, First Affiliated Hospital of Xi'an Jiaotong University, Xi'an, China, [9] Department of Women's Health, University of Tuebingen, University Women's Hospital and Research Centre for Women's Health, Tuebingen, Germany

OPEN ACCESS

Edited by:
Yuting Fan,
Boston IVF, United States

Reviewed by:
Giuliano Marchetti Bedoschi,
University of São Paulo, Brazil
Timothy Lautz,
Ann & Robert H. Lurie Children's Hospital of Chicago, United States
Gianandrea Pasquinelli,
University of Bologna, Italy
Monica M Laronda,
Ann & Robert H. Lurie Children's Hospital of Chicago, United States

***Correspondence:**
Xiangyan Ruan
ruanxiangyan@ccmu.edu.cn

Specialty section:
This article was submitted to Reproduction, a section of the journal Frontiers in Endocrinology

Received: 28 April 2022
Accepted: 25 May 2022
Published: 29 June 2022

Citation:
Ruan X, Cheng J, Du J, Jin F, Gu M, Li Y, Ju R, Wu Y, Wang H, Yang W, Cheng H, Li L, Bai W, Kong W, Yang X, Lv S, Wang Y, Yang Y, Xu X, Jiang L, Li Y and Mueck AO (2022) Analysis of Fertility Preservation by Ovarian Tissue Cryopreservation in Pediatric Children in China. Front. Endocrinol. 13:930786. doi: 10.3389/fendo.2022.930786

Background: Ovarian tissue cryopreservation (OTC) is the only method of fertility preservation (FP) in prepubertal girls, but the experience remains limited. This study investigates the effectiveness and feasibility of FP of OTC in children facing gonadotoxicity treatment in Chinese first ovarian tissue cryobank.

Procedure: OTC and evaluation of 49 children ≤14 years old in the cryobank of Beijing Obstetrics and Gynecology Hospital, Capital Medical University, from July 2017 to May 19, 2022, were analyzed retrospectively. We compared children's general characteristics, follicle numbers, and hormone levels with and without chemotherapy before OTC.

Results: The age of 49 children at the time of OTC was 7.55 (1–14) years old. There were 23 cases of hematological non-malignant diseases, eight cases of hematological malignant diseases, four cases of gynecological malignant tumors, one case of neurological malignant tumors, one case of bladder cancer, five cases of sarcoma, three cases of mucopolysaccharidosis, one case of metachromatic leukodystrophy, two cases of dermatomyositis, one case of Turner's syndrome. The median follicular count per 2-mm biopsy was 705. Age and AMH were not correlated (r = 0.084, $P = 0.585$). Age and follicle count per 2-mm biopsy was not correlated (r = –0.128, $P = 0.403$). Log10 (follicle count per 2-mm biopsy) and Log10 (AMH) were not correlated (r = –0.118, $P = 0.456$). Chemotherapy before OTC decreased AMH levels but had no significant effect on the number of follicles per 2-mm biopsy.

Conclusions: OTC is the only method to preserve the fertility of prepubertal girls, and it is safe and effective. Chemotherapy before OTC is not a contraindication to OTC.

Keywords: ovarian tissue cryopreservation, children, fertility preservation, ovarian tissue transplantation, reproduction, endocrine function, gonadal toxicity

1 INTRODUCTION

The overall incidence of cancer in children has increased slightly (0.7% per year), and the reason is unclear (1). Because of significant treatment advances in recent decades, 85% of children with cancer now survive more than 5 years (1). Childhood cancer treatment may include surgery, chemotherapy, radiotherapy, and/or hematopoietic stem cell transplantation (HSCT) (2). Except for non-pelvic surgery, these treatments impair ovarian function, which is related to the oocyte/follicle DNA double-strand break (DSB) and apoptosis (3). Gonadal toxicity of anticancer therapy depends on the type, dose, and extent of chemotherapeutic agents and radiotherapy (4). HSCT is a standard treatment for hematological diseases, including high-dose chemotherapy with or without whole-body radiotherapy. Patients cured by myeloablative HSCT have a very high risk of premature ovarian insufficiency (POI) (5).

Decline or loss of fertility and POI are well-known side effects of anticancer therapy, and infertility is a significant concern for childhood cancer survivors (6). Estrogen deficiency also affects uterine development and increases the risk of osteoporosis, cardiovascular disease, and impaired cognitive function. In adolescent girls, POI also leads to developmental impairment and delayed puberty and affects self-esteem (7). Although fertility preservation (FP) in patients with cancer has become an essential issue in the clinic, previous studies have shown that young patients with cancer are not always adequately counseled about the potential adverse effects of cancer treatment on reproductive function and FP options nor are they referred to a fertility specialist (8). This issue has yet to be addressed in a proper manner, especially in low-income settings (9).

The ovarian tissue cryopreservation (OTC) technique is the only FP method for prepubertal girls. Cortical tissue is obtained by laparoscopic minimally invasive surgery under general anesthesia (10, 11). The adolescent or young adults could have ovarian stimulation and oocytes retrieval once they have recovered and before they develop to POI. In 2019, the American Society for Reproductive Medicine (ASRM) claimed that the OTC technique is no longer an experimental technique but has become standard clinical FP technology (12). Because of the small ovary size in children, the unilateral ovary is usually retrieved for OTC (13).

More than 200 babies have been born through OTC technology worldwide (14), and cryopreserved ovarian tissue from children has been successfully used to induce puberty (15). Recently, there have been reports of successful pregnancy after retransplantation of cryopreserved ovarian tissue at the age of 13 (16) and 9 (17) and in patients with acute lymphoblastic leukemia at the age of 14 (18). The International Guideline Harmonization Group pointed out that all children with cancer and their families have the right to be informed of the risk of gonadal damage and recommends that children and young patients who will receive a cumulative dose of 6,000~8,000 mg/m^2 or greater alkylating agent, ovarian radiotherapy, and HSCT undergo FP of OTC (8).

The global clinical practice information on OTC of prepubertal girls and adolescent women is still limited, and the FP experience in children is limited compared to adults. To better apply OTC for prepubertal girls, the valuable experience of each center is worth reporting. This study mainly analyzed the age, disease, transport and cryopreservation, follicle number, and hormone level of 49 children who underwent OTC in the cryobank of Beijing Obstetrics and Gynecology Hospital, Capital Medical University, the first and largest OTC center in China. It compares the age, disease, transport and cryopreservation, follicle count, and hormone level of patients with or without chemotherapy before OTC.

2 METHODS

2.1 Ethics Statement

The Ethics Committee approved OTC of Beijing Obstetrics and Gynecology Hospital, Capital Medical University (ethics code: 2017-KY-020-01; date: March 15, 2017) to provide centralized OTC and use up to 10% of ovarian tissue for quality control measures and patient-related research. Ovarian tissue was collected from clinical sub-centers and transferred to the ovarian tissue cryobank.

2.2 Retrieval, Transportation, and Preparation of Ovarian Tissue

Forty-one children who underwent OTC in the cryobank of Beijing Obstetrics and Gynecology Hospital, Capital Medical University, from July 2017 to May 19, 2022 (mean ± SD, range: 7.55 ± 3.64 years, 1–14 years) were selected as subjects. Twenty-four of them underwent a few cycles of chemotherapy before OTC to alleviate the symptoms of the disease and most of them reach the remission stage and plan to undergo HSCT. Because of the small size of the ovary in children (13), the amount of ovarian tissue retrieval is generally the unilateral ovary, equivalent to 50% of all ovarian tissue, *via* laparoscopy (**Figure 1**) or laparotomy (primary tumor resection at the same time).

The ovarian tissue was transferred to the cooled Custodiol immediately after retrieval. During ovarian tissue transport, the temperature was maintained at 4°C–8°C. The mean temperature reached the cryobank was 5.47°C, and the average transport time was less than 12 h. In a pollution-free environment, ovarian tissue was prepared in a sterile laminar flow cabinet at 4°C. The cortex was prepared to 1 mm thick, then cut into cortical slices of size about 6 mm × 3 mm, and cryopreserved for future transplantation. For the remaining cortical tissue, standardized cortical samples (diameter of 2 mm) were obtained from different areas using punches (PFM Medical AG, Cologne, Germany) for follicle density analysis and routine viability assay. After slow programmed freezing, the ovarian cortex was stored in a gas phase liquid nitrogen tank. The operation is according to the previously published protocol (19, 20).

2.3 Hormone Level Analysis Before Ovarian Tissue Cryopreservation

The levels of follicle-stimulating hormone (FSH), luteinizing hormone (LH), and estradiol (E2) in serum before OTC were

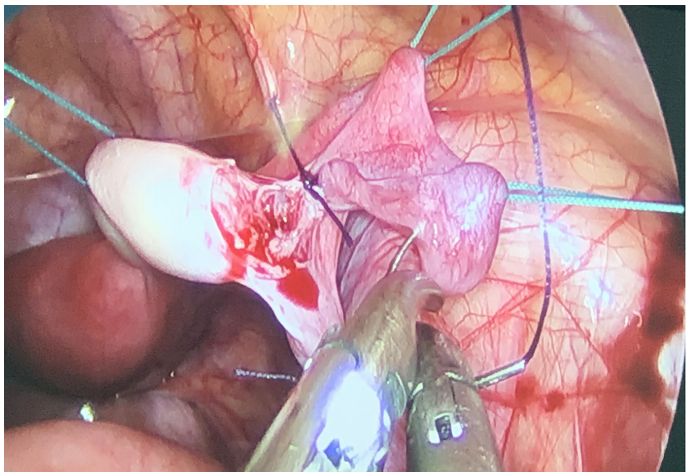

FIGURE 1 | Intraoperative photo demonstrating ovarian anatomy in a 11-year-old female with chronic active Epstein-Barr virus infection.

determined by Centaur automatic chemiluminescence immunoassay produced by Bayer Company in the United States. AMH was determined using the AMH kit (Guangzhou Kangrun Company, China) by enzyme-linked immunosorbent assay. The intra-assay and inter-assay errors were 3.3% and 6.7%, respectively.

2.4 Analysis of Follicle Density

The count of surviving primordial and primary follicles was analyzed in standardized biopsied cortices, with circular cortical slices 2 mm in diameter collected from different cortex regions with a volume of 3.14 mm^3 per biopsy. The follicles count per 2-mm biopsy, and the follicles density per mm^3 were statistically analyzed. The follicular count assessment method is the same as the previous articles published by our team (21).

2.5 Statistical Analyses

SPSS 22.0 (IBM SPSS Statistics, IBM software) was used for data analysis. The data in accordance with normal distribution were expressed by "mean ± standard deviation", the mean between groups was compared by independent sample t-test, and the data in accordance with non-normal distribution were represented by "median, range". The Mann–Whitney U-test compared the median between groups. Spearman correlation analysis was used to analyze the variables that did not conform to the normal distribution. $P < 0.05$ indicates that the difference is statistically significant.

3 RESULTS

3.1 Patient Characteristics

3.1.1 Ages and Diagnosis

Characteristics of children with OTC are shown in **Table 1**. The age of 49 children was 7.55 ± 3.64 years old, range: 1 to 14 years. The disease distribution of 49 patients was (**Figure 2**): 23 cases of hematological non-malignant diseases, eight cases of hematological malignant diseases, four cases of gynecological malignant tumors, one case of neurological malignant tumor, one case of bladder cancer, three cases of mucopolysaccharidosis, one case of metachromatic leukodystrophy, two cases of dermatomyositis, one case of Turner's syndrome, and five cases of sarcoma. Thirty-six patients (36 of 49, 73.5%) with hematological

TABLE 1 | Patient characteristics and comparison with chemotherapy and without chemotherapy before OTC.

Characteristics	Overall children	Chemo before OTC	No-Chemo before OTC	*P*-value
Age (mean ± SD) (n)	7.55 ± 3.64 (49)	8.54 ± 4.06 (24)	6.60 ± 2.94 (25)	0.061
Transport temperature (mean ± SD) (n)	5.47 ± 1.34 (49)	5.76 ± 1.53 (24)	5.20 ± 1.10 (25)	0.156
The proportion of ovarian retrieval in the total ovary (median, range) (n)	0.50, 0.15-0.75 (48)	0.50, 0.25-0.75 (24)	0.50, 0.15-0.50 (24)	0.957
Number of cryopreserved cortex pieces (mean ± SD) (n)	20.52 ± 7.63 (48)	21.42 ± 8.04 (24)	19.63 ± 7.26 (24)	0.422
Follicle number per 2-mm biopsy (median, range) (n)	705, 122–3628 (45)	868, 158–2,250 (21)	507, 122–3628 (24)	0.290
Follicle density per mm^3 (median, range) (n)	224.52, 38.85–1,155.41 (45)	276.43, 50.32–716.56 (21)	161.47, 38.85–1155.41 (24)	0.290
FSH (IU/L) before OTC (median, range) (n)	2.34, 0.00–17.66 (41)	2.20, 0.58–6.83 (21)	3.18, 0–17.66 (20)	0.182
LH (IU/L) before OTC (median, range) (n)	0.00, 0.00–63.23 (41)	0.10, 0.00–63.23 (21)	0.00, 0.00–4.26 (20)	0.270
E2 (pg/ml) before OTC (median, range) (n)	12.21, 11.80–326.72 (41)	12.28, 11.80–326.52 (21)	12.06, 11.80–93.13 (20)	0.834
AMH (ng/ml) before OTC (median, range) (n)	0.89, 0.06–5.94 (45)	0.27, 0.06–3.21 (23)	1.51, 0.4–5.94 (22)	0.000***

****refers to P < 0.001.*

OTC, ovarian tissue cryopreservation; SD, standard deviation; FSH, follicle stimulating hormone; LH, luteinizing hormone; E2, estradiol; AMH, anti-Müllerian hormone.

non-malignant diseases, hematological malignant diseases, mucopolysaccharidosis, and dermatomyositis were cryopreserved because of planned HSCT. The number of patients with or without chemotherapy before OTC was 24 and 25, respectively. The cycles of chemotherapy before OTC were 3 (1–11) (median, range).

3.1.2 Number of Children Undergoing OTC Per Year

From July 2017 to May 19, 2022, 52 children come to counseling OTC at our center, and 49 children have performed the OTC. Among the patients who underwent OTC in 2017, there was only one child patient (1 of 35, 2.9%), and none of the patients experienced OTC in 2018 (0). In 2019, there were five child patients (5 of 57 8.8%). In 2020, there were five child patients (6 of 36, 16.7%). In 2021, there were 21 children (21 of 61, 34.4%) and eight patients who underwent OTC in 2022 (16 of 26, 61.5%). The proportion of children in patients with cryopreserved ovaries increased significantly (**Figure 3**).

3.1.3 Ovarian Tissue Retrieval, Transportation, Cryopreservation, and Follicle Density

In **Table 1**, the temperature of ovarian tissue transport to a centralized cryobank is 5.47 ± 1.34°C. The proportion of ovarian retrieval in the total ovary is 0.50, 0.15–0.75 (median, range), the number of cryopreserved cortex pieces is 20.52 ± 7.63 (mean ± SD), and the follicle number per 2-mm biopsy is 705, 122–3,628 (median, range). Follicle density per mm^3 is 224.52, 38.85–1,155.41 (median, range).

3.1.4 Hormone Levels Before OTC

In **Table 1**, FSH level before OTC is 2.34, 0.00–17.66 IU/L (median, range); LH level before OTC is 0.00, 0.00–63.23 IU/L (median, range); E2 level before OTC is 12.21, 11.80–326.72 pg/ml (median, range). The patients with the highest values of LH and E2 were in the same patient aged 14 years, with menarche at 11 years old. AMH level before OTC is 0.89, 0.06–5.94ng/ml (median, range).

3.1.5 Correlation Analysis and Linear Regression Analysis

Age and AMH were not significantly correlated (n = 45, r = 0.084 P = 0.585). Age and follicle count per 2-mm biopsy were not significantly correlated (n = 45, r = −0.128, P = 0.403). Log10 (follicle count per 2-mm biopsy) and Log10 (AMH) were not significantly correlated (n = 45, r = −0.118, P = 0.456) (**Figure 4**).

3.2 Comparison of Chemotherapy and No Chemotherapy Before OTC

3.2.1 Ages and Diagnosis

In **Table 1**, There was no significant difference in the age of patients with or without chemotherapy before OTC (8.54 ± 4.06, 6.60 ± 2.94, P = 0.061) (**Figure 5**). The main diseases in patients with chemotherapy (n = 24) before OTC were eight cases of hematological non-malignant diseases, seven cases of hematological malignant diseases (leukemia), five cases of sarcoma (one case of Ewing's sarcoma and four cases of rhabdomyosarcoma), one case of gynecological malignant tumor, one case of neurological malignant disease, and one case of bladder cancer. Malignant diseases accounted for 62.5% (15 of 24). The main diseases of patients without chemotherapy (n = 25) before OTC were 15 hematological non-malignant diseases, three cases of gynecological malignant tumors, six other non-malignant diseases, and one hematological malignant disease. Malignant diseases accounted for 16% (4 of 25).

3.2.2 Ovarian Tissue Retrieval, Transportation, Cryopreservation, and Follicle Density

In **Table 1**, there was no significant difference in transport temperature (mean ± SD, 5.76 ± 1.53 vs. 5.20 ± 1.10), the proportion of ovarian retrieval in the total ovary (median, range,

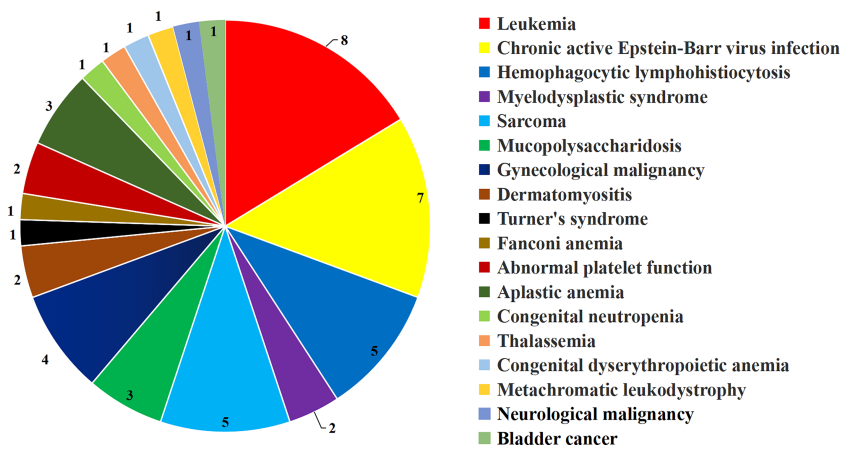

FIGURE 2 | Disease classification of 49 children undergone OTC. OTC, ovarian tissue cryopreservation.

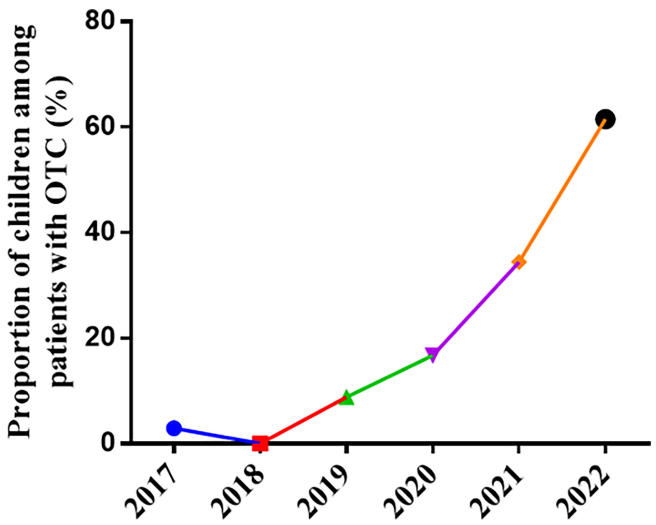

FIGURE 3 | The proportion of children among patients with OTC per year. OTC, ovarian tissue cryopreservation.

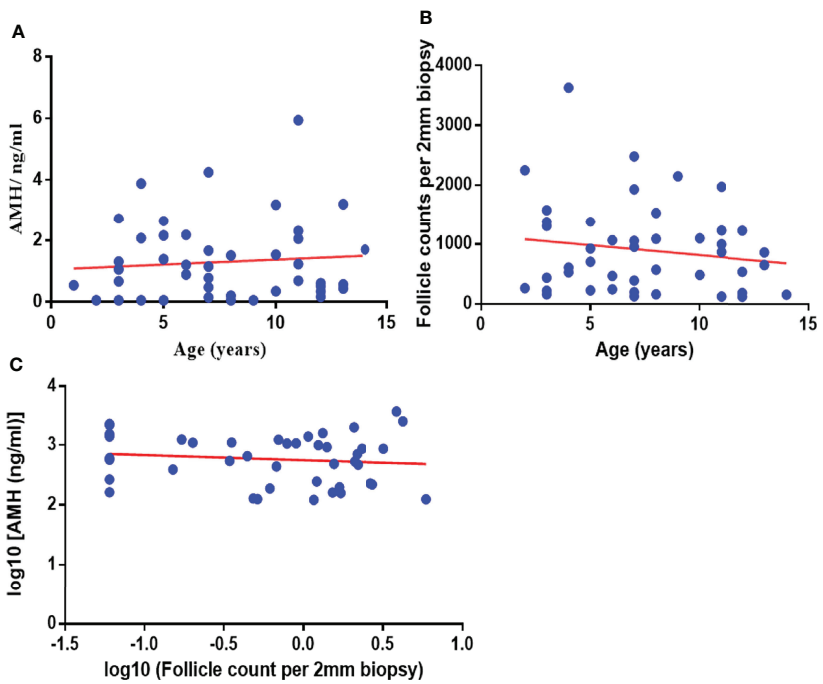

FIGURE 4 | Correlation analysis and linear regression analysis between Age and AMH **(A)** (n = 45, r = 0.084, *P* = 0.585), between age and follicle count per 2-mm biopsy **(B)** (n = 45, r = –0.128, *P* = 0.403), between log10 (follicle count per 2-mm biopsy) and log10 (AMH) **(C)** (n = 45, r = –0.118, *P* = 0.456). AMH, anti-Müllerian hormone.

0.50, 0.25–0.75 vs. 0.50, 0.15–0.50), the number of cryopreserved cortex pieces (mean ± SD, 21.42 ± 8.04 vs. 19.63 ± 7.26), follicle number per 2-mm biopsy (median, range, 868, 158–2250 vs. 507, 122–3628), and follicle density per mm^3 (median, range, 276.43, 50.32–716.56 vs. 161.47, 38.85–1,155.41) between the two groups with or without chemotherapy before OTC (all $P > 0.05$) (**Figure 5**).

3.2.3 Hormone Levels Before OTC

In **Table 1**, There was no significant difference in FSH, LH, and E2 levels between the two groups with or without chemotherapy before OTC (all *P*>0.05). AMH levels in patients with chemotherapy before OTC were significantly lower than those without chemotherapy (median, range: 0.27, 0.06–3.21 vs. 1.51, 0.48–5.94, *P* = 0.000) (**Figure 5**).

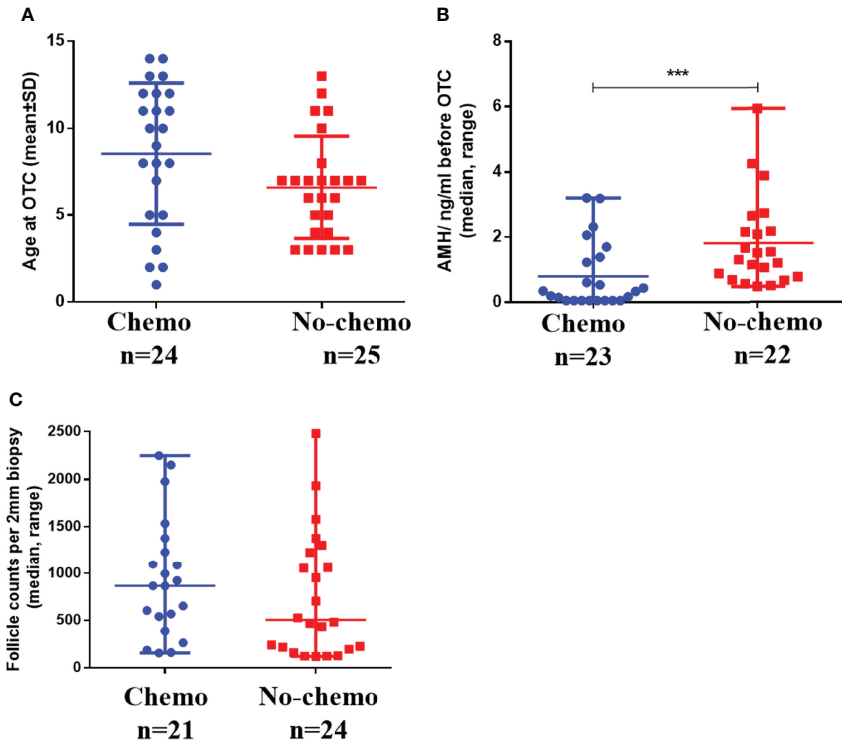

FIGURE 5 | Comparison of age **(A)**, AMH **(B)**, and follicle count per 2-mm biopsy **(C)** in children with and without chemotherapy before OTC. *** refers to P<0.001. OTC, ovarian tissue cryopreservation.

4 DISCUSSION

Our center is the first ovarian tissue cryobank in China and is also currently the largest ovarian tissue cryobank in China. More than 400 cases of ovarian tissue have been successfully cryopreserved, 10 cases of adult ovarian tissue have been successfully transplanted, and the ovarian function has been restored after transplantation (19). One of the adult patients with MDS has successfully conceived naturally and delivered a healthy baby girl through OTC and transplantation. This is also the first baby born in China through OTC and transplantation (22). With the cooperation of pediatrics, the proportion of OTC of children in our center has increased over the past 2 years.

Cyclophosphamide and other alkylating agents are commonly used to treat cancer in children. They induce apoptosis of cancer cells by destroying DNA and inhibiting cell metabolism, DNA replication, and transcription but cause vascular toxicity to ovaries and direct DNA damage to growing and dormant follicles, resulting in acute ovarian failure (23). Radiotherapy also increases the risk of infertility, depending on age, ovarian reserve, total radiation dose, and radiation plan. Head radiation destroys the hypothalamus and pituitary function, leading to hypogonadism. Fifty percent of follicular loss can be caused by direct pelvic radiation of 2 Gy, and pelvic irradiation can lead to myometrial fibrosis. More than 25-Gy radiation seems to lead to irreversible damage to the uterus (24).

HSCT is a standard treatment option that usually cures severe benign and malignant diseases. Of the 49 children who underwent OTC for FP in this study, 73.5% planned HSCT treatment. In this study, seven children with chronic active EB virus infection underwent OTC. As far as we know, there are only two cases of OTC in patients with this disease (25). This study describes for the first time that OTC was performed in children with mucopolysaccharidosis and included different types, such as type I, type IVa, and type IH. We also performed OTC for five patients with hemophagocytic lymphohistiocytosis. It was reported that the ovaries of three patients with hemophagocytic lymphohistiocytosis were cryopreserved, but two patients died before the application of cryopreserved ovarian tissue (26). The study has reported that the ovarian tissue of adult patients with hemophagocytic lymphohistiocytosis was cryopreserved, ovarian function recovered after OTT, and the pregnancy was successful (27). The HSCT of leukemia patients is applied in remission, and the patients may have received chemotherapy for months or years before HSCT (28). Referral to fertility counseling before HSCT is the most important for patients. The study has shown that, even after receiving HSCT in childhood, fertility counseling and assessment of residual fertility potential can provide opportunities for FP (28).

AMH is produced almost entirely by granulosa cells of small antral follicles between 5 and 8 mm, reflecting gonadotropin-

independent follicle genesis (29). In adults with regular menstrual cycles, serum FSH can be considered a marker of pituitary function. The peak level of serum AMH is in puberty or early adulthood. It has been proved that AMH correlates with the antral follicle count in healthy women. Still, it is not recommended as the primary monitoring method to evaluate POI in the childhood cancer group (30, 31). The continuous longitudinal follow-up study is significant (32). The hypothalamus–pituitary–ovary axis is stationary in childhood, and the evaluation of FSH, LH, E2, and AMH levels is not practical in children. There was no significant correlation between age and AMH level and the number of follicles in this study. There was no significant correlation between AMH level and the number of follicles.

ASRM stressed the importance of surgical techniques in retrieving ovarian tissue and the importance of tissue preparation for cryopreservation, which is the core of the quality of cryopreservation and ultimately crucial to the success of the future application of ovarian tissue to restore fertility (33). Laparoscopic ovarian tissue retrieval has been proven safe for children and adults, with low intraoperative and postoperative risks. Because of the small size of the ovaries in children, laparoscopic unilateral ovariectomy is the first choice, maximizing the number of cortical tissue for cryopreservation and future retransplantation and avoiding bleeding complications. Multiple cortical slices can allow multiple attempts at OTT, and if the hormone recovery effect is weakened, then OTT can be repeated (34). Ovarian tissue retrieval for OTC does not seem to affect patients significantly. Unilateral ovariectomy may advance the age of menopause by about 1.8 years, which may be due to a compensatory mechanism, leading to a low recruitment rate of primordial follicles (25, 35).

At present, the low temperature (4°C to 8°C) is a widely used standard tissue transportation method. Low temperatures decrease cellular metabolism in ovarian tissue, reduce cellular oxygen demand and consumption, and preserve tissue without vascular perfusion (36, 37). Because of the high density of follicles in children, we generally prepared ovarian cortical slices with the size of 6 mm × 3 mm × 1 mm, which is consistent with the international community (38). At present, ovarian tissue slow-programming cryopreservation is internationally recognized as the gold standard procedure for OTC (38). Except for the five reported babies born after vitrification of ovarian tissue, other more than 200 new births were born through slow-programming of OTC (39).

For patients with a high risk of ovarian tissue transplantation, such as leukemia and non-Hodgkin's lymphoma, part of the ovarian tissue was taken for histopathology to evaluate whether there was cancer cell infiltration before OTC. In addition, the thawed part of the cryopreserved ovarian tissue before transplantation was analyzed by histological and molecular biology techniques to evaluate that there were no cancer cells in the cryopreserved ovarian tissue (40). No evidence of malignant cell contamination was observed in cryopreserved ovarian tissues from patients with non-metastatic solid tumors and Hodgkin's lymphoma (41, 42). The evidence cited in the existing guidelines does not indicate cancer recurrence in transplanted ovarian tissue (40, 43). There were no pregnancy complications or congenital abnormalities in women after transplantation of cryopreserved ovarian tissue (44). However, the safety of ovarian tissue at high risk of the disease still needs to be thoroughly evaluated.

During the preparation of ovarian tissue, the small antral follicles in the medulla are destroyed, and cumulus-oocyte complexes (COCs) are released into the medium. These COCs can be recovered and matured *in vitro* to obtain MII oocytes and cryopreserved for future application (2, 45). Live birth from the source of the oocytes has been reported (46, 47). Most *in vitro* maturation (IVM) results are from adults, and more research is needed to determine how to mature preadolescent gametes into high-quality eggs. Telfer et al. have grown and matured human primordial follicles to the preantral and antral follicle stages (48). More work is required before *in vitro* culture can be clinically applied and offered. In the future, artificial ovaries will reduce the possibility of reintroducing malignant cells into the body and eliminate the need for ovarian tissue autotransplantation, such as *in vitro* growth and IVM of primordial follicles (49).

Most of the patients who underwent chemotherapy before OTC were malignant diseases, and the proportion of malignant diseases was higher than that of patients without chemotherapy before OTC. This is consistent with the results of another study, which showed that 95% of patients who receive chemotherapy before OTC have hematological malignant diseases (50). There was no significant difference in the number of follicles, FSH, LH, and E2 between children undergoing chemotherapy before OTC and those without chemotherapy, but the level of AMH in children undergoing chemotherapy before OTC was significantly lower than that in children without chemotherapy. AMH is mainly secreted by granulosa cells of small antral follicles, and chemotherapy may significantly damage metabolically active follicles, such as growing follicles. Therefore, the level of AMH in patients with chemotherapy before OTC is significantly lower than that in patients without chemotherapy, and it may take 1~3 years to recover (31). For diseases with a high risk of cancer cell contamination in the ovary, such as leukemia, OTC after complete remission with chemotherapy reduces the risk. In our study, the population is heterogeneous, the sample number is limited, the cryopreserved ovarian tissue in childhood has not been transplanted, and we cannot prove that chemotherapy before OTC does not affect the outcome of OTT. However, other studies have shown that chemotherapy before OTC has little effect on the number of follicles, does not affect the outcome of OTT, and is no longer a contraindication for OTC (50, 51).

Still, the study has shown that the interaction between immature ovarian tissue and the hypothalamus and pituitary is similar to that of the adult ovary, indicating that ovarian maturation needs appropriate FSH and LH stimulation. These results support the use of OTC in prepubertal girls. The current study does not cover the functional lifespan of cryopreserved prepubertal ovary grafts after transplantation. Long-term follow-up is still needed to monitor whether a large number of non-growing follicles transplanted due to younger age will prolong the grafted life (52).

5 CONCLUSION

Advances in clinical oncology care in children have greatly improved survival and now pose challenges to the long-term quality of life during survival, including fertility and hormonal function. Pediatric surgeons need to continue to advocate FP, incorporate FP methods before and early treatment, and perform ovarian tissue surgery on children at high risk of POI if safe and necessary. OTC in children seems to be a safe procedure and needs to be confirmed in large prospective studies to provide data for developing guidelines for OTC in children.

DATA AVAILABILITY STATEMENT

The raw data supporting the conclusions of this article will be made available by the authors, without undue reservation.

ETHICS STATEMENT

The studies involving human participants were reviewed and approved by Beijing Obstetrics and Gynecology Hospital, Capital Medical University. Written informed consent to participate in this study was provided by the participants' legal guardian/next of kin.

AUTHOR CONTRIBUTIONS

All authors qualify for authorship by contributing substantially to this article. XR: project leader, project supervision, interpretation of results, provided critical comments, and revised the first draft. JC: article preparation, ovarian tissue transportation, preparation, and cryopreservation. JD, FJ, MG, and YLL: ovarian tissue preparation and cryopreservation. RJ, YRW, HW, HC, WY, LL, WB, WK, XY, and SL: biopsied ovarian tissue. YW, YY, XX, LJ, YQL: ovarian tissue transportation, AM: experimental supervision, interpretation of results, and article revision. All authors contributed to the article and approved the submitted version.

FUNDING

This study was supported by Beijing Natural Science Foundation (7202047), Capital's Funds for Health Improvement and Research (2020-2-2112), Beijing Municipal Administration of Hospitals' Ascent Plan (DFL20181401), Capital's Funds for Health Improvement and Research (2016-2-2113), Beijing Municipal Science and Technology Commission (Z161100000516143), and Beijing Municipal Administration of Hospitals Clinical Medicine Development of Special Funding Support (XMLX201710).

ACKNOWLEDGMENTS

The authors gratefully acknowledge Markus Montag and Jana Liebenthron for their technical assistance. The authors thank Li Rong (Department of Hematology, Children's Hospital, Capital Institute of Pediatrics), Qin Maoquan and Yang Jun (Hematology Oncology Center, Beijing Children's Hospital, Capital Medical University), and Chen Jiao (Beijing JingDu Children's Hospital) for their referring patients for fertility preservation counseling on ovarian tissue cryopreservation.

REFERENCES

1. Siegel RL, Miller KD, Jemal A. Cancer Statistics, 2020. *CA Cancer J Clin* (2020) 70:7–30. doi: 10.3322/caac.21590
2. Lautz TB, Burns K, Rowell EE. Fertility Considerations in Pediatric and Adolescent Patients Undergoing Cancer Therapy. *Surg Oncol Clin N Am* (2021) 30:401–15. doi: 10.1016/j.soc.2020.11.009
3. Bedoschi GM, Navarro PA, Oktay KH. Novel Insights Into the Pathophysiology of Chemotherapy-Induced Damage to the Ovary. *Panminerva Med* (2019) 61:68–75. doi: 10.23736/S0031-0808.18.03494-8
4. Barton SE, Najita JS, Ginsburg ES, Leisenring WM, Stovall M, Weathers RE, et al. Infertility, Infertility Treatment, and Achievement of Pregnancy in Female Survivors of Childhood Cancer: A Report From the Childhood Cancer Survivor Study Cohort. *Lancet Oncol* (2013) 14:873–81. doi: 10.1016/S1470-2045(13)70251-1
5. Vatanen A, Wilhelmsson M, Borgstrom B, Taskinen M, Saarinen-Pihkala UM, Winiarski J, et al. Ovarian Function After Allogeneic Hematopoietic Stem Cell Transplantation in Childhood and Adolescence. *Eur J Endocrinol* (2014) 170:211–8. doi: 10.1530/EJE-13-0694
6. Anderson RA, Brewster DH, Wood R, Nowell S, Fischbacher C, Kelsey TW, et al. The Impact of Cancer on Subsequent Chance of Pregnancy: A Population-Based Analysis. *Hum Reprod* (2018) 33:1281–90. doi: 10.1093/humrep/dey216
7. Cattoni A, Parissone F, Porcari I, Molinari S, Masera N, Franchi M, et al. Hormonal Replacement Therapy in Adolescents and Young Women With Chemo- or Radio-Induced Premature Ovarian Insufficiency: Practical Recommendations. *Blood Rev* (2021) 45:100730. doi: 10.1016/j.blre.2020.100730
8. Mulder RL, Font-Gonzalez A, Hudson MM, van Santen HM, Loeffen EAH, Burns KC, et al. Fertility Preservation for Female Patients With Childhood, Adolescent, and Young Adult Cancer: Recommendations From the PanCareLIFE Consortium and the International Late Effects of Childhood Cancer Guideline Harmonization Group. *Lancet Oncol* (2021) 22:e45–56. doi: 10.1016/S1470-2045(20)30594-5
9. Bedoschi G, Navarro PA. Oncofertility Programs Still Suffer From Insufficient Resources in Limited Settings. *J Assist Reprod Genet* (2022) 39:953–5. doi: 10.1007/s10815-022-02452-w
10. Wallace WH, Kelsey TW, Anderson RA. Fertility Preservation in Pre-Pubertal Girls With Cancer: The Role of Ovarian Tissue Cryopreservation. *Fertil Steril* (2016) 105:6–12. doi: 10.1016/j.fertnstert.2015.11.041
11. Dinikina Y, Belogurova M, Zaritskey A, Govorov I, Tsibizova V, Gamzatova Z, et al. Ovarian Tissue Cryopreservation in Prepubertal Patients With Oncological Diseases: Multidisciplinary Approach and Outcomes. *J Matern Fetal Neonatal Med* (2021) 34:2391–8. doi: 10.1080/14767058.2019.1666364
12. ASRM. Fertility Preservation in Patients Undergoing Gonadotoxic Therapy or Gonadectomy: A Committee Opinion. *Fertil Steril* (2019) 112:1022–33. doi: 10.1016/j.fertnstert.2019.09.013
13. Arian SE, Flyckt RL, Herman R, Erfani H, Falcone T. Fertility Preservation in Pediatric Female Cancer Patients. *Fertil Steril* (2018) 109:941. doi: 10.1016/j.fertnstert.2018.02.112
14. Dolmans MM, Falcone T, Patrizio P. Importance of Patient Selection to Analyze *In Vitro* Fertilization Outcome With Transplanted Cryopreserved Ovarian Tissue. *Fertil Steril* (2020) 114:279–80. doi: 10.1016/j.fertnstert.2020.04.050

15. Ernst E, Kjaersgaard M, Birkebaek NH, Clausen N, Andersen CY. Case Report: Stimulation of Puberty in a Girl With Chemo- and Radiation Therapy Induced Ovarian Failure by Transplantation of a Small Part of Her Frozen/Thawed Ovarian Tissue. *Eur J Cancer* (2013) 49:911–4. doi: 10.1016/j.ejca.2012.09.028
16. Demeestere I, Simon P, Dedeken L, Moffa F, Tsépélidis S, Cecile B, et al. Live Birth After Autograft of Ovarian Tissue Cryopreserved During Childhood. *Hum Reprod* (2015) 30:2107–9. doi: 10.1093/humrep/dev128
17. Matthews SJ, Picton H, Ernst E, Andersen CY. Successful Pregnancy in a Woman Previously Suffering From Beta-Thalassemia Following Transplantation of Ovarian Tissue Cryopreserved Before Puberty. *Minerva Ginecol* (2018) 70:432–5. doi: 10.23736/S0026-4784.18.04240-5
18. Rodriguez-Wallberg KA, Milenkovic M, Papaikonomou K, Keros V, Gustafsson B, Sergouniotis F, et al. Successful Pregnancies After Transplantation of Ovarian Tissue Retrieved and Cryopreserved at Time of Childhood Acute Lymphoblastic Leukemia - A Case Report. *Haematologica* (2021) 106:2783–7. doi: 10.3324/haematol.2021.278828
19. Ruan X, Cheng J, Korell M, Du J, Kong W, Lu D, et al. Ovarian Tissue Cryopreservation and Transplantation Prevents Iatrogenic Premature Ovarian Insufficiency: First 10 Cases in China. *Climacteric* (2020) 23:574–80. doi: 10.1080/13697137.2020.1767569
20. Liebenthron J, Montag M. Chapter 15 Development of a Nationwide Network for Ovarian Tissue Cryopreservation. *Methods Mol Biol* (2017) 1568:205–20. doi: 10.1007/978-1-4939-6828-2_15
21. Li Y, Ruan X, Liebenthron J, Montag M, Zhou Q, Kong W, et al. Ovarian Tissue Cryopreservation for Patients With Premature Ovary Insufficiency Caused by Cancer Treatment: Optimal Protocol. *Climacteric* (2019) 22:383–9. doi: 10.1080/13697137.2018.1554644
22. Ruan X, Du J, Lu D, Duan W, Jin F, Kong W, et al. First Pregnancy in China After Ovarian Tissue Transplantation to Prevent Premature Ovarian Insufficiency. *Climacteric* (2021) 24:624–8. doi: 10.1080/13697137.2021.1956453
23. van der Kooi A, van Dijk M, Broer L, van den Berg MH, Laven JSE, van Leeuwen FE, et al. Possible Modification of BRSK1 on the Risk of Alkylating Chemotherapy-Related Reduced Ovarian Function. *Hum Reprod* (2021) 36:1120–33. doi: 10.1093/humrep/deaa342
24. Rozen G, Rogers P, Chander S, Anderson R, McNally O, Umstad M, et al. Clinical Summary Guide: Reproduction in Women With Previous Abdominopelvic Radiotherapy or Total Body Irradiation. *Hum Reprod Open* (2020) 2020:a45. doi: 10.1093/hropen/hoaa045
25. Takae S, Furuta S, Iwahataa H, Iwahata Y, Keino D, Kanamori R, et al. Cryopreservation of Paediatric Ovarian Tissue With an Updated Version of the Edinburgh Criteria for Appropriate Patient Selection. *Reprod BioMed Online* (2022) 44:667–76. doi: 10.1016/j.rbmo.2021.10.009
26. Macklon KT. Prevalence of Deaths in a Cohort of Girls and Women With Cryopreserved Ovarian Tissue. *Acta Obstet Gynecol Scand* (2019) 98:625–9. doi: 10.1111/aogs.13576
27. Oktay K, Bedoschi G, Pacheco F, Turan V, Emirdar V. First Pregnancies, Live Birth, and *In Vitro* Fertilization Outcomes After Transplantation of Frozen-Banked Ovarian Tissue With a Human Extracellular Matrix Scaffold Using Robot-Assisted Minimally Invasive Surgery. *Am J Obstet Gynecol* (2016) 214:91–4. doi: 10.1016/j.ajog.2015.10.001
28. Wikander I, Lundberg FE, Nilsson H, Borgström B, Rodriguez-Wallberg KA. A Prospective Study on Fertility Preservation in Prepubertal and Adolescent Girls Undergoing Hematological Stem Cell Transplantation. *Front Oncol* (2021) 11:692834. doi: 10.3389/fonc.2021.692834
29. Jeppesen JV, Anderson RA, Kelsey TW, Christiansen SL, Kristensen SG, Jayaprakasan K, et al. Which Follicles Make the Most Anti-Mullerian Hormone in Humans? Evidence for an Abrupt Decline in AMH Production at the Time of Follicle Selection. *Mol Hum Reprod* (2013) 19:519–27. doi: 10.1093/molehr/gat024
30. ACOG Committee Opinion No. 747. Gynecologic Issues in Children and Adolescent Cancer Patients and Survivors. *Obstet Gynecol* (2018) 132:e67–77. doi: 10.1097/AOG.0000000000002763
31. Anderson RA, Su HI. The Clinical Value and Interpretation of Anti-Mullerian Hormone in Women With Cancer. *Front Endocrinol (Lausanne)* (2020) 11:574263. doi: 10.3389/fendo.2020.574263
32. Lotz L, Barbosa PR, Knorr C, Hofbeck L, Hoffmann I, Beckmann MW, et al. The Safety and Satisfaction of Ovarian Tissue Cryopreservation in Prepubertal and Adolescent Girls. *Reprod BioMed Online* (2020) 40:547–54. doi: 10.1016/j.rbmo.2020.01.009
33. Lautz TB, Harris CJ, Laronda MM, Erickson LL, Rowell EE. A Fertility Preservation Toolkit for Pediatric Surgeons Caring for Children With Cancer. *Semin Pediatr Surg* (2019) 28:150861. doi: 10.1016/j.sempedsurg.2019.150861
34. Corkum KS, Laronda MM, Rowell EE. A Review of Reported Surgical Techniques in Fertility Preservation for Prepubertal and Adolescent Females Facing a Fertility Threatening Diagnosis or Treatment. *Am J Surg* (2017) 214:695–700. doi: 10.1016/j.amjsurg.2017.06.013
35. Brouillet S, Ferrieres-Hoa A, Fournier A, Martinez G, Bessonnat J, Gueniffey A, et al. Cryopreservation of Oocytes Retrieved From Ovarian Tissue to Optimize Fertility Preservation in Prepubertal Girls and Women. *J Vis Exp* (2020) 164. doi: 10.3791/61777
36. Vilela J, Dolmans MM, Maruhashi E, Blackman MCNM, Sonveaux P, Miranda-Vilela AL, et al. Evidence of Metabolic Activity During Low-Temperature Ovarian Tissue Preservation in Different Media. *J Assist Reprod Genet* (2020) 37:2477–86. doi: 10.1007/s10815-020-01935-y
37. Cheng J, Ruan X, Zhou Q, Li Y, Du J, Jin F, et al. Long-Time Low-Temperature Transportation of Human Ovarian Tissue Before Cryopreservation. *Reprod BioMed Online* (2021) 43:172–83. doi: 10.1016/j.rbmo.2021.05.006
38. Liebenthron J, Montag M. Cryopreservation and Thawing of Human Ovarian Cortex Tissue Slices. *Methods Mol Biol* (2021) 2180:485–99. doi: 10.1007/978-1-0716-0783-1_23
39. Khattak H, Malhas R, Craciunas L, Afifi Y, Amorim CA, Fishel S, et al. Fresh and Cryopreserved Ovarian Tissue Transplantation for Preserving Reproductive and Endocrine Function: A Systematic Review and Individual Patient Data Meta-Analysis. *Hum Reprod Update* (2022) 28:400–16. doi: 10.1093/humupd/dmac003
40. Dolmans MM, von Wolff M, Poirot C, Diaz-Garcia C, Cacciottola L, Boissel N, et al. Transplantation of Cryopreserved Ovarian Tissue in a Series of 285 Women: A Review of Five Leading European Centers. *Fertil Steril* (2021) 115:1102–15. doi: 10.1016/j.fertnstert.2021.03.008
41. Dolmans MM, Iwahara Y, Donnez J, Soares M, Vaerman JL, Amorim CA, et al. Evaluation of Minimal Disseminated Disease in Cryopreserved Ovarian Tissue From Bone and Soft Tissue Sarcoma Patients. *Hum Reprod* (2016) 31:2292–302. doi: 10.1093/humrep/dew193
42. Jensen AK, Rechnitzer C, Macklon KT, Ifversen MRS, Birkebæk N, Clausen N, et al. Cryopreservation of Ovarian Tissue for Fertility Preservation in a Large Cohort of Young Girls: Focus on Pubertal Development. *Hum Reprod* (2017) 32:154–64. doi: 10.1093/humrep/dew273
43. Fernbach A, Lockart B, Armus CL, Bashore LM, Levine J, Kroon L, et al. Evidence-Based Recommendations for Fertility Preservation Options for Inclusion in Treatment Protocols for Pediatric and Adolescent Patients Diagnosed With Cancer. *J Pediatr Oncol Nurs* (2014) 31:211–22. doi: 10.1177/1043454214532025
44. Donnez J, Dolmans MM. Fertility Preservation in Women. *N Engl J Med* (2017) 377:1657–65. doi: 10.1056/NEJMra1614676
45. Rowell EE, Duncan F, Laronda MM. ASRM Removes the Experimental Label From Ovarian Tissue Cryopreservation (OTC): Pediatric Research Must Continue. *Fertil Steril* (2020). https://www.fertstertdialog.com/posts/asrm-removes-the-experimental-label-from-ovarian-tissue-cryopreservation-otc-pediatric-research-must-continue.
46. Segers I, Mateizel I, Van Moer E, Smitz J, Tournaye H, Verheyen G, et al. *In Vitro* Maturation (IVM) of Oocytes Recovered From Ovariectomy Specimens in the Laboratory: A Promising *"Ex Vivo"* Method of Oocyte Cryopreservation Resulting in The First Report of an Ongoing Pregnancy in Europe. *J Assist Reprod Genet* (2015) 32:1221–31. doi: 10.1007/s10815-015-0528-9
47. Yin H, Jiang H, Kristensen SG, Andersen CY. Vitrification of *In Vitro* Matured Oocytes Collected From Surplus Ovarian Medulla Tissue Resulting From Fertility Preservation of Ovarian Cortex Tissue. *J Assist Reprod Genet* (2016) 33:741–6. doi: 10.1007/s10815-016-0691-7
48. McLaughlin M, Albertini DF, Wallace W, Anderson RA, Telfer EE. Metaphase II Oocytes From Human Unilaminar Follicles Grown in a Multi-Step Culture System. *Mol Hum Reprod* (2018) 24(3):135–42. doi: 10.1093/molehr/gay002
49. Dolmans MM, Masciangelo R. Risk of Transplanting Malignant Cells in Cryopreserved Ovarian Tissue. *Minerva Ginecol* (2018) 70:436–43. doi: 10.23736/S0026-4784.18.04233-8
50. Poirot C, Fortin A, Lacorte JM, Akakpo JP, Genestie C, Vernant JP, et al. Impact of Cancer Chemotherapy Before Ovarian Cortex Cryopreservation on Ovarian Tissue Transplantation. *Hum Reprod* (2019) 34:1083–94. doi: 10.1093/humrep/dez047

51. Nurmio M, Asadi-Azarbaijani B, Hou M, Kiviö R, Toppari J, Tinkanen H, et al. Effect of Previous Alkylating Agent Exposure on Follicle Numbers in Cryopreserved Prepubertal and Young Adult Ovarian Tissue After Long-Term Xenografting. *Cancers (Basel)* (2022) 14(2):399. doi: 10.3390/cancers14020399
52. Hornshoj VG, Dueholm M, Mamsen LS, Ernst E, Andersen CY. Hormonal Response in Patients Transplanted With Cryopreserved Ovarian Tissue is Independent of Whether Freezing was Performed in Childhood or Adulthood. *J Assist Reprod Genet* (2021) 38:3039–45. doi: 10.1007/s10815-021-02320-z

Conflict of Interest: The authors declare that the research was conducted in the absence of any commercial or financial relationships that could be construed as a potential conflict of interest.

Publisher's Note: All claims expressed in this article are solely those of the authors and do not necessarily represent those of their affiliated organizations, or those of the publisher, the editors and the reviewers. Any product that may be evaluated in this article, or claim that may be made by its manufacturer, is not guaranteed or endorsed by the publisher.

frontiers | Frontiers in Endocrinology

ORIGINAL RESEARCH
published: 22 July 2022
doi: 10.3389/fendo.2022.938926

Clinical Features and Management of Suboptimal Ovarian Response During *in vitro* Fertilization and Embryo Transfer: Analysis Based on a Retrospective Cohort Study

Yizhi Yan[1], Ruomu Qu[2], Xiaodong Ma[2], Siyuan Qin[2], Lixue Chen[1], Xiaoxiao Ni[1], Rui Yang[1], Ying Wang[1], Rong Li[1] and Jie Qiao[1]*

[1] Department of Obstetrics and Gynecology, Reproductive Medical Center, Peking University Third Hospital, Beijing, China, [2] Peking University Health Science Center, Beijing, China

OPEN ACCESS

Edited by:
Yuting Fan,
Boston IVF, United States

Reviewed by:
Jing-Yan Song,
Shandong University of Traditional Chinese Medicine, China
Zhengao Sun,
Affiliated Hospital of Shandong University of Traditional Chinese Medicine, China
Tsung-Hsien Lee,
Chung Shan Medical University, Taiwan

***Correspondence:**
Ying Wang
wangying02114@bjmu.edu.cn

Specialty section:
This article was submitted to Reproduction, a section of the journal Frontiers in Endocrinology

Received: *08 May 2022*
Accepted: *15 June 2022*
Published: *22 July 2022*

Citation:
Yan Y, Qu R, Ma X, Qin S, Chen L, Ni X, Yang R, Wang Y, Li R and Qiao J (2022) Clinical Features and Management of Suboptimal Ovarian Response During in vitro Fertilization and Embryo Transfer: Analysis Based on a Retrospective Cohort Study. Front. Endocrinol. 13:938926. doi: 10.3389/fendo.2022.938926

Background: Based on dynamic changes of indicators during controlled ovarian hyperstimulation and of clinical outcomes of suboptimal ovarian response with different protocols, this study aimed to summarize the clinical characteristics of SOR and provide clinical recommendations.

Methods: Data of 125 patients with SOR and 125 controls who had undergone appropriate protocols for *in vitro* fertilization-embryo transfer were collected from a single medical center from January 2017 to January 2019. Basic clinical indexes, including age, BMI, antral-follicle count, infertility time, basic follicle-stimulating hormone, luteinizing hormone, LH/FSH ratio, estradiol, progesterone, testosterone, androstenedione, prolactin, anti-Mullerian hormone, and thyroid stimulating hormone levels, were analyzed using T-test. Dynamic indexes during COH, including amount and days of gonadotropin, sex hormone levels, and number of large/medium/small follicles at specified time periods, were analyzed using T-test and joint diagnosis analysis with ROC curves. Indexes of laboratory and clinical indicators were analyzed using the chi-square test.

Results: For the SOR group, BMI, duration time, and dosage of gonadotropin used for SOR were significantly higher. In the ultra-long/long group, ROC curve analysis showed that the LH/FSH ratio and BMI yielded cutoff values of 0.61 and 21.35 kg/m^2, respectively. A combined diagnosis of the two indexes showed higher sensitivity (90%) and specificity (59%). In the GnRH-ant group, ROC curve analysis showed an LH level, an LH/FSH ratio on COH day 2, and BMI yielded cutoff values of 2.47 IU/L, 0.57, and 23.95 kg/m^2, respectively. Combining the two indexes with BMI, both showed increased sensitivity (77%) and specificity (72% and 74%). The estradiol level and progesterone level during the late follicular stage in SOR patients were significantly lower than those in control patients for both protocol groups. At each monitoring time, delayed follicular development was observed. The live-birth rate in fresh cycles of the ultra-long/long group and the live-birth

rate in cumulative cycles of the antagonist group in the SOR group were lower than those in the control group.

Conclusion: SOR had adverse effects on clinical outcome. We provide some threshold values of basic LH/FSH ratio, BMI, COH day 2 LH, counts of follicles, and levels of estradiol/progesterone to be taken as reference to assist the early recognition of SOR.

Keywords: controlled ovarian hyperstimulation, *in vitro* fertilization & embryo transfer, suboptimal ovarian response, super-long protocol, long protocol, antagonist protocol, retrospective cohort study

1 INTRODUCTION

In controlled ovulation hyperstimulation (COH) during *in vitro* fertilization-embryo transfer (IVF-ET), the optimal selection of an ovulation hyperstimulation protocol is one of the key factors affecting the success rate of IVF. During the IVF process, most patients undergo normal reactions, which have not been clearly defined. According to experts, indicators, including age, ovarian reserve function, and past history of COH (low or high reaction), could be used to comprehensively evaluate ovarian reactions. Women with pure oviduct factors and/or male infertility belong to the population with normal ovarian reactions. Specific indicators predicting ovarian normal reaction (1) include age <35 years, normal ovarian reserve function, 1.0–1.4 g/l < anti-Mullerian hormone (AMH) <3.5–4.0 g/l, 7 < antral follicle counts (AFC) <14, follicle-stimulating hormone (FSH) level <10 IU/l, and no previous cancelled cycles due to low or high ovarian response. The most suitable ovum number after IVF is 5–15, with a high ovum maturity rate and high quality, which can achieve better clinical outcomes after IVF.

In addition to the normal response, a considerable proportion of patients showed high and low ovarian responses, accounting for approximately 20% and 10%, respectively (**Figure 1**) (2). High ovarian response refers to an abnormal sensitivity of the ovary to gonadotrophin (Gn) stimulation during COH. Currently, no unified diagnostic criteria toward high ovarian response have been established. Previous reports mostly define high ovarian response as acquired ovum number >15 or estradiol (E2) peak >3,000 pg/ml (3), which mainly occurs in patients with PCOS, patients with low body weight or low BMI, or patients with a previous history of high ovarian response. High estrogen levels lead to increased vascular permeability and eventual extravasation of blood into the third body cavity (4). As a result, varying degrees of hydrothorax, ascites, and cerebral edema, as well as varying degrees of blood concentration, hypovolemic shock, and/or venous thrombosis, may occur with severe consequences. Low ovarian response refers to the decreased ability of cortical follicles to grow, develop, or be fertilized to form embryos. The characteristics of poor ovarian response to Gn stimulation during the COH process include decreased developing follicle number, decreased peak of serum E2 level on the day of human chorionic gonadotropin (HCG) administration, increased use of Gn, decreased acquired ovum number, and poor clinical pregnancy rate (5). Patients with a low ovarian response usually have advanced age or normal age (less than 35-year old) with poor ovarian reserve function. Additionally, another ovarian response type, suboptimal ovarian response (SOR), has similar clinical manifestations but different mechanisms from low ovarian response. About 10%–15% of patients using gonadotropin-releasing hormone agonist (GnRH-a) exhibit SOR after downregulation of the pituitary gland (6). Different from low ovarian response, SOR is not induced by a decline in ovarian reserve function. Patients with SOR have normal age (less than 35 years old) with normal sex hormone levels, AMH level, and AFC. However, they exhibit abnormally slow follicular growth in the IVF process. If SOR is recognized in time and managed with appropriate remedial measures, it could still be converted into normal ovarian response, with optimal number of acquired ova (7). The diagnostic criteria of SOR are as follows: 1) no presence of follicles with a diameter >10 mm on the 6th–8th days of ovarian stimulation; 2) serum E2 level <655.1–728.3 pmol/l on the 6th day of ovarian stimulation; 3) slow follicular development and increased follicular diameter <3 mm within 3 days (1).

Currently, several studies have been conducted on SOR, but its mechanism of occurrence and related factors remain elusive. Additionally, its effect on COH and pregnancy outcomes is inconclusive. SOR may have a negative effect on the outcome of ovulation induction and pregnancy (8). Since SOR can be easily ignored, inappropriate handling of SOR cases may lead to a transition to low ovarian response with higher risk of cycle cancellation and increase in patients' economic and psychological burdens. In this study, a retrospective cohort analysis was performed on the clinical data of patients with SOR and normal ovarian response from January 2017 to January 2019. These patients must have undergone procedures following the ultra-long protocol, long protocol, and antagonist protocol for IVF-ET at the Reproductive Center of the Peking University Third Hospital. Additionally, the study explored the influencing factors on SOR, predictive value of indicators, and effect of SOR on the outcome of ovulation induction and clinical pregnancy outcome. Findings from this study may establish a theoretical basis and data summary for improving the poor outcomes of SOR cases.

2 MATERIALS AND METHODS

2.1 Patients

A retrospective analysis was performed on clinical data from 125 patients with SOR (slow growth of follicles during COH and low serum E2 level, based on diagnostic criteria of SOR talked above) who underwent IVF-ET at Peking University Third Hospital from January 2017 to January 2019. According to the COH ovarian

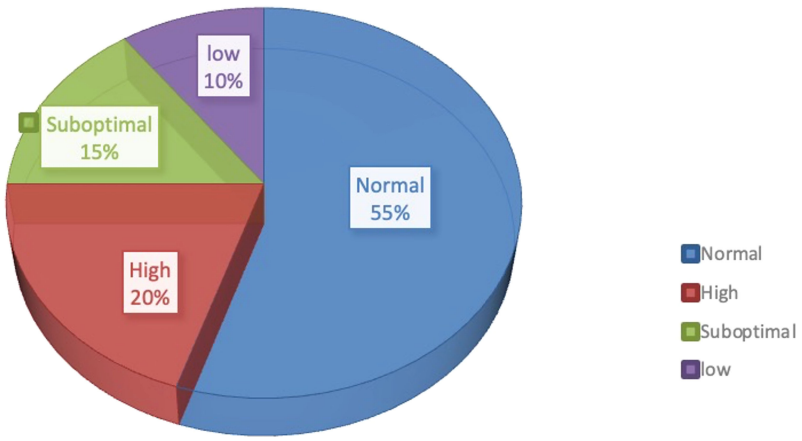

FIGURE 1 | Proportion of different ovarian responses during controlled ovarian responses types in IVF.

stimulation protocol, they were divided into ultra-long and long protocol group (71 cases) and antagonist protocol group (54 cases). Due to the limited sample size and similarity between the mechanisms of the ultra-long protocol and long protocol, both groups were combined into a single group for the analysis. The control group consisted of 125 patients with normal ovarian response who had undergone IVF-ET during the same period as the SOR group, with a similar number of patients in the corresponding protocol group in the SOR group. Due to attrition resulting from patients who canceled the cycle, some medical records were incomplete. Therefore, canceled cycles were not analyzed in this study. An overview of the patient recruitment process is shown in **Figure 2**.

2.2 IVF-ET Treatment Protocol

Generally, evaluation of ovarian function is based on age, weight, AFC, serum level of AMH, and basal serum level of hormones, followed by the development of COH protocols. Commonly used drugs during standardized long or ultra-long protocols include GnRH-agonist (GnRH-a) and Gn, while those during antagonist protocol are Gn and GnRH-antagonist (GnRH-ant). GnRH-a mainly used in our center include Diphereline (Ipsen Pharma Biotech, Signes, France) or Enantone (Leuprorelin, Takeda Pharma Company, Tokyo, Japan), and Gn used in our center include 1) recombinant FSH: Gonal-F (Merck Serono, Geneva, Switzerland), Puregon (Organon, P.O. Box 20 OssNL5340BH, Netherlands), and Urofollitropin (uFSH, Livzon Pharmaceutical Group Inc., Zhuhai, China); 2) menotropins for injection (urine-derived HMG, Livzon Pharmaceutical Group Inc., Zhuhai, China) and Menopur (high-purity urine-derived HMG, Ferring GmbH, Kiel, Germany); and 3) recombinant LH: Luveris (Merck Serono S.A). Antagonists used in our center include cetrorelix acetate (Pierre Fabre Pharmaceuticals, Castres, France) and Ganirek (N.V. Organon, Nijmegen, Netherlands).

Recombinant HCG (Merck Serono SA Aubonne Branch) was injected to retrieve oocytes. COH protocols refer to expert consensus on assisted reproduction ovulation induction drug treatment (9). The treatment process of each protocol, the exact drugs used during process, and the standards for pituitary regulation are described in Appendix E1 and Appendix E2.

2.3 Oocyte Retrieval and Transplantation

2.3.1 The Timing of Oocyte Retrieval

The dose and type of Gn were adjusted based on the patient's age and follicular development. The patient's level of serum LH, E2, and P and diameter of the follicles were monitored. When the patient's dominant follicles' diameter reached ≥18 mm, 250 μg of HCG (Shanghai Livzon Pharmaceutical) or Ovidrel (recombinant HCG, Merck Serono SPA) was injected intramuscularly. Thirty-six hours later, the oocytes were retrieved under vaginal ultrasound guidance. IVF or intracytoplasmic sperm injection (ICSI) fertilization was chosen based on the condition of the semen.

2.3.2 Embryo Transfer

The embryos transferred were clinically transferable embryos, and the embryo transfer program included the cleavage embryo transfer and blastocyst transfer. The Reproductive Medical Center of Peking University Third Hospital assessed the morphology of cleavage embryos based on the number of blastomeres for uniformity in size and fragmentation of the blastomeres. The embryos could be used with at least four cells and cell fragments below 30%. The blastocyst-stage embryo scoring used the blastocyst grading system proposed by Gardner et al. (10). According to the size of the blastocyst cavity and whether it was hatched, the development of the blastocyst was divided into six stages: stage I (early stage, blastocyst with cavity, the volume of the embryo cavity was less than one-half of the total volume); stage II (the volume of the blastocyst cavity was ≥1/2 of the embryo volume); stage III (the blastocyst cavity completely occupied the total volume of the embryo); stage IV (the blastocyst expanded, the blastocyst cavity when the embryo was completely occupied, the total volume of the embryo became larger, and the zona pellucida became thin); stage V (the blastocyst was hatching, part of the blastocyst escaped from the zona pellucida [ZP]); and stage VI (the blastocyst was hatched, completely escaped from the ZP).

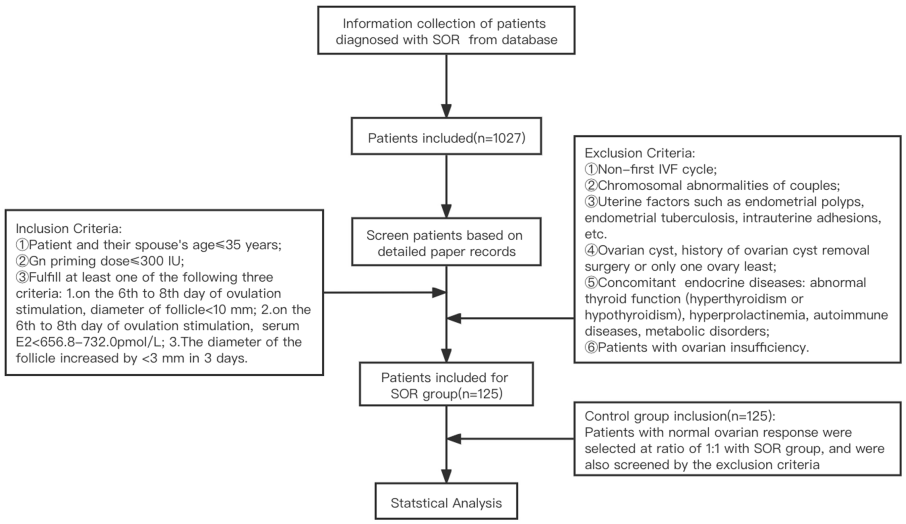

FIGURE 2 | Process of the Patients Recruitment.

Blastocysts in stages IV and V and some embryos in stage VI (including VIBC, VICB) could be used for embryo transfer.

Our center routinely performed fresh embryo transfer on day 3 post-fertilization. In the presence of factors that were not suitable for fresh embryo transfer, such as high risk of ovarian hyperstimulation syndrome (OHSS), endometrial factors, uterine effusion, progesterone elevation, and personal factors, the transfer would be cancelled, and remaining embryos or blastocysts would be vitrified and frozen, and thawed embryo transfer (FET) would be performed at an optimal time.

2.3.3 Follow-Up After Transplantation

Luteal phase support would be provided routinely after embryo transfer, involving oral, vaginal, or intramuscular progesterone. A blood test was performed after 14–16 days of transplantation. Serum HCG >5 mIU/ml was defined as a positive result (the detection of blood HCG in the Endocrinology Laboratory of Peking University Third Hospital Reproductive Medical Center adopts double-site enzyme immunoassay (double-antibody sandwich) kit from Beckman Coulter, Brea, CA, USA). Biochemical pregnancy referred to the pregnancy in which the blood HCG was positive, but the gestational sac echo was not detected by ultrasound. When serum HCG levels were elevated, transvaginal ultrasound was performed about 4–5 weeks after embryo transfer, and the pregnancy sac was found in or outside the uterine cavity, clinical pregnancy was diagnosed. In the absence of pregnancy, corpus luteum support was stopped. If intrauterine pregnancy was confirmed, luteal support was continued until 9–10 weeks of pregnancy.

2.4 Indicators for Further Observation

2.4.1 General Information of Patients

Age, age of spouse, body mass index (BMI), AFC, years of infertility, basic FSH, basic LH, basic E2, basic pituitary prolactin (prolactin, PRL), basic testosterone (T), basic androstenedione (AND), basic thyroid stimulating hormone (TSH) levels, levels of AMH, LH, FSH, E2, and P on 2nd day of COH, and vaginal ultrasound were used to detect the number of ovarian antral follicles. Follicle sizes were defined as follows: minimum follicle, diameter ≤10 mm; small follicle, 10 mm < diameter ≤15 mm; medium follicle, 15 mm < diameter of follicle ≤18 mm; large follicle, diameter >18 mm. Hormone levels were measured by electrochemiluminescence (Roche Diagnostics, Mannheim, Germany), and the operation was performed according to the manufacturer's instructions.

2.4.2 Indicators of Ovulation Induction

Gn using days; Gn using dose; COH 2nd-day FSH, LH, P, and E2 levels; changes in follicle number and diameter; LH, P, and E2 levels on COH 6th–8th, 9th–11th, 12th–14th, and 15th–17th days, and others; P/number of large follicles (progesterone to follicle index, PFI); and P/E2 ratio on HCG day were the indicators of ovulation induction.

2.4.3 Laboratory Indicators of Ovulation Outcome

These indicators included number of oocytes obtained, 2PN oocytes, fertilization number, cleavage number, high-quality embryo number, and corresponding 2PN rate, fertilization rate, cleavage rate, and high-quality embryo rate.

2.4.4 Indicators of Pregnancy Outcome

They included biochemical pregnancy rate, clinical pregnancy rate, live birth rate, abortion rate, and term birth rate. As the data of patients whose cycles were cancelled due to SOR in our center were lost to follow-up due to the patients' personal reasons, the statistics of SOR incidence and cycle cancellation rates were not accurate. Therefore, these two indicators were not calculated.

2.5 Statistical Analysis

All statistical analyses were performed using SPSS 24.0 (IBM SPSS Statistics CRZ1AML for Windows). Measurement data were expressed as mean ± standard deviation, and enumeration data were expressed as rates (%). Measurement data were tested for normality ($P > 0.05$). The data were normally distributed; therefore, t-test was used. The enumeration data were assessed using the chi-square test. The ROC survival curve was used to calculate the cutoff value, and the unconditional binary regression model was used for multivariate analysis. $P < 0.05$ indicated that the difference was statistically significant.

3 RESULTS

3.1 Baseline Information of All Patients

Among patients enrolled, the baseline data of patients in the ultra-long and long protocol group were compared separately, and no statistical difference was observed ($P > 0.05$) (**Supplementary Table 1**). Therefore, the two groups were combined into the ultra-long/long group for subsequent analyses. In the ultra-long/long group, compared with the control group, the SOR group had a higher BMI ($P < 0.05$) and higher AMH ($P < 0.05$); in the antagonist group, the SOR group was observed to have a higher BMI ($P < 0.05$) and lower TSH. No difference was observed between SOR patients and control patients in both protocol groups in age, spouse age, years of infertility, types of infertility, basal sex hormone levels, and basal follicle number ($P > 0.05$) (**Table 1**).

3.2.1 Comparison of Indexes in the COH Process

3.2.1 Ultra-Long/Long Group Population

3.2.1.1 Univariate Analysis

In the ultra-long and long protocol group, the SOR group had a longer response time to downregulation and longer Gn application time than the control group, and their total dose of Gn using was more than that of the control group. The basic LH/FSH ratio of the SOR group was 0.63 ± 0.37, significantly lower than the value of 0.84 ± 0.65 in the control group ($P < 0.05$) (**Supplementary Table 2**). The serum E2 level of COH on days 6–8 was 231.85 ± 108.58 pmol/l, significantly lower than the value of 1007.58 ± 1002.80 pmol/l in the control group (**Figure 3A**), and the serum P level of COH on days 12–14 was 1.09 ± 0.55 nmol/l, significantly lower than the value of 2.02 ± 1.11 nmol/l in the control group ($P < 0.05$) (**Figure 3B**) (**Supplementary Table 2**). On HCG day, the PFI and P/E2 ratios in the SOR group were 0.59 ± 0.25 and 0.33 ± 0.24 respectively, higher than those in the control group (0.56 ± 0.41 and 0.12 ± 0.68, respectively), but without statistical significance (**Supplementary Table 2**).

The minimum follicle number in the SOR group on days 6–8, 9–11, and 12–14 of COH were 11.78 ± 4.29, 12.42 ± 5.15, and 10.49 ± 4.91 respectively, all higher than the values in the control group (9.86 ± 4.63, 6.24 ± 3.02, 3.00 ± 1.41, respectively) with significance ($P < 0.05$). The number of small follicles in the SOR group on days 15–17 of COH was 7.03 ± 4.21, significantly higher than that of the control group, which was 4.75 ± 1.73 ($P < 0.05$), whereas the number of small follicles on days 9–11 of COH in the SOR group, the number of medium follicles on days 12–14 of COH in the SOR group, and the number of large follicles on days 15–17 of COH in the SOR group were lower than those in the control group ($P < 0.05$)(3.75 ± 3.26 vs. 8.42 ± 3.85, 2.89 ± 1.90 vs. 5.60 ± 3.53, and 3.24 ± 2.09 vs. 5.27 ± 1.49, respectively. Shown in **Figure 4**). Other details are included in **Supplementary Table 2**. Some of the indicators on certain measurement dates were not included in the statistical comparison due to the limited number of recorded medical records.

3.2.1.2 ROC Curve Analysis and Joint Diagnosis

Since the early identification and remediation of SOR is important, this study used the ROC curve to analyze the relatively early (COH ≦14 days) indicators with statistical differences between the SOR group and control group in each protocol group.

In the univariate analysis, the data with statistical differences in the early follicular phase and the median follicular phase were

TABLE 1 | Baseline information of all patients in IVF.

Index	Ultra-long/long protocol			Antagonist protocol		
	SOR group(n = 71)	Control group (n = 71)	*P value*	SOR group (n = 54)	Control group (n = 54)	*P value*
Age	29.68 ± 2.94	30.41 ± 3.18	0.156	28.87 ± 3.42	29.04 ± 3.08	0.791
Spouse age'	30.65 ± 2.88	31.08 ± 2.99	0.377	29.46 ± 2.85	29.67 ± 3.09	0.722
Infertility year	2.90 ± 2.22	3.04 ± 1.93	0.688	3.57 ± 2.55	3.41 ± 2.81	0.748
Primary infertility	41	47	0.300	34	33	0.843
Secondary infertility	30	24		20	21	
BMI(kg/m^2)	24.75 ± 3.47	21.64 ± 3.11	0.000	26.31 ± 3.47	23.52 ± 3.94	0.001
Basal FSH(IU/l)	6.56 ± 2.50	6.08 ± 2.01	0.240	6.19 ± 1.78	5.88 ± 1.68	0.406
Basal LH(IU/l)	3.93 ± 2.34	4.65 ± 2.73	0.116	5.59 ± 5.19	5.67 ± 3.35	0.073
Basal E2(pmol/l)	170.11 ± 110.02	172.24 ± 65.49	0.896	171.55 ± 82.43	202.32 ± 267.25	0.468
Basal PRL(ng/ml)	24.17 ± 45.30	17.95 ± 42.04	0.438	11.15 ±4.18	26.09 ± 61.12	0.113
Basal T(nmol/l)	2.85 ± 9.22	1.22 ± 3.55	0.220	2.89 ± 9.50	4.67 ± 11.42	0.431
Basal AND(nmol/l)	7.16 ± 3.51	5.98 ± 2.77	0.060	7.18 ± 3.63	8.31 ± 4.92	0.249
AMH(ng/ml)	4.76 ± 3.19	3.41 ± 2.32	0.013	5.29 ± 3.48	5.03 ± 4.06	0.769
TSH(μIU/ml)	2.54 ± 1.74	2.34 ± 1.33	0.465	2.12 ± 0.77	3.21 ± 2.18	0.001
AFC(bilateral)	13.39 ± 4.87	11.98 ± 5.45	0.117	16.13 ± 6.71	15.58 ± 5.74	0.653

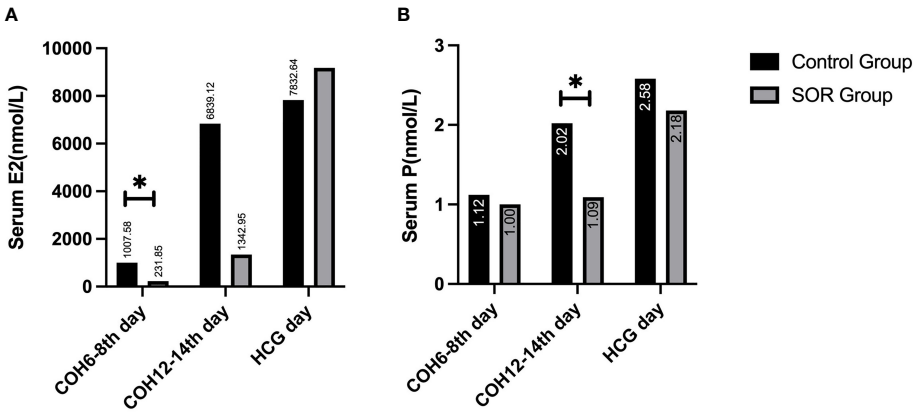

FIGURE 3 | **(A)** Comparison of serum E2 levels during the COH process in the ultra-long/long group; **(B)** Comparison of serum P levels during the COH process in the ultra-long/long group (note: (1).*Indicates statistically significant difference (P < 0.05); (2) n (SOR group) = 71, n (control group) = 71).

analyzed using the ROC curve according to the COH time sequence. Additionally, the threshold of SOR occurrence and the corresponding sensitivity and specificity of each index were calculated. The results are shown in **Table 2**. The combined diagnostic analysis of BMI and basal LH/FSH ratio showed that sensitivity increased to 90% and specificity was 59% (AUC, 0.814; 95% Cl, 0.738–0.889).

3.2.2 Antagonist Group Population

3.2.2.1 Univariate Analysis

In the antagonist protocol group, the SOR group had a longer downregulation time and ovulation induction time than the control group, and the total amount of Gn used was more than that of the control group. The level of serum LH of the SOR group on day 2 of COH was 3.28 ± 2.22 IU/l, significantly lower than 4.79 ± 3.57 IU/l in the control group (P < 0.05). Conversely, the LH level on HCG day in the SOR group was 3.10 ± 2.50 IU/l, higher than 1.91 ± 1.16 IU/l in the control group (**Figure 5B**) (**Supplementary Table 3**). The level of LH/FSH ratio of the SOR group on day 2 of COH was 0.54 ± 0.30, also significantly lower than 0.87 ± 0.88 in the control group (P < 0.05) (**Supplementary Table 3**). The levels of serum E2 of the SOR group on COH days 6–8 and 9–11 were 430.19 ± 314.40 pmol/l and 1,170.88 ± 1,138.11 pmol/l, respectively, lower than 2,150.61 ± 2,790.17 pmol/l and 5,933.60 ± 4,309.70 pmol/l in the control group (**Figure 5A**). The level of serum P of the COH SOR group was 1.16 ± 0.47 nmol/l, lower than 1.88 ± 0.85 nmol/l in the control group on COH days 9–11 (P < 0.05) (**Figure 5C**). The PFI and P/E2 ratio in the SOR group on the HCG day were not statistically different (**Supplementary Table 3**). The minimum follicle number in the SOR group on days 6–8, 9–11, and 12–14 of COH was higher than that of the control group (12.28 ± 5.10 vs. 9.14 ± 5.80, 10.41 ± 5.68 vs. 5.81 ± 4.04, 9.50 ± 5.09 vs. 3.00 ± 1.00, respectively) (P < 0.05), and the number of large follicles in

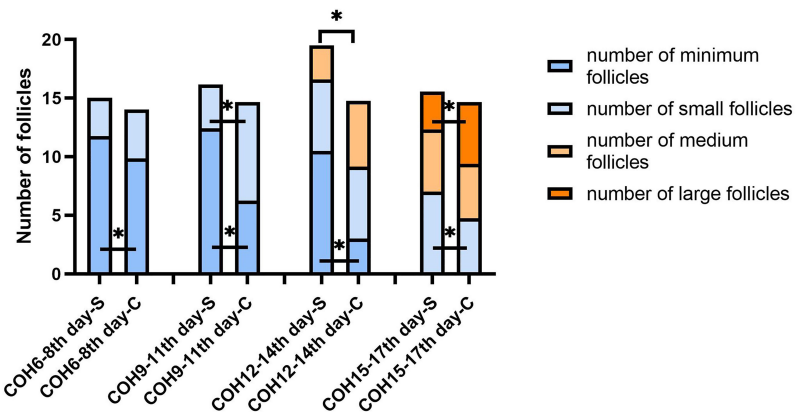

FIGURE 4 | Changes in the number of follicles of different sizes during the COH process in the ultra-long/long group patient (note (1): *Indicates statistically significant difference (P < 0.05); (2) S:SOR group; C: control group; (3) n (SOR group) = 71, n (control group) = 71).

the SOR group on COH days 12–14 was 1.40 ± 0.70, significantly lower than 4.58 ± 2.28 in the control group (P < 0.05)(**Figure 6**). Other details are included in **Supplementary Table 3**.

3.2.2.2 ROC Curve Analysis and Joint Diagnosis

In the univariate analysis, the data with statistical differences in the early and median follicular phases were analyzed using the ROC curve, according to the COH time sequence separately. The threshold of SOR occurrence and the corresponding sensitivity and specificity were calculated. The results are shown in **Table 3**. The level of LH and the LH/FSH ratio on COH day 2 were combined with BMI respectively for analysis, which resulted in a sensitivity of 77% and specificity of 72% (AUC, 0.758; 95% CI, 0.665–0.853) and sensitivity of 77% and specificity of 74% (AUC, 0.773; 95% CI, 0.681–0.865), respectively.

3.3 Laboratory Outcome of patients in IVF

Among the three COH protocol groups, compared with the control group, the SOR group had no statistical difference (P > 0.05) in the number of oocytes obtained, fertilized oocytes, 2PN oocytes, cleavage, and high-quality embryos and the rate of 2PN and high-quality embryos (**Table 4**).

3.4 Clinical Pregnancy Outcome of patients in IVF

The cumulative live-birth rate of the SOR group (40.54%) in the antagonist protocol group was lower than that of the control group (79.36%); the difference was statistically significant (P < 0.05). Compared with the control group, the biochemical pregnancy rate, clinical pregnancy rate, live-birth rate, miscarriage rate, and full-term birth rate of the SOR group were not different from those of the control group (P > 0.05) (see **Supplementary Tables 4–7** for details).

4 DISCUSSION

4.1 Signs of Patients with SOR

The results of this study showed that the occurrence of SOR has a correlation with patients' higher BMI, which is consistent with previous studies (11). It is worth noting that the AMH of SOR patients is even higher than that of the control group in the ultra-long/long protocol group, indicating that AMH does not only stand for the ovarian reserve but could play roles in abnormal follicular formation (12, 13). Results also show that, in the antagonist group, the TSH level of SOR patients is lower than that of the control group, but both of them are within the normal range clinically, and thus will not affect following treatment.

Of note, our results showed that the serum E2 level during the COH process of the SOR group was lower than that of the control group. This could be caused by relatively insufficient E2 metabolism because of more adipose tissues in patients with obesity who had a larger body surface area, so that they need more Gn during the COH process to obtain mature follicles. Previous studies have shown (11) that patients who are overweight and obese have different degrees of metabolic disorders, such as insulin resistance and hyperleptinemia, which can affect oocyte maturation and embryonic development potential (14). Although some patients enrolled in this study were clinically overweight, we did not screen the level of metabolic indexes such as insulin, glucose tolerance, or blood lipid profiles for these patients because their previous assessments showed normal ovarian response. Therefore, we did not include the analysis about metabolic factors in this study.

4.2 Dynamics of Hormone Levels During the COH Process

4.2.1 Analysis of the LH/FSH Ratio

Our study showed a lower basic LH/FSH ratio at the beginning of the COH process in SOR patients compared with the control group (basic LH/FSH ratio in ultra-long/long protocol, LH/FSH ratio on COH day 2 in antagonist protocol, respectively). A small section of the population could be more sensitive to downregulation, exhibiting excessive pituitary suppression and insufficient LH levels (4, 15). Usually, GnRH agonists inhibit 90% of the LH level but only inhibit about 40%–50% of the FSH level. The residual LH in the serum of most patients after downregulation is sufficient to support the development of multiple follicles in most cases; however, differences may exist in the sensitivity of the adenohypophysis to GnRH-a among different patients, for whom the relative or absolute lack of LH after pituitary downregulation could be the main reason for SOR when the long protocol is used (16).

4.2.2 Analysis of E2 and P

Our results indicated that during the process of COH, the levels of E2 and P in each protocol group of the SOR group were lower than those of the control group. The relatively lower E2 is mainly manifested in the early follicular phase, whereas the lower serum P is mainly manifested in the late follicular phase. This reason of lower E2 lies in that, in the early follicular phase, LH can stimulate the theca cells (TCs) to synthesize androgens, which are substrates for estrogen synthesis, and estrogen plays an

TABLE 2 | Results of single-factor indexes during the COH process in the ultra-long/long group patients.

Time	Index	AUC	Threshold	Sensitivity	Specificity	95% confidence interval
BMI (kg/m^2)		0.722	21.35	87%	35%	0.695-0.850
Basal LH/FSH ratio		0.631	<0.61	68%	63%	0.532-0.731
COH days 9–11	Number of minimum follicles	0.847	>10.5	72%	93%	0.763–0.931
	Number of small follicles	0.822	<3.5	63%	95%	0.693–0.951
COH days 12–14	Level of serum P	0.846	<1.52 nmol/L	95%	65%	0.734–0.959
	Number of minimum follicles	0.969	>5.5	93%	100%	0.923–1.000
	Number of medium follicles	0.760	<2.5	56%	82%	0.605–0.914

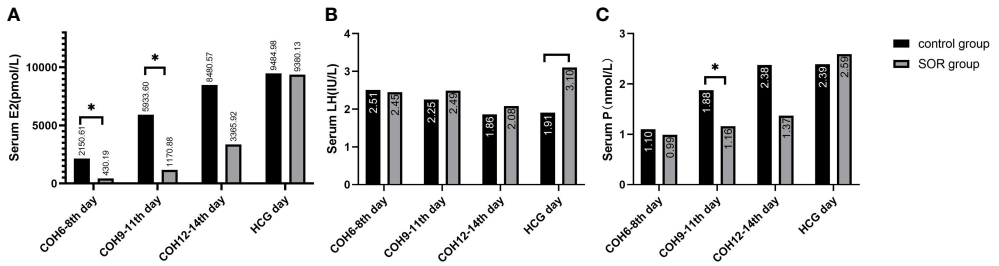

FIGURE 5 | **(A)** Level of serum E2 during the COH process in the antagonist group; **(B)** Level of serum LH during the COH process in the antagonist group patient; **(C)** Level of serum P during the COH process in the antagonist group patient (note: (1) *Indicates statistically significant difference ($P < 0.05$); (2) n (SOR group) = 54, n (control group) = 54).

important role in follicular growth and development. When the downregulation is too deep and the level of serum LH is too low, androgen synthesis will be insufficient, leading to a poor increase in serum E2 level and follicular development stagnation.

With regard to lower serum P, of note, it mainly happened at the late follicular phase in our study. Progesterone in the early follicular phase is mainly secreted by the adrenal glands, whereas progesterone in the late follicular phase is mainly derived from the ovaries, and this steroidal conversion by the adrenal gland is regulated by the ovaries (17). GCs express small amounts of LHR on the cell surface and respond to LH in the follicular stage; when multiple follicles mature, the number of luteinized GCs increases, which accordingly causes synthetic progesterone to gradually increase within 12–24 h before the appearance of the LH peak (18). With relatively insufficiency of LH, GCs synthesize less progesterone, as manifested in our study.

4.2.3 Analysis of the P/E2 Ratio and PFI

Previous studies have shown that a high PFI (18, 19) and a higher P/E2 ratio (20) each on the HCG day are independent risk factors for the reduction of live-birth rate in long protocol: for individuals with normal ovarian responses and high ovarian response, P/E2 ≥0.48 (unit of P, ng/ml) and ≥0.42, respectively, the live-birth rate is significantly reduced. In our study, the P/E2 ratio on the HCG day in each protocol group showed a higher trend in the SOR group than in the control group, but without significant statistical difference, which may be related to our limited sample size, and SOR has been recognized and the poor follicular development has been rescued to some extent by experienced clinicians. Further prospective study with a larger sample size is needed to verify the efficiency of P/E2 ratio on HCG day to predict the clinical outcome for SOR patients.

4.3 Follicle Growth During the COH Process

In the ultra-long/long protocol group, the minimum follicle number in the SOR group on COH days 6–8 was more than that in the control group, and this difference persisted until COH days 12–14, whereas the number of relatively larger follicles was lower than that in the control group, which is shown by the fact that in the cross section of each monitoring time, the retardation of follicular development persists and gradually accumulates.

Notably, the number of large follicles in the SOR group in the late follicular phase was lower than that in the control group in both protocol groups, but statistical difference only showed in the ultra-long/long protocol group. It might be caused by our limitation to a single center and small sample size but more likely due to the pituitary downregulation treatment in the ultra-

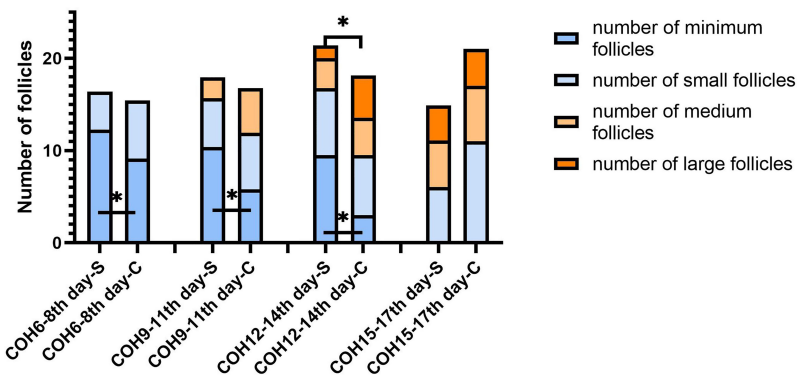

FIGURE 6 | Changes in the number of follicles of different sizes during the COH process in the antagonist group patient (note: (1) *Indicates statistically significant difference ($P < 0.05$); (2) S: SOR group; C: control group; (3) n (SOR group) = 54, n (control group) = 54).

TABLE 3 | Results of single-factor indexes during the COH process in the ultra-long/long group patients.

Time	Index	AUC	Threshold	Sensitivity	Specificity	95% confidence interval
BMI (kg/m^2)		0.743	23.95	76%	68%	0.646–0.839
COH day 2	LH	0.685	2.47 IU/l	49%	85%	0.584–0.787
	LH/FSH ratio	0.675	0.57	64%	70%	0.573–0.777
COH days 9–11	Serum E2	0.912	3,372 pmol/l	100%	73%	0.822–1.000
	Serum P	0.773	1.62 nmol/l	88%	58%	0.633–0.913
	Number of minimum follicles	0.741	8.5	68%	81%	0.605–0.877
COH days 12–14	Number of minimum follicles	0.944	5	92%	100%	0.857–1.000
	Number of large follicles	0.929	2.5	90%	88%	0.844–1.000

long/long protocol, because correction of the excessively deep pituitary inhibition state through the adjustment of Gn in the later stage is more difficult in this group, resulting in the difficulty for the final number of mature follicles to reach the normal level, whereas for patients in the antagonist protocol group, Gn is activated without pre-pituitary downregulation.

4.4 Laboratory Outcome and Clinical Outcome

There is no significant difference in laboratory outcomes between SOR patients and control patients in both protocol groups, possibly due to the prolonged use of Gn because clinicians in our reproductive center identified SOR in the early stage of the COH process and added r-LH/HMG or prolonged the time frame of treatment to revert SOR to a normal response. Early identification and remedial measures are essential to transforming SOR to a normal response to obtain good clinical outcomes.

Lower fresh-cycle live-birth rates of the SOR group were recorded in the ultra-long/long protocol group ($P < 0.05$), and lower cumulative-cycle live-birth rates of the SOR group were recorded in the antagonist protocol group ($P < 0.05$), indicating that the occurrence of SOR has an adverse effect on pregnancy outcome, although no significant difference of laboratory outcomes between SOR patients and control group. Because of technical limitation, we can only asses the outcome of COH referring to the number of oocytes retrieved and the morphology of oocytes and embryos, but not the quality of the oocytes in in essence (8). On the other hand, Gn dosage and Gn days for SOR patients are significantly higher than in the control group (**Supplementary Tables 2, 3**); possibilities remain that prolonged Gn exposure may detrimentally affect endometrial receptivity (21, 22).

4.5 Clinical Features in the Early Follicular Phase

Recognizing that SOR in time is important clinically, in most cases sensitivity has greater clinical significance than specificity; clinicians should at least detect patients at higher risk first and distinguish real SOR patients. A comprehensive evaluation of these indicators can improve the detection sensitivity of SOR.

Based on our results, for patients who adopt the ultra-long/long protocol, when the basic LH/FSH ratio <0.61 and the BMI >21.35 kg/m^2, the patient is more likely to have SOR, and clinicians need to have a high index of suspicion to deal with such cases in time. In the follow-up period of follicular monitoring, when the minimum follicle number on COH days 9–11 >10.5, number of small follicles on COH days 9–11 <3.5, minimum follicle number on COH days 12–14 >5.5, or number of medium follicles <2.5, and serum P <1.52 nmol/l, the patient may have already experienced SOR at this time, and the clinician should be able to manage. COH days 12–14 belong to the middle follicular phase; therefore, if not treated in time, SOR may not be rescued.

For patients undergoing the antagonist protocol, when LH on COH day 2 <2.47 IU/l and BMI >21.35 kg/m^2, or the LH/FSH ratio on COH day 2 <0.57 and BMI >21.35 kg/m^2, SOR may possibly occur, and clinicians should have a high index of suspicion to detect and manage the patient early. In the follow-up follicle monitoring period, COH days 9–11, serum E2 <3,372.0 pmol/l, serum P < 1.62 nmol/l, minimum follicle number >8.5,

TABLE 4 | Comparison of the laboratory outcomes of IVF patients.

Index	Ultra-long/long protocol			Antagonist protocol		
	SOR group (n = 71)	Control group (n = 71)	*P value*	SOR group (n = 54)	Control group (n = 54)	*P* value
Total number of oocytes obtained	13.46 ± 5.68	16.52 ± 8.95	0.157	13.91 ± 7.78	14.74 ± 9.96	0.595
Number of fertilized oocytes	12.63 ± 5.74	15.00 ± 8.69	0.261	12.24 ± 7.17	13.38 ± 9.34	0.437
Fertilization rate (%)	94.73 ± 14.20	91.36 ± 12.43	0.370	89.81 ± 16.92	92.20 ± 12.96	0.370
Number of 2PN oocytes	6.46 ± 3.53	6.96 ± 3.59	0.614	7.02 ± 5.54	8.50 ± 6.19	0.144
2PN rate (%)	51.94 ± 20.00	52.77 ± 26.39	0.901	56.76 ± 24.71	64.54 ± 22.16	0.348
Number of cleavage	8.21 ± 4.51	10.11 ± 6.72	0.247	9.08 ± 6.73	10.34 ± 7.04	0.285
Cleavage rate (%)	66.25 ± 24.83	67.91 ± 23.82	0.808	72.04 ± 29.29	78.42 ± 19.23	0.154
Number of high-quality embryos	4.83 ± 2.68	4.89 ± 3.08	0.946	4.98 ± 4.13	5.63 ± 4.23	0.362
High-quality embryo rate (%)	62.29 ± 23.88	51.30 ± 30.62	0.163	53.37 ± 22.53	57.63 ± 31.07	0.339

*2PN rate = (number of 2PN oocytes/number of fertilized oocytes) *100%; Cleavage rate = (Number of cleavage/Number of fertilized oocytes) *100%; High-quality embryo rate = (Number of high-quality embryos/Number of cleavage) *100%*

minimum follicle number on COH days 12–14 >5, or number of large follicles <2.5 indicates that the patient has already experienced SOR at this time and needs to be treated in time; otherwise, SOR may not be rescued.

Due to the limitation of sample size, this study did not separately calculate the indicators of the ultra-long protocol and long protocol. Therefore, the results are limited in clinical application, but they serve as reference and foundation for future studies with larger sample sizes.

4.6 Treatment of patients with SOR

4.6.1 Early Recognition of SOR

Based on our study, some points should be emphasized. In treating patients with SOR, first, an experienced doctor should comprehensively and accurately assess the patient's general condition to the greatest extent. Previous history of SOR or even a poor COH outcome and all possible related risk factors of SOR should be brought to the forefront, including general condition such as BMI, previous IVF records, ovarian reserve, uterine condition, and basal serum hormone condition, to assess the function of the hypothalamic–pituitary–ovarian (HPO) axis. Patients with obesity should be recommended to lose weight (23).

Next, during the COH process, clinicians should carefully observe the patient's follicular growth, serum E2 level, and COH time to identify abnormal growth conditions. Here based on our analysis, some threshold values of some clinical indexes including BMI and levels of serum sex hormones are provided to be taken as reference for the early recognition of SOR.

4.6.2 Supplement of Gn

In our reproductive center, Gn dosage was calculated according to the estimated ovarian function based on clinical routines and adjusted during the COH process according to the experience of clinicians. In most cases, the application of FSH should be sufficient, and even if insufficient, the monitoring doctors make adjustments to supplement the FSH dosage when patients first return to the hospital on days 4–6 following FSH severing; therefore, the majority of patients have good outcomes. However, SOR still occurs, indicating the complexity of SOR. We could preliminarily divide the possible causes of SOR into the following categories: 1) too deep pituitary function suppression by GnRH-a; 2) different sensitivity to Gn in the patient population, some of which might be explained by FSH receptor and/or LH receptor gene polymorphism (24) (20); 3) clinicians are unaware of the occurrence of SOR and do not supplement enough Gn in time. Of note, the GnRH antagonist protocol does not require downregulation pretreatment. Previous studies indicated that the incidence of SOR on the antagonist protocol was 4.8%, which was lower than that of the long protocol (15). However, it was a single-center study and the sample size of the SOR group in this study was limited (<100). The mechanism of occurrence of SOR in the antagonist protocol is more likely to be related with LH receptor mutation or an insensitive LH receptor (25).

Currently, receptor polymorphism inspection is not able to be widely used in clinic because it is time-consuming and money-consuming for most patients; of course, for patients with unexplained refractory SOR, FSH/LH receptor gene polymorphism inspection should be suggested to patients. Half-dose long-acting injection of GnRH-a or even 1/4~1/3 dosage can be considered to prevent excessive suppression of the pituitary gland for some patients with a history of SOR (1, 4). When serum LH <1.0 IU/l, the startup time of Gn can be considered for postponement or that LH can be used at the startup time.

In most cases, supplement of Gn is still the main method. Simply increasing FSH cannot improve the lack of endogenous LH (26); either LH or HMG is more efficient. Recombinant human luteinizing hormone (r-hLH) can highly mimic the biological function of LH *in vivo* (7, 27, 28); LH in the early follicular phase can act on TCs, increasing the production of E2 from GCs by promoting androgen synthesis and enhancing the sensitivity of GCs to FSH to improve ovarian responsiveness (29, 30). Moreover, the number of oocytes retrieved and the mature oocyte percentage obtained by adding 150 LH are higher than those added to 75 U (26); Jing et al. (31) revealed that when HMG (containing both FSH and LH) at 75 U/day was added during the early follicular phase (COH days 4–8), the number of oocytes obtained, number of available embryos, implantation rate, and clinical pregnancy rate were apparently higher than when it was added during the late follicular phase. Some studies (24) also show that in patients with SOR on the long protocol, adding HMG with a growth hormone (GH) at 4.5 IU/day until the HCG day is more effective than adding HMG only.

4.6.3 Monitor Development of Follicles

Patients with suspected SOR should be evaluated for FSH dose sufficiency, follicular growth rate, and E2 rate of increase, to assess whether LH is sufficient. Since LH is secreted in pulses, the detected serum LH level during the COH process does not completely represent the actual LH level *in vivo*; relying solely on the serum LH level to assess the occurrence or prediction of SOR may not be beneficial. Serum E2 and follicular growth are still the main focus during the COH monitoring process; if follicular growth and E2 rise show an upward trend, the time of Gn use can be continued to ensure that the oocytes fully mature. Otherwise, LH or HMG should be added in time.

Our study indicates that SOR has adverse effects on clinical outcome. Early recognition of SOR can be of great importance for rescuing it. Specific treatment protocol for SOR needs to be clarified by more detailed prospective controlled studies.

DATA AVAILABILITY STATEMENT

The original contributions presented in the study are included in the article/**Supplementary Material**. Further inquiries can be directed to the corresponding author.

ETHICS STATEMENT

The studies involving human participants were reviewed and approved by the Ethics Committee of Peking University Third Hospital (No. IRB00006761-M2020004). Informed consent was

waived because this was a data analysis with no personally identified information. Written informed consent for participation was not required for this study in accordance with the national legislation and the institutional requirements.

AUTHOR CONTRIBUTIONS

YY performed the literature search, collected and analyzed the data, and wrote the manuscript; RQ, XM, and SQ helped screening the medical records and collecting the data; XN and LC helped analyzing the data; RY, YW, RL, and JQ critically reviewed and revised the manuscript. All authors read and approved the final submission.

FUNDING

This work was supported by National Natural Science Foundation of China [81873833], National Natural Science Foundation of China [81550022], and Key Clinical Research Project of Peking University Third Hospital (BYSY2018016).

ACKNOWLEDGMENTS

I would like to thank my supervisor, Prof. Wang, sincerely. Without her consistent guidance and encouragement, I would not have completed this study. She has been my beacon in life in and outside academia.

SUPPLEMENTARY MATERIAL

The Supplementary Material for this article can be found online at: https://www.frontiersin.org/articles/10.3389/fendo.2022.938926/full#supplementary-material

REFERENCES

1. Ferraretti AP, Gianaroli L, Magli MC, D'angelo A, Farfalli V, Montanaro N. Exogenous Luteinizing Hormone in Controlled Ovarian Hyperstimulation for Assisted Reproduction Techniques. *Fertil Steril* (2004) 82:1521–6. doi: 10.1016/j.fertnstert.2004.06.041
2. Ke D, Ling L, Chang X, Rong L, Kang Z, Xin S. Criteria and Clinical Predictors of High Ovarian Response: A Systematic Review. *Chin J Reprod Contracep* (2019) 39:376–84. doi: 10.3760/cma.j.issn.2096-2916.2019.05.006
3. Wei J, Yuan J, Bai J, Zhu J, Tan L. Comparison of the Value of Commonly Used Indicators for Evaluating Ovarian Reserve in Predicting Ovarian Responsiveness. *J Reprod Med* (2020) 29:27–32. https://szyx.cbpt.cnki.net/WKB3/WebPublication/paperDigest.aspx?paperID=604761ba-b670-4d58-94ce-4885f24e310d#
4. Mahajan N. Ovarian Hyperstimulation Syndrome. *Int J Infertil Fetal Med* (2013) 4:71–8. doi: 10.5005/jp-journals-10016-1065
5. Li T, Wu M, Huang H, Huang Y. Meta-Analysis of the Clinical Effects of IVF-ET With Different Ovulation Induction Protocol on Patients With Low Ovarian Response. *J Reprod Med* (2019) 28:1289–95. https://www.cnki.com.cn/Article/CJFDTOTAL-ZYX201911009.htm
6. Wang B, Liu W, Liu Y, Zhang W, Ren C, Guan Y. What Does Unexpected Suboptimal Response During Ovarian Stimulation Suggest, an Overlooked Group? *Front Endocrinol (Lausanne)* (2021) 12:795254. doi: 10.3389/fendo.2021.795254
7. Alviggi C, Conforti A, Esteves SC, Andersen CY, Bosch E, Bühler K, et al. Recombinant Luteinizing Hormone Supplementation in Assisted Reproductive Technology: A Systematic Review. *Fertil Steril* (2018) 109:644–64. doi: 10.1016/j.fertnstert.2018.01.003
8. Broekmans FJ. The Sub-Optimal Response to Controlled Ovarian Stimulation: Manageable or Inevitable? *Hum Reprod* (2015) 30:2009–10. doi: 10.1093/humrep/dev150
9. Qiao J, Ma C, Liu J, Ma X, Li S, Yang Y, et al. Expert Consensus on the Treatment of Assisted Reproduction and Ovulation Stimulation Drugs. . *Reprod Contracep* (2015) 35:211–23.
10. Gardner DK, Balaban B. Assessment of Human Embryo Development Using Morphological Criteria in an Era of Time-Lapse, Algorithms and 'Omics': Is Looking Good Still Important? *Mol Hum Reprod* (2016) 22:704–18. doi: 10.1093/molehr/gaw057
11. Zhang D, Zhu Y, Gao H, Zhou B, Zhang R, Wang T, et al. Overweight and Obesity Negatively Affect the Outcomes of Ovarian Stimulation and *In Vitro* Fertilisation: A Cohort Study of 2628 Chinese Women. *Gynecol Endocrinol* (2010) 26:325–32. doi: 10.3109/09513591003632100
12. Hughes CHK, Murphy BD. Nuclear Receptors: Key Regulators of Somatic Cell Functions in the Ovulatory Process. *Mol Aspects Med* (2021) 78:100937. doi: 10.1016/j.mam.2020.100937
13. Tanimoto R, Sekii K, Morohaku K, Li J, Pépin D, Obata Y. Blocking Estrogen-Induced AMH Expression is Crucial for Normal Follicle Formation. *Development* (2021) 148:dev197459. doi: 10.1242/dev.197459
14.
15. Feng S. *A Preliminary Study on the Causes, Management and Clinical Outcome of Sub-Optimal Ovarian Response in GnRH Antagonist Regimen*. Southern Medical University (2017).
16. Yazıcı Yılmaz F, Görkemli H, Çolakoğlu MC, Aktan M, Gezginç K. The Evaluation of Recombinant LH Supplementation in Patients With Suboptimal Response to Recombinant FSH Undergoing IVF Treatment With GnRH Agonist Down-Regulation. *Gynecol Endocrinol* (2015) 31:141–4. doi: 10.3109/09513590.2014.965675
17. De Geyter C. Progesterone Serum Levels During the Follicular Phase of the Menstrual Cycle Originate From the Crosstalk Between the Ovaries and the Adrenal Cortex. *Hum Reprod* (2002) 17:933–9. doi: 10.1093/humrep/17.4.933
18. Ding J, Yang J, Zhao M, Zhang Y. The Relationship Between the Ratio of Serum Progesterone Levels and the Number of Follicles With Diameter ≥14mm on hCG Days and the Outcome of IVF-Et. *J Int Reprod Health/Family Plann* (2016) 35:13–6. https://www.cnki.com.cn/Article/CJFDTOTAL-GWJS201601003.htm
19. Shufaro Y, Sapir O, Oron G, Haroush AB, Garor R, Pinkas H, et al. Progesterone-To-Follicle Index is Better Correlated With *In Vitro* Fertilization Cycle Outcome Than Blood Progesterone Level. *Fertil Steril* (2015) 103:669–674.e3. doi: 10.1016/j.fertnstert.2014.11.026
20. Zhang J, Guan Y. The Effect of Serum Progesterone and the Ratio of Progesterone to Estradiol on HCG Day on the Live Birth Rate of Long-Acting Long-Protocol in the Early Follicular Phase. *J Reprod Med* (2019) 28:1137–43. https://www.cnki.com.cn/Article/CJFDTOTAL-SZYX201910007.htm
21. Mann ON, Kong C-S, Lucas ES, Brosens JJ, Hanyaloglu AC, Brighton PJ. Expression and Function of the Luteinizing Hormone Choriogonadotropin Receptor in Human Endometrial Stromal Cells. *Sci Rep* (2022) 12:8624. doi: 10.1038/s41598-022-12495-9
22. Evans J, Salamonsen LA. Too Much of a Good Thing? Experimental Evidence Suggests Prolonged Exposure to hCG is Detrimental to Endometrial Receptivity. *Hum Reprod* (2013) 28:1610–9. doi: 10.1093/humrep/det055

23. Moragianni VA, Jones S-ML, Ryley DA. The Effect of Body Mass Index on the Outcomes of First Assisted Reproductive Technology Cycles. *Fertil Steril* (2012) 98:102–8. doi: 10.1016/j.fertnstert.2012.04.004
24. Zhao Z, Qi R, Wu X, Zhou L, Liang Y, Wang J. Evaluation of the Efficacy of Growth Hormone Supplementation in Patients With Sub-Optimal Ovarian Response. *Chin Family Plann Obstet Gynecol* (2019) 11:41–44+59. https://www.cnki.com.cn/Article/CJFDTotal-JHFC201907012.htm
25. Loutradis D, Patsoula E, Minas V, Koussidis GA, Antsaklis A, Michalas S, et al. FSH Receptor Gene Polymorphisms Have a Role for Different Ovarian Response to Stimulation in Patients Entering IVF/ICSI-ET Programs. *J Assist Reprod Genet* (2006) 23:177–84. doi: 10.1007/s10815-005-9015-z
26. De Placido G, Alviggi C, Mollo A, Strina I, Ranieri A, Alviggi E, et al. Effects of Recombinant LH (rLH) Supplementation During Controlled Ovarian Hyperstimulation (COH) in Normogonadotrophic Women With an Initial Inadequate Response to Recombinant FSH (rFSH) After Pituitary Downregulation. *Clin Endocrinol* (2004) 60:637–43. doi: 10.1111/j.1365-2265.2004.02027.x
27. Maher JY, Segars J. When is Recombinant Luteinizing Hormone Supplementation Beneficial During Ovarian Stimulation? *Fertil Steril* (2018) 109:611–2. doi: 10.1016/j.fertnstert.2018.01.041
28. Younis JS, Laufer N. Recombinant Luteinizing Hormone Supplementation to Recombinant Follicle Stimulating Hormone Therapy in Gonadotropin Releasing Hormone Analogue Cycles: What is the Evidence? *Curr Med Res Opin* (2018) 34:881–6. doi: 10.1080/03007995.2017.1417827
29. Practice Committee of the American Society for Reproductive MedicineUse of Clomiphene Citrate in Infertile Women: A Committee Opinion. *Fertil Steril* (2013) 100:341–8. doi: 10.1016/j.fertnstert.2013.05.033
30. Conforti A, Esteves SC, Cimadomo D, Vaiarelli A, Di Rella F, Ubaldi FM, et al. Management of Women With an Unexpected Low Ovarian Response to Gonadotropin. *Front Endocrinol (Lausanne)* (2019) 10:387. doi: 10.3389/fendo.2019.00387
31. Tang J, Zhao Z, Li Y, Liu D. The Effect of Adding Luteinizing Hormone During Different Periods on the Clinical Outcome of Patients With Polycystic Ovary Syndrome Together With Sub-Optimal Ovarian Response in Long-Protocol. *J Hunan Normal Univ (Medical Edition)* (2018) 15:56–60. doi: 10.3969/j.issn.1673-016X.2018.04.018

Conflict of Interest: The authors declare that the research was conducted in the absence of any commercial or financial relationships that could be construed as a potential conflict of interest.

Publisher's Note: All claims expressed in this article are solely those of the authors and do not necessarily represent those of their affiliated organizations, or those of the publisher, the editors and the reviewers. Any product that may be evaluated in this article, or claim that may be made by its manufacturer, is not guaranteed or endorsed by the publisher.

frontiers | Frontiers in Endocrinology

ORIGINAL RESEARCH
published: 22 July 2022
doi: 10.3389/fendo.2022.907286

NAT10 Maintains *OGA* mRNA Stability Through ac4C Modification in Regulating Oocyte Maturation

Jiayu Lin[1†], *Yuting Xiang*[1,2†], *Jiana Huang*[1†], *Haitao Zeng*[1], *Yanyan Zeng*[1], *Jiawen Liu*[1], *Taibao Wu*[1], *Qiqi Liang*[1], *Xiaoyan Liang*[1*], *Jingjie Li*[1*] *and Chuanchuan Zhou*[1*]

[1] *Reproductive Medicine Center, Sixth Affiliated Hospital of Sun Yat-sen University, Guangzhou, China,* [2] *Department of Obstetrics and Gynecology, Affiliated Dongguan People's Hospital, Southern Medical University, Dongguan, China*

In vitro maturation (IVM) refers to the process of developing immature oocytes into the mature *in vitro* under the microenvironment analogous to follicle fluid. It is an important technique for patients with polycystic ovary syndrome and, especially, those young patients with the need of fertility preservation. However, as the mechanisms of oocyte maturation have not been fully understood yet, the cultivation efficiency of IVM is not satisfactory. It was confirmed in our previous study that oocyte maturation was impaired after N-acetyltransferase 10 (NAT10) knockdown (KD). In the present study, we further explored the transcriptome alteration of NAT10-depleted oocytes and found that *O-GlcNAcase* (*OGA*) was an important target gene for NAT10-mediated ac4C modification in oocyte maturation. NAT10 might regulate *OGA* stability and expression by suppressing its degradation. To find out whether the influence of NAT10-mediated ac4C on oocyte maturation was mediated by *OGA*, we further explored the role of *OGA* in IVM. After knocking down OGA of oocytes, oocyte maturation was inhibited. In addition, as oocytes matured, *OGA* expression increased and, conversely, O-linked N-acetylglucosamine (O-GlcNAc) level decreased. On the basis of NAT10 KD transcriptome and OGA KD transcriptome data, NAT10-mediated ac4C modification of *OGA* might play a role through G protein–coupled receptors, molecular transduction, nucleosome DNA binding, and other mechanisms in oocyte maturation. *Rsph6a*, *Gm7788*, *Gm41780*, *Trpc7*, *Gm29036*, and *Gm47144* were potential downstream genes. In conclusion, NAT10 maintained the stability of *OGA* transcript by ac4C modification on it, thus positively regulating IVM. Moreover, our study revealed the regulation mechanisms of oocytes maturation and provided reference for improving IVM outcomes. At the same time, the interaction between mRNA ac4C modification and protein O-GlcNAc modification was found for the first time, which enriched the regulation network of oocyte maturation.

Keywords: oocyte, *in vitro* maturation, NAT10, N4-acetylcytidine, OGA, O-GlcNAc, transcription

OPEN ACCESS

Edited by:
Yuting Fan,
Boston IVF, United States

Reviewed by:
Junfeng Ma,
Georgetown University, United States
Chad Slawson,
University of Kansas Medical Center Research Institute, United States
Arnab Banerjee,
Birla Institute of Technology and Science, India

***Correspondence:**
Chuanchuan Zhou
zhouchch7@mail.sysu.edu.cn
Jingjie Li
lijjie3@mail.sysu.edu.cn
Xiaoyan Liang
liangxy2@mail.sysu.edu.cn

[†]These authors have contributed equally to this work

Specialty section:
This article was submitted to Reproduction, a section of the journal Frontiers in Endocrinology

Received: *29 March 2022*
Accepted: *16 May 2022*
Published: *22 July 2022*

Citation:
Lin J, Xiang Y, Huang J, Zeng H, Zeng Y, Liu J, Wu T, Liang Q, Liang X, Li J and Zhou C (2022) NAT10 Maintains OGA mRNA Stability Through ac4C Modification in Regulating Oocyte Maturation. Front. Endocrinol. 13:907286. doi: 10.3389/fendo.2022.907286

INTRODUCTION

In vitro oocyte maturation (IVM) is a promising assisted reproductive technology simulating the physiological development of oocytes from the immature, also called germinal vesicle (GV) stage, to the mature, which was also called metaphase II (MII) (1, 2). IVM presents great clinical application values, especially for those patients with indications for fertility preservation requirement, with polycystic ovary syndrome or high risk of ovarian hyperstimulation syndrome, etc. (3, 4). However, because the underlying mechanisms involved in oocyte maturation have not been fully understood, IVM has not achieved satisfying clinical outcomes compared with conventional *in vitro* fertilization and other assisted reproductive techniques. Therefore, it is very necessary to explore the mechanisms of IVM, which will help to discover new molecular targets and directions for improving its clinical application.

The process of oocyte maturation is temporally and spatially monitored to permit the proper and accurate expression of genes, which is highly dependent upon post-transcriptional regulation of messenger RNA (mRNA) (5, 6). In early gametes, it is mainly achieved through epigenetic mechanisms, which is necessary for ovulation and zygote to build up competence during the maternal-to-zygotic genome transition (MZT) (7, 8). Therefore, the role of epigenetic modifications is crucial, and the underlying mechanisms remain to be further explored.

More than 100 epigenetic modifications of mRNA, including N6-adenosine methylation (m6A), cytosine hydroxylation (m5C), and N1-adenosine methylation (m1A), have been revealed in mediating the stability, function, and splicing process of targeted mRNAs (9–11). Previous studies on m6A have reported that two important readers, YTHDF2 and YTHDC1, were respectively located in the nucleus and cytoplasm of oocytes, which played crucial roles in mRNA degradation, transcriptome switching, and selective splicing during oocyte maturation. KIAA1429 is a recently identified component of the m6A writers, affecting the quality of oocytes by mediating meiosis, chromatin remodeling, and selective splicing of genes associated with oogenesis (12).

N4-acetylcytidine (ac4C) is the first acetylcytidine event and highly conserved epigenetic modification in eukaryotic mRNAs reported in recent years (13, 14). Enriched in the coding sequence (CDS) region of genes, it gradually decreases along the 5′ end to the 3′ end of the aimed transcripts (15). NAT10, as the only identified acetyltransferase, is thought to play critical roles in promoting mRNA stability and maintaining translation fidelity through ac4C modification on the specific sequence of target mRNAs (16). The dysregulation of NAT10 inhibited cell development progress and led to various diseases, such as gastric cancer and systemic lupus erythematosus (17–19).

Our team has previously demonstrated that NAT10-mediated ac4C modification affected oocyte maturation. In the NAT10 KD group, GV stage oocytes could not reach a satisfying first polar body extrusion rate compared with the negative control one (20). However, related downstream genes and potential mechanisms underneath it remain unclear. By analyzing transcriptomic data of the NAT10-depleted oocytes, *OGA* (also known as *Mgea5*) was verified as one of the important targets of NAT10-mediated ac4C modification in regulating oocyte maturation. OGA depletion caused impaired oocyte maturation, which resulted in the fluctuation in O-GlcNAc in IVM. NAT10 might regulate the stability of *OGA* transcript by ac4C modification on it, which further mediated oocyte maturation through G protein–coupled receptors, molecular transduction, and nucleosome DNA binding. *Rsph6a*, *Gm7788*, *Gm41780*, *Trpc7*, *Gm29036*, and *Gm*47144 were identified as candidate downstream genes.

Our study aimed to investigate the mechanisms of NAT10-mediated ac4C during IVM and further explored the role of downstream gene *OGA* in oocyte maturation. As OGA is an important regulatory enzyme of O-GlcNAc modification, our research will provide reference for understanding the interaction between ac4C modification and O-GlcNAcylation.

MATERIALS AND METHODS

Mice

Three- to 4-week-old female C57BL/6 mice were purchased from Vital River Laboratory Animal Technology Co., Ltd (Beijing, China). The mice were housed in the animal laboratory center with a controlled 12-h:12-h light/dark cycle, humidity (50%–60%), and temperature (22°C–24°C). Before experiments, there was 1 week for the mice to adapt to the environment. Water and food were freely accessed to. In addition, all the interventions were approved by the Animal Care and Use Committee of the Sixth Affiliated Hospital, Sun Yat-sen University (Guangzhou, China) (ethical approval number: IACUC-2021112502).

Oocytes Collection

Female C57BL/6 mice were intraperitoneally injected with 10 International Units of pregnant mare's serum gonadotropin (PMSG) (Ningbo Second Hormone Factory, Zhejiang, China) 46–48 h earlier. The ovaries were then dissected and obtained. After the fat around the ovarian tissue being removed, the antral follicles were punctured with a sterile needle in a petri dish containing M2 medium (Sigma-Aldrich, M7167) and cumulus-oocyte complexes (COCs) were released.

Oocyte *In Vitro* Maturation

The IVM medium was made from TCM-199 (Gibco, 31100035), 0.2 mM sodium pyruvate, and 10% fetal bovine serum (FBS). GV oocytes were cultured in IVM medium in a cell incubator of 5% CO_2 at 37°C for 14–16 h. Then, GV oocytes were isolated gently from COCs in the hyaluronidase (Sigma-Aldrich, 37326-33-3) by repeatedly pipetting. The oocytes were collected for maturation rates calculation and further analyses.

NAT10/OGA Knockdown by Trim-Away and Electroporation

Trim-Away is a newly discovered degradation method that recruits proteasome to hydrolysis antibody-bound proteins through *Trim 21* mRNA (21). Because of its high specificity,

Trim-Away has been wildly used in oocytes and embryos (22, 23). To explore the effect of NAT10-mediated ac4C modification on *OGA*, *OGA* on oocyte maturation, and further on O-GlcNAc modification, we conducted targeted degradation of endogenous NAT10 and OGA in oocytes based on electroporation and Trim-Away. NAT10 antibody (ProteinTech, 13365-1-AP) and OGA antibody (ProteinTech, 14711-1-AP) were purified in advance to reduce harmful chemicals intervening in oocyte maturation such as sodium azide. First, 20 μl of antibody was pipetted into an Eppendorf tube and then 180 μl of phosphate-buffered saline (PBS) was added to dilute the antibody. Ultrafiltration tube (Millipore, UFC5100BK) was used to concentrate the antibody at 14,000 g for 10 min. The filtrate was discarded, and the inner tube was placed into a new Eppendorf tube invertedly. After centrifugation at 1,000 g for 2 min, the antibody was collected and prepared. Later, denuded GV oocytes were placed in the Tyrode's solution (Leagene, CZ0060) for 10 s to weaken the zona pellucida. Then, they were washed for three times in Opti-MEM medium to reduce the Tyrode's solution as much as possible. In addition, the oocytes were transferred to the antibody-containing Opti-MEM medium (total volume of 5 μl), which were then transferred into the electrode groove and waited to be electroporated. The electroporation procedure was executed according to what we have reported (1-ms pulse width, 30 volts in amplitude, and 4 pulses at intervals of 50 ms) (20). For the experimental group, we electroporated *Trim 21* mRNA and NAT10 antibody or OGA antibody in Opti-MEM medium at a final concentration of 200 ng/μl into GV stage oocytes. As a control, homologous IgG (Fine Test, PNSA-0106) and *Trim 21* mRNA were delivered into at the same concentration. Afterward, the oocytes were washed for three times and incubated in Opti-MEM medium to recover for 30 min. Then, the oocytes would be transferred to IVM medium for evaluating maturation rates 14–16 h later or transferred to a cell incubator with 3-isobutyl-1-methyl-xanthine (IBMX)–containing IVM medium (50 μM IBMX) to be kept arrested at GV stage and waited for the adequate degradation of the aimed proteins until immunofluorescence. The IBMX (HY-12318) was purchased from MCE, Shanghai, China.

Fluorescent-Labeled Antibody Technique

To avoid the combination of the secondary antibodies in immunofluorescence with the antibodies used in electroporation, the OGA antibody was labeled with 647 fluorescence, the NAT10 antibody with 488 fluorescence, and the OGT antibody (CST, D1D8Q) with 555 fluorescence. The experiments were performed almost according to the manufacturer's instructions of LinKine AbFluorTM 647/488/555 Labeling Kit (LinKine, KTL0560; LinKine, KTL0520; Linkine, KTL0530). To get the optimal labeling effect, the unlabeled antibody should be purified in advance. In addition, the final concentration should reach 2 mg/ml. Then, 1 μl of AbFluorTM 647/488/555 labeling solution was added to the 20 μl of the aimed antibody and gently mixed with a pipette. Activated AbFluorTM 647/488/555 solution (0.5 μl) was later added into, mixed evenly, and incubated in 37°C under the dark for 1 h. Centrifuged at 12,000 g, 4°C for 20 min, the supernatant was collected and the filtrate was discarded. PBS (30 μl) was added into and, after being mixed evenly, the liquid was centrifuged at 12,000 g, 4°C for another 20 min. The purification column was then taken out and upturned into a new a clean centrifugal tube. Then, it was centrifuged for the last 2 min, 4,000 g, 4°C. The solution collected from the centrifugal tube was the final labeled antibody.

Immunofluorescence Staining of Oocytes

The oocytes were fixed in 1% paraformaldehyde and 0.2% Triton X-100 in PBS for 1 h at room temperature. After 1 h, the oocytes were transferred into 3% bovine serum albumin (BSA) in PBS to be blocked for another 1 h. Next, the oocytes were incubated with fluorescent-labeled antibodies against OGA (1:200), NAT10 (1:200), O-GlcNAc Transferase (OGT) (1:200), and/or another first antibody RL2 (1:200, Abcam, ab2739) at 4°C overnight. After three washes with 0.3% BSA, oocytes incubated with RL2 first antibody were then incubated with Cy3-conjugated secondary antibody (1:500, Earthox, E031620) at room temperature for 1 h in the dark condition. The oocytes were then washed with 0.3% BSA for three times. In addition, images were taken under the inverted phase contrast confocal microscope (LSM 880, Zeiss, JENA, Germany).

NAT10/ac4C RNA Immunoprecipitation

Human embryonic kidney HEK293 cells (FuHeng Biology, FH0244) were cultured in high-glucose DMEM medium (Gibco, C11960500BT) supplemented with 10% FBS and 1% penicillin-streptomycin, at 37°C and 5% CO_2 in a humidified atmosphere. According to manufacturer's instructions of PEI Transfection Reagent (ProteinTech, PR40001), the NAT10-overexpressing plasmids (GeneCopeia, EX-I5674-M11) were transfected into HEK293 cells. After 48 h, the NAT10-overexpressed HEK293 cells were washed by cold PBS, mechanically isolated with a cell scraper, and centrifuged at 1,500 rpm for 5 min at 4°C. The supernatant was discarded, and the sediment was resuspended by 1 ml of purification buffer, 0.5% NP40, and 1% protease inhibitor (APExBIO, K1007). The mixture was pre-cooled in ice for 5 min and then transferred to −80°C for more than 15 min. Then, it was centrifuged at 12,000 g, 4°C for 10 min. Protein A/G magnetic beads (MCE, HY-K0202) were activated with purification buffer and conjugated with 5 μg of polyclonal anti-NAT10 antibody, 5 μg of anti-ac4C antibody (Abcam, ab252215), and 5 μg of rabbit IgG antibody (FineTest, FNSA-0106) at room temperature for 2 h, respectively. After that, the beads were washed with purification buffer for two to three times. In addition, 10% of the cell lysate was saved as input at -80°C. Antibody-conjugated A/G magnetic beads were incubated with 45% of cell lysate, 0.25 M EDTA, and 1 μl RNase inhibitor (APExBIO, K1046) at 4°C for 4 h separately. Then, the beads were washed with purification buffer for another two to three times, and all the solution was discarded. Later, the A/G magnetic beads were incubated with 117 μl of lysis buffer, 15 μl of 10% SDS, and 18 ul proteinase K of 10 mg/ml at 55°C for 30 min to purify mRNA. Moreover the reverse transcription was performed, and PCR was followed to test the binding of target RNA.

RNA Degradation Test, RNA Extraction, and Quantitative Real-Time PCR

Human embryonic kidney HEK293 cells were firstly seeded in six wells in 24-well plates (4×10^5 cells per well). They were cultured in high-glucose DMEM medium containing 10% FBS and 1% penicillin-streptomycin at 37°C and 5% CO_2 in humidified atmosphere. According to manufacturer's instructions of PEI Transfection Reagent, the NAT10-overexpressing plasmids were transfected into HEK293 cells in the experimental group, and the control group cells were transfected with no-load plasmids. After 48 h, the cells were exposed to Actinomycin D (5 μg/ml, Aladdin, A113142) to block RNA synthesis as previously described (24). In addition, HEK293 cells were then harvested at 0, 2, and 12 h, respectively. The total RNA of cells was then extracted and reversely transcribed using the RNeasy Micro Kit (Qiagen, 74004) and HiScript III RT SuperMix for Quantitative PCR (qPCR) (Vazyme, R323-01) according to the manufacturer's instructions. RealStar Green Power Mixture (2×) (Genstar, A311-101) was used to carry out qPCR on the Roche LightCycler 480 II (Roche Diagnostics, Germany). The expression levels of *OGA* mRNA in the experimental group and the control group at 0 h were normalized to 1, and the relative expression levels at 2 and 12 h were calculated respectively based on $2^{-\Delta\Delta CT}$ method. In addition, the primers are displayed in **Table 1**.

Single-Cell Transcriptome Sequencing and Data Analysis

According to the manufacturer's instructions, we used the Single-Cell Full-Length mRNA-Amplification Kit (Vazyme, n712) to extract and reversely transcribe the total RNA of oocytes. Each group had five oocytes. The cDNA products were purified by VAHTS DNA Clean Beads (Vazyme, N411). The amount and purity of cDNA were evaluated by Qubit (Invitrogen, USA) and Bioanalyzer 2100 (Agilent, USA). Finally, we used the TruePrep DNA Library Prep Kit V2 for Illumina (Vazyme, TD502) to prepare RNA libraries. Furthermore, Illumina Novaseq™ 6000 (LC Bio Technology CO., Ltd. Hangzhou, China) was used to conduct pair-end sequencing according to the standard operation protocol, with the sequencing mode of PE150. The quality control of FASTQ files was performed by Trim Galore software. The adaptors, low-quality sequences with the default parameters, and repeated sequences were removed. The paired-end clean reads were mapped to the reference genome of Mus musculus GRCh38 using HISAT2 (25). We used the feature Counts function of subread software to analyze gene quantification (26). In addition, the differential expression analysis was conducted by DESeq2 R package (27). The count value of gene expression was standardized to transcripts per kilobase of exon model per million mapped reads value. The genes with fold change >1.5 or < 0.7 and p-value < 0.05 were considered differentially expressed genes (DEGs).

TABLE 1 | Primers.

Gene	The primer sequence (5′-3′)
OGA	Forward: AGCCAAATGGTGACAAGGAACTCTC
	Reverse: GCTCCGACCAAGTATAACCACATCC
β-actin	Forward: ACGGCCAGGTCATCACCATT
	Reverse: CGGAGTACTTGCGCTCAGG

Statistical Analysis

SPSS 25.0 (SPSS Inc., IL, USA) was used for statistical analyses, and GraphPad Prism 8 (GraphPad Software, CA, USA) was conducted for graph visualization. Data are presented as the mean ± standard error of mean (SEM). Comparison between two groups was analyzed by Student's t-test (two-tailed). Results were considered statistically significant when $P < 0.05$(*$P < 0.05$, **$P < 0.01$, and ***$P < 0.001$).

RESULTS

Expression Profiling of NAT10-Depleted Mouse Oocytes

We have previously reported that NAT10 depletion resulted in retarded meiotic progression in mouse oocytes, and NAT10-mediated ac4C modification was a crucial regulator during oocyte maturation (20). In the current study, we knocked down NAT10 in GV stage mouse oocytes and performed transcriptome analysis to further identify the regulated genes and investigated the underlying mechanisms. As shown in **Figure 1A**, the volcano plot demonstrated the DEGs between NAT10-depleted and control oocytes. Clusters of differential expression were shown by the heatmap, and most of the genes were downregulated with NAT10 depletion (**Figure 1B**). Bioinformatic analysis identified 280 DEGs with NAT10 KD, including 99 upregulated genes and 181 downregulated genes, implying that NAT10 KD resulted in enhanced degradation of transcripts (**Figure 1C**). All of the 280 identified DEGs were subjected to GO enrichment and KEGG pathway analysis to better understand their biological functions. These genes were mainly enriched in the biological processes related to cellular amino acid metabolic process and cytoplasmic sequestering of protein (**Figure 1D**). Analysis of KEGG pathway showed that DEGs were enriched in the metabolism and signal transduction (**Figure 1E**).

Transcripts Modulated by NAT10-Mediated ac4C Modification in Oocytes

To identify the genes modulated by NAT10-mediated ac4C modification, we obtained 2,135 genes that have been reported to be acetylated in a previous study (28). There were 18 transcripts with potential ac4C sites among the 280 DEGs. Among them, as many as 17 genes were downregulated with NAT10 KD. Given that ac4C has been shown to enhance mRNA stability, these findings suggested that NAT10 might modulate gene expression in an ac4C-dependent manner (16, 28). As for the 262 NAT10-modulated genes without potential ac4C sites, 62.60% were downregulated and 37.40% were upregulated. NAT10 might have an indirect effect on these genes (**Figure 2A**). With NAT10 depletion, the overall expression of genes with and without potential ac4C sites were both downregulated, but the decline of

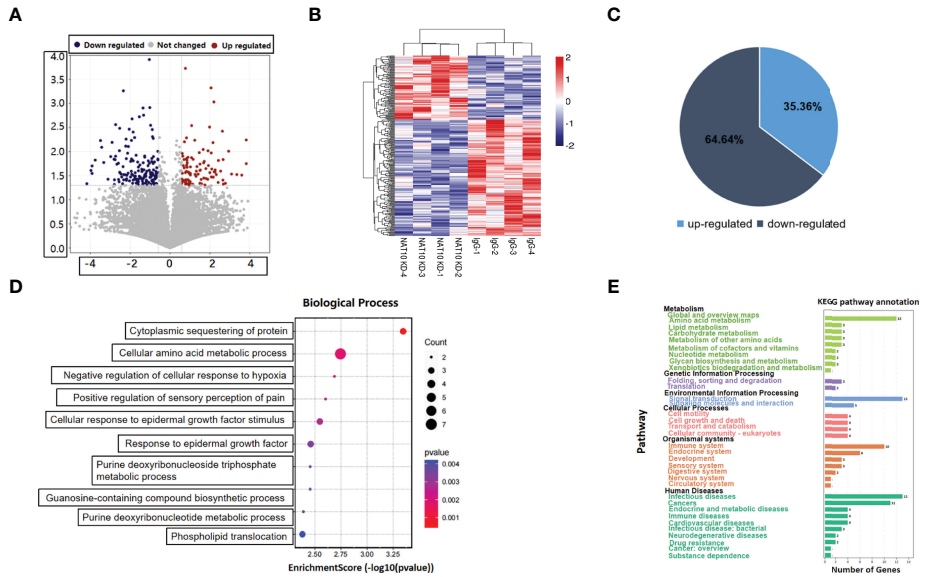

FIGURE 1 | Expression profiling of NAT10-depleted mouse oocytes. **(A)**Volcano map showed the gene expression with NAT10 KD. Blue dots represented downregulation, and red dots represented upregulation. **(B)** The heatmap showed clusters of differential expression of genes. **(C)** Pie chart presented the proportion of up/downregulated genes in 280 DEGs. **(D)** Cellular amino acid metabolic process and cytoplasmic sequestering of protein were main biological process of 280 DEGs. **(E)** A total of 280 DEGs were enriched in metabolism and signal transduction according to KEGG enrichment analysis.

potentially acetylated genes was more pronounced (**Figure 2B**). These data were consistent with the known functions of ac4C, implying that NAT10 exerts its function on downstream genes mainly through ac4C modification. GO enrichment and KEGG pathway analyses were conducted for the downregulated ac4C transcripts. *GPR153* was not included in the analyses because of a fold change of 0. Functional annotation showed that these transcripts were enriched in biological functions as regulation of protein binding and positive regulation of transcription, DNA-templated (**Figure 2C**). In addition, they were enriched in pathways associated with cancer, signal transduction, folding, sorting, and degradation (**Figure 2D**).

OGA Stability Was Modulated by NAT10-Mediated ac4C Modification

Because NAT10-mediated ac4C modification was demonstrated to participate in post-transcriptional regulation of mouse oocyte maturation *in vitro* (20), we intended to identify that the NAT10-targeted acetylated transcripts might play a role in modulating IVM. Thus, we further investigated the 18 DEGs with potential ac4C site, among which the abundance of *OGA* was high (>1), and it showed the lowest *P*-value and highest absolute value of fold change. In mammals, OGA is the enzyme to catalyze the removal of O-GlcNAc of proteins (29). O-GlcNAc is recognized as an important regulatory mechanism of cytosolic and nuclear proteins (30). The involvement of O-GlcNAc in regulating mammalian oocyte maturation has been determined in previous literature (31, 32). Frank and colleagues have reported that *in vitro* developmental competence of mouse oocytes was impaired by O-GlcNAc of heat shock protein 90 under hyperglycemic conditions (32). Another study noted that disruption of O-GlcNAc homeostasis during mammalian oocyte meiotic maturation impacted fertilization (31). Therefore, we further explored the regulatory mechanisms of *OGA* as well as its function in IVM modulation.

Our data demonstrated that NAT10 KD resulted in significant downregulation of *OGA* (**Figure 3A**). According to the literature, the acetylated site of *OGA* from Hela cells is located within 484–498 (28). We investigated the sequences of *OGA* from murine and human origins and found that a region of human *OGA* (265–279) is highly conserved with the murine ac4C site (**Figure 3B**). By performing NAT10 RIP and ac4C RIP, we confirmed that *OGA* was modulated by both NAT10 ($P < 0.001$) and ac4C modification ($P < 0.01$) (**Figure 3C**). Because NAT10 is the only known mRNA acetyltransferase in mammals and mainly regulates gene expression in an ac4C-dependant way (28), we inferred that NAT10 regulated *OGA* gene expression by altering ac4C modification. It is well known that transcription ceases and mRNA decay are fundamental events during mammalian oocyte maturation. Oocyte meiosis triggers instability of a subset of mRNAs, leading to active degradation of approximately 20% of accumulated maternal transcripts (33, 34). Because ac4C is known to stabilize mRNA, the degradation of *OGA* was also measured in our study. The results showed that the degradation of *OGA* mRNA was markedly inhibited by NAT10 overexpression (**Figure 3D**). Immunostaining of oocytes showed that NAT10 KD led to decreased expression of *OGA*, further confirming that *OGA* was modulated by NAT10, possibly through an ac4C-dependent way (**Figure 3E**). These results indicated that NAT10-mediated ac4C modulated the expression of *OGA* by inhibiting its decay. Because the modulation of OGA expression level would result in a compensatory change of OGT, we performed

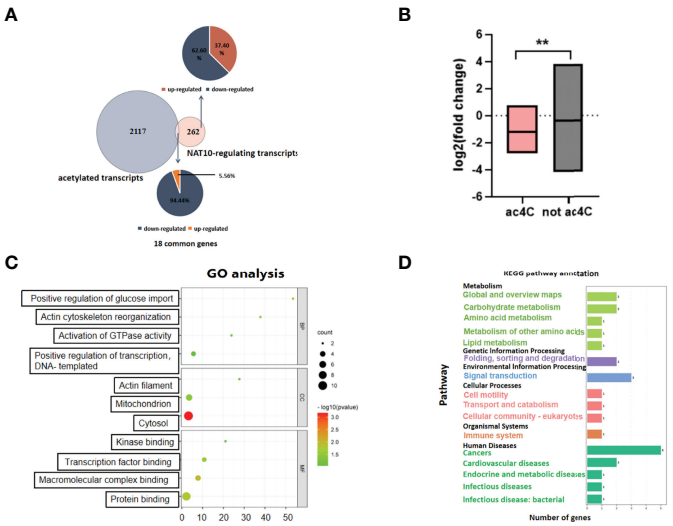

FIGURE 2 | Transcripts modulated by NAT10-mediated ac4C modification in oocytes. **(A)** Venn diagram and pie chart showed the proportion of NAT10-regulated ac4C genes and non–ac4C-modified genes. **(B)** Box diagram displayed the fold change difference between NAT10-regulated ac4C-modified DEGs and non–ac4C-modified DEGs. **(C)** Sixteen downregulated ac4C-modified DEGs regulated by NAT10 mainly participated in regulation of protein binding and positive regulation of transcription, DNA-templated. **(D)** KEGG analysis showed 16 downregulated ac4C-modified DEGs regulated by NAT10 were enriched in cancer, signal transduction, folding, sorting, and degradation. Unpaired t-test was used in **(B)** to compare the expression of genes because the number of genes did not match between two groups. $^{**}P < 0.01$.

immunofluorescence of OGT in oocytes after NAT10 KD to verify the compensatory regulation in our experiment (35). In addition, the results showed that OGA downregulation after NAT10 KD would lead to the decrease of OGT level to maintain the O-GlcNAc homeostasis (**Figure S1**).

OGA Depletion Retarded Mouse Oocyte Maturation *In Vitro*

Although O-GlcNAc modification is known as a regulatory mechanism during mammalian oocyte development (31, 32), the role of *OGA* in oocyte maturation remains unclarified. Thus,

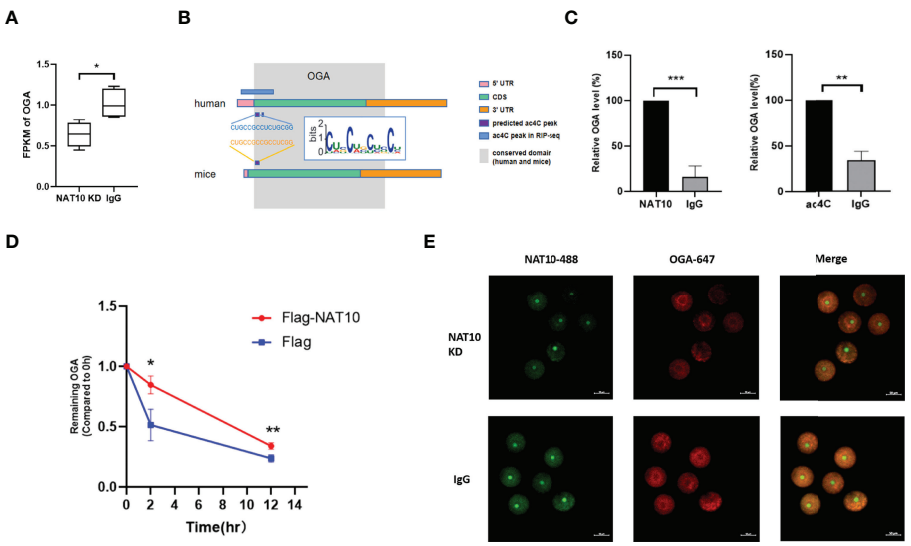

FIGURE 3 | *OGA* Stability was modulated by NAT10-mediated ac4C modification. **(A)** Expression of *OGA* was downregulated significantly by comparing NAT10 KD transcriptome with the control. **(B)** The diagram displayed ac4C-modified potential sites of *OGA* in homo sapiens and Mus musculus. **(C)** Bar chart showed *OGA* could bind to NAT10 and be ac4C-modified by RIP. **(D)** The degradation of *OGA* was suppressed in NAT10-overexpressing compared with negative control group. **(E)** Immunofluorescence showed NAT10 degradation and OGA downregulation after NAT10 KD by Trim-Away. Data represent the mean ± SEM of at least three independent experiments. $^{*}P < 0.05$, $^{**}P < 0.01$, and $^{***}P < 0.001$.

GV-stage and mouse oocytes matured *in vitro* were collected for immunostaining. The results revealed significantly increased expression of *OGA* from GV to MII oocytes (**Figure 4A**). To further investigate the role of *OGA* in modulating oocyte maturation, OGA in GV oocytes was knocked down through electroporation, and the effective depletion of OGA was confirmed by immunofluorescence staining (**Figure 4B**). The intervened GV oocytes were cultured in IVM medium for 14–16 h. Interestingly, the *in vitro* maturation rate was significantly reduced with OGA KD ($P < 0.05$) (**Figures 4C, D**). In mammals, OGA is recognized as the critical enzyme to remove O-GlcNAc of proteins (36). We further investigated the role of O-GlcNAc in oocyte maturation. During mouse oocyte meiotic progression, markedly decreased level of O-GlcNAc was observed. In addition, with OGA depletion, impaired meiotic maturation was accompanied with enhanced level of O-GlcNAc (**Figure 4E**). Collectively, OGA depletion led to impaired meiotic progression of mouse oocytes, possibly *via* enhancing O-GlcNAc of proteins. These results indicated that OGA-modulated O-GlcNAc of proteins acted as a critical regulatory mechanism in oocyte maturation.

Expression Profiling of Oocytes With OGA Knockdown

OGA has been identified as the gene modulated by NAT10-mediated ac4C, which played an important role in oocyte maturation. We depleted OGA in GV stage oocytes and performed transcriptome analysis to further unravel the altered genes and the possible mechanisms. The volcano plot showed the differential expressed genes between OGA-depleted and control oocytes (**Figure 5A**). As demonstrated in **Figure 5B**, most genes were upregulated with OGA KD, possibly associated with an elevated level of O-GlcNAc modification. GO enrichment analysis confirmed that the differentially expressed transcripts were associated with metabolic processes (**Figure 5C**). Pathway analysis was also performed on the basis of KEGG database and the most significant pathways were displayed in **Figure 5D**, including cell cycle and oocyte meiosis. To investigate the downstream mechanisms by which NAT10 regulated OGA through ac4C modification and thus modulated oocyte maturation, the expression profiling with OGA KD, NAT10-depleted transcriptome, and ac4C RIP data was analyzed jointly (28). A total of 27 DEGs were identified in common, out of which 22 genes were not ac4C-modified (**Figure 5E**). The altered expression of these 22 genes cannot be mediated directly by ac4C. Instead, these genes might be modulated by OGA, which could be modified by NAT10, too.

Joint Analysis of NAT10-Depleted and OGA-Depleted Transcriptomes

Gene set enrichment analyses (GSEA) of NAT10-depleted and OGA-depleted transcriptomes were further performed to gain insights about the biological significance of DEGs. The results suggested that NAT10 was associated with G protein–coupled receptor activity, molecular transducer activity, and nucleosomal DNA binding (**Figures 6A–C**). Interestingly, the OGA-depleted expression profiling was enriched in similar gene sets (**Figures 6D–F**). Taken together, NAT10 might affect these aforementioned biological processes by regulating ac4C modification of *OGA* mRNA and thus participate in the regulation of oocyte maturation. We next investigated each DEG and identified several genes co-regulated by NAT10 and OGA. As shown in **Figure 7A**,

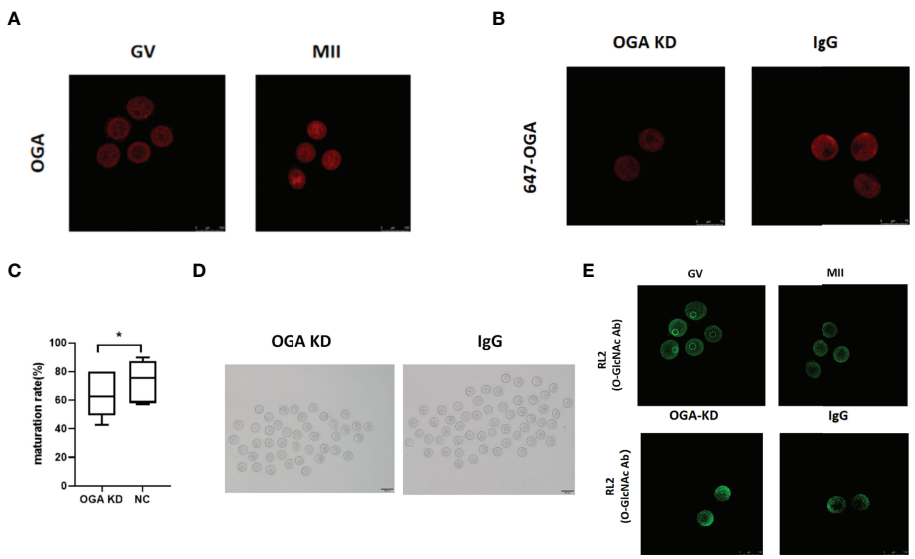

FIGURE 4 | *OGA* depletion retarded mouse oocyte maturation *in vitro*. **(A)** Compared with GV oocytes, *OGA* gene expression was upregulated in MII oocytes. **(B)** OGA was significantly downregulated by Trim-Away. **(C)** Box plot showed the difference of oocyte maturation rates between OGA KD group and the control group. **(D)** Representative pictures of oocyte maturation in OGA KD group and the control group. **(E)** Different expression of O-GlcNAc in GV and MII oocytes was verified by immunofluorescence, and O-GlcNAc modification was upregulated after OGA intervention. Data represent the mean ± SEM of at least three independent experiments. *$P < 0.05$.

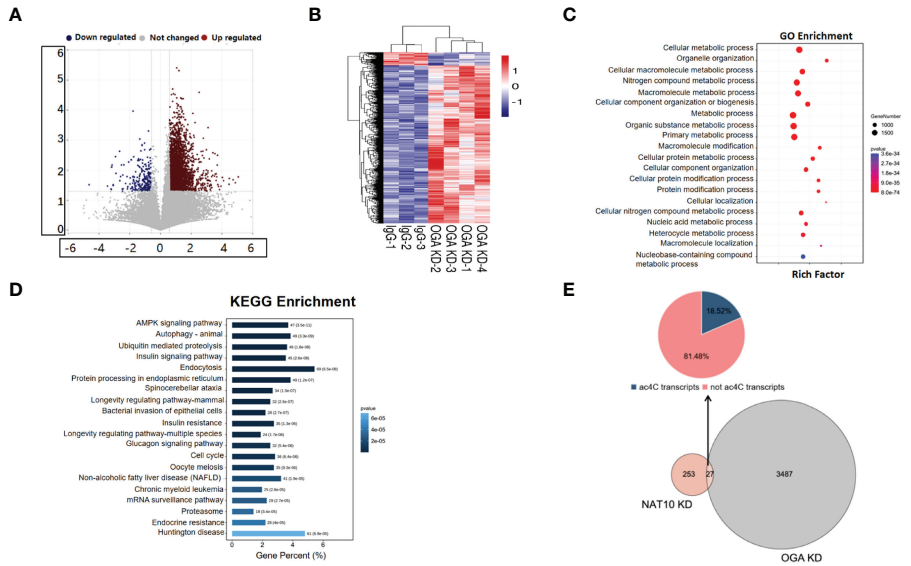

FIGURE 5 | Expression Profiling of Oocytes with OGA Knockdown. **(A)** Volcano map showed global genes change after OGA KD, with blue dots representing downregulation and red dots representing upregulation. **(B)** Heatmap showed the overall clusters of differential expression of genes. **(C)** A total of 3,514 DEGs with OGA KD were mainly associated with metabolic processes according to GO enrichment. **(D)** KEGG analysis displayed top 20 pathways where 3,514 DEGs were involved in. **(E)** Pie chart showed the distribution of DEGs by joint analysis of OGA KD, NAT10-KD transcriptomes, and ac4C RIP data.

the expression of *Rsph6a*, *Gm7788*, and *Gm41780* was downregulated in both NAT10-depleted and OGA-depleted oocytes. Among them, *Rsph6a* is associated with mammalian fertility and is recognized as a potential marker for fertility (37). In addition,*Trpc7*, *Gm29036*, and *Gm47144* were upregulated in both NAT10-silenced and OGA-silenced groups (**Figure 7B**). Among them, *Trpc7* is involved in the regulation of calcium ion transmembrane transport and cytoplasmic calcium ion concentration, which are critical for oocyte maturation and activation (38, 39). *Rsph6a* and *Trpc7* were possible downstream genes modulated by NAT10-mediated ac4C on *OGA* mRNA, and their dysregulation could result in impaired oocyte maturation.

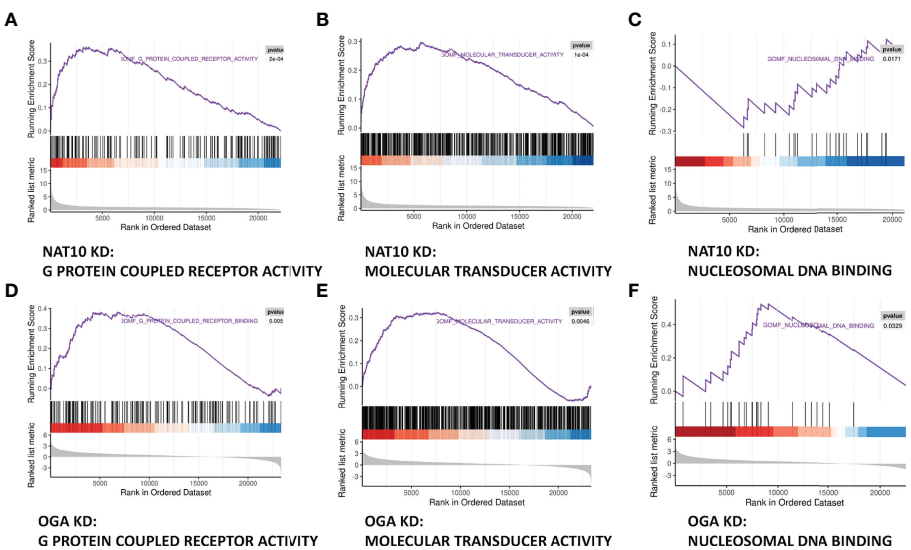

FIGURE 6 | Joint Analysis of NAT10-depleted and OGA-depleted Transcriptomes. **(A–C)** GSEA analysis showed that NAT10 KD transcriptome genes were mainly enriched in G protein–coupled receptor activity, molecular transducer activity, and nucleosomal DNA binding. **(D–F)** OGA-depleted expression profiling was enriched in similar gene sets as NAT10-KD according to GSEA analysis.

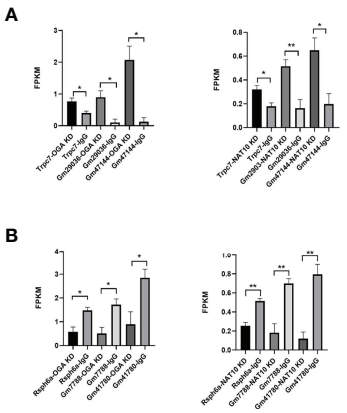

FIGURE 7 | Co-regulated genes of NAT10 and OGA in oocyte maturation. **(A)** Common upregulated DEGs and their expression in NAT10 KD and OGA KD transcriptomes. **(B)** Common downregulated DEGs and expression in NAT10 KD and OGA KD transcriptomes. *$P < 0.05$ and **$P < 0.01$.

DISCUSSION

The purpose of this study is to explore the important downstream genes and mechanisms of NAT10-mediated ac4C modification during oocyte maturation. In a previous study, we found that ac4C downregulation after NAT10 KD inhibited oocyte maturation, but the underlying mechanisms remained unknown (20). To further explore the underlying mechanisms, we conducted a transcriptomic study on oocytes with NAT10 KD and analyzed it with ac4C RIP data jointly (28). Our result revealed that *OGA* was one of the important target genes of NAT10-mediated ac4C modification during oocyte maturation.

First, *OGA* was verified to bind to NAT10 and be ac4C-modified based on NAT10/ac4C RIP results. Furthermore, to explore the function of NAT10-mediated ac4C modification on *OGA*, we conducted degradation experiments and found that NAT10 might regulate the expression of *OGA* by suppressing the degradation of it.

We furthered on investigating whether NAT10-mediated ac4C modification affected oocyte maturation through *OGA*. As the role of *OGA* in mammalian oocyte maturation has not been reported yet, we compared the fluorescent expression of *OGA* in GV and MII oocytes, and the latter was significantly higher than the former. *OGA* seemed to be a beneficial factor for oocyte maturation, whereas the maturation was impaired after OGA KD compared with the control group. According to the previous studies, OGA is a key protein in O-GlcNAc modification, which regulates the progression of cell cycle, cell signal transduction, and mitochondrial function by removing O-GlcNAc from the target proteins (40). Thus, we further explored the O-GlcNAc fluctuation by comparing RL2 expression between GV and MII oocytes, and interestingly, as oocytes maturated, the O-GlcNAc modification decreased significantly, which indicated the importance of OGA regulating O-GlcNAc level during IVM. On the basis of the above results, it is reasonable to speculate that *OGA* was the important regulated gene of NAT10-mediated ac4C modification in IVM.

To further explore the role and mechanisms of NAT10-mediated *OGA* ac4C in oocyte maturation, we knocked down *OGA* of oocytes for transcriptome sequencing. In addition, through joint analysis with the transcriptome data of oocytes depleted NAT10, we found that NAT10-mediated *OGA* ac4C regulated oocyte maturation mainly through G protein–coupled receptor, molecular transducer activity, and nucleosomal DNA binding. *Rsph6a*, *Gm7788*, and *Gm41780* were downregulated in NAT10-depleted and OGA-depleted transcriptomes, whereas *Trpc7*, *Gm29036*, and *Gm47144* were upregulated. As *Rsph6a and Trpc7* played an important part in fertility, we speculated that both of them might be the important downstream genes in NAT10-mediated *OGA* ac4C modification in oocyte maturation.

Previous literatures have reported the function of O-GlcNAc modification in oocyte development and maturation (31, 32, 41–43). Slawson et al. found that glucosamine or PUGNAc treatment impaired the maturation kinetics of Xenopus laevis oocytes because the O-GlcNAc level increased, and oocytes at advanced stages (III–IV) were less O-GlcNAc–modified compared with that of stages I–II (44). Dehennaut et al. got the similar results and identified that OGA activity attributed to the decreased O-GlcNAc level as oocytes maturated in Xenopus laevis but not decreased OGT expression nor the decrease of the substrate (42). It supports our finding that OGA KD resulted in elevated O-GlcNAc modification and thus jeopardized oocyte development potential. It is worthy to note that most studies about O-GlcNAcylation in oocytes were carried out in the non-mammal such as Xenopus because of the technology limit and the available number of oocytes (45). We performed it in mice oocytes, which might be more consistent with the maturation progress of human oocytes.

Because oocyte maturation is a finely regulated process, epigenetic modifications play a crucial role to ensure timely and selective translation or degradation of specific RNAs (46). Sequencing and omic techniques should be emphasized in exploring the specific characterization and key events in oocyte maturation (8). Our study combined two transcriptome data and proved that *OGA* was regulated by NAT10-mediated ac4C modification, which might affect oocyte maturation through G protein–coupled receptors, molecular transduction, and nucleosome DNA binding. It will also provide insights for the modification interaction between ac4C modification and O-GlcNAcylation. What is noteworthy is that both of the two epigenetic modifications are new and that there are few studies on the role and mechanisms of them in mammalian oocyte maturation, so this is the main innovation of our research.

In conclusion, our results demonstrated that NAT10 might stabilize *OGA* through ac4C modification and mediated oocyte maturation. In addition, our results suggested that NAT10 might affect O-GlcNAc level by regulating OGA, thus regulating key proteins that could be O-GlcNAc–modified in IVM. Therefore, our study further explored the mechanisms of epigenetic

modification in oocyte maturation and would be used as reference for clinical improvement of IVM.

DATA AVAILABILITY STATEMENT

The data presented in the study are deposited in the GSA repository (https://bigd.big.ac.cn/gsa/browse/CRA007092, accession number CRA007092).

ETHICS STATEMENT

Animal experiments were approved by the Animal Care and Use Committee of the Sixth Affiliated Hospital, Sun Yat-sen University (Guangzhou, China) (ethical approval number: IACUC-2021112502).

AUTHOR CONTRIBUTIONS

CZ and JLi designed the study. XL supervised the progress of it and provided the funding. JLin performed the experiment with the help of HZ, YZ, JLin, QL, and TW. JLin drafted the manuscript with the support of YX and JH. All authors contributed to the article and approved the submitted version.

FUNDING

This study was supported by the National Key Research and Development Program of China (2021YFC2700403), National Natural Science Foundation of China (82071713), Natural Science Foundation of Guangdong Province (2019A1515011764), and Youth Project-Joint Foundation for Basic and Applied Basic Research of Guangdong Province (2021A1515110977).

SUPPLEMENTARY MATERIAL

The Supplementary Material for this article can be found online at: https://www.frontiersin.org/articles/10.3389/fendo.2022.907286/full#supplementary-material

Supplementary Figure 1 | The modulation of OGA level after NAT10 knockdown induced a compensatory regulation of OGT. Affected by NAT10 knockdown, the decreased level of OGA resulted in the downregulation of OGT in oocytes.

REFERENCES

1. Yang H, Kolben T, Meister S, Paul C, van Dorp J, Eren S, et al. Factors Influencing the *In Vitro* Maturation (IVM) of Human Oocyte. *Biomedicines* (2021) 9(12):1904. doi: 10.3390/biomedicines9121904
2. Sauerbrun-Cutler MT, Vega M, Keltz M, McGovern PG. *In Vitro* Maturation and its Role in Clinical Assisted Reproductive Technology. *Obstet Gynecol Surv* (2015) 70(1):45–57. doi: 10.1097/OGX.0000000000000150
3. Hart RJ. Optimizing the Opportunity for Female Fertility Preservation in a Limited Time-Frame for Patients With Cancer Using *In Vitro* Maturation and Ovarian Tissue Cryopreservation. *Fertil Steril* (2019) 111(2):258–9. doi: 10.1016/j.fertnstert.2018.10.027
4. Lin Y, Zheng X, Ma C, Li X, Zhang X, Yang P, et al. Human Chorionic Gonadotropin Priming Does Not Improve Pregnancy Outcomes of PCOS-IVM Cycles. *Front Endocrinol (Lausanne)* (2020) 11:279. doi: 10.3389/fendo.2020.00279
5. Prather RS, Ross JW, Isom SC, Green JA. Transcriptional, Post-Transcriptional and Epigenetic Control of Porcine Oocyte Maturation and Embryogenesis. *Soc Reprod Fertil Suppl* (2009) 66:165–76.
6. Slaidina M, Lehmann R. Translational Control in Germline Stem Cell Development. *J Cell Biol* (2014) 207(1):13–21. doi: 10.1083/jcb.201407102
7. Blatt P, Martin ET, Breznak SM, Rangan P. Post-Transcriptional Gene Regulation Regulates Germline Stem Cell to Oocyte Transition During Drosophila Oogenesis. *Curr Top Dev Biol* (2020) 140:3–34. doi: 10.1016/bs.ctdb.2019.10.003
8. He M, Zhang T, Yang Y, Wang C. Mechanisms of Oocyte Maturation and Related Epigenetic Regulation. *Front Cell Dev Biol* (2021) 9:654028. doi: 10.3389/fcell.2021.654028
9. Yang C, Wu T, Zhang J, Liu J, Zhao K, Sun W, et al. Prognostic and Immunological Role of mRNA Ac4c Regulator NAT10 in Pan-Cancer: New Territory for Cancer Research? *Front Oncol* (2021) 11:630417. doi: 10.3389/fonc.2021.630417
10. Licht K, Jantsch MF. Rapid and Dynamic Transcriptome Regulation by RNA Editing and RNA Modifications. *J Cell Biol* (2016) 213(1):15–22. doi: 10.1083/jcb.201511041
11. Roundtree IA, Evans ME, Pan T, He C. Dynamic RNA Modifications in Gene Expression Regulation. *Cell* (2017) 169(7):1187–200. doi: 10.1016/j.cell.2017.05.045
12. Hu Y, Ouyang Z, Sui X, Qi M, Li M, He Y, et al. Oocyte Competence Is Maintained by M(6)A Methyltransferase KIAA1429-Mediated RNA Metabolism During Mouse Follicular Development. *Cell Death Differ* (2020) 27(8):2468–83. doi: 10.1038/s41418-020-0516-1
13. Zhao W, Zhou Y, Cui Q, Zhou Y. PACES: Prediction of N4-Acetylcytidine (Ac4c) Modification Sites in mRNA. *Sci Rep* (2019) 9(1):11112. doi: 10.1038/s41598-019-47594-7
14. Arango D, Sturgill D, Oberdoerffer S. Immunoprecipitation and Sequencing of Acetylated RNA. *Bio Protoc* (2019) 9(12):e3278. doi: 10.21769/BioProtoc.3278
15. Jin G, Xu M, Zou M, Duan S. The Processing, Gene Regulation, Biological Functions, and Clinical Relevance of N4-Acetylcytidine on RNA: A Systematic Review. *Mol Ther Nucleic Acids* (2020) 20:13–24. doi: 10.1016/j.omtn.2020.01.037
16. Dominissini D, Rechavi G. N(4)-Acetylation of Cytidine in mRNA by NAT10 Regulates Stability and Translation. *Cell* (2018) 175(7):1725–7. doi: 10.1016/j.cell.2018.11.037
17. Karthiya R, Wasil SM, Khandelia P. Emerging Role of N4-Acetylcytidine Modification of RNA in Gene Regulation and Cellular Functions. *Mol Biol Rep* (2020) 47(11):9189–99. doi: 10.1007/s11033-020-05963-w
18. Zhang Y, Jing Y, Wang Y, Tang J, Zhu X, Jin WL, et al. NAT10 Promotes Gastric Cancer Metastasis *via* N4-Acetylated Col5a1. *Signal Transduct Target Ther* (2021) 6(1):173. doi: 10.1038/s41392-021-00489-4
19. Guo G, Shi X, Wang H, Ye L, Tong X, Yan K, et al. Epitranscriptomic N4-Acetylcytidine Profiling in CD4(+) T Cells of Systemic Lupus Erythematosus. *Front Cell Dev Biol* (2020) 8:842. doi: 10.3389/fcell.2020.00842
20. Xiang Y, Zhou C, Zeng Y, Guo Q, Huang J, Wu T, et al. NAT10-Mediated N4-Acetylcytidine of RNA Contributes to Post-Transcriptional Regulation of Mouse Oocyte Maturation. *vitro Front Cell Dev Biol* (2021) 9:704341. doi: 10.3389/fcell.2021.704341
21. Clift D, McEwan WA, Labzin LI, Konieczny V, Mogessie B, James LC, et al. A Method for the Acute and Rapid Degradation of Endogenous Proteins. *Cell* (2017) 171(7):1692–1706.e1618. doi: 10.1016/j.cell.2017.10.033

22. Drutovic D, Duan X, Li R, Kalab P, Solc P. RanGTP and Importin Beta Regulate Meiosis I Spindle Assembly and Function in Mouse Oocytes. *EMBO J* (2020) 39(1):e101689. doi: 10.15252/embj.2019101689
23. Gerri C, McCarthy A, Alanis-Lobato G, Demtschenko A, Bruneau A, Loubersac S, et al. Initiation of a Conserved Trophectoderm Program in Human, Cow and Mouse Embryos. *Nature* (2020) 587(7834):443–7. doi: 10.1038/s41586-020-2759-x
24. Tsai K, Jaguva Vasudevan AA, Martinez Campos C, Emery A, Swanstrom R, Cullen BR. Acetylation of Cytidine Residues Boosts HIV-1 Gene Expression by Increasing Viral RNA Stability. *Cell Host Microbe* (2020) 28(2):306–312.e306. doi: 10.1016/j.chom.2020.05.011
25. Kim D, Langmead B, Salzberg SL. HISAT: A Fast Spliced Aligner With Low Memory Requirements. *Nat Methods* (2015) 12(4):357–60. doi: 10.1038/nmeth.3317
26. Liao Y, Smyth GK, Shi W. The R Package Rsubread is Easier, Faster, Cheaper and Better for Alignment and Quantification of RNA Sequencing Reads. *Nucleic Acids Res* (2019) 47(8):e47. doi: 10.1093/nar/gkz114
27. Love MI, Huber W, Anders S. Moderated Estimation of Fold Change and Dispersion for RNA-Seq Data With Deseq2. *Genome Biol* (2014) 15(12):550. doi: 10.1186/s13059-014-0550-8
28. Arango D, Sturgill D, Alhusaini N, Dillman AA, Sweet TJ, Hanson G, et al. Acetylation of Cytidine in mRNA Promotes Translation Efficiency. *Cell* (2018) 175(7):1872–1886.e1824. doi: 10.1016/j.cell.2018.10.030
29. Dong DL, Hart GW. Purification and Characterization of an O-GlcNAc Selective N-Acetyl-Beta-D-Glucosaminidase From Rat Spleen Cytosol. *J Biol Chem* (1994) 269(30):19321–30. doi: 10.1016/S0021-9258(17)32170-1
30. Dong H, Liu Z, Wen H. Protein O-GlcNAcylation Regulates Innate Immune Cell Function. *Front Immunol* (2022) 13:805018. doi: 10.3389/fimmu.2022.805018
31. Zhou LT, Romar R, Pavone ME, Soriano-Ubeda C, Zhang J, Slawson C, et al. Disruption of O-GlcNAc Homeostasis During Mammalian Oocyte Meiotic Maturation Impacts Fertilization. *Mol Reprod Dev* (2019) 86(5):543–57. doi: 10.1002/mrd.23131
32. Frank LA, Sutton-McDowall ML, Brown HM, Russell DL, Gilchrist RB, Thompson JG. Hyperglycaemic Conditions Perturb Mouse Oocyte *In Vitro* Developmental Competence *via* Beta-O-Linked Glycosylation of Heat Shock Protein 90. *Hum Reprod* (2014) 29(6):1292–303. doi: 10.1093/humrep/deu066
33. Su YQ, Sugiura K, Woo Y, Wigglesworth K, Kamdar S, Affourtit J, et al. Selective Degradation of Transcripts During Meiotic Maturation of Mouse Oocytes. *Dev Biol* (2007) 302(1):104–17. doi: 10.1016/j.ydbio.2006.09.008
34. Ma J, Fukuda Y, Schultz RM. Mobilization of Dormant Cnot7 mRNA Promotes Deadenylation of Maternal Transcripts During Mouse Oocyte Maturation. *Biol Reprod* (2015) 93(2):48. doi: 10.1095/biolreprod.115.130344
35. Decourcelle A, Loison I, Baldini S, Leprince D, Dehennaut V. Evidence of a Compensatory Regulation of Colonic O-GlcNAc Transferase and O-GlcNAcase Expression in Response to Disruption of O-GlcNAc Homeostasis. *Biochem Biophys Res Commun* (2020) 521(1):125–30. doi: 10.1016/j.bbrc.2019.10.090
36. Stephen HM, Adams TM, Wells L. Regulating the Regulators: Mechanisms of Substrate Selection of the O-GlcNAc Cycling Enzymes OGT and OGA. *Glycobiology* (2021) 31(7):724–33. doi: 10.1093/glycob/cwab005
37. Laseca N, Demyda-Peyras S, Valera M, Ramon M, Escribano B, Perdomo-Gonzalez DI, et al. A Genome-Wide Association Study of Mare Fertility in the Pura Raza Espanol Horse. *Animal* (2022) 16(3):100476. doi: 10.1016/j.animal.2022.100476
38. Wang F, Fan LH, Li A, Dong F, Hou Y, Schatten H, et al. Effects of Various Calcium Transporters on Mitochondrial Ca(2+) Changes and Oocyte Maturation. *J Cell Physiol* (2021) 236(9):6548–58. doi: 10.1002/jcp.30327
39. Liu X, Zhao R, Ding Q, Yao X, Tsang SY. TRPC7 Regulates the Electrophysiological Functions of Embryonic Stem Cell-Derived Cardiomyocytes. *Stem Cell Res Ther* (2021) 12(1):262. doi: 10.1186/s13287-021-02308-7
40. Chatham JC, Zhang J, Wende AR. Role of O-Linked N-Acetylglucosamine Protein Modification in Cellular (Patho)Physiology. *Physiol Rev* (2021) 101(2):427–93. doi: 10.1152/physrev.00043.2019
41. Dehennaut V, Slomianny MC, Page A, Vercoutter-Edouart AS, Jessus C, Michalski JC, et al. Identification of Structural and Functional O-Linked N-Acetylglucosamine-Bearing Proteins in Xenopus Laevis Oocyte. *Mol Cell Proteomics* (2008) 7(11):2229–45. doi: 10.1074/mcp.M700494-MCP200
42. Dehennaut V, Lefebvre T, Leroy Y, Vilain JP, Michalski JC, Bodart JF. Survey of O-GlcNAc Level Variations in Xenopus Laevis From Oogenesis to Early Development. *Glycoconj J* (2009) 26(3):301–11. doi: 10.1007/s10719-008-9166-0
43. Lefebvre T, Baert F, Bodart JF, Flament S, Michalski JC, Vilain JP. Modulation of O-GlcNAc Glycosylation During Xenopus Oocyte Maturation. *J Cell Biochem* (2004) 93(5):999–1010. doi: 10.1002/jcb.20242
44. Slawson C, Shafii S, Amburgey J, Potter R. Characterization of the O-GlcNAc Protein Modification in Xenopus Laevis Oocyte During Oogenesis and Progesterone-Stimulated Maturation. *Biochim Biophys Acta* (2002) 1573(2):121–9. doi: 10.1016/s0304-4165(02)00369-0
45. Wu Y, Li M, Yang M. Post-Translational Modifications in Oocyte Maturation and Embryo Development. *Front Cell Dev Biol* (2021) 9:645318. doi: 10.3389/fcell.2021.645318
46. Christou-Kent M, Dhellemmes M, Lambert E, Ray PF, Arnoult C. Diversity of RNA-Binding Proteins Modulating Post-Transcriptional Regulation of Protein Expression in the Maturing Mammalian Oocyte. *Cells* (2020) 9(3):662. doi: 10.3390/cells9030662

Conflict of Interest: The authors declare that the research was conducted in the absence of any commercial or financial relationships that could be construed as a potential conflict of interest.

Publisher's Note: All claims expressed in this article are solely those of the authors and do not necessarily represent those of their affiliated organizations, or those of the publisher, the editors and the reviewers. Any product that may be evaluated in this article, or claim that may be made by its manufacturer, is not guaranteed or endorsed by the publisher.

frontiers | Frontiers in Endocrinology

ORIGINAL RESEARCH
published: 25 July 2022
doi: 10.3389/fendo.2022.882214

Electro-Acupuncture Regulates Metabolic Disorders of the Liver and Kidney in Premature Ovarian Failure Mice

Min Chen[1,2†], Qi-da He[1†], Jing-jing Guo[3†], Qi-biao Wu[1,4], Qi Zhang[3], Yuen-ming Yau[3], Yu-feng Xie[1], Zi-yi Guo[1], Zi-yan Tong[1], Zong-bao Yang[3*] and Lu Xiao[5*]*

[1] Faculty of Chinese Medicine and State Key Laboratory of Quality Research in Chinese Medicines, Macau University of Science and Technology, Macau, Macau SAR, China, [2] Department of Chinese Medicine, The Fifth Affiliated Hospital of Zunyi Medical University, Zhuhai, China, [3] Department of Traditional Chinese Medicine, School of Medicine, Xiamen University, Xiamen, China, [4] Zhuhai MUST Science and Technology Research Institute, Zhuhai, China, [5] Department of Basic Medicine, Zunyi Medical University, Zhuhai, China

As per the theory of traditional Chinese medicine (TCM), the liver and kidney dysfunction are important pathogenies for premature ovarian failure (POF). POF is a common gynecological disease that reduced the pregnancy rate. Electro-acupuncture (EA) is a useful non-pharmaceutical therapy that supposedly regulates the function of the liver and kidney in the treatment of POF with TCM. However, the underlying mechanism of EA in the treatment of POF has not been adequately studied through metabonomics with reference to the theory of TCM. Accordingly, we investigated the effect of EA on the liver and kidney metabolites in POF mice through metabolomics. POF mice were established *via* intraperitoneal injection of cisplatin. Both Sanyinjiao (SP6) and Guanyuan (CV4) were stimulated by EA for 3 weeks. The biological samples (including the serum and the ovary, liver, and kidney tissues) were evaluated by histopathology, molecular biology, and hydrogen-1 nuclear magnetic resonance (^{1}HNMR)–based metabolomics to assess the efficacy of EA. ^{1}HNMR data were analyzed by the orthogonal partial least squares discriminant analysis (OPLS-DA). The results revealed that EA was beneficial to ovarian function and the menstrual cycle of POF. Both the energy metabolism and neurotransmitter metabolism in the liver and kidney were regulated by EA. Notably, EA played an important role in regulating energy-related metabolism in the kidney, and the better effect of neurotransmitter-related metabolism in the liver was regulated by EA. These findings indicated that the ovarian functions could be improved and the metabolic disorder of the liver and kidney caused by POF could be regulated by EA. Our study results thus suggested that the EA therapy, based on the results for the liver and kidney, were related to POF in TCM, as preliminarily confirmed through metabolomics.

Keywords: premature ovarian failure, electro-acupuncture, metabonomics, ^{1}HNMR, energy metabolism, neurotransmitter metabolism

OPEN ACCESS

Edited by:
Yuting Fan,
Boston IVF, United States

Reviewed by:
Lei Chen,
Guangdong Ocean University, China
Xin Dong,
Shanghai University, China

****Correspondence:***
Min Chen
minchenmust@163.com
Zong-bao Yang
yangzb@xmu.edu.cn
Lu Xiao
hbxl1527@163.com

†These authors have contributed equally to this work and share first authorship

Specialty section:
This article was submitted to Reproduction, a section of the journal Frontiers in Endocrinology

Received: *23 March 2022*
Accepted: *31 May 2022*
Published: *25 July 2022*

Citation:
Chen M, He Q-d, Guo J-j, Wu Q-b, Zhang Q, Yau Y-m, Xie Y-f, Guo Z-y, Tong Z-y, Yang Z-b and Xiao L (2022) Electro-Acupuncture Regulates Metabolic Disorders of the Liver and Kidney in Premature Ovarian Failure Mice. Front. Endocrinol. 13:882214. doi: 10.3389/fendo.2022.882214

INTRODUCTION

Premature ovarian failure (POF) is characterized by follicle-stimulating hormone (FSH) levels higher than 40 U/L and amenorrhea for more than 6 months before the age of 40. The symptoms of POF include amenorrhea, infertility, night sweats, hot flashes, and vaginal dryness (1). Globally, 1%–3% of adult women are diagnosed with POF (2). Presently, hormone therapy (HT) is a widely recommended therapy for patients with POF (3). Patients with POF are advised to intake sufficient calcium and vitamin D to prevent osteoporosis caused by low estrogen levels (4). Although the management of hormones and symptoms in patients with POF has made progress in the past years, the efficacy and cost are not satisfactory. In addition, the risk of ovarian cancer and endometrial cancer can be increased because of HT (5, 6). Therefore, complementary and alternative therapy is required.

Electro-acupuncture (EA) is a non-pharmaceutical therapy that is widely used for POF in China. The efficacy and safety of EA for POF have been approved (7). Traditional Chinese medicine (TCM) states that the occurrence of POF is closely associated with the function of the liver and kidney. The function of the liver and kidney can be regulated *via* stimulated acupoints, which are related to the meridians of the liver and kidney. In addition, TCM states that the Ren channel is one of the prerequisites for maintaining the regularity of the menstrual cycle. Therefore, Guanyuan (CV4) is located at Ren channel and is considered to have a positive curative effect on POF. We selected Sanyinjiao (SP6), which passes through the liver-meridian and kidney-meridian (8). In our previous study, we found that the phosphatidylinositol-3-kinase (PI3K)/Akt/mammalian target of rapamycin (mTOR) signaling pathway in follicles could be activated by EA to promote the proliferation of granulosa cells (9).

Metabonomics is used to study physiological and pathological metabolites under the guidance of the holistic concept, which is consistent with the holistic regulation of acupuncture based on TCM. Recently, metabonomics has been used to determine the changes in metabolites after EA (10). In our previous study, we found that metabolic disorders in the liver and kidney would be caused by chronic diseases. Meanwhile, the abnormal level of metabolites in the liver and kidney can be bidirectionally regulated, and metabolic homeostasis by EA can be maintained (11).

The ovarian reserve function and pregnancy rate in patients with POF can be improved by EA (7). However, only a few studies have elucidated the underlying mechanism of EA in the treatment of POF by metabonomics based on the theory of TCM. Therefore, to elucidate the underlying therapeutic mechanisms of EA on POF, the metabolic profiles of the liver and kidney were detected by hydrogen-1 nuclear magnetic resonance (^{1}HNMR).

Abbreviations: POF, Premature ovarian failure; TCM, Traditional Chinese medicine; ^{1}HNMR, Hydrogen-1 nuclear magnetic resonance; HT, Hormone therapy; EA, Electro-acupuncture; EN, Electro-acupuncture at the non-acupoints; CV4, Guanyuan acupoint; SP6, Sanyinjiao acupoint; PLS-DA, Partial least squares discriminant analysis; OPLS-DA, Orthogonal partial least squares discriminant analysis; HE, Hematoxylin–eosin; TUNEL, Terminal deoxynucleotidyl transferase dUTP nick-end labeling; ELISA, Enzyme-linked immunosorbent assay; FSH, Follicle-stimulating hormone; LH, Luteinizing hormone; E_2, Estradiol; AMH, Anti-Mullerian hormone; qPCR, Quantitative real-time PCR; ER-α, Estrogen receptor-α; ER-β, Estrogen receptor-β; GPR30, G protein–coupled estrogen receptor.

MATERIALS AND METHODS

Animals Handing

A total of 40 Institute of Cancer Research (ICR) female mice (weight: 35 ± 5 g) were obtained and raised at the experimental animal center of the Xiamen University. The animal study was reviewed and approved by the Xiamen University's Animal Ethics Committee (Permit Number: SCXK2018-0003). All procedures were conducted in accordance with the regulations of the "International Council for Laboratory Animal Science". The experimental mice were randomly assigned to the control, POF, electro-acupuncture at the acupoints (EA), and electro-acupuncture at the non-acupoints (EN) groups (n = 10 in each group). All mice were fed and drank freely during the experimental process. The POF mice were established *via* intraperitoneal injection of cisplatin (2 mg/kg) daily for 2 weeks, except for the control group (12).

EA Treatment

CV4 and SP6, as the acupoints, were selected in the EA group. SP6 was located at 0.5 cm above the medial malleolus of the hind limb, whereas CV4 was located 1 cm below the navel (the navel was located at the lower third of the line between the xiphoid process and perineum). Correspondingly, the non-acupoints were at 3-mm horizontal distance to CV4 and 3 mm higher than SP6 (**Figure 1A**). Generally, the non-acupoints did not belong to any known meridians. In the process of treatment, a breathable and opaque headgear was used to completely cover the head of the mice so as to help the mice remain calm during the treatment. Both acupoints and non-acupoints were inserted at 0.8 mm with acupuncture needles. The frequency of the EA instrument was adjusted until a slight beating of the skin was observed. Stainless steel acupuncture needle (0.25 mm × 13 mm; Suzhou Medical Supplies Factory Co., Ltd, Suzhou, China) was used (**Figures 1B, C**). All mice in the EA and EN groups were treated for 30 min, daily, for 3 weeks.

Vaginal Cytology

Into the vagina of the mice, 20 μl of 0.9% NaCl solution was dripped from 09:00 AM to 10:00 AM daily. Then, 0.9% of the NaCl solution was mixed gently and repeatedly dropped in the mice vagina with a pipette gun. Next, the solution was sucked out with a pipette gun and dropped on a slide. Nucleated epithelial, cornified epithelial, and leukocytes of mice in each group were observed under a light microscope to determine the estrous cycle.

Hematoxylin–Eosin Staining

All mice were anaesthetized with 10% chloral hydrate after treatment. One side of the ovary from the mice was collected surgically and placed in 4% paraformaldehyde. Next, these dehydrated ovaries were embedded in paraffin and sectioned

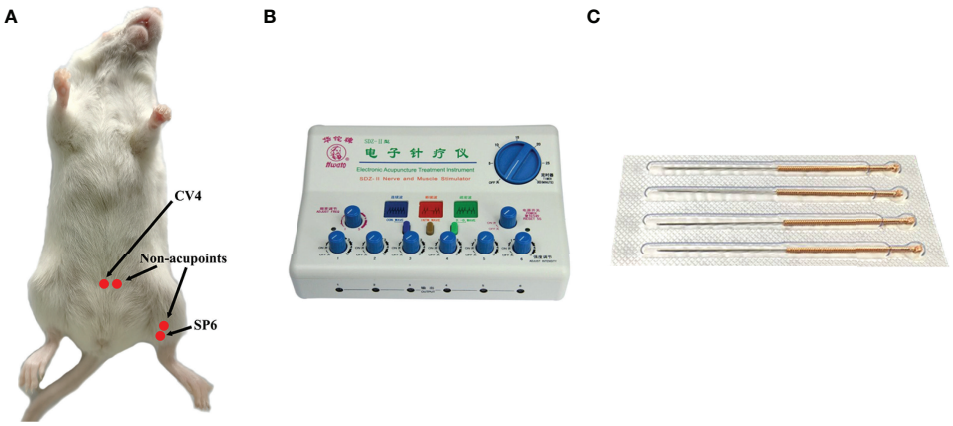

FIGURE 1 | The location of acupoints (CV4 and SP6) and corresponding non-acupoints on mice **(A)**; the EA instrument **(B)**; stainless steel acupuncture needle of 0.25 mm × 13 mm **(C)**.

into 5-μm-thick slices with a freezing microtome (CM1950, Leica Biosystems Division of Leica Microsystems Inc., Germany). Subsequently, the slices were dehydrated in alcohol and stained with hematoxylin–eosin (HE). The pathological morphology of the ovary was observed under the light microscope.

Terminal Deoxynucleotidyl Transferase dUTP Nick-End Labeling

The apoptosis of granulosa cells in the ovary was detected by terminal deoxynucleotidyl transferase dUTP nick-end labeling (TUNEL). All processes were conducted as per the instructions of the TUNEL Assay kit (G1501, Wuhan Servicebio Technology Co., Ltd., China). The apoptotic granulosa cells were labeled green with a fluorescent reagent and observed under the fluorescence microscope. To avoid any pathological differences between the samples, three ovarian sections were prepared for each sample. The percentage of TUNEL-positive granulosa cells was calculated and analyzed by the Image-Pro Plus 6.0 software.

Enzyme-Linked Immunosorbent Assay

Blood samples were collected from the orbital artery and sacrificed after treatment. FSH, luteinizing hormone (LH), estradiol (E_2), and anti-Mullerian hormone (AMH) in the serum were detected by using the enzyme-linked immunosorbent assay (ELISA) kit (0555M2/44039M2/0546M1/44204M2, Jiangsu Meimian Industrial Co., Ltd, China). All procedures were conducted as per the manufacturer's instructions.

Quantitative Real-Time PCR

The relative expression of estrogen receptor-α (ER-α), receptor-β (ER-β), and G protein-coupled ER (GPR30) in the ovary were detected by quantitative real-time (qPCR). Total RNA was extracted from the ovary by the Trizol method and reversed transcribed into cDNA. Subsequently, cDNA was used as the template for amplification. All data were analyzed by the software of Quantity One, and the relative expressions were calculated according to the $2^{-\triangle\triangle}$CT method.

^{1}HNMR Experiments

The liver and kidney were removed by surgery after all the mice were sacrificed. The metabolites of the liver and kidney were performed with the ^{1}HNMR spectrometer (Bruker AVANCE-III 600MHz, Switzerland) at 298 K. The samples of the liver and kidney were weighed (300 mg), and the homogenate was mixed with 600 μl of methanol and 300 μl of double-distilled water. All the samples were placed and allowed to stand for 10 min on an ice bath. Next, the samples were centrifuged (10,000 rpm/10 min at 4°C) and dried with nitrogen. Then, 600 μl of D2O was mixed, and 500 μl of the solution was extracted into a nuclear magnetic tube. For all samples, 64 FIDs were collected into 64K data points over a spectral width of 12,000 Hz with a relaxation delay of 6.5 μs.

Statistical Analyses

MestReNova software (Mestrelab Research, Santiago de Compostela, Spain) was used to calibrate and optimize the ^{1}HNMR spectra. Specifically, the ^{1}HNMR spectra of each sample were processed through baseline calibration, phase correction, and water peak removal. To accurately analyze the ^{1}HNMR spectrum, the chemical shift interval (0.5–9) was selected for piecewise integration, and the resulting data were imported into the SIMCA-P software (Umetrics, Sweden). Next, the regression model was established through partial least squares discriminant analysis (PLS-DA) along with the discriminant analysis. In addition, to improve the effectiveness of data analyses, orthogonal partial least squares discriminant analysis (OPLS-DA) was performed to correct the orthogonal transformation based on PLS-DA. OPLS-DA was applied to construct the relationship model between the metabolite expression and the sample category. The detected characteristic metabolites by ^{1}HNMR spectroscopy were identified with reference to the National Center for Biotechnology Information database (https://www.ncbi.nlm.nih.gov/) and Human Metabolome Database (http://www.hmdb.ca/). Furthermore, the metabolic pathway of the characteristic

metabolites was established according to the MetaboAnalyst 5.0 database (https://www.metaboanalyst.ca/).

RESULTS

Effect of EA on Weight

To compare the differences in weight, all mice were weighed daily. The weight after modeling decreased significantly ($P < 0.01$). Although the weight of POF mice increased after EA ($P < 0.05$), it was still lower than that of the control group ($P < 0.01$). The weights of the POF group and the EN group were not significantly different ($P > 0.05$) **(Figure 2A)**.

Effect of EA on Estrous Cycle

On the basis of the different types of vaginal exfoliated cells, the estrous cycle of mice was identified as proestrus, estrus, metestrus, and diestrus. The estrous cycle of normal mice was 4–6 days. In proestrus, the vaginal exfoliated cells were mainly composed of nuclear epithelial cells and keratinocytes **(Figure 2B)**. As the estrous cycle changed, most keratinocytes were observed in the estrous period **(Figure 2C)**. In the metestrus period, nucleated epithelial cells, keratinocytes, and leukocytes were observed **(Figure 2D)**. In the diestrus period, mainly nuclear epithelial cells and leukocytes were observed **(Figure 2E)**. The vaginal exfoliated cells were mainly composed of nuclear epithelial cells and leukocytes after POF modeling was established **(Figure 2F)**. Interestingly, the estrous cycle of mice in the EA group was changed regularly as the proestrus–estrus–metestrus–diestrus cycle progressed after treatment. On the contrary, all vaginal exfoliated cells in the mice of the EN group were still mainly composed of nuclear epithelial cells and leukocytes.

Effect of EA on Histopathology

As shown in **Figure 3A**, atresia follicles increased, which was observed in the ovaries of POF mice. The number of mature follicles and primary follicles increased, and atresia follicles decreased in the EA group. Although a few antral follicles were observed in the EN group, no significant difference was found between the antral follicles in the EN group and the POF group **(Figures 3A).**

The positive rate of granulosa cell apoptosis increased in the POF group ($P < 0.01$). Compared with the POF group, the positive rate of granulosa cell apoptosis in the EA group was reduced ($P < 0.05$). However, the positive rate of the EA group was still higher than that of the control group ($P < 0.01$). Although the positive rate of the EN group was lower than that of the POF group, it was higher than that of the EA group ($P < 0.01$) **(Figures 3B)**.

Effect of EA on the Levels of FSH, LH, E_2, and Anti-Mullerian Hormone

Compared with the control group, the serum levels of FSH and LH in the POF group increased ($P < 0.05$). Meanwhile, the levels of E_2 and AMH decreased after POF was established ($P < 0.05$). The levels of FSH and LH between the control group and the EA group were approached ($P > 0.05$). On the contrary, although the levels of FSH, LH, E_2, and AMH in the EN group were also regulated, they were significantly different from the control group. In addition, no significant difference was found in the levels of AMH among the EA group, EN group, and POF group ($P > 0.05$) **(Figures 4A–D)**.

Effect of EA on the Relative Expression of ERs

To determine the effect of EA on ovarian ERs, the relative expression of ER-α, ER-β, and ERP30 was assessed. The results showed that the expression of ER-α, ER-β, and ERP30

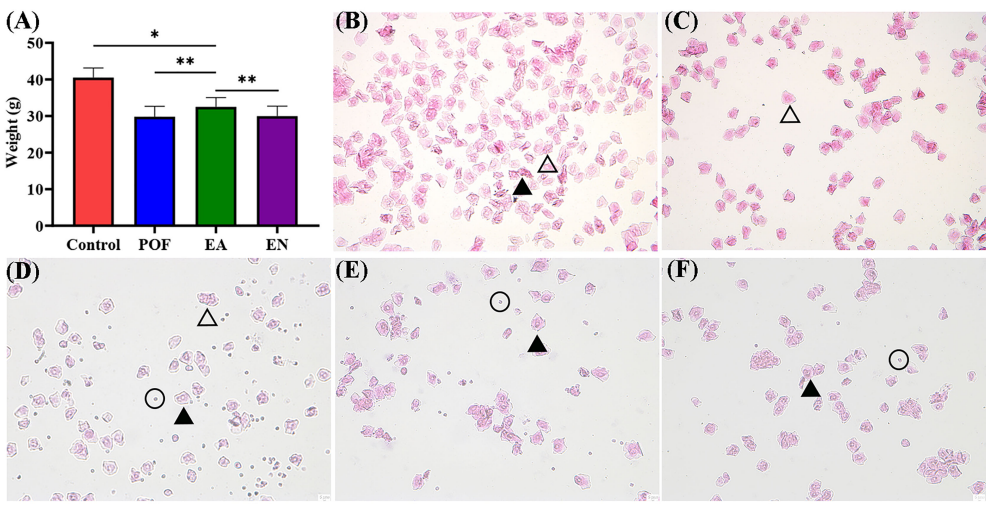

FIGURE 2 | The weight of four groups **(A)**, and the typical morphology of vaginal exfoliated cells in each estrous cycle **(B)**, proestrus; **(C),** estrus; **(D)**, metestrus; **(E)**, diestrus; **(F)**, POF model; ×40 magnification) (* means $P < 0.05$; ** means $P < 0.01$).

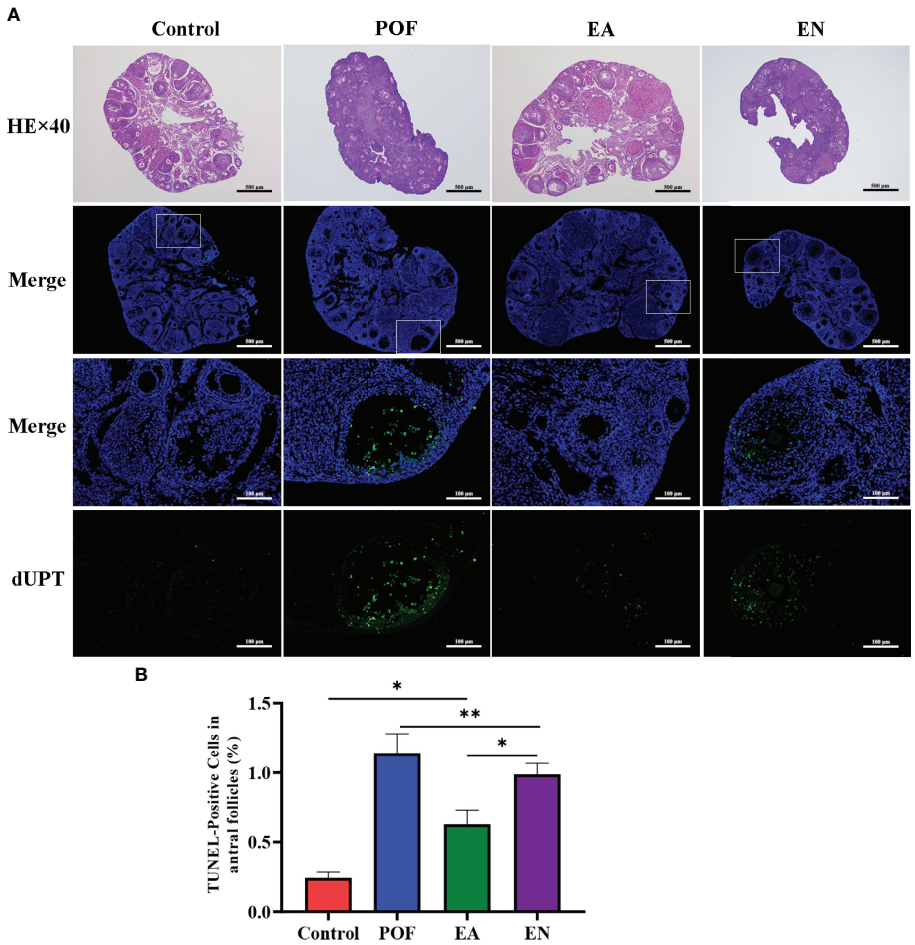

FIGURE 3 | Pathological morphology and granulosa cell apoptosis of ovaries in four groups **(A)**, HE staining and TUNEL detection; **(B)**, the positive rate of granulosa cell apoptosis in antral follicles) (×40 and ×200 magnification; * means $P < 0.05$; ** means $P < 0.01$).

was lower than those in the control group after the POF modeling was established ($P < 0.01$). We found that ER-α, ER-β, and ERP30 increased after EA; however, they were lower than those in the control group ($P < 0.01$) (**Figures 4E–G**).

Effect of EA on ^{1}HNMR Profiles of Liver and Kidney

To determine the characteristic metabolites underlying the mechanism of EA on POF, the ^{1}HNMR profiles of extracts from the liver and kidney were performed and analyzed. The characteristic metabolites in the obtained ^{1}HNMR profiles of the liver and kidney were difficult to identify intuitively (**Figure 5**). Therefore, the PLS-DA and orthogonal projections to latent structures discriminant analysis (OPLS-DA) were performed according to ^{1}HNMR profiles.

The four groups of ^{1}HNMR profiles were merged and analyzed. As shown in **Figures 6A, B**, the control group and the POF groups in the liver and kidney were distinctly dispersed. Concurrently, a good dispersion was present between the POF group and the EA group. Although the dispersion between the POF group and the EN group was observed intuitively in the liver, no significant difference was found in the metabolites between them. Poor dispersion was observed between the POF group and the EN group in the kidney. Therefore, the metabolism of the liver and kidney in POF mice was abnormal. The metabolites in the EN group and POF group were similar.

To determine the effect of EA on liver and kidney metabolism in POF, the metabolic profile of each group were analyzed in pairs. The analysis further proved that the dispersions between the control group and the POF group in the liver and kidney was good (**Figures 6C, D**). This finding indicated that the metabolites in the liver and kidney were abnormal after POF modeling. Similarly, the metabolites in the liver and kidney of POF mice were changed distinctly due to EA. The OPLS-DA of the liver and kidney showed that the metabolites of the EA group were greatly different from the POF group (**Figures 7A, B**). The result showed that the metabolites of the liver and kidney in POF can be regulated by EA. Therefore, S-plot and T-test were performed to identify the characteristic metabolites between the POF group

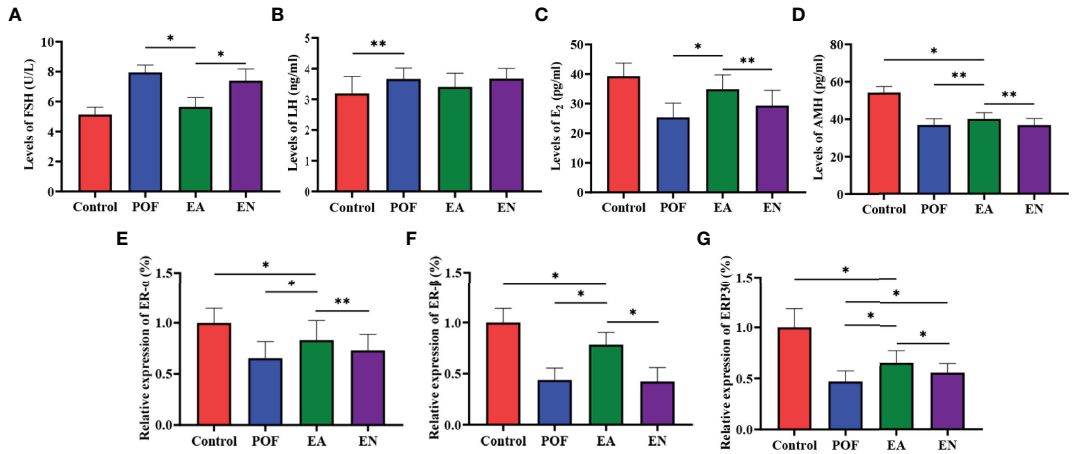

FIGURE 4 | The levels of sex hormones were detected by ELISA **(A)**, FSH; **(B)**, LH; **(C)**, E2; **(D)**, AMH.) and the relative expression of estrogen receptor **(E)**, ER-α; **(F)**, ER-β; **(G)**, GRP30) (* means $P < 0.05$; ** means $P < 0.01$).

and the EA group (**Figures 7a, b**). In contrast, OPLS-DA showed that no significant difference was present in the metabolites of the liver and kidney between the POF group and EN group. The result showed that EN could not improve the metabolic disorder of the liver and kidney in POF mice.

In the liver, the relative levels of lysine, glucose, phosphocholine, taurine, glycine, and glycerol increased after EA. On the contrary, the levels of glutamate, and creatine decreased. In the kidney, the relative levels of lactate and glycerol increased by EA. Furthermore, compared with the POF group, the relative levels of glutamate, creatine, threonine, serine, alanine, and lysine decreased. Creatine, glutamate, glycerol, and lysine were the overlapping metabolites between the liver and kidney after being treated by EA. Interestingly, the levels of overlapping characteristic metabolites in the liver and kidney showed consistent trends after EA.

All the characteristic metabolites of the liver and kidney in the EA group were regulated (**Figures 8**, **9**). Compared with the POF group, the level of characteristic metabolites in the EA group was closer to that in the control group. The characteristic metabolites in the EN group and the POF group were similar. All metabolic pathways containing the above characteristic metabolites in the liver and kidney were established based on the MetaboAnalyst 5.0 database (**Figure 10**).

Effect of EA on the Relationship Between POF and Characteristic Metabolites

To determine the relationship between POF and metabolites, the correlation of POF with characteristic metabolites was obtained by performing the Pearson analysis.

In the liver, FSH and LH were positively correlated with creatine, glutamate, glycerol, lysine, and taurine. FSH and LH

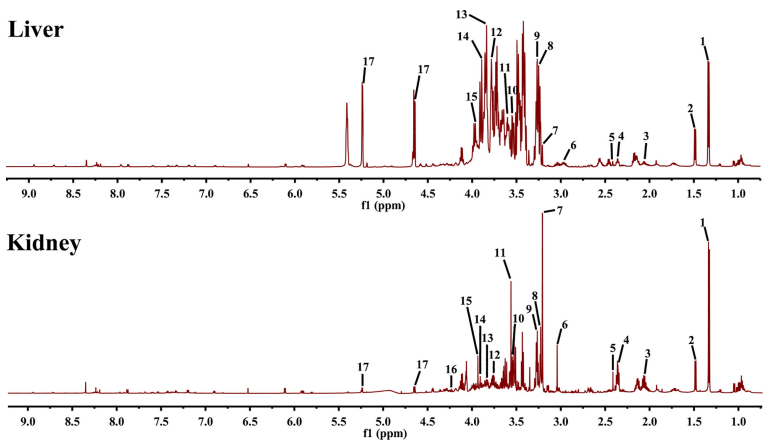

FIGURE 5 | ^{1}HNMR spectra of liver and kidney extracts (1, lactate; 2, alanine; 3, methionine; 4, glutamate; 5, pyruvate; 6, creatine; 7, phosphocholine; 8, betaine; 9, taurine; 10, glycine; 11, glycerol; 12, lysine; 13, serine; 14, aspartate; 15, cysteine; 16, threonine; and 17, glucose).

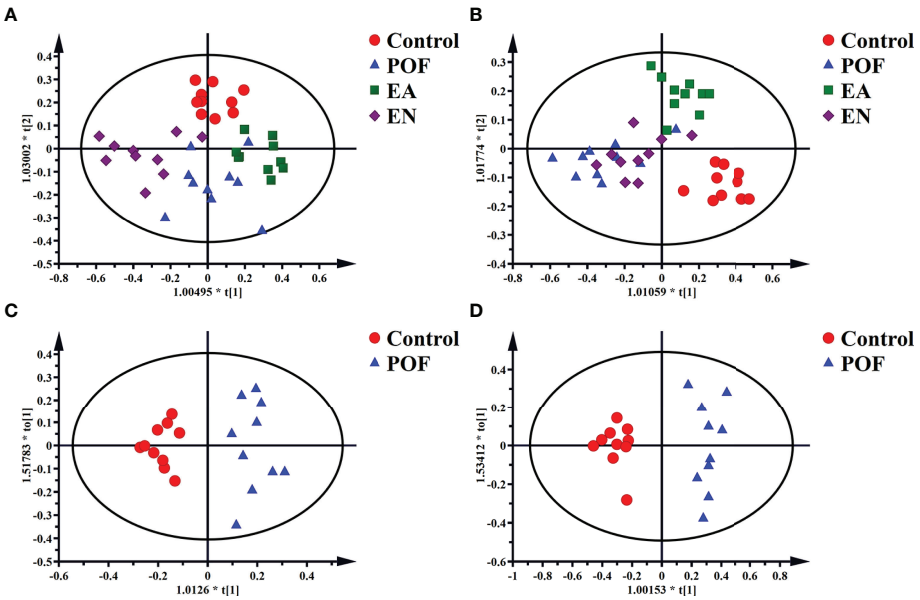

FIGURE 6 | The OPLS-DA scores plots of four groups in liver [**A**, R2X(cum) = 0.632, R2Y(cum) = 0.748, Q2(cum) = 0.55] and kidney (**B**, R2X(cum) = 0.498, R2Y (cum) = 0.75, Q2(cum) = 0.378]. The OPLS-DA scores plots of the control group and the POF group in liver [**C**, R2X(cum) = 0.326, R2Y(cum) = 0.916, Q2(cum) = 0.621] and kidney [**D**, R2X(cum) = 0.535, R2Y(cum) = 0.947, Q2(cum) = 0.754].

were negatively correlated with glucose, glycine, and phosphocholine. AMH, E_2, ER-α, ER-β, and GPR30 were positively correlated with glucose, glycine, and phosphocholine. AMH, E_2, ER-α, ER-β, and GPR30 were negatively correlated with creatine, glutamate, glycerol, lysine, and taurine (**Figure 11**).

In the kidney, FSH and LH were positively correlated with alanine, creatine, glutamate, glycerol, lysine, serine, and threonine. FSH and LH were negatively correlated with lactate. AMH, E_2, ER-α, ER-β, and GPR30 were positively correlated with lactate. AMH, E_2, ER-α, ER-β, and GPR30 were negatively

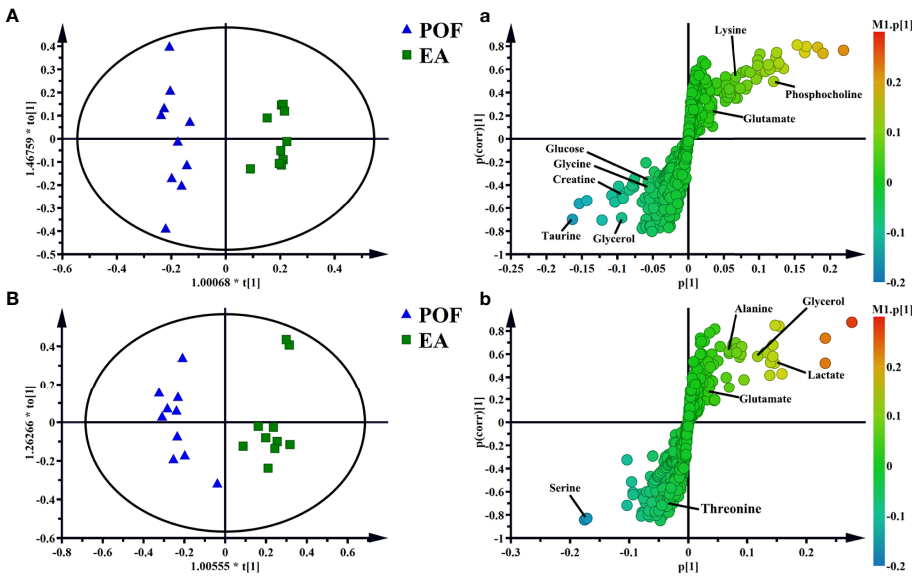

FIGURE 7 | OPLS-DA and S-plots of liver [**A** and **a**, R2X(cum) = 0.606, R2Y(cum) = 0.966, Q2(cum) = 0.689] and kidney extracts in POF group and EA group **B** and **b**, R2X(cum) = 0.499, R2Y(cum) = 0.913, Q2(cum) = 0.65].

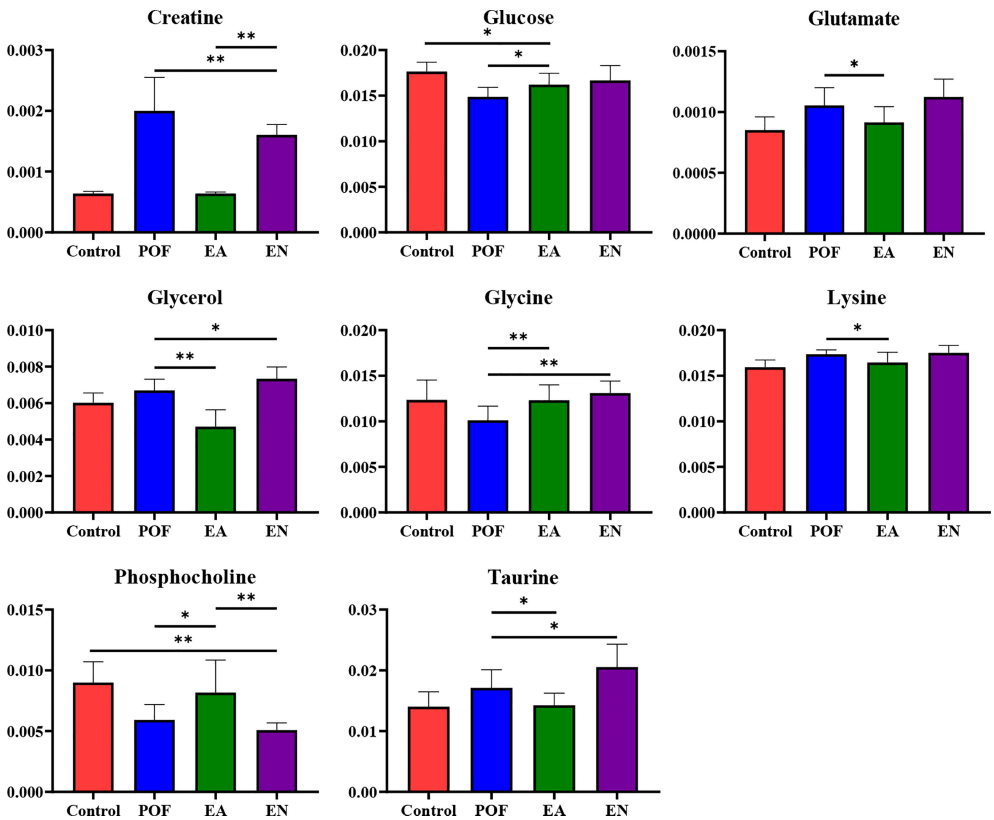

FIGURE 8 | The relative concentrations of characteristic metabolites in the liver (* means $P < 0.05$; ** means $P < 0.01$).

correlated with alanine, creatine, glutamate, glycerol, lysine, serine, and threonine (**Figure 12**).

DISCUSSION

Follicle development is complex and dynamic. A follicle is a basic functional unit of the endocrine and reproduction systems in the ovary (13). The reproductive capacity and reproductive age of females are determined by the number and quality of follicles (14). After secondary follicle formation, granulosa cells express FSH, E_2, and progesterone receptors, and intimal cells express LH receptors (15). FSH and E_2 stimulate granulosa cells, promoting granulosa cell proliferation and follicular cavity formation. Furthermore, the distribution of granulosa cells could reflect the physiological and pathological state of the ovary. Moreover, the estrous cycle changes regularly with changing hormone levels (16). In the present study, ovarian granulosa cells were proliferated by EA, which is one of the important signs of follicular development. Moreover, the regular alteration of the menstrual cycle may be closely related to granulosa cell proliferation by EA. On the whole, EA can promote granulosa cell proliferation and restore the menstrual cycle.

FSH combines with its receptor in granulosa cells, promoting granulosa cell proliferation and follicle maturation. After LH stimulates mature follicles, ovulation is induced and the corpus luteum is generated (17, 18). Interestingly, the levels of FSH and LH in POF mice were restored to normal by EA. EA is beneficial for the development of ovarian granulosa cells and the negative feedback regulation of sex hormones. AMH is secreted by granulosa cells and plays a role in inhibiting the primordial follicle recruitment to prevent the premature consumption of follicles (19). Our result suggests that EA is beneficial in preventing premature consumption of follicles. Further, this finding verifies whether EA could promote ovarian function.

ER-α, ER-β, and ERP30 are considered to be the key mediators of estrogen in ovarian function (20, 21). ER-α is mainly distributed in the interstitial part of the ovary, whereas ER-β is considered to exist mainly in granulosa cells of the ovary. ERP30 is an ER among membrane receptors (19). Estrogen activates the PI3K-Akt signaling pathway after binding to the ER (22, 23). Furthermore, the PI3K-Akt signaling pathway is one of the pathways that promote cell proliferation (24). EA can proliferate ovarian granulosa cells; similarly, EA proliferated ovarian interstitial cells in the present study. This process may be related to the activation of the estrogen-PI3K-Akt signaling pathway. The finding is consistent with the results of histological morphology examinations and TUNEL examinations.

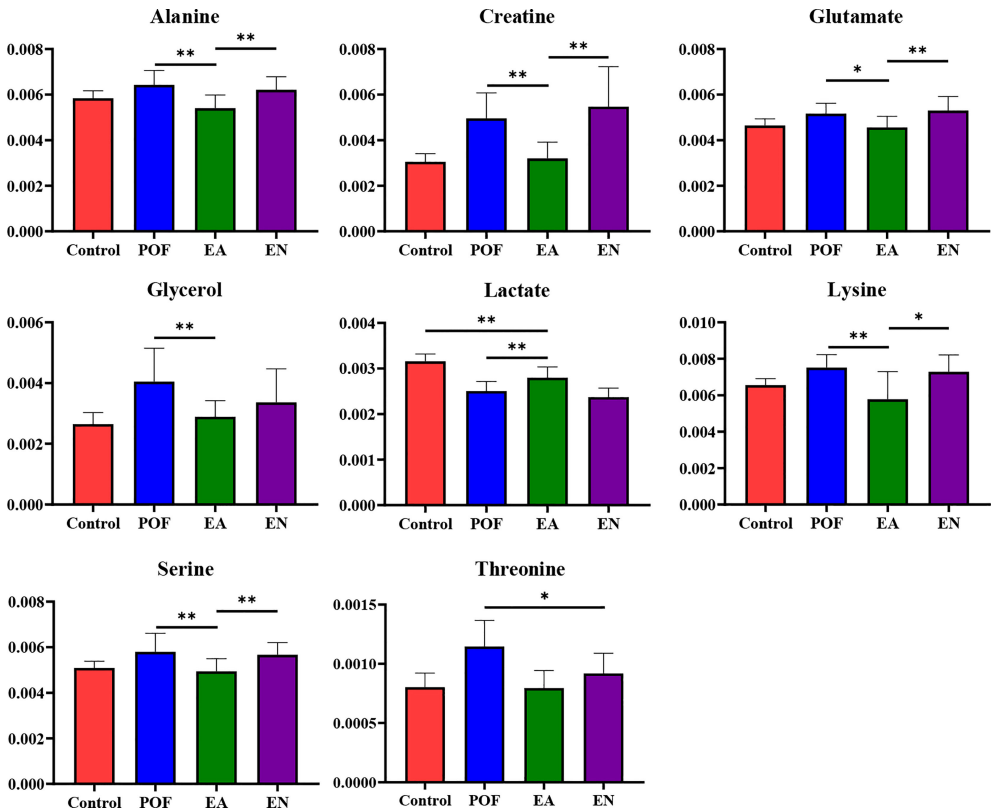

FIGURE 9 | The relative concentrations of characteristic metabolites in the kidney (* means $P < 0.05$; ** means $P < 0.01$).

The application of metabonomics provides an innovative method for constructing the diagnostic strategy of POF. Moreover, metabonomics was widely used to detect the underlying mechanism of acupuncture treatment in the past years. In general, metabolomics is an important part of system biology, which can comprehensively and directly connect diseases

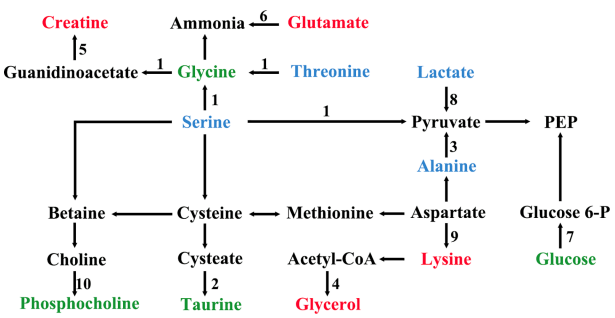

FIGURE 10 | The metabolic pathways of characteristic metabolites in liver and kidney after EA (1, glycine, serine and threonine metabolism; 2, taurine and hypotaurine metabolism; 3, alanine, aspartate, and glutamate metabolism; 4, glycerolipid metabolism; 5, arginine and proline metabolism; 6, arginine biosynthesis; 7, glycolysis/gluconeogenesis; 8, pyruvate metabolism; 9, lysine degradation; 10, glycerophospholipid metabolism; green shows metabolites in liver; blue shows metabolites in kidney; red shows metabolites in liver and kidney).

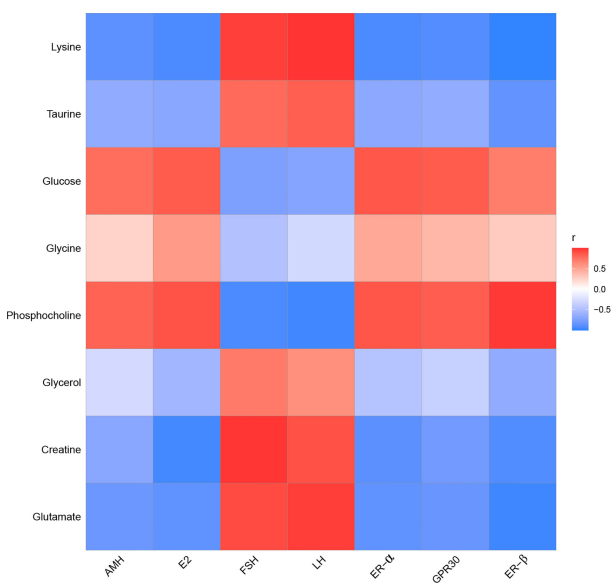

FIGURE 11 | The correlation analysis between POF and characteristic metabolites in the liver.

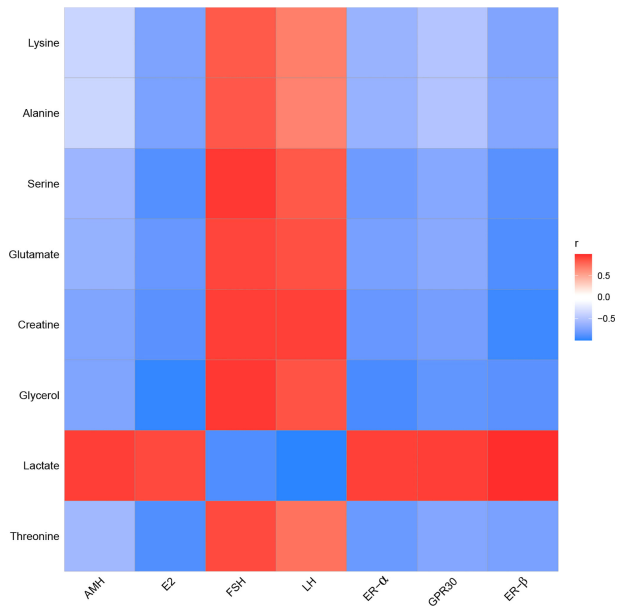

FIGURE 12 | The correlation analysis between POF and characteristic metabolites in the kidney.

with physiological changes. As a common technique in metabolomics, ^{1}HNMR is widely used to identify metabolites associated with the curative effect of treating (25).

The metabolic disorders of the liver and kidney in POF could be regulated by EA, which was beneficial for ovarian function in the present study. On the contrary, EN had no obvious regulatory effect on the metabolic disorders of the liver and kidney in POF. This is consistent with the finding of our previous study, which verified that EA could improve metabolic disorders (11). Metabolic disorders may be evidence for TCM theories such as POF is associated with the function of the liver and kidney. The physiological function of each characteristic metabolite was analyzed. Alanine, creatine, glucose, glycerol, lactate, lysine, and threonine were involved in the energy-related metabolism per the physiological functions of the characteristic metabolites. Glutamate, glycine, phosphocholine, and taurine were involved in the neurotransmitter-related metabolism. Overall, the energy- and neurotransmitter-related metabolic pathways can be regulated in the liver and kidney during POF treatment by EA. As follows, the functions of the obtained characteristic metabolites are described in detail.

ENERGY-RELATED METABOLISM

Alanine, a non-essential amino acid, is one of the regulators of glucose metabolism. Alanine is an important source of energy for humans, as well as it is involved in lymphocyte regeneration, thus maintaining immune homeostasis (26). Alanine, a characteristic metabolite in the kidney, was regulated by EA in the present study. The result suggests that EA may improve glucose metabolism and immune homeostasis in the kidney to treat POF. Creatine participates in the energy metabolism of muscle and nerve cells, which is related to a variety of endocrine diseases. Meanwhile, creatine also plays a role in various enzymatic reactions (27). Creatine was an overlapping characteristic metabolite in the liver and kidney, which showed that EA is involved in enzymatic reactions. Glucose is the main metabolite of energy metabolism and is involved in glycolysis and gluconeogenesis (28). Glycerol can be converted into glucose by a glucose metabolism pathway in the liver, providing energy for cell metabolism (29, 30). Therefore, glycerol is also an important metabolite involved in energy metabolism. Lactate is a common metabolite in glycolysis, which can be converted into glucose by the Cori cycle, thus providing energy during gluconeogenesis in the liver (31). Glucose, glycerol, and lactate as metabolites of the aforementioned processes are regulated by EA in POF mice, indicating that EA may treat POF by regulating glycolysis and gluconeogenesis. Lysine plays a vital role in promoting cell proliferation and enhancing immunity. In the liver, lysine participates in protein synthesis along with other amino acids (32). Therefore, lysine might be related to energy metabolism. Threonine is associated with energy metabolism and promotes the defense function of the cellular immune system (33). Moreover, threonine promotes phosphorus synthesis and fatty acid oxidation, thereby protecting cell membranes (34). By analyzing the physiological functions of lysine and threonine, we speculate that EA plays a role in improving immune function and protecting cell membranes in the liver and kidney of POF mice.

In summary, EA regulates glucose metabolism and immune homeostasis in the liver and kidney of POF mice. Furthermore, POF occurrence may be related to the metabolite disorder of glucose metabolism and immune homeostasis in the liver and kidney. The energy associated with the metabolic disorder is considered to be an important factor in the occurrence of many diseases. The finding indicates that EA can regulate the energy metabolism pathway, which may be related to POF treatment. Importantly, more energy-related metabolites are present in the kidney than in the liver, which indicates that EA may affect the regulation of energy metabolism in the kidney.

NEUROTRANSMITTER-RELATED METABOLISM

Glutamate is one of the important metabolites in neurons (35). EA regulated neuron metabolism to restore glutamate levels in the liver and kidney. Taurine plays various biological roles such as a neurotransmitter, a stabilizer of the cell membrane, and a promoter of ion transport (36). Therefore, EA is beneficial for cell membrane stabilization and neuroprotection in the liver. Glycine is an inhibitory neurotransmitter, where glycine and serine affect antioxidants (37). Serine synthesis is regulated by the diet and hormones in the liver. Serine and its metabolites are necessary for cell proliferation and the central nervous system (38). Phosphocholine takes a part in the synthesis of acetylcholine and activates the autonomic nervous system (39). Furthermore, phosphocholine can promote lipid metabolism and accelerate hepatocyte regeneration (40). Phosphocholine levels increased after EA treatment, which may be related to the promotion of lipid metabolism and hepatocyte regeneration.

Taken together, EA is beneficial for neurotransmitter-related metabolic homeostasis in the liver and kidney. Moreover, POF occurrence may be related to the metabolite disorder of neurotransmitter-related metabolism in the liver and kidney. The aforementioned characteristic metabolites that existed in the liver indicate that EA exhibits a greater effect in the liver than in the kidney on the neurotransmitter-related metabolism in POF.

To conclude, the metabolic profiles in the liver and kidney of POF mice were changed, where EA regulated the characteristic metabolites of energy- and neurotransmitter-related metabolism. EA plays an important role in regulating energy-related metabolism in the kidney. Moreover, EA exhibited a better effect on the neurotransmitter-related metabolism in the liver than in the kidney. The Pearson analysis showed that the metabolomics in the liver and kidney were closely associated with ovarian function. Our study suggests that EA therapy plays a crucial role in liver and kidney metabolism, thereby proving its usefulness in treating POF, as the liver and kidney are related to POF according to a TCM theory. This was preliminarily confirmed by metabolomics. However, speaking of limitations, the metabolites were not quantitatively detected using ^{1}HNMR; liquid chromatography–mass spectrometry will be used and the sample size will be increased in the future study.

DATA AVAILABILITY STATEMENT

The raw data supporting the conclusions of this article will be made available by the author (hokida@163.com), without undue reservation.

ETHICS STATEMENT

The animal study was reviewed and approved by Xiamen University Animal Ethics Committee.

AUTHOR CONTRIBUTIONS

QH, ZY, LX, and MC designed the project; QH, QW, JG, YX, and QZ conducted the experiments; YY, ZG, and ZT analyzed all data; QH wrote original draft preparation; ZY, LX, and MC revised the manuscript. All authors contributed to the article and approved the submitted version.

FUNDING

This work was supported by the Special Project of Academic New Seedling Cultivation and Innovation Exploration of Zunyi Medical University, No. QKH-Platform-Talents [2017]5733-080; the project of Guizhou Provincial Natural Science Foundation, QKH-J [2020]1Y378; the open project from the Key Laboratory of Basic Pharmacology of Ministry of Education at Zunyi Medical University, Education Department of Guizhou Province Cooperation, KY [2018]484; the project of Science and Technology Bureau in Zunyi City, Zunyi Science and Technology Cooperation, HZ (2019) No. 40; and the Science and Technology Development Fund, Macau SAR [file nos. 0099/2018/A3, 0098/2021/A2, and SKL-QRCM(MUST)-2020-2022].

REFERENCES

1. Jankowska K. Premature Ovarian Failure. *Prz Menopauzalny* (2017) 16 (2):51–6. doi: 10.5114/pm.2017.68592
2. Igboeli P, El Andaloussi A, Sheikh U, Takala H, ElSharoud A, McHugh A, et al. Intraovarian Injection of Autologous Human Mesenchymal Stem Cells Increases Estrogen Production and Reduces Menopausal Symptoms in Women With Premature Ovarian Failure: Two Case Reports and a Review of the Literature. *J Med Case Rep* (2020) 14(1):108. doi: 10.1186/s13256-020-02426-5
3. Swee DS, Javaid U, Quinton R. Estrogen Replacement in Young Hypogonadal Women-Transferrable Lessons From the Literature Related to the Care of Young Women With Premature Ovarian Failure and Transgender Women. *Front Endocrinol* (2019) 10:685. doi: 10.3389/fendo.2019.00685
4. Szeliga A, Maciejewska-Jeske M, Męczekalski B. Bone Health and Evaluation of Bone Mineral Density in Patients With Premature Ovarian Insufficiency. *Prz Menopauzalny* (2018) 17(3):112–6. doi: 10.5114/pm.2018.78552
5. Vinogradova Y, Coupland C, Hippisley-Cox J. Use of Hormone Replacement Therapy and Risk of Breast Cancer: Nested Case-Control Studies Using the QResearch and CPRD Databases. *BMJ* (2020) 371:m3873. doi: 10.1136/bmj.m3873
6. Ueda K, Fukuma N, Adachi Y, Numata G, Tokiwa H, Toyoda M, et al. Sex Differences and Regulatory Actions of Estrogen in Cardiovascular System. *Front Physiol* (2021) 12:738218. doi: 10.3389/fphys.2021.738218
7. Zhang J, Huang X, Liu Y, He Y, Yu H. A Comparison of the Effects of Chinese non-Pharmaceutical Therapies for Premature Ovarian Failure: A PRISMA-Compliant Systematic Review and Network Meta-Analysis. *Medicine* (2020) 99(26):e20958. doi: 10.1097/MD.0000000000020958
8. Wang SC, Jiang YM, Qiu LR, Su M. Efficacy of Needling Acupoints of Guanyuan (CV4), Sanyinjiao (SP6), Zusanli (ST36), Pishu (BL20), Shenshu (BL23), Zigong (EX-CA1) on Expression of P38 Mitogen-Activated Protein Kinase in Ovarian Tissue in Rats With Premature Ovarian Failure Induced by Cyclophosphamide. *J Tradit Chin Med* (2021) 41(6):953–8. doi: 10.19852/j.cnki.jtcm.2021.06.012
9. He QD, Guo JJ, Zhang Q, Yau YM, Yu Y, Zhong ZH, et al. Effects of Electroacupuncture on the Gut Microbiome in Cisplatin-Induced Premature Ovarian Failure Mice. *Evid Based Complement Alternat Med* (2022) 2022:9352833. doi: 10.1155/2022/9352833
10. Lin X, Liu X, Xu J, Cheng KK, Cao J, Liu T, et al. Metabolomics Analysis of Herb-Partitioned Moxibustion Treatment on Rats With Diarrhea-Predominant Irritable Bowel Syndrome. *Chin Med* (2019) 14:18. doi: 10.1186/s13020-019-0240-2
11. He QD, Huang YP, Zhu LB, Shen JC, Lian LY, Zhang Y, et al. Difference of Liver and Kidney Metabolic Profiling in Chronic Atrophic Gastritis Rats Between Acupuncture and Moxibustion Treatment. *Evid Based Complement Alternat Med* (2018) 2018:6030929. doi: 10.1155/2018/6030929
12. Lee EH, Han SE, Park MJ, Kim HJ, Kim HG, Kim CW, et al. Establishment of Effective Mouse Model of Premature Ovarian Failure Considering Treatment Duration of Anticancer Drugs and Natural Recovery Time. *J Menopausal Med* (2018) 24(3):196–203. doi: 10.6118/jmm.2018.24.3.196
13. Pan B, Li J. The Art of Oocyte Meiotic Arrest Regulation. *Reprod Biol Endocrinol* (2019) 17(1):8. doi: 10.1186/s12958-018-0445-8
14. Gershon E, Dekel N. Newly Identified Regulators of Ovarian Folliculogenesis and Ovulation. *Int J Mol Sci* (2020) 21(12):4565. doi: 10.3390/ijms21124565
15. Dupont J, Scaramuzzi RJ. Insulin Signalling and Glucose Transport in the Ovary and Ovarian Function During the Ovarian Cycle. *Biochem J* (2016) 473 (11):1483–501. doi: 10.1042/BCJ20160124

16. Tan R, He Y, Zhang S, Pu D, Wu J. Effect of Transcutaneous Electrical Acupoint Stimulation on Protecting Against Radiotherapy- Induced Ovarian Damage in Mice. *J Ovarian Res* (2019) 12:65. doi: 10.1186/s13048-019-0541-1
17. Wang J, Cheng K, Qin Z, Wang Y, Zhai L, You M, et al. Effects of Electroacupuncture at Guanyuan (CV 4) or Sanyinjiao (SP 6) on Hypothalamus-Pituitary-Ovary Axis and Spatial Learning and Memory in Female SAMP8 Mice. *J Tradit Chin Med* (2017) 37(1):96–100. doi: 10.1016/s0254-6272(17)30032-8
18. Thompson IR, Kaiser UB. GnRH Pulse Frequency-Dependent Differential Regulation of LH and FSH Gene Expression. *Mol Cell Endocrinol* (2014) 385 (1-2):28–35. doi: 10.1016/j.mce.2013.09.012
19. Jiao X, Meng T, Zhai Y, Zhao L, Luo W, Liu P, et al. Ovarian Reserve Markers in Premature Ovarian Insufficiency: Within Different Clinical Stages and Different Etiologies. *Front Endocrinol (Lausanne)* (2021) 12:601752. doi: 10.3389/fendo.2021.601752
20. Tang ZR, Zhang R, Lian ZX, Deng SL, Yu K. Estrogen-Receptor Expression and Function in Female Reproductive Disease. *Cells* (2019) 8(10):1123. doi: 10.3390/cells8101123
21. Hara Y, Waters EM, McEwen BS, Morrison JH. Estrogen Effects on Cognitive and Synaptic Health Over the Lifecourse. *Physiol Rev* (2015) 95(3):785–807. doi: 10.1152/physrev.00036.2014
22. Shi D, Zhao P, Cui L, Li H, Sun L, Niu J, et al. Inhibition of PI3K/AKT Molecular Pathway Mediated by Membrane Estrogen Receptor GPER Accounts for Cryptotanshinone Induced Antiproliferative Effect on Breast Cancer SKBR-3 Cells. *BMC Pharmacol Toxicol* (2020) 21(1):32. doi: 10.1186/s40360-020-00410-9
23. Xia X, Zhou C, Sun X, He X, Liu C, Wang G. Estrogen Improved the Regeneration of Axons After Subcortical Axon Injury *via* Regulation of PI3K/Akt/CDK5/Tau Pathway. *Brain Behav* (2020) 10(9):e01777. doi: 10.1002/brb3.1777
24. Yu JS, Cui W. Proliferation, Survival and Metabolism: The Role of PI3K/AKT/mTOR Signalling in Pluripotency and Cell Fate Determination. *Development* (2016) 143(17):3050–60. doi: 10.1242/dev.137075
25. Wang P, Wang Q, Yang B, Zhao S, Kuang H. The Progress of Metabolomics Study in Traditional Chinese Medicine Research. *Am J Chin Med* (2015) 43 (7):1281–310. doi: 10.1142/S0192415X15500731
26. Ron-Harel N, Ghergurovich JM, Notarangelo G, LaFleur MW, Tsubosaka Y, Sharpe AH, et al. T Cell Activation Depends on Extracellular Alanine. *Cell Rep* (2019) 28(12):3011–21.e4. doi: 10.1016/j.celrep.2019.08.034
27. Hall CHT, Lee JS, Murphy EM, Gerich ME, Dran R, Glover LE, et al. Creatine Transporter, Reduced in Colon Tissues From Patients With Inflammatory Bowel Diseases, Regulates Energy Balance in Intestinal Epithelial Cells, Epithelial Integrity, and Barrier Function. *Gastroenterology* (2020) 159 (3):984–98.e1. doi: 10.1053/j.gastro.2020.05.033
28. Han HS, Kang G, Kim JS, Choi BH, Koo SH. Regulation of Glucose Metabolism From a Liver-Centric Perspective. *Exp Mol Med* (2016) 48(3): e218. doi: 10.1038/emm.2015.122
29. Gambert S, Héliès-Toussaint C, Grynberg A. Extracellular Glycerol Regulates the Cardiac Energy Balance in a Working Rat Heart Model. *Am J Physiol Heart Circ Physiol* (2007) 292(3):H1600–6. doi: 10.1152/ajpheart.00563.2006
30. Jin ES, Browning JD, Murphy RE, Malloy CR. Fatty Liver Disrupts Glycerol Metabolism in Gluconeogenic and Lipogenic Pathways in Humans. *J Lipid Res* (2018) 59(9):1685–94. doi: 10.1194/jlr.M086405
31. Suhara T, Hishiki T, Kasahara M, Hayakawa N, Oyaizu T, Nakanishi T, et al. Inhibition of the Oxygen Sensor PHD2 in the Liver Improves Survival in Lactic Acidosis by Activating the Cori Cycle. *Proc Natl Acad Sci U S A* (2015) 112(37):11642–7. doi: 10.1073/pnas.1515872112
32. Zhao S, Xu W, Jiang W, Yu W, Lin Y, Zhang T, et al. Regulation of Cellular Metabolism by Protein Lysine Acetylation. *Science* (2010) 327(5968):1000–4. doi: 10.1126/science.1179689
33. Herzig S, Shaw RJ. AMPK: Guardian of Metabolism and Mitochondrial Homeostasis. *Nat Rev Mol Cell Biol* (2018) 19(2):121–35. doi: 10.1038/nrm.2017.95
34. House JD, Hall BN, Brosnan JT. Threonine Metabolism in Isolated Rat Hepatocytes. *Am J Physiol Endocrinol Metab* (2001) 281(6):E1300–7. doi: 10.1152/ajpendo.2001.281.6.E1300
35. Bak LK, Schousboe A, Waagepetersen HS. The Glutamate/GABA-Glutamine Cycle: Aspects of Transport, Neurotransmitter Homeostasis and Ammonia Transfer. *J Neurochem* (2006) 98(3):641–53. doi: 10.1111/j.1471-4159.2006.03913.x
36. Wu JY, Prentice H. Role of Taurine in the Central Nervous System. *J BioMed Sci* (2010) 17 Suppl 1(Suppl 1):S1. doi: 10.1186/1423-0127-17-S1-S1
37. Amelio I, Cutruzzolá F, Antonov A, Agostini M, Melino G. Serine and Glycine Metabolism in Cancer. *Trends Biochem Sci* (2014) 39(4):191–8. doi: 10.1016/j.tibs.2014.02.004
38. Suzuki M, Imanishi N, Mita M, Hamase K, Aiso S, Sasabe J. Heterogeneity of D-Serine Distribution in the Human Central Nervous System. *ASN Neuro* (2017) 9(3):1759091417713905. doi: 10.1177/1759091417713905
39. Amenta F, Tayebati SK. Pathways of Acetylcholine Synthesis, Transport and Release as Targets for Treatment of Adult-Onset Cognitive Dysfunction. *Curr Med Chem* (2008) 15(5):488–98. doi: 10.2174/092986708783503203
40. Li Z, Vance DE. Phosphatidylcholine and Choline Homeostasis. *J Lipid Res* (2008) 49(6):1187–94. doi: 10.1194/jlr.R700019-JLR200

Conflict of Interest: The authors declare that the research was conducted in the absence of any commercial or financial relationships that could be construed as a potential conflict of interest.

Publisher's Note: All claims expressed in this article are solely those of the authors and do not necessarily represent those of their affiliated organizations, or those of the publisher, the editors and the reviewers. Any product that may be evaluated in this article, or claim that may be made by its manufacturer, is not guaranteed or endorsed by the publisher.

frontiers | Frontiers in Endocrinology

ORIGINAL RESEARCH
published: 27 July 2022
doi: 10.3389/fendo.2022.893506

Future Fertility of Patients With No Embryo Transfer in Their First IVF Cycle Attempts

*Xuli Zhu†, Mingya Cao†, Zhaohui Yao, Peiyang Lu, Yueming Xu, Guimin Hao and Zhiming Zhao**

Department of Reproduction Medicine, The Second Hospital of Hebei Medical University, Shijiazhuang, China

OPEN ACCESS

Edited by:
Yuting Fan,
Boston IVF, United States

Reviewed by:
Alice Albu,
Carol Davila University of Medicine and Pharmacy, Romania
Juanzi Shi,
Northwest Women's and Children's Hospital, China
Yihong Guo,
First Affiliated Hospital of Zhengzhou University, China
Yuhua Shi,
Guangdong Provincial People's Hospital, China

***Correspondence:**
Zhiming Zhao
doctor_zhaozhao@sina.com

†These authors have contributed equally to this work and share first authorship

Specialty section:
This article was submitted to Reproduction, a section of the journal Frontiers in Endocrinology

Received: *10 March 2022*
Accepted: *27 May 2022*
Published: *27 July 2022*

Citation:
Zhu X, Cao M, Yao Z, Lu P, Xu Y, Hao G and Zhao Z (2022) Future Fertility of Patients With No Embryo Transfer in Their First IVF Cycle Attempts. Front. Endocrinol. 13:893506. doi: 10.3389/fendo.2022.893506

Objective: We aimed to evaluate the future outcomes of patients undergoing their first IVF (*in vitro* fertilization) attempt with no oocyte retrieved, no normal zygotes formed, or no embryos available for transfer and to identify factors affecting the live birth rate.

Methods: Patients who underwent no transplantable embryo in their first IVF cycles but carried out several consecutive cycles between January 2012 to December 2020 were retrospectively enrolled and divided into three groups:group A (no egg retrieval), group B (no normal zygotes formed), and group C (no embryos available to transfer). The patients were also divided into the live birth group and non-live birth group according to whether they got a live baby or not. The clinical data and the cumulative clinical outcomes of groups were compared.

Results: 496 patients met the inclusion criteria and enrolled, with 121 patients with no oocytes retrieved in group A, 138 patients with no normal zygotes formed in group B, and 237 patients with no embryos available to transfer in group C. The age [(34.75(5.82) *vs* 31.91(5.31), $P<0.001$; 34.75(5.82) *vs* 32.25(5.72), $P<0.001$)] and baseline FSH level [(13.04(8.82) *vs* 10.52(7.39), $P=0.005$; 13.04(8.82) *vs* 9.91(5.95), $P<0.001$)] of women in group A were significantly higher than those in groups B and C. The stable cumulative live birth rate/patient of three groups achieved 18.18% (after 5 cycles, group A), 28.98% (after 3 cycles, group B) and 20.25% (after 7 cycles, group C). Moreover, the multivariate regression analysis showed that female age and basic FSH were main factors affecting live birth outcome of patients with no embryo transfer in their first IVF cycle attempts.

Conclusions: The future clinical outcome may be better in women with no normal zygotes than those with no oocyte retrieved or no available embryo at their first IVF cycle attempts. The main factors influencing the live birth are age and ovarian reserve.

Keywords: *in vitro* fertilization, no embryo transfer, cycle cancellation rate, poor ovarian response, cumulative live birth rate

INTRODUCTION

Embryo transfer is a key step for successful pregnancy of women through assisted reproduction, but this process may face cycle cancellation because of no oocyte retrieved, no normal zygote formed, or no available embryos. Considering the inherent poor outcomes, most studies have excluded patients with cycle cancellation at the beginning of research (1–3). The ESPART study reported the prevalence of cycle cancellation was 4.7% in poor responders (4), and another survey showed the risk of cycle cancellation caused by poor ovarian response was about 20% (5). However, the prevalence in the general population receiving *in vitro* fertilization (IVF) is obscure. A French study examined medical factors associated with early cessation of IVF in 5135 couples and found that couples who did undergo no embryo transfer during the first IVF cycle attempt were more likely to stop treatment early (6). Other studies (7–10) have found that the psychological burden of failure in non-pregnancy treatment is the reason for withdrawing from further treatment. There are currently few reports on the clinical outcome of follow-up treatment in these patients, but it is necessary to provide these patients with information about the final clinical outcome in all institutions carrying out the artificial reproduction technology (ART).

Based on the above observational studies and to answer the consultation of patients with no transplantable embryo in their first IVF cycle attempt, this study was performed to investigate the outcome of future fertility of patients undergoing their first IVF cycle attempt with no embryos transplanted as well as to identify factors that might affect the possibility to get a baby in subsequent IVF cycle attempt.

MATERIALS AND METHODS

Subject

The retrospective study was performed in consecutive women attending the IVF procedure in our hospital from January 2012 to December 2020. Inclusion criteria were women who wanted more cycle attempts after their first IVF cycles had been cancelled for some reasons even if they had reached the oocyte pick-up (OPU) stage and had undergone egg retrieval in their first IVF cycle. The first delivery was used as the end point of the study. Exclusion criteria include: (i) chromosomal abnormalities in either their spouse or pre-implantation genetic testing cycles; (ii) patients who did not continue the IVF cycle after the first cancelled cycle; (iii) patients who had no clinical outcome at the end of follow-up. This study was approved by the ethics committee of our hospital, and all patients had signed the informed consent to participate (**Figure 1**).

Treatment Protocol and Pregnancy Criteria

The stimulation protocol was performed according to our center's guidelines and was determined by the treating clinician based on individualized conditions. The stimulation protocol in fresh cycles included GnRH-a long protocol (luteal phase short-acting GnRH-a long protocol), short-acting GnRH-a protocol, GnRH-ant protocol (GnRH antagonist protocol), EFLL protocol (early-follicular phase long-acting GnRH agonist long protocol), PPOS protocol (progestin-primed ovarian stimulation protocol), and milder ovarian stimulation protocol. Different protocles may be used in the same person in different cycles.

Follicle growth and hormone levels were continuously monitored by ultrasound and blood tests. Human chorionic gonadotropin (hCG) was injected when the largest follicle diameter was bigger than 18 mm or the diameter of at least three follicles was bigger than 17 mm during the fresh cycle, and the oocytes were collected 36-38h after hCG injection. The oocytes were inseminated through conventional IVF/ICSI (intracytoplasmic sperm injection), and fertilization was observed 16-18h after insemination. Seventy-two hours after oocyte retrieval, whether to transplant or to freeze the embryo was based on embryo grading and the individual clinical situation of each patient. Blood β-hCG (+) was measured 14d after transfer as biochemical pregnancy, and clinical pregnancy was determined by ultrasonography at 28-30d when a gestational sac and primordial ventricular pulsation were observed.

Embryo Score and Cycle Outcome Definition

The ASEBIR scoring criteria was used to assess the embryo at the cleavage stage (11). Embryos were classified into grades I-IV according to the number of blastomeres on day 3, proportion of fragmentation, uniformity of blastomeres, multinucleation, number of vacuoles, and normalness of the zona pellucida. The criteria for good quality embryos were 2PN (2 pronucleus) origin, 7-9 cells, fragmentation <10%, and basic homogeneity of the cleavage. Non-transferable embryos were defined as embryos with grade IV with no fused embryos formed in further culture at Day3; non-insemination was defined as no MII (mature) eggs 2 hours after degranulation; non-fertilization was defined as no normal progenitor nuclei observed after IVF fertilization with no oocyte cleavage. Group B (no normal zygote formation group) included non-fertilization and no normal progenitor nuclei.

Grouping and Indicators

Patients were divided into three groups depending on the cause for the cancellation in their first IVF cycle: group A (no egg retrieval group), group B (no normal zygote formation group) including patients with non-insemination and non-fertilization, and group C (no embryos available to transfer). According to whether they had got a live baby or not, the patients were divided into live birth and non-live birth groups. The patients' age, BMI (Body mass index), infertility years, infertility type, infertility factors (male or female), basic FSH or LH level, Gn (gonadotropin) dose and days, cumulative clinical pregnancy rate, and cumulative live birth rate of the three groups were compared. The Gn days, Gn dose, mean Oocytes/opu, total oocytes retrieved, average number of 2PN fertilization/opu, average number of transferred embryos/opu, cumulative clinical pregnancy rate/opu, cumulative clinical pregnancy rate/

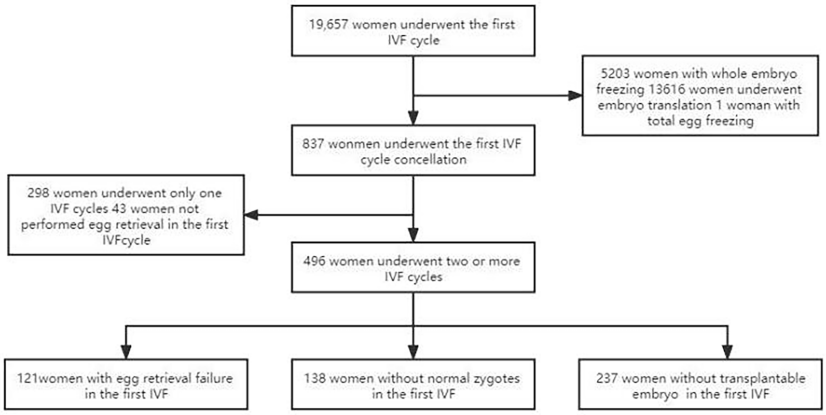

FIGURE 1 | Flowchart of patient selection. A total of 19,657 couples underwent IVF cycle with oocytes to pick up, and 837 patients had cycle cancellation in their first IVF cycle attempts. 298 women underwent only one IVF cycle, of which 50 women were with no egg retrieved, 48 women with no normal zygotes formed and 200 women with the cancellation cycle due to poor embryo quality. 496 women met the study inclusion criteria and were enrolled.

patient, https://fanyi.baidu.com/translate?aldtype=16047&query=%E7%AC%AC%E4%B8%80%E5%91%A8%E6%9C%9F%E6%82%A3%E8%80%85%E7%89%B9%E5%BE%81&keyfrom=baidu&smartresult=dict&lang=auto2zh - ##cumulative live birth rate/opu, https://fanyi.baidu.com/translate?aldtype=16047&query=%E7%AC%AC%E4%B8%80%E5%91%A8%E6%9C%9F%E6%82%A3%E8%80%85%E7%89%B9%E5%BE%81&keyfrom=baidu&smartresult=dict&lang=auto2zh - ##cumulative live birth rate/patient were recorded, respectively, among three groups according to the cycle rank, and the basic characteristics including age, BMI, basic FSH or LH level, Gn dose and days between the live birth and non-live birth groups in the first cycle were investigated.

Statistical Analysis

The SPSS23.0 software (IBM, Chicago, IL, USA) was used for statistical analysis. Continuous variables were expressed as mean (standard deviation or SD) and categorical variable data were expressed as numbers and percentages. One-Way ANOVA was used to analyze the mean difference among groups, the Chi squre test was used to compare the classified data between groups, and the binary Logistic regression (Enter) was used to calculate the OR (odds ratio) value. The statistically significant difference was set at $P<0.05$.

RESULTS

Subject

During the study period, a total of 19,657 couples underwent the first IVF cycle and with oocytes being picked up, and 837 patients had cycle cancellation in their first IVF cycle attempts, resulting in a cancellation rate of 4.26% (837/19657). Among the 837 patients with cycle cancellation, 496 women who met the study inclusion criteria, with no embryo transfer, were enrolled to attend more cycles attempts. Among them, 121 cases of egg retrieval failure were assigned to group A, 138 cases who failed to form normal zygotes (including 83 cases of non-fertilization, 21 cases of abnormal fertilization, 33 cases of non-insemination, 1 case of non-cleavage) were assigned group B, and 237 without available embryo were assigned to group C. Baseline clinical characteristics and clinical outcomes of the three groups in the first IVF cycle are summarized in **Table 1**. Characteristics of the subsequent IVF cycles and the final reproductive outcomes stratified according to the IVF cycle rank between three groups are presented in **Tables 2.1**–**2.3** and **Figure 2**. The characteristics of live birth and non-live birth groups are showed in **Table 3**, and the outcomes of multivariate regression analysis between the two groups are demonstrated in **Table 4**.

Baseline and Characteristics Among Three Groups

A significant difference existed in female age, basic FSH level and Gn days between group A and group B ($P< 0.001$, $P=0.005$, $P=0.001$)as well as between groups A and C ($P< 0.001$, $P< 0.001$, $P< 0.001$). Cumulative clinical pregnancy rates per OPUand per patient in group B were 14.75% and 39.13%, respectively, which were better than those in other two groups. Cumulative live birth rates per OPU and per patient were 10.92% and 28.98%, respectively, in group B, which were significantly higher than those in group A ($P=0.027$, $P=0.042$), but not significantly ($P>0.05$)different from those in group C. Both cumulative pregnancy rate and cumulative live birth rates were not significantly ($P>0.05$) different between group A and C (**Table 1**).

Cumulative Clinical Outcomes at Cycle Rank

In group A, the cumulative clinical pregnancy rates were 7.14% per OPU and 20.66% per patient, and the cumulative live birth rates were 6.28% per OPU and 18.18% per patient, all of which reached a plateau at the 5th OPU cycle (**Table 2.1** and **Figure 2**).

TABLE 1 | Comparison of baseline values and final reproductive outcomes in the first IVF cycle among the three groups.

groups	Group A	P1 (AvsB)	Group B	P2 (AvsC)	Group C	P3 (BvsC)
Characteristics of patients in the first cycle						
Number of patients	121		138		237	
Age (years)	34.75 (5.82)	<0.001	31.91 (5.31)	<0.001	32.25 (5.72)	ns
BMI (kg/m2)	23.41 (5.18)	ns	23.70 (3.71)	ns	23.4 (3.51)	ns
FSH/mIU	13.04 (8.82)	0.005	10.52 (7.39)	<0.001	9.91 (5.95)	ns
LH/mIU	5.81 (5.75)	ns	5.14 (4.03)	ns	7.93 (46.97)	ns
AMH (ng/ml)	0.50 (0.56)	ns	0.68 (0.65)	0.044	1.15 (1.53)	0.002
Infertility years	4.42 (3.97)	ns	4.21 (3.33)	ns	4.29 (3.45)	ns
Infertility type						
Primary infertility	61/121	ns	91/138	<0.001	132/237	ns
Secondary infertility	60/121	0.011	47/138	ns	105/237	ns
Infertility factors						
Male (%)	16/121 (13.22%)	ns	21/138 (15.22%)	ns	33/237 (13.92%)	ns
Tubal (%)	58/121 (47.93%)	ns	57/138 (41.30%)	ns	101/237 (42.62%)	ns
Endometriosis (%)	7/121 (5.79%)	ns	6/138 (4.35%)	ns	15/237 (6.33%)	ns
Unexplained infertility (%)	5/121 (4.13%)	ns	13/138 (9.42%)	ns	20/237 (8.44%)	ns
Uterine factor (%)	2/121 (1.65%)	ns	3/138 (2.17%)	ns	0/237	ns
Ovulatory disorder (%)	25/121 (20.66%)	ns	28/138 (20.29%)	ns	46/237 (19.41%)	ns
Others (%)	4/121 (3.31%)	ns	46/138 (33.33%)	ns	4/237 (1.69%)	ns
https://fanyi.baidu.com/translate?aldtype=16047&query=%E7%AC%AC%E4%B8%80%E5%91%A8%E6%9C%9F%E6%82%A3%E8%80%85%E7%89%B9%E5%BE%81&keyfrom=baidu&smartresult=dict&lang=auto2zh - ##Treatment characteristics						
Ovarian stimulation protocol						
GnRH-a long protocol	15/121	<0.001	46/138	ns	70/237	<0.001
EFLL protocol	7/121	ns	17/138	ns	41/237	0.005
GnRH-ant protocol	30/121	ns	22/138	0.001	72/237	ns
Others	69/121	0.004	54/138	<0.001	54/237	<0.001
Gn days (days)	7.67 (4.98)	0.001	9.28 (3.30)	<0.001	9.93 (3.68)	ns
Gn dose (IU)	2126.01 (1474.67)	0.104	2367.66 (1127.77)	<0.001	2622.98 (1138.61)	0.063
Clinical outcome						
Number of OPU cycles	350		366		610	
Clinical pregnancy (n)	25		54		60	
Live birth(n)	22		40		48	
Cumulative clinical pregnancy/opu (%)	25/350 (7.14%)	0.08	54/366 (14.75%)	ns	60/610 (9.84%)	0.021
Cumulative clinical pregnancy/patient (%)	25/121 (20.66%)	0.001	54/138 (39.13%)	ns	60/237 (25.32%)	0.005
Cumulative live birth/opu (%)	22/350 (6.28%)	0.027	40/366 (10.92%)	ns	48/610 (7.88%)	ns
Cumulative live birth/patient (%)	22/121 (18.18%)	0.042	40/138 (28.98%)	ns	48/237 (20.25%)	0.054

Values are presented as number or mean (SD).

EFLL protocol, early-follicular phase long-acting GnRH agonist long protocol.

Others of ovarian stimulation protocol mean PPOS protocol, short-acting GnRH-a protocol, micro stimulation protocol, etc.

ns, non-singnificant.

TABLE 2.1 | IVF cycles' characteristics and their final reproductive outcomes of group A stratified according to IVF cycle rank.

cycle rank	1	2	3	4	5	6	7	8	9	10
Gn days	7.57 (4.90)	7.99 (3.68)	9.04 (4.86)	7.26 (4.02)	7.36 (3.64)	7.67 (3.56)	5.00 (2.65)	2.00(-)	5.50 (2.12)	–
Gn dose	2100 (1476)	2148 (1184)	2545 (1798)	1892 (1345)	1932 (1356)	1800 (1168)	1225 (943)	300(-)	1425 (954)	–
No. of patients of opu with zero oocytes/total patients of opu	121/121	16/121	13/57	3/23	2/13	2/7	0/4	0/2	0/2	–
Mean Oocytes/opu	0	2.77 (3.64)	1.80 (1.623)	1.96 (1.64)	1.77 (1.691)	1.00 (0.816)	1.33 (0.577)	1.00 (0.00)	2.00 (1.41)	–
Total of oocytes retrieved	0	316	101	45	23	7	4	2	4	–
Number Fertilizes oocytes of 2PN	0	166	55	25	12	2	2	1	1	–
Average number of 2PN fertilization/opu	0	2.07 (2.74)	1.67 (1.58)	1.56 (1.55)	1.33 (1.12)	0.67 (0.58)	1.00 (0.00)	1.00	1.00	–
Number of high quality embryos	0	43	17	7	2	1	0	0	0	–
Average number of high quality embryos/opu	0	0.57 (1.11)	0.55 (0.89)	0.44 (0.63)	0.29 (0.49)	0.33 (0.577)	–	–	–	–
Number of transferred embryos	0	53	25	8	5	2	1	1	1	–
Average number of transferred embryos/opu	0	1.77 (0.73)	1.39 (0.78)	1.60 (0.894)	1.67 (1.16)	1.00 (0.00)	1	1	1	–
total patients of opu	121	121	57	23	13	7	4	2	2	0
https://fanyi.baidu.com/translate?aldtype=16047&query=%E7%AC%AC%E4%B8%80%E5%91%A8%E6%9C%9F%E6%82%A3%E8%80%85%E7%89%B9%E5%BE%81&keyfrom=baidu&smartresult=dict&lang=auto2zh - zh/en/javascript:void(0);https://fanyi.baidu.com/translate?aldtype=16047&query=%E7%AC%AC%E4%B8%80%E5%91%A8%E6%9C%9F%E6%82%A3%E8%80%85%E7%89%B9%E5%BE%81&keyfrom=baidu&smartresult=dict&lang=auto2zh - zh/en/javascript:void(0);Number of clinical pregnancies	0	12	9	2	2	0	0	0	0	0
Number of live births	0	10	8	2	2	0	0	0	0	0
Cumulative clinical pregnancy/opu (%)	0	12/242 (4.96%)	21/299 (7.02%)	23/322 (7.14%)	25/335 (7.46%)	25/342 (7.31%)	25/346 (7.23%)	25/348 (7.18%)	25/350 (7.14%)	25/350 (7.14%)
Cumulative clinical pregnancy/patient(%)	0	12/121 (9.92%)	21/121 (17.36%)	23/121 (19.01%)	25/121 (20.66%)	25/121 (20.66%)	25/121 (20.66%)	25/121 (20.66%)	25/121 (20.66%)	25/121 (20.66%)
https://fanyi.baidu.com/translate?aldtype=16047&query=%E7%AC%AC%E4%B8%80%E5%91%A8%E6%9C%9F%E6%82%A3%E8%80%85%E7%89%B9%E5%BE%81&keyfrom=baidu&smartresult=dict&lang=auto2zh - ##Cumulative live birth/opu(%)	0/121	10/242 (2.86%)	18/299 (6.02%)	20/322 (6.21%)	22/335 (6.57%)	22/342 (6.43%)	22/346 (6.36%)	22/348 (6.32%)	22/350 (6.28%)	22/350 (6.28%)
https://fanyi.baidu.com/translate?aldtype=16047&query=%E7%AC%AC%E4%B8%80%E5%91%A8%E6%9C%9F%E6%82%A3%E8%80%85%E7%89%B9%E5%BE%81&keyfrom=baidu&smartresult=dict&lang=auto2zh - ##Cumulative live birth/patient(%)	0/121	10/121 (8.26%)	18/121 (14.88%)	20/121 (16.53%)	22/121 (18.18%)	22/121 (18.18%)	22/121 (18.18%)	22/121 (18.18%)	22/121 (18.18%)	22/121 (18.18%)

Values are presented as number or mean (SD).

The cumulative live birth rates/patient in group B was 28.98% and did not increase any more after cycle 3 (**Table 2.2** and **Figure 2**), whereas the cumulative live birth rates/patient in group C was 20.25% and reached a plateau after cycle 7 (**Table 2.3** and **Figure 2**).

Comparison Between Live Birth and Non-Live Birth Groups and Factors Influencing Live Birth

Both age (31.21 ± 4.65 *vs* 33.22 ± 5.95, *P*=0.001) and basic FSH level (9.08 ± 6.15 *vs* 11.41 ± 7.49, *P*=0.004) in the live birth group were statistically signficantly lower than those in other groups (**Table 3**). The multivariate regression analysis showed that age and basic FSH level were predict factors for live birth (ORadjusted 0.935, 95% CI 0.876-0.997, *P*=0.042; ORadjusted 0.937, 95% CI 0.878-0.999, *P*=0.046) (**Table 4**).

DISCUSSION

This study evaluated the chance of a live birth in women with no embryo transfer at their first IVF cycle attempt over their subsequent IVF treatment course and factors affecting the live birth.

In our center, the total cycle cancellation rate was nearly 10%, and the cancellation rate of the first cycle was 4.9%. This may be related to embryo transfer strategies as well as the ovarian stimulation protocols used in our hospital. For example, the cycle cancellation rate of low ovarian response with minimal stimulation was 10% while that with long protocol was 2.9% (12). A meta-analysis in 2021 showed that the cycle cancellation rate of mild stimulation was higher than that of conventional ovarian stimulation in the low ovarian response group (13). Siristatidis et al (14) also found that the

TABLE 2.2 | IVF cycles' characteristics and their final reproductive outcomes of group B stratified according to IVF cycle rank.

cycle rank	1	2	3	4	5	6	7	8	9	10
Gn days	9.28 (3.30)	8.32 (3.65)	8.91 (3.56)	6.72 (3.01)	8.14 (2.08)	7.0(1.63)	8	2	8	12
Gn dose	2367 (1127)	2242 (1154)	2369 (1194)	1633 (979)	2121 (716)	1650 (851)	2400	300	1800	3600
Total of oocytes retrieved	571	560	162	55	22	6	4	2	2	3
Mean Oocytes/opu	4.17 (5.70)	4.59 (4.81)	3.31 (3.57)	2.89 (3.70)	2.44 (2.92)	1.50 (1.00)	2	1	2	3
Number Fertilizes oocytes of 2PN	0	173	56	15	14	2	2	2	2	3
Average number of 2PN fertilization/opu	0	3.20 (3.87)	1.93 (2.99)	1.36 (1.12)	2.00 (2.71)	0.67 (0.577)	2	2	2	3
Number of high quality embryos	0	57	15	6	3	0	0	0	0	0
Average number of high quality embryos/opu	0	0.78 (1.85)	0.60 (1.96)	0.67 (1.66)	0.60 (0.89)	–	–	–	–	–
Number of transferred embryos	0	93	19	3	0	0	2	2	0	0
Average number of transferred embryos/opu	0	1.82 (0.65)	1.73 (0.65)	1.50 (1.15)	–	–	2	2	–	–
Number of no normal zygotes/opu	138	7	3	0	1	1	0	0	0	0
total patients of opu	138	138	50	22	10	4	1	1	1	1
https://fanyi.baidu.com/translate?aldtype=16047&query=%E7%AC%AC%E4%B8%80%E5%91%A8%E6%9C%9F%E6%82%A3%E8%80%85%E7%89%B9%E5%BE%81&keyfrom=baidu&smartresult=dict&lang=auto2zh - ##https://fanyi.baidu.com/translate?aldtype=16047&query=%E7%AC%AC%E4%B8%80%E5%91%A8%E6%9C%9F%E6%82%A3%E8%80%85%E7%89%B9%E5%BE%81&keyfrom=baidu&smartresult=dict&lang=auto2zh - zh/en/javascript:void(0);Number of clinical pregnancies	0	42	9	1	2	0	0	0	0	0
https://fanyi.baidu.com/translate?aldtype=16047&query=%E7%AC%AC%E4%B8%80%E5%91%A8%E6%9C%9F%E6%82%A3%E8%80%85%E7%89%B9%E5%BE%81&keyfrom=baidu&smartresult=dict&lang=auto2zh - zh/en/javascript:void(0);https://fanyi.baidu.com/translate?aldtype=16047&query=%E7%AC%AC%E4%B8%80%E5%91%A8%E6%9C%9F%E6%82%A3%E8%80%85%E7%89%B9%E5%BE%81&keyfrom=baidu&smartresult=dict&lang=auto2zh - zh/en/javascript:void(0);Number of live births	0	31	8	1	0	0	0	0	0	0
Cumulative clinical pregnancy rate/opu(%)	0	42/276 (15.22%)	51/326 (15.64%)	52/348 (14.94%)	54/358 (15.08%)	54/362 (14.92%)	54/363 (14.88%)	54/364 (14.84%)	54/365 (14.79%)	54/366 (14.75%)
Cumulative clinical pregnancy rate/patient(%)	0	42/138 (30.43%)	51/138 (36.96%)	52/138 (37.68%)	54/138 (39.13%)	54/138 (39.13%)	54/138 (39.13%)	54/138 (39.13%)	54/138 (39.13%)	54/138 (39.13%)
https://fanyi.baidu.com/translate?aldtype=16047&query=%E7%AC%AC%E4%B8%80%E5%91%A8%E6%9C%9F%E6%82%A3%E8%80%85%E7%89%B9%E5%BE%81&keyfrom=baidu&smartresult=dict&lang=auto2zh - ##Cumulative live birth rate/opu(%)	0/138	31/276 (11.23%)	39/326 (11.96%)	40/348 (11.49%)	40/358 (11.17%)	40/362 (11.05%)	40/363 (11.02%)	40/364 (10.99%)	40/365 (10.96%)	40/366 (10.92%)
https://fanyi.baidu.com/translate?aldtype=16047&query=%E7%AC%AC%E4%B8%80%E5%91%A8%E6%9C%9F%E6%82%A3%E8%80%85%E7%89%B9%E5%BE%81&keyfrom=baidu&smartresult=dict&lang=auto2zh - ##Cumulative live birth rate/patient(%)	0/138	31/138 (22.46%)	39/138 (28.26%)	40/138 (28.98%)	40/138 (28.98%)	40/138 (28.98%)	40/138 (28.98%)	40/138 (28.98%)	40/138 (28.98%)	40/138 (28.98%)

Values are presented as number or mean (SD).

cycle cancellation rate of mild stimulation was significantly higher than that of long-term and antagonist regimens (36.4% *vs* 12%). A recent study showed that participants experienced an overall feeling of "loss and loneliness" when they had no experience of embryo transfer. The situation was described as a shock unprepared for them. Their need for relevant information has not been met (15). The results of the present study showed that some data could provide these patients with some information in terms of no embryo transfer in their first IVF cycle attempt.

In the group with no egg retrieved, the proportion of the patients in the first IVF cycle cancellation was 21.54% [(121 + 50)/(496 + 298)], and 22 of these women achieved a live birth in their subsequent cycles. Furthermore, there was no significant difference in the cycle source and the mode of fertilization through analysis of the original data. In patients with no eggs being retrieved in our study, the ovarian response was low, and their average age was higher than those in the other two groups. In the end, a 18% cumulative live birth rate was achieved in these patients after the 5th IVF cycle, which was similar to that of the

TABLE 2.3 | IVF cycles' characteristics and their final reproductive outcomes of group c stratified according to IVF cycle rank.

cycle rank	1	2	3	4	5	6	7	8	9	10
Gn days	9.97 (3.63)	9.366 (2.92)	8.25 (3.80)	8.69 (4.07)	8.06 (3.51)	9.43 (4.54)	5.00 (4.24)	6.66 (5.13)	7.00 (9.90)	7.50 (0.71)
Gn dose	2621 (1136)	2427 (983)	2150 (1155)	2181 (1366)	2107 (1280)	1882 (917)	1087 (1007)	1300 (1128)	1575 (2227)	1687 (159)
Total of oocytes retrieved	1079	1367	288	68	47	17	3	4	3	4
Mean Oocytes/opu	4.55 (4.80)	5.84 (5.62)	4.57 (7.34)	2.34 (2.73)	2.94 (3.25)	1.89 (1.36)	0.60 (0.84)	1.33 (0.57)	1	2
Number Fertilizes oocytes of 2PN	374	467	144	29	17	8	2	2	2	1
Average number of 2PN fertilization/opu	1.82 (2.65)	3.16 (3.50)	3.35 (5.61)	1.53 (1.17)	1.42 (1.08)	1.14 (0.37)	–	–	–	–
Number of high quality embryos	0	42	6	3	1	1	0	0	0	0
Average number of high quality embryos/opu	0	0.45 (1.06)	0.26 (0.54)	0.33 (0.50)	0.14 (0.38)	0.20 (0.447)		0	–	
Number of transferred embryos	0	79	17	4	4	2	1	–	–	–
Average number of transferred embryos/transplantation cycle	0	1.68 (0.63)	1.89 (0.61)	2	2	2	–	–	–	–
No transplantable embryo/opu	237	38	11	3	3	3	2	2	1	2
total patients of opu	237	237	67	30	16	10	5	3	3	2
https://fanyi.baidu.com/translate?aldtype=16047&query=%E7%AC%AC%E4%B8%80%E5%91%A8%E6%9C%9F%E6%82%A3%E8%80%85%E7%89%B9%E5%BE%81&keyfrom=baidu&smartresult=dict&lang=auto2zh - zh/en/javascript:void(0);https://fanyi.baidu.com/translate?aldtype=16047&query=%E7%AC%AC%E4%B8%80%E5%91%A8%E6%9C%9F%E6%82%A3%E8%80%85%E7%89%B9%E5%BE%81&keyfrom=baidu&smartresult=dict&lang=auto2zh - zh/en/javascript:void(0);Number of clinical pregnancies	0	41	6	7	4	1	1	0	0	0
https://fanyi.baidu.com/translate?aldtype=16047&query=%E7%AC%AC%E4%B8%80%E5%91%A8%E6%9C%9F%E6%82%A3%E8%80%85%E7%89%B9%E5%BE%81&keyfrom=baidu&smartresult=dict&lang=auto2zh - ##https://fanyi.baidu.com/translate?aldtype=16047&query=%E7%AC%AC%E4%B8%80%E5%91%A8%E6%9C%9F%E6%82%A3%E8%80%85%E7%89%B9%E5%BE%81&keyfrom=baidu&smartresult=dict&lang=auto2zh - zh/en/javascript:void(0);Number of live births	0	31	6	6	3	1	1	0	0	0
Cumulative clinical pregnancy rate/opu(%)	0	41/474 (8.65%)	47/541 (8.69%)	54/571 (9.46%)	58/587 (9.88%)	59/587 (10.05%)	60/602 (9.97%)	60/605 (9.92%)	60/608 (9.87%)	60/610 (9.84%)
Cumulative clinical pregnancy rate/patient(%)	0	41/237 (17.29%)	47/237 (19.83%)	54/237 (22.78%)	58/237 (24.47%)	59/237 (24.89%)	60/237 (25.32%)	60/237 (25.32%)	60/237 (25.32%)	60/237 (25.32%)
https://fanyi.baidu.com/translate?aldtype=16047&query=%E7%AC%AC%E4%B8%80%E5%91%A8%E6%9C%9F%E6%82%A3%E8%80%85%E7%89%B9%E5%BE%81&keyfrom=baidu&smartresult=dict&lang=auto2zh - ##Cumulative live birth rate/opu(%)	0/237	31/474 (6.54%)	37/541 (6.84%)	43/571 (7.54%)	46/587 (7.85%)	47/597 (7.89%)	48/602 (7.99%)	48/605 (7.95%)	48/608 (7.91%)	48/610 (7.88%)
https://fanyi.baidu.com/translate?aldtype=16047&query=%E7%AC%AC%E4%B8%80%E5%91%A8%E6%9C%9F%E6%82%A3%E8%80%85%E7%89%B9%E5%BE%81&keyfrom=baidu&smartresult=dict&lang=auto2zh - ##Cumulative live birth rate/patient(%)	0/237	31/237 13.08%	37/237 15.61%	43/237 18.14%	46/237 19.41%	47/237 19.83%	48/237 20.25%	48/237 20.25%	48/237 20.25%	48/237 20.25%

Values are presented as number or mean (SD).

study by Raoul Orvieto et al. (16). For these patients, the reproductive outcome will not change after the 5th IVF OPU cycle being tried, and the next ovulation stimulation cycle is suggested to be abandoned. Nonetheless, the patient's own decision should always be respected.

The proportion of women with no normal zygotes formed in the first IVF cycle cancellation was 23.43% [(138 + 48)/(496 + 298)], and 40 of the 138 patients achieved a live birth eventually. In our hospital, when the number of eggs retrieved was less than or equal to 3, ICSI was not rescued. The majority of these patients had fewer eggs retrieved, which might be one reason for fertilization failure. Even though there was no significant difference in the fertilization methods (IVF *vs* ICSI) in the live birth cycle (9.46%*vs*13.27%), 54 cases were changed to ICSI after the first cycle of IVF, and 13 cases obtained a live birth, with the live birth rate of 24.07%. According to these outcomes, changing the mode of insemination in the second cycle may bring a better outcome. Some scholars (17) found that compared with the hCG single trigger group, the oocyte fertilization rate (73.1% *vs* 58.6%), clinical pregnancy rate (33% *vs* 20.7%), live birth rate

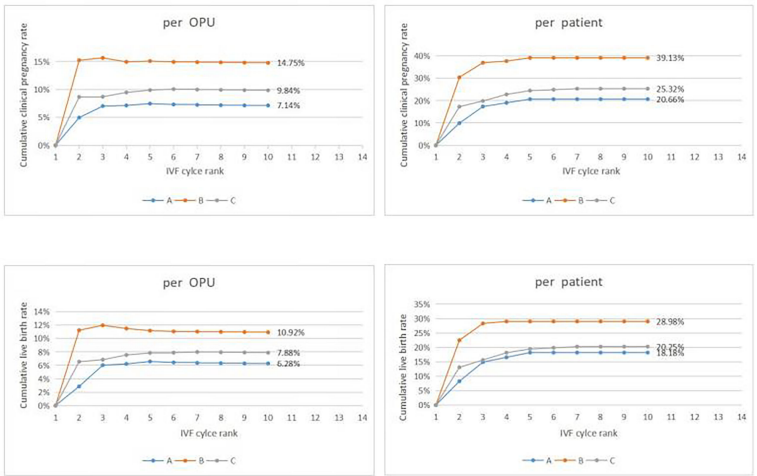

FIGURE 2 | Cumulative clinical outcomes at cycle rank. In group A, The cumulative clinical pregnancy rates were 7.14% per OPU and 20.66% per patient, and the cumulative live birth rates were 6.28% per OPU and 18.18% per patient, with both rates reaching a plateau at the 5th OPU cycle. The cumulative live birth rate/patient in group B was 28.98%, which did not increase any more after cycle 3, whereas the cumulative live birth rates/patient in group C was 20.25% and reached a plateau after cycle 7.

(26.9% *vs* 14.5%), abortion rate (17.4% *vs* 37.0%), and embryo transfer elimination rate (6.1% *vs* 15.4%) in the double trigger group were significantly different. This may suggest that changing the trigger scheme, grasping the correct trigger time so as to get the target follicles as far as possible, and getting the MII (mature) eggs may improve the pregnancy outcomes. Furthermore, some patients may improve the clinical outcomes by using some new techniques like AOA (assisted oocyte activation), IVM (*in vitro* maturation), and testing for associated genes. A retrospective study (18) showed that AOA intervention after ICSI fertilization failure significantly increased the normal fertilization rate (52.1%), the cumulative clinical pregnancy rate (47.1%) and the live birth rate (29.4%).

The proportion of patients with the cancellation cycle caused by poor embryo quality in the first IVF cycle was 55.04% [(237 + 200)/(496 + 298)]. These patients are more challenging for the

TABLE 3 | Basic characteristics of the first cycle in live birth group and non-live birth group.

	Live birth group	non live birth group	p
Proportion of patients			0.06
Group A	22	99	
Group B	40	98	
Group C	48	189	
Age (years)	31.21 (4.65)	33.22 (5.95)	0.001
BMI (kg/m2)	23.36 (3.55)	23.51 (4.14)	ns
FSH/mIU	9.08 (6.15)	11.41 (7.49)	0.004
LH/mIU	5.43 (4.05)	7.02 (3.72	ns
Infertility years	4.05 (3.24)	4.37 (3.62)	ns
AMH (ng/ml)	1.71 (2.91)	1.06 (1.18)	ns
Infertility type			ns
Primary infertility	65	219	
Secondary infertility	45	167	
Ovarian stimulation protocol			ns
GnRH-a long protocol	35	96	
EFLL protocol	20	45	
GnRH-ant protocol	21	103	
others	34	142	
Gn days (days)	10.05 (3.98)	8.99 (3.95)	0.01
Gn dose (IU)	2464 (1121)	2428 (1265)	ns

Values are presented as number or mean (SD).
EFLL protocol, early-follicular phase long-acting GnRH agonist long protocol.
Others of ovarian stimulation protocol mean PPOS protocol, short-acting GnRH-a protocol, micro stimulation protocol, etc.
ns, non-singnificant.

TABLE 4 | Multivariate regression analysis of IVF cycle between the live birth group and non-live birth group.

	Live birth group	non live birth group	*P*	OR value (95%CI)	*p*	OR adjusted value(95% CI)
Number of cycles	110	1216				
Cycle outcome type						
Not transplanted	0	785	–	–	–	–
Fresh cycle transplantation	65	227	–	–	–	–
https://fanyi.baidu.com/translate?aldtype=16047&query=%E7%AC%AC%E4%B8%80%E5%91%A8%E6%9C%9F%E6%82%A3%E8%80%85%E7%89%B9%E5%BE%81&keyfrom=baidu&smartresult=dict&lang=auto2zh - ##Thawed embryo transfer from Whole embryo freezing	45	204	–	–	–	–
Fertilization mode						
No insemination	0	217	–	–	–	–
IVF	65	664	–	–	–	–
ICSI	45	335	–	–	–	–
Patient first cycle type						
Type A	22	328		1		1
Type B	40	326	0.388	1.28 (0.726,2.28)	0.189	0.438 (0.128,1.500)
Type C	48	562	0.272	1.33 (0.80,2.21)	0.091	3.174 (0.884,5.345)
age	31.21 (4.65)	33.22 (5.95))	0.04	0.956 (0.916, 0.998)	0.042	0.935 (0.876,0.997)
BMI	23.36 (3.55)	23.51 (4.14)	ns	0.984 (0.928, 1.043)	ns	1.030 (0.965,1.100)
FSH	9.08 (6.15)	11.41 (7.49)	0.032	0.953 (0.911, 0.996)	0.046	0.937 (0.878,0.999)
LH	5.43 (4.05)	7.02 (37.22)	ns	0.999 (0.994, 1.005)	ns	1.000 (0.996,1.004)
Gn days	10.05 (3.98)	8.99 (3.95)	ns	1.067 (0.964, 1.181)	ns	1.073 (0.984,1.171)
Gn dose	2464 (1122)	2428 (1265)	ns	1	ns	1

Values are presented as number or mean (SD), the OR (odds ratio) value and 95% CI (confidence interval), and OR adjusted value (95% CI) are obtained by adjusting the male factor, ovarian stimulation program and other confounding factors.
ns, non-singnificant.

ART. In our study, these patients' age was not high, they had more eggs, but the CLBR was low. In the ovulation induction of these patients, 25 cases with the antagonist regimen obtained a live birth, whereas 23 cases with other protocols did not. It seems that the antagonist regimen had a trend of increasing the live birth rate, but no significant difference was found in our study (10.25% *vs* 6.28%, P =0.07). Similarly, the fertilization mode of the live birth cycle was not signfiicantly different. Moreover, although no differences were found in various infertility factors among these patients in our study, a recent study (19) reported that AOA could improve the clinical pregnancy and live birth rate in patients with male factors (oligoasthenospermia [OAT]), advanced age, polycystic ovary syndrome (PCOS), and unexplained infertility. In current literature, blastocyst transfer after ICSI-AOA according to different infertility factors may help to improve the clinical outcome of these patients. Besides, shortening the embryo culture time to the first or second day and carrying out gamete transfer or zygote transfer may be a goodway to improve the reproductive outcome of patients with embryonic development block from the embryologists' point of view.

Female age and ovarian reserve are still the main factors influencing the live birth of patients with first IVF cycle cancellation. However, clinical quality control, personalized treatment, or changes in ovulation induction and fertilization mode may help them achieve a live birth. Therefore, for patients with good financial resources, the findings of the present study suggest extending the number of OPU cycles up to the 3rd, 5th, or 7th cycle even if the reasons for cancellation of the first IVF cycle are different.

Some limitations existed in this study, including the retrospective and one-center design, a small cohort of patients, and Chinese patients enrolled only. Moreover, the reasons for patient cycle cancellation are multifarious and complex, and patients with non-fertilization, fertilization failure and abnormal fertilization might have been assigned to one group for analysis, which limits the ability to control for potential unknown confounding factors. All these factors may affect the

generalization of the outcome of this study. Future studies will have to resolve all these issues for better outcomes.

In conclusion, future clinical outcomes may be better in women with no normal zygotes than those with no oocyte retrieved or no available embryo at their first IVF cycle attempts. The main factors influencing the live birth are age and ovarian reserve.

DATA AVAILABILITY STATEMENT

The raw data supporting the conclusions of this article will be made available by the authors without undue reservation.

ETHICS STATEMENT

The studies involving human participants were reviewed and approved by Ethics Committee of The Second Hospital of Hebei Medical University. The patients/participants provided their written informed consent to participate in this study.

AUTHOR CONTRIBUTIONS

Study design: ZZ and GH. Data collection: XZ, MC, ZY, and PL. Data analysis: XZ and MC. Supervision: YX. Writing the original article: MC. Revision: ZZ. All authors contributed to the article and approved the submitted version.

FUNDING

This study was supported by S&T Program of Hebei (22377742D), Natural Science Foundation of Hebei Province(Beijing-Tianjin-Hebei Cooperation Special Project) (H2019206712).

REFERENCES

1. Drakopoulos P, Blockeel C, Stoop D, Camus M, de Vos M, Tournaye H, et al. Conventional Ovarian Stimulation and Single Embryo Transfer for IVF/ICSI. How Many Oocytes do We Need to Maximize Cumulative Live Birth Rates After Utilization of All Fresh and Frozen Embryos. *Hum Reprod* (2016) 31 (2):370–6. doi: 10.1093/humrep/dev316
2. Polyzos NP, Drakopoulos P, Parra J, Pellicer A, Santos-Ribeiro S, Tournaye H, et al. Cumulative Live Birth Rates According to the Number of Oocytes Retrieved After the First Ovarian Stimulation for *In Vitro* Fertilization/ Intracytoplasmic Sperm Injection: A Multicenter Multinational Analysis Including 15,000 Women. *Fertil Steril* (2018) 110(4):661–70. doi: 10.1016/ j.fertnstert.2018.04.039
3. Sunkara SK, Rittenberg V, Raine-Fenning N, Bhattacharya S, Zamora J, Coomarasamy A, et al. Association Between the Number of Eggs and Live Birth in IVF Treatment: An Analysis of 400135 Treatment Cycles. *Hum Reprod* (2011) 26(7):1768–74. doi: 10.1093/humrep/der106
4. Humaidan P, Chin W, Rogoff D, D'Hooghe T, Longobardi S, Hubbard J, et al. ESPART Study Investigators. Efficacy and Safety of Follitropin Alfa/ Lutropin Alfa in ART: A Randomized Controlled Trial in Poor Ovarian Responders. *Hum Reprod* (2017) 32(3):544–55. doi: 10.1093/humrep/ dew360
5. Giovanale V, Pulcinelli FM, Ralli E, Primiero FM, Caserta D. Poor Responders in IVF: An Update in Therapy. *Gynecol Endocrinol* (2015) 31 (4):253–7. doi: 10.3109/09513590.2014.987228
6. Troude P, Guibert J, Bouyer J, de la Rochebrochard EDAIFI Group. Medical Factors Associated With Early IVF Discontinuation. *Reprod Biomed Online* (2014) 28(3):321–9. doi: 10.1016/j.rbmo.2013.10.018
7. Olivius C, Friden B, Borg G, Bergh C. Psychological Aspects of Discontinuation of *In Vitro* Fertilization Treatment. *Fertil Steril* (2004) 81 (2):276. doi: 10.1016/j.fertnstert.2003.09.026
8. Smeenk JM, Verhaak CM, Braat DD. Psychological Interference in *In Vitro* Fertilization Treatment. *Fertil Steril* (2004) 81(2):277. doi: 10.1016/ j.fertnstert.2003.09.025
9. Gameiro S, Boivin J, Peronace L, Verhaak CM. Why do Patients Discontinue Fertility Treatment? A Systematic Review of Reasons and Predictors of Discontinuation in Fertility Treatment. *Hum Reprod Update* (2012) 18 (6):652–69. doi: 10.1093/humupd/dms031
10. Domar AD, Rooney K, Hacker MR, Sakkas D, Dodge LE. Burden of Care is the Primary Reason Why Insured Women Terminate *In Vitro* Fertilization Treatment. *Fertil Steril* (2018) 109(6):1121–6. doi: 10.1016/j.fertnstert. 2018.02.130
11. Alpha scientists in reproductive medicine and ESHRE special interest group of embryology. The Istanbul Consensus Workshop on Embryo Assessment: Proceedings of an Expert Meeting. *Hum Reprod* (2011) 26(6):1270–83. doi: 10.1093/humrep/der037
12. Baka S, Makrakis E, Tzanakaki D, Konidaris S, Hassiakos D, Moustakarias T, et al. Poor Responders in IVF: Cancellation of a First Cycle is Not Predictive of a Subsequent Failure. *Ann N Y Acad Sci* (2006) 1092:418–25. doi: 10.1196/ annals.1365.040
13. Datta AK, Maheshwari A, Felix N, Campbell S, Nargund G. Mild Versus Conventional Ovarian Stimulation for IVF in Poor, Normal and Hyper-Responders: A Systematic Review and Meta-Analysis. *Hum Reprod Update* (2021) 27(2):229–53. doi: 10.1093/humupd/dmaa035
14. Siristatidis C, Salamalekis G, Dafopoulos K, Basios G, Vogiatzi P, Papantoniou N. Mild Versus Conventional Ovarian Stimulation for Poor Responders Undergoing IVF/ICSI. *In Vivo (Athens Greece)* (2017) 31(2):231–7. doi: 10.21873/invivo.11050
15. Holter H, Bergh C, Gejervall AL. Lost and Lonely: A Qualitative Study of Women's Experiences of No Embryo Transfer Owing to non-Fertilization or Poor Embryo Quality. *Hum Reprod Open* (2021) 19(1):hoaa062. doi: 10.1093/hropen/hoaa062
16. Orvieto R, Farhi J, Nahum R, Basch S, Haas J, Aizer A. Future Fertility of Patients With Zero Oocytes Yield in Their First IVF Cycle Attempt. *PloS One* (2021) 16(2):e0246889. doi: 10.1371/journal.pone.0246889
17. Lin MH, Wu FS, Hwu YM, Lee RK, Li RS, Li SH. Dual Trigger With Gonadotropin Releasing Hormone Agonist and Human Chorionic Gonadotropin Significantly Improves Live Birth Rate for Women With Diminished Ovarian Reserve. *Reprod Biol Endocrinol* (2019) 17(1):7. doi: 10.1186/s12958-018-0451-x
18. Lam KKW, Wong JYY, Cheung TM, Li RHW, Ng EHY, Yeung WSB. A Retrospective Analysis of Artificial Oocyte Activation in Patients With Low or No Fertilisation in Intracytoplasmic Sperm Injection Cycles. *J Obstet Gynaecol* (2021) 12:1–6. doi: 10.1080/01443615.2021.1922878
19. Lv M, Zhang D, He X, Chen B, Li Q, Ding D, et al. Artificial Oocyte Activation to Improve Reproductive Outcomes in Couples With Various Causes of Infertility: A Retrospective Cohort Study. *Reprod BioMed Online* (2020) 40 (4):501–9. doi: 10.1016/j.rbmo.2020.01.001

Conflict of Interest: The authors declare that the research was conducted in the absence of any commercial or financial relationships that could be construed as a potential conflict of interest.

this article, or claim that may be made by its manufacturer, is not guaranteed or endorsed by the publisher.

frontiers | Frontiers in Endocrinology

TYPE Original Research
PUBLISHED 29 July 2022
DOI 10.3389/fendo.2022.936765

OPEN ACCESS

EDITED BY
Yuting Fan,
Boston IVF, United States

REVIEWED BY
Tianren Wang,
Shenzhen Hospital, The University of Hong Kong, China
Ariella Shikanov,
University of Michigan, United States
Tzeng Chii Ruey,
Taipei Medical University, Taiwan

*CORRESPONDENCE
Susana M. Chuva De Sousa Lopes
lopes@lumc.nl

SPECIALTY SECTION
This article was submitted to Reproduction, a section of the journal Frontiers in Endocrinology

RECEIVED 05 May 2022
ACCEPTED 05 July 2022
PUBLISHED 29 July 2022

CITATION
Del Valle JS, Mancini V, Laverde Garay M, Asseler JD, Fan X, Metzemaekers J, Louwe LA, Pilgram GSK, Westerlaken LAJvd, van Mello NM and Chuva de Sousa Lopes SM (2022) Dynamic *in vitro* culture of cryopreserved-thawed human ovarian cortical tissue using a microfluidics platform does not improve early folliculogenesis. *Front. Endocrinol.* 13:936765. doi: 10.3389/fendo.2022.936765

Dynamic *in vitro* culture of cryopreserved-thawed human ovarian cortical tissue using a microfluidics platform does not improve early folliculogenesis

Julieta S. Del Valle[1], Vanessa Mancini[1], Maitane Laverde Garay[1], Joyce D. Asseler[2], Xueying Fan[1], Jeroen Metzemaekers[3], Leoni A. Louwe[3], Gonneke S. K. Pilgram[3], Lucette A. J. van der Westerlaken[3], Norah M. van Mello[2] and Susana M. Chuva De Sousa Lopes[1,4]*

[1]Department of Anatomy and Embryology, Leiden University Medical Center, Leiden, Netherlands, [2]Department of Obstetrics and Gynaecology, Amsterdam University Medical Center (UMC), Amsterdam, Netherlands, [3]Department of Gynaecology, Leiden University Medical Center, Leiden, Netherlands, [4]Ghent-Fertility and Stem Cell Team (G-FAST), Department of Reproductive Medicine, Ghent University Hospital, Ghent, Belgium

Current strategies for fertility preservation include the cryopreservation of embryos, mature oocytes or ovarian cortical tissue for autologous transplantation. However, not all patients that could benefit from fertility preservation can use the currently available technology. In this regard, obtaining functional mature oocytes from ovarian cortical tissue *in vitro* would represent a major breakthrough in fertility preservation as well as in human medically assisted reproduction. In this study, we have used a microfluidics platform to culture cryopreserved-thawed human cortical tissue for a period of 8 days and evaluated the effect of two different flow rates in follicular activation and growth. The results showed that this dynamic system supported follicular development up to the secondary stage within 8 days, albeit with low efficiency. Surprisingly, the stromal cells in the ovarian cortical tissue were highly sensitive to flow and showed high levels of apoptosis when cultured under high flow rate. Moreover, after 8 days in culture, the stromal compartment showed increase levels of collagen deposition, in particular in static culture. Although microfluidics dynamic platforms have great potential to simulate tissue-level physiology, this system still needs optimization to meet the requirements for an efficient *in vitro* early follicular growth.

KEYWORDS

folliculogenesis, human, follicular growth, microfluidics, ovarian cortical tissue, cryopreservation, secondary follicle, fertility preservation

Introduction

According to the World Health Organization (WHO), infertility is a global disease affecting more than 186 million people mainly from developed countries (https://www.who.int/news-room/fact-sheets/detail/infertility). While infertility is often associated with defects in the male or female reproductive systems, it may also result from other factors such as lifestyle, stress or the progressively older age of the female partner at conception (1). In the last decades, innovative techniques in medically assisted reproduction, such as *in vitro* fertilization, have helped an increasingly large group of patients to overcome infertility (2). For patients exposed to either gonadotoxic treatment, predisposed to premature ovarian insufficiency or undergoing surgical removal of both ovaries, there are several options for fertility preservation, that include the cryopreservation of mature oocytes to be used during medically assisted reproduction, or ovarian tissue cryopreservation for autografting (3, 4). However, for patients such as pre-pubertal oncological patients with hematological malignancies, none of the currently available strategies are adequate due to the absence of mature oocytes and the high risk of reintroducing cancer cells after autografting (5–7). For this growing group of patients, that undergoes ovarian tissue cryopreservation to preserve the ovarian follicular reserve and survives to adulthood, obtaining mature oocytes from cortical ovarian tissue cultured *in vitro*, could be considered a safe alternative method in the context of fertility preservation (8).

In humans, folliculogenesis is a complex process that starts with the formation of primordial follicles before birth (9). After birth, small groups of primordial follicles, formed by one primary oocyte arrested in dictyate (diplotene stage from meiotic prophase I) surrounded by a single layer of flat granulosa cells and a layer of basement membrane, undergo follicular activation, as the granulosa cell layer adopts a cuboidal morphology and the primordial follicle transits to primary follicle (10, 11). During follicular growth, the cuboidal granulosa cells undergo proliferation, forming several cell layers around the oocyte (secondary follicle) and start accumulating follicular fluid in a growing central cavity or antrum (antral follicle). In mono-ovulatory species such as humans, typically one antral follicle becomes dominant, growing from 5 up to 20 millimeters in diameter and undergoing ovulation (12–14), whereas the other antral follicles regress through atresia (15). In the ovulatory follicle, the oocyte resumes meiosis and arrests in metaphase II, the competent stage for fertilization. It is only after fertilization that the oocyte completes meiosis with the extrusion of the second polar body. During adulthood, the process from follicular activation until ovulation requires several months (16, 17).

The development of robust clinically-applicable protocols remains challenging despite ongoing efforts to culture cryopreserved (or fresh) ovarian cortical tissue *in vitro* through *in vitro* follicular activation, *in vitro* follicular growth and oocyte *in vitro* maturation to ultimately obtain mature oocytes (metaphase II) that could be fertilized (18). One of the main reasons for this is the lack of knowledge regarding the control mechanisms that regulate follicular activation and growth (19) due to the relative rarity of healthy human ovarian tissue available for scientific research. Several studies have reported the formation of antral follicles *in vitro* from cultured pre-antral/secondary follicles present in human ovarian cortical tissue (20–24). However, the follicular population that shows the highest survival rate after cryopreservation and thawing procedures are the primordial follicles (25). To date, only two groups have reported the growth and maturation to metaphase II oocytes starting from unilaminar (primordial/primary) follicles present in fresh human ovarian cortical tissue, by using a multistep static culture system (26, 27), but attempts to fertilize such obtained metaphase II oocytes have not been reported.

The traditional static ovarian culture system is a robust and simple system that mimics the complexity of physiological conditions only to a limited extend. This system allows the accumulation in the culture media of compounds released by the tissue that may act as paracrine signals for cell growth and survival. However, due to follicular growth, the culture media needs to be replaced with some frequency to provide the cells with fresh nutrients and remove waste products. This manipulation disturbs the medium composition and consequently the cellular state. Dynamic culture systems using microwells have the possibility of culturing tissue in a small volume, where the concentration of paracrine factors can reach high values, while making use of a large reservoir of circulating medium and adjustable flow rates that allow a continuous supply of nutrients.

Innovative organ-on-chip models, microfluidic platforms and engineered culture systems are increasing in complexity to recreate the physiological conditions of the reproductive system and stimulate follicular growth and maturation (28, 29). One example of these advanced culture systems is the microfluidics platform EVATAR, whereby several organ modules (ovary, fallopian tube, uterus, cervix and liver) were connected by circulating flow between the organ modules (30). Another example is the transwell-based system that was used to co-culture human fallopian tube epithelium and murine ovarian follicles in two different compartments (31). These innovative tissue culture systems to improve folliculogenesis *in vitro* have shown promising results, but have so far only been used with mouse follicles. Hence, the application of engineered systems to follicles present in cryopreserved-thawed human cortical tissue is urgently needed.

Using a microfluidics platform, our study aims to investigate the effects of dynamic culture conditions on human ovarian cortex to stimulate follicular activation and growth *in vitro*.

10.3389/fendo.2022.936765

Cryopreserved-thawed ovarian cortical tissue was cultured in a microfluidic chip in static and dynamic conditions using two different flow rates and the quantity and quality of secondary follicles was investigated after four and eight days in culture. The culture period used was based on the multistep static culture system developed by McLaughlin and colleagues (26), where secondary follicles could be obtained from unilaminar follicles present in human ovarian cortex *in vitro* within 8 days (Step I).

Materials and methods

Ethics and patient characteristics

The study was conducted according to the guidelines of the Declaration of Helsinki. The study design was submitted to the Medical Ethical Committee of the LUMC and a letter of no objection was obtained (B18.029) prior to the study. Signed informed consent was obtained from the tissue donors (N=13) undergoing gender-affirming surgery at the VUmc hospital (Amsterdam, Netherlands) and at the Amstelland hospital (Amsterdam, Netherlands). Patient characteristics, such as age, gender-affirming hormone treatment (testosterone-based) and treatment duration prior to gender-affirming surgery are provided in Table S1.

Ovarian cortex isolation, cryopreservation and thawing

Ovaries were processed and cryopreserved using a slow freezing method as described (32). Briefly, the ovaries were bisected and placed 0.9% NaCl solution (B230551, Fresenius Kabi, France). The outer cortex, with a thickness of about 1mm, was separated from the inner cortex and medulla using scalpels (0508, Swann-Morton, UK) and was cut into smaller pieces of 10mm x 5mm. Thereafter, individual ovarian cortex pieces were put into cryovials (126263, Greiner, Netherlands) containing 1ml of cryoprotectant solution [0.1M sucrose (S9378-1KG, Sigma Chemicals, Netherlands) and 1.5M ethylene glycol (102466, Sigma Chemicals, Netherlands) in phosphate-buffered saline (PBS) (14190094, Merck, Germany)]. The tissue was left in the cryoprotectant solution for 30 minutes (min) before starting the slow freezing program performed by a programmable Planer freezer (GDMRV, PLANNER, UK). The freezing protocol applied was the following: 2°C/min to −9°C, 5min of soaking, manual seeding for ice crystal nucleation induction using a cotton swab dipped into liquid nitrogen, 0.3°C/min to −40°C, 10°C/min to −140°C and the cryovials were placed into liquid nitrogen (−196°C) containers for storage.

For thawing, the cryovials were kept in a water bath at 37°C until the medium around the frozen tissue had thawed (3-5min). To remove the cryoprotectant solution, the tissue was washed for 10min at room temperature (RT) with occasional shaking in a solution of 0.75M ethylene glycol and 0.25M sucrose in PBS, followed by a 10min wash in 0.35M sucrose in PBS, and finally a 10min wash in PBS.

Ovarian cortex culture

Thawed cortical ovarian tissue pieces (N=6 donors) were cut into 1mm × 1mm × 1mm cubes using scalpels in PBS. After thawing (day 0), the cortical cubes were either fixed (n=8-15) or placed in microwells (n=12, 2 cubes per well) from a µ-slide III 3D perfusion plates (80376, Ibidi GmbH, Gräfelfing, Germany) for *in vitro* culture. After closing the open microwells using an adhesive coverslip, the microchannels were filled with culture medium using a 1ml syringe (303172, Dalsup BD, Netherlands) through the inlet ports of the slides (each inlet port is connected to 2 microwells of 30µl volume). The culture medium used was McCoy's 5a with bicarbonate and 20mM HEPES (22330021, Invitrogen, Paisley, UK) supplemented with 3mM glutamine (25030-024, Invitrogen, Paisley, UK), 0.5% human serum albumin (C1309/490, Alburex20, CSL Behring, UK), 1x penicillin and streptomycin (P4458-100ML, Sigma Chemicals, Netherlands), 0.1% amphotericin B (A2942-20ML, Sigma Chemicals, Netherlands), 1x Insulin-Transferrin-Selenium-Ethanolamine (ITS -X) (51500-056, Invitrogen, Paisley, UK) and 50µg/ml ascorbic acid (A8960, Sigma Chemicals, Netherlands) adapted from McLaughlin and colleagues (McLaughlin et al., 2018). For the first 24 hours, 12µM sphingosine-1-phosphate (S1P) (860492P-1MG, Merk, Netherlands) was added to the media to promote follicular growth (33). Fragments were cultured for four or eight days at 37°C in humidified air and 5% CO_2.

During static culture, the media was replaced every 2 days by adding 70µl of fresh media through each inlet (connected to 2 microwells in series). In the dynamic culture, each plate was connected to a Ibidi pump system (Ibidi, GmbH, Gräfelfing, Germany). The characteristics of the perfusion set were: tubing with 15cm length and 0.8mm internal diameter (ID) to provide a high flow rate (0.5ml/min) and tubing with 50cm length and 0.5mm ID to provide a low flow rate (0.1ml/min). The fluidic unit was assembled in the hood, transferred to an incubator and connected to the pump system. Up to four fluidic units were connected to the pump in the same experiment. Each unit had two 10ml reservoirs and, for each experiment, 5ml of media was added to each reservoir before starting the experiment.

Fresh ovarian cortex pieces (N=3 donors) were cut into 1mm × 1mm × 1mm cubes using scalpels in PBS and cultured in static condition in 12-well plates (Thermo Fisher Scientific) (n=12 cubes per well) in 500µl culture medium (as above) with or without 1ng/ml recombinant follicle-stimulating hormone (FSH) (F4021-2µg, Sigma Chemicals, Netherlands).

10.3389/fendo.2022.936765

Half of the medium was replaced every 2 days. Fragments were cultured for 8 days at 37°C in humidified air and 5% CO_2.

Histochemistry, immunofluorescence and TUNEL assay

Freshly collected ovaries as well as fresh or cryopreserved-thawed ovarian cortex tissue samples collected on day 0, day 4, or day 8 after culture were fixed in 4% paraformaldehyde (Merck, Germany) in PBS overnight at 4°C. Thereafter, the tissue was washed overnight in PBS, transferred to 70% ethanol and embedded in paraffin using a Shandon Excelsior tissue processor (Thermo Scientific, Altrincham, UK). After embedding, the tissue was sectioned (5µm) using an RM2065 microtome (Leica Instruments GmbH, Wetzlar, Germany) and the sections stretched onto StarFrost microscope slides (3057-1, Waldemar Knittel, Germany). Hematoxylin and eosin (HE) staining on paraffin sections was performed as previously described (Heeren et al., 2015).

For immunofluorescence, the sections were deparaffinized and treated with Tris–EDTA buffer (10mM Tris, 1 mM EDTA solution, pH 9.0) for 12min at 98°C in a microwave (TissueWave 2, Thermo Scientific). The sections were allowed to cool down, rinsed with PBS (2 × 5min) and 0.05% Tween-20 (822184, Merck, Germany) in PBS (PBST) (5min) and blocked 1 hour with 1% bovine serum albumin (BSA) (A8022-100G, Life Technologies, USA) in PBST at RT in a humidified chamber. After blocking, the primary antibodies diluted in blocking buffer were added and the slides were incubated overnight at 4°C. Subsequently, the slides were rinsed with PBS (2 × 5min) and PBST (5min) and incubated 1 hour with the secondary antibodies diluted in blocking buffer at RT. Next, the slides were rinsed with PBS (2 × 2min), PBST (2min), distilled water (2min) and mounted with Pro-Long Gold (P36930, Life Technologies, USA). Negative controls were obtained by omitting the primary antibodies.

The primary antibodies used were goat anti-FOXL2 (1:200, NB100-1277, Bio-Techne), mouse anti-AMH (1:30, MCA2246, R&D system), rabbit anti-KRT19 (1:100, ab76539, Abcam), rabbit anti-COLIV (1:50, AB748, Abcam) and mouse anti-PCNA (1:100, sc-56, Bio-connect). The secondary antibodies used were Alexa Fluor 488 donkey anti-rabbit IgG (1:500, A21206, Life Technologies), Alexa Fluor 647 donkey anti-goat IgG (1:500, A-21447, Life Technologies) and Alexa Fluor 594 donkey anti-mouse IgG (1:500, A21203, Life Technologies). TUNEL-assay was performed using the *In Situ* Cell Detection Kit FITC (11684817910, Roche, Germany) according to manufacturer's instructions. The nuclei were stained with 4′,6-diamidino-2-phenyl-indole (DAPI) (1:1000, D1306, Life Technologies, USA) and sections were mounted using Pro-Long Gold.

Imaging and quantification

Confocal fluorescence images were obtained on a TC SP8 inverted confocal microscope (Leica, Wetzlar, Germany), using a ×40 oil immersion objective and LAS X software (Leica, Wetzlar, Germany), and color adjustments were performed using Fiji (34).

The HE-stained slides were scanned using a Panoramic 250 digital scanner (3DHISTECH Ltd., Budapest, Hungary) and viewed using CaseViewer software (3DHISTECH Ltd., Budapest, Hungary). For the quantification of the follicles, the total number of follicles present in 8 different HE-stained sections, apart 40µm to prevent double-counting, per cortical ovarian cube were counted and pooled per culture condition. To overcome intrinsic differences in follicular number between ovarian cubes, we have summed the number of follicles per cube per donor. In addition, to reduce the variation between donors, instead of comparing the total number of follicles per donor, we have compared the percentage of follicular types present in all cubes per donor and provided the mean percentage between the donors per condition.

The criteria to classify the different follicular stages was: primordial follicles had a single layer of flat granulosa cells; transitional/primary follicles were unilaminar, but contained at least some cuboidal granulosa cells; secondary follicles had at least two layers of granulosa cells and no antrum; antral follicles had five or more layers of surrounding granulosa cells and an antral cavity. Atretic follicles were follicles that contained pyknotic nuclei in the oocyte and granulosa cells, and presented oocyte shrinkage with red-coloration in HE and/or cell detachment from the basement membrane. Early atretic follicles were unilaminar and secondary atretic follicles presented multiple layers of granulosa cells.

To measure the relative fluorescence intensity of TUNEL and COLIV, arbitrary images essentially containing stromal compartment and no secondary follicles per condition (N=6 images from three different donors) were taken using a TC SP8 inverted confocal microscope (Leica) with ×40 oil immersion objective. The fluorescence intensity signal from TUNEL, COLIV and DAPI were measured using Fiji software. The corrected total cell fluorescence (CTCF) was calculated by measuring TUNEL or COLIV fluorescence signal on the whole image area and normalized against the fluorescence intensity signal from DAPI present in the same image.

Statistical analysis

The results, presented as mean ± standard deviation or mean ± standard error of the mean (SEM), were analyzed with GraphPad Prism v9.0.1 software (Graph Pad Software Inc., California, USA). Statistical significance was determined by

using Shapiro-Wilk test for normal distribution followed by multiple t-test (Figure 3A), one-way ANOVA followed by Fisher test(Figure 3D and Figure 6B and 6D) and two-way ANOVA followed by Fisher test (Figure S2D). P_value < 0.05 (*), < 0.01 (**) and < 0.001 (***) were considered statistically significant.

Results

Folliculogenesis in transmasculine ovaries

In this study, the population of transmasculine donors (Table S1) showed ovaries in the follicular phase, but surprisingly also in the luteal phase after histological analysis (Figure 1), suggesting that active folliculogenesis is taking place at least in some donors. Although this may be a sporadic observation, it contrasts with the suggestion that testosterone treatment may suppress ovulation in transmasculine donors (35). More importantly, this suggests that ovaries from transmasculine donors may be adequate to investigate folliculogenesis *in vitro*.

Distribution and characterization of follicular stages in cortical ovarian fragments

Cryopreserved-thawed cortical ovarian fragments from 6 different donors undergoing gender-affirming surgery (Table S1) were cut into cubes of approximately 1mm^3 size (Figure 2A) and fixed at day 0 (D0) for baseline follicular population analysis. A total of 73 cubes containing 474 follicles were analyzed at D0 and showed an average of 79.0 ± 13.0 follicles per donor (Figure 2B). The distribution of the different follicular stages was 45.2 ± 6.2% primordial follicles, 35.9 ± 6.6% primary and transitional follicles, 18.9 ± 5.2% early atretic follicles, and no secondary follicles (healthy or atretic)

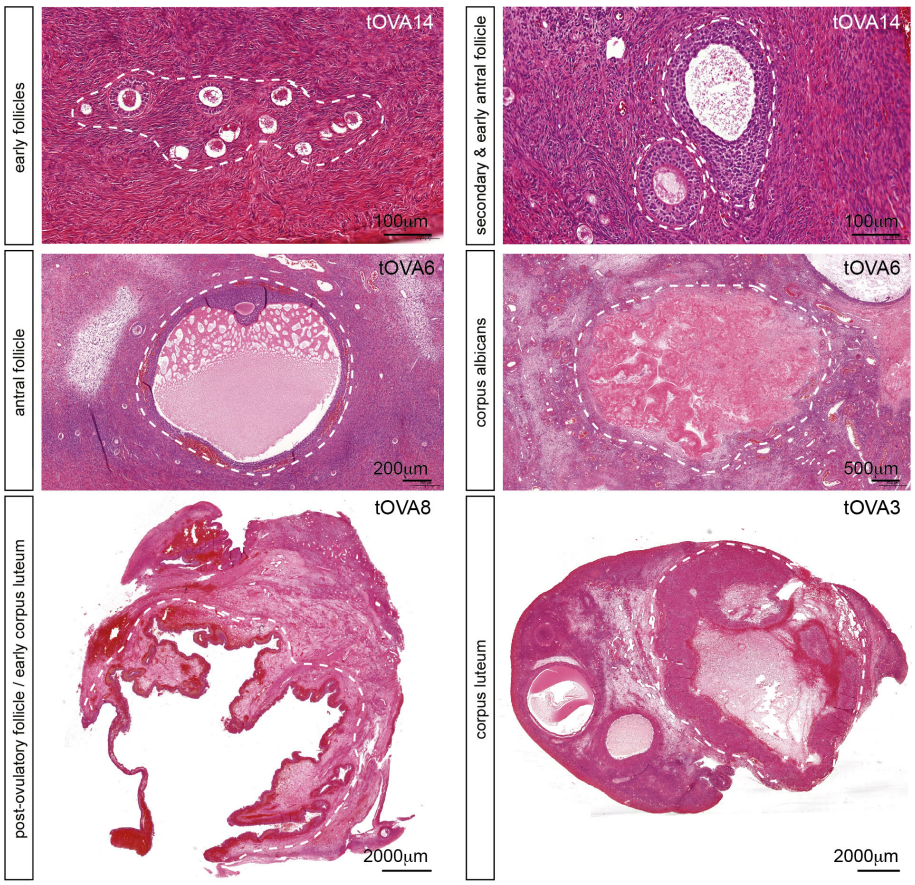

FIGURE 1
Folliculogenesis in transmasculine ovaries. Hematoxilin-eosin staining on ovarian histological sections from several transmasculine donors showing different follicular stages, such as early follicles (primordial, transitional, primary and early secondary), secondary and early antral follicles, antral follicles, post-ovulatory follicles (or early corpus lutea), corpus lutea and corpus albicans. Scale bars are indicated.

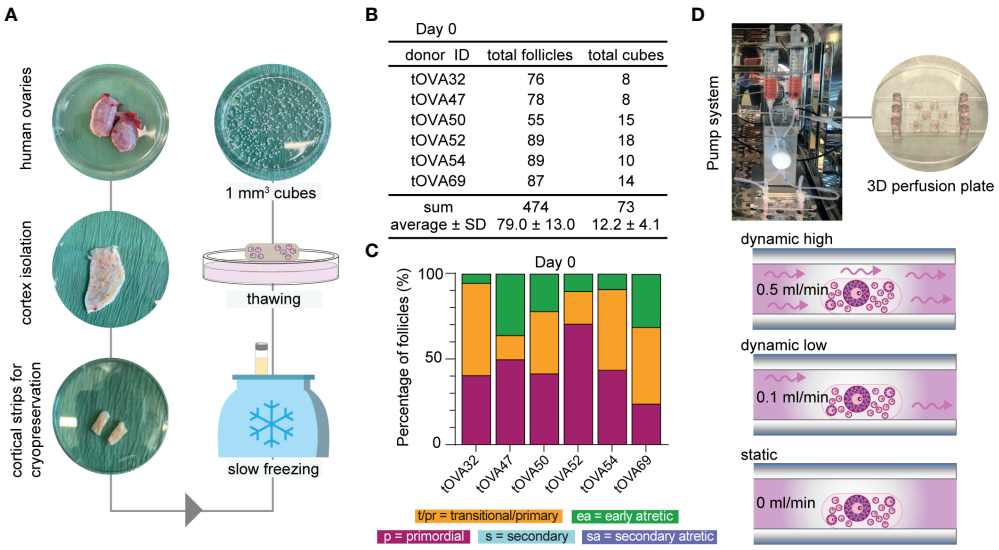

FIGURE 2
Study design and follicular distribution at D0. **(A)** Schematic workflow from collection until culture. Upon arrival, the ovaries were bisected and the outer cortex was isolated by scraping the medulla and inner cortex. Cortical strips were prepared for cryopreservation using slow freezing. Thawed-cortical tissue was cut into approximately 1mm3 cubes to fix or culture. **(B)** Total number of follicles and cubes analyzed per donor at D0, sum and average ± standard deviation (SD). **(C)** Follicular distribution per donor at D0. **(D)** Ovarian cortical cubes were placed in microwells (1-2/well) from µ-slide III 3D perfusion plates. Microchannels were filled with culture medium and plates were either connected to the perfusion pump for dynamic culture applying high flow rate (0.5ml/min), low flow rate (0.1ml/min) or no flow (0ml/min).

(Figure 2C and Figures S1A–C). Cryopreserved-thawed cortical cubes were placed into the Ibidi III 3D perfusion system and cultured for 4 days (D4) or 8 days (D8) under different flow rates (0.5 ml/min; 0.1 ml/min; 0 ml/ml) (Figure 2D).

The culture medium used was essentially as previously published (33, McLaughlin et al., 2018) with the main differences that FSH was not added. The reason being that 1) the activation of primordial follicles is independent of FSH (17) and 2) we observed no statistical differences in the distribution of follicular types after culturing fresh cortical ovarian cubes in static condition for eight days in the presence or absence of FSH (Figure 3A).

Histological analysis of the cryopreserved-thawed cortical cubes showed remarkable variation in follicular distribution after culture. Moreover, it is noteworthy that many fragments from all 6 donors were empty of any type of follicles (Figure 3B and Figure S1A), in agreement with reports showing that the human ovarian cortex contains an uneven follicular distribution (36–38), hence it is important to analyze a large number ovarian cortical cubes.

As in freshly isolated ovaries (*in vivo*), we observed all stages of preantral follicles after culture (Figure 3C). Regarding the morphology of the follicles after culture, primordial follicles containing a single layer of flat granulosa cells could be distinguished from follicles that showed the presence of cuboidal granulosa cells, often surrounding the oocyte only partially (Figure 3C). As from one single section it was not possible to distinguish between primary follicles (completely surrounded by cuboidal granulosa cells) and transitional follicles (partially surrounded by cuboidal granulosa cells), we quantified those into a single group (primary and transitional follicles). Furthermore, two types of secondary follicles could be distinguished after culture: one type with a centrally located oocyte (Figure 3C middle- bottom) and another with a peripherally located oocyte (Figure 3C middle-top). Both types were quantified together as secondary follicles. The atretic follicles were distinguished by an oocyte with a red cytoplasm and characteristic pyknotic nucleus also observed in the surrounding granulosa cells (Figure 3C).

Influence of the flow rate in the culture of human cortical tissue

Compared to the follicular distribution at D0, all conditions showed a significant decreased in the percentage of primordial follicles (p_value < 0.001) displaying 4.6 ± 1.7% at D4 static; 9.1 ± 3.2% at D8 static; 6.7 ± 2.4% at D4 dynamic low; 13.2 ± 3.4% at D8 dynamic low; 2.1 ± 1.5% at D4 dynamic high; and 9.6 ± 2.8% D8 dynamic high (Figure 3D and Figures S1B–D).

After four days of culture, the percentage of primary/transitional follicles obtained in the absence of flow 33.3 ±

10.3389/fendo.2022.936765

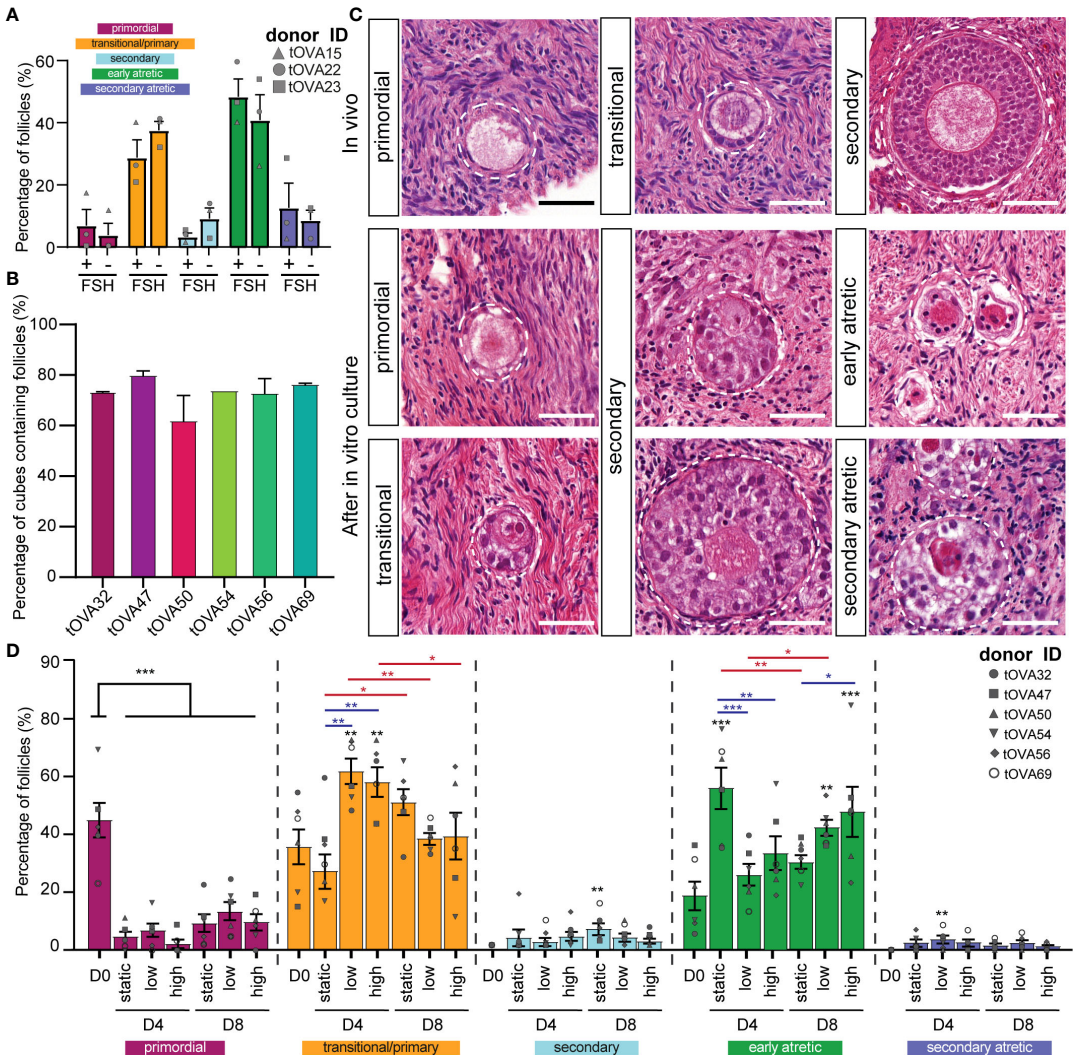

FIGURE 3
Distribution of follicles in ovarian cortical cubes after *in vitro* culture. **(A)** Distribution of follicular stages after eight days in culture with or without 1ng/ml of FSH. Results depict the percentage of each follicular stage per condition (mean ± SEM) compared per follicular stage. A total of N=120 cortical tissue cubes containing in total 321 follicles were classified. Statistical analysis was performed using Shapiro-Wilk test for normal distribution followed by multiple t-test. *=p_value < 0.05; ** = p_value < 0.01; ***=p_value <0.001. **(B)** Percentage of cortical tissue cubes containing follicles per donor (mean ± SEM). **(C)** Follicular classification used in this study. Top row shows *in vivo* control ovarian follicles in histological sections from freshly-isolated transmasculine donors. Bottom rows show *in vitro* cultured ovarian follicles. Scale bars = 40 µm. **(D)** Distribution of follicular stages after D4 and D8 in static, dynamic low and dynamic high culture. Results depict the percentage of each follicular stage per condition (mean ± SEM) compared per follicular stage. A total of N=497 cortical tissue cubes containing in total 3676 follicles were classified. Statistical analysis was performed using one-way ANOVA followed by Fisher test comparing each condition to D0 and statistical significance visualized on top of each respective bar (*=p_value < 0.05; ** = p_value < 0.01; ***=p_value <0.001). Statistical analysis was also performed among the three culture conditions within the same time point (blue lines) and between D4 and D8 within the same condition (red lines).

6.1% was comparable to that observed at D0, but the number of early atretic follicles (55.9 ± 7.1%) was significantly higher than that observed at D0 (p_value=0.0001). This suggested that this culture condition was not beneficial for folliculogenesis. By contrast, the ovarian cubes exposed to flow (low and high) exhibited a significant increase in the percentage of primary/transitional follicles (61.6 ± 4.4% and 57.9 ± 5.1%, respectively), compared to D0 (p_value=0.003 and p_value=0.009, respectively) (Figure 3D and Figures S1B–D). Moreover, several secondary follicles were observed after four days of culture, but the number was relatively low in all culture conditions (Figure 3D and Figures S1B–D). Together, this suggested that exposure to flow during four days stimulated follicular activation.

Interestingly, the ovarian cubes cultured for eight days without flow showed the highest percentages of both primary

10.3389/fendo.2022.936765

and transitional (51.0 ± 4.6%) and secondary follicles (7.0 ± 1.9%) from all culture conditions (Figure 3D and Figures S1B–D). Moreover, the increment in secondary follicles after eight days of culture was only statistically significant in the static condition when compared to D0 (p_value=0.006). It is important to note that the total number of secondary follicles obtained after culture was low in all conditions (Figure S1B).

Together our results suggest that the use of flow may accelerate follicular activation until four days of culture, but may not be beneficial for further follicular growth at least in combination with the used culture media.

Characterization of the granulosa cells in the secondary follicles after culture

To further investigate the quality of the secondary follicles obtained after culture under different flow rates, we performed immunofluorescence for anti-Müllerian hormone (AMH) and keratin 19 (KRT19) (Figure 4 and Figure S2). AMH is a member of the TGFβ-family involved in the regulation of folliculogenesis and expressed in human ovarian follicles from the secondary stage onwards (39) (Figure 4). KRT19 belongs to the keratin family of intermediate filaments, with a main role in the structural integrity of epithelial cells. The expression of KRT19 in preantral follicles in humans has not been previously reported, however we observed specific expression of KRT19 in granulosa cells of unilaminar follicles, but not in granulosa cells of secondary follicles at D0 (Figure 4). Hence, we considered the dynamic expression pattern of AMH and KRT19 suitable to assess the transition from unilaminar to secondary follicles after culture.

After four and eight days of culture, we observed an increased disorganization in the granulosa cells of secondary follicles, marked by the transcription factor forkhead box L2 (FOXL2), when compared to the granulosa cells in non-cultured secondary follicles (Figure 4 and Figure S2). After four days in culture, granulosa cells in secondary follicles showed both expression of AMH and KRT19. By contrast, after eight days in culture the granulosa cells of the secondary follicles cultured under low flow rate showed both expression of AMH and KRT19, whereas the granulosa cells of the secondary follicles cultured under high flow rate or static showed expression of AMH and absence of KRT19 (Figure 4). This suggested that the granulosa cells present in the secondary follicles after eight days in culture under low flow rate still retained characteristics of those in unilaminar follicles.

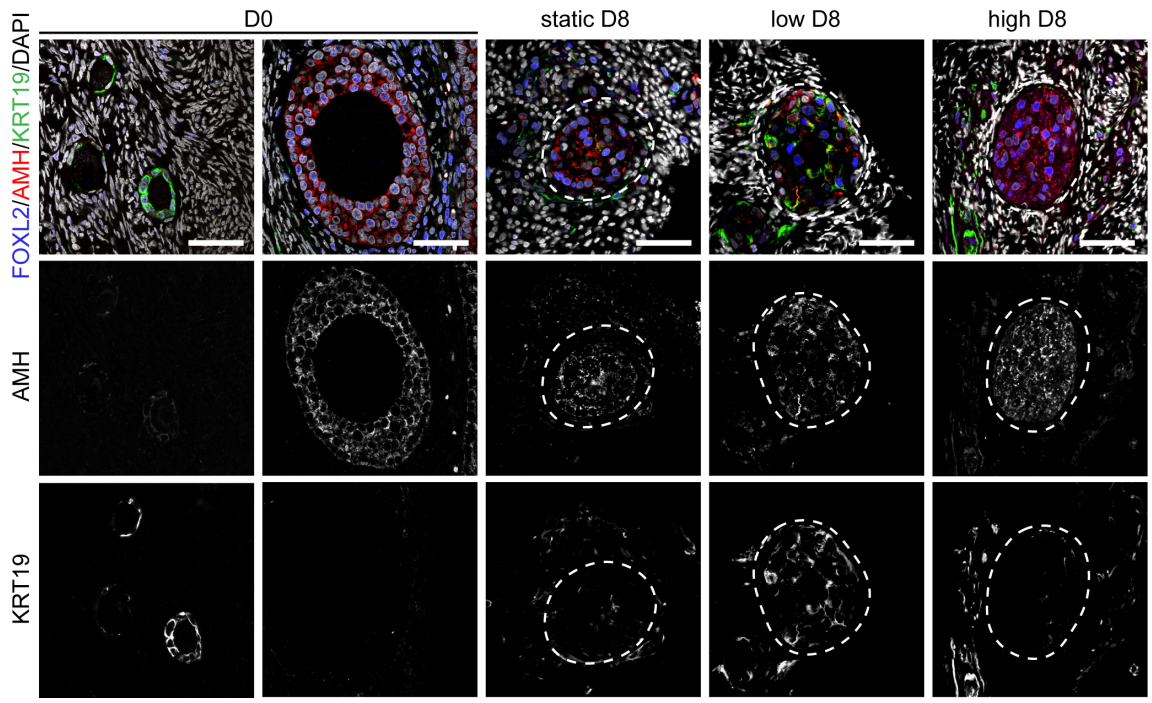

FIGURE 4
Expression of FOXL2, AMH and KRT19 in secondary follicles after culture. Immunofluorescence for FOXL2, AMH and KRT19 in primordial, primary and secondary follicles at D0 and after eight days (D8) culture in static, low and high flow rate. Scale bars = 50 µm.

Cell viability and proliferation of the granulosa cells in the secondary follicles after culture

To study the viability of the cultured follicles and surrounding stromal tissue, the TUNEL assay was used to detect apoptosis through DNA fragmentation. Moreover, we evaluated the presence of a continuous uninterrupted follicular basement membrane using immunofluorescence for collagen type IV (COLIV). The basement membrane surrounding the ovarian follicles is rich in extracellular matrix proteins, such as COLIV (40) and plays a fundamental role on follicular survival, since its disruption compromises follicular viability (41, 42).

After four days in culture, secondary follicles showed no TUNEL+ follicular cells. Only the stromal cells at the edge of the cubes showed signs of apoptosis (Figure 5A), perhaps due to tissue damage during sample preparation. Furthermore, all secondary follicles exhibited an intact COLIV+ basement membrane, as well as proliferative PCNA+ granulosa cells, comparable to that observed in D0 (Figure 5B). After eight days in culture, there were still no double positive FOXL2+TUNEL+ granulosa cells in all culture conditions (Figure 6A). However, there was a statistically significant increase in TUNEL+ cells in the stromal compartment of the ovarian cubes under high flow compared to both DO ($p<0.0001$) and to the other D8 conditions ($p=0.001$) (Figure 6B). Interestingly, the levels of proliferation (PCNA) observed after eight days in culture were opposite to those of TUNEL, with high levels of PCNA in the granulosa cells of secondary follicles whereas the stroma was mostly PCNA-negative (Figure 6C).

Secondary follicles obtained after eight days of culture showed a continuous COLIV+ basement membrane, comparable with that of secondary follicles at D0 (Figure 6C). In addition, the deposition of COLIV between the granulosa cells (Call-Exner bodies) (43) was also present in the secondary follicles in all culture conditions. Interestingly, after eight days in culture, we observed a statistically significant increase in COLIV deposition in the stromal compartment of the ovarian cubes cultured with low or no flow ($p\_value=0.004$ and $p\_value=0.03$, respectively), when compared to ovarian cubes at D0 (Figure 6D). It remains to be investigated whether the higher levels of COLIV deposition on the stromal compartment have a detrimental effect on follicular growth in long-term culture.

Discussion

Microfluidic devices including dynamic culture conditions have proved to be an innovative system for creating a more physiological microenvironment during *in vitro* culture of embryos (44), ovarian cells (30), ovarian cortical tissue and isolated follicles from animal models (45). Here, we aimed to test whether the culture of human ovarian cortical tissue under dynamic conditions for eight days improved activation, growth and viability of early follicles. We used human ovarian cortical samples that have been cryopreserved-thawed following clinical-grade protocols to increase applicability.

In vivo folliculogenesis from primordial to pre-ovulatory follicle takes several months in humans (16, 17), but it has been shown that *in vitro* this process is strongly accelerated (26, 27). De Roo and colleagues have proposed that mechanical fragmentation of the cortical tissue during sample preparation for *in vitro* culture disrupts the Hippo pathway, promoting the activation of dormant follicles as well as the growth of other follicular stages (46). This could explain the formation of preantral follicles in such a short period of culture. Moreover, we have included a short-term treatment with S1P, a follicular growth-promoting lipid that is involved in both the Hippo- and PI3K- pathways (33) and could therefore promote and accelerate *in vitro* folliculogenesis.

The quantification of the follicles in cryopreserved-thawed cortex samples from gender-affirming donors at D0 already revealed that an average of 19% of the follicles were atretic, a much higher percentage than that reported in cisgender young donors (47). As reported in non-human primates (48), a detrimental effect from the androgen treatment on follicular quality in the transmasculine ovarian samples at D0 cannot be excluded, although De Roo and colleagues reported both a comparable follicular distribution and *in vitro* maturation potential of oocytes isolated from cumulus-oocyte-complex between androgen-treated and untreated ovaries (49). Alternatively, the cryopreserved-thawing procedure could directly affect the percentage of atretic follicles at D0.

The number of secondary follicles that was formed in cryopreserved-thawed ovarian cortical cubes after eight days of culture in both static and dynamic conditions was low. Moreover, although the secondary follicles obtained showed an intact basement membrane and their granulosa cells showed proliferative capacity and production of AMH, suggesting both viability and functionality, the granulosa cells showed in general a high level of cellular disorganization in the follicle that resulted in the peripheral location of the oocyte. In agreement, Wang and colleagues showed that a larger number of abnormal follicles was observed as well as significantly lower expression of follicular markers, as ZP3, CYP11A and AMH in ovarian tissue after cryopreservation, slow freezing and vitrification, compared to fresh counterparts after culture (50). By contrast, work by Sanfilippo and colleagues did not find significant differences regarding the percentage of viable follicles from frozen-thawed versus fresh ovarian cortical tissue, and they reported 20% of secondary follicles in cryopreserved fragments after culture (51). In order to validate the *in vitro* growth capacity of the cryopreserved-thawed cortical tissue obtained from

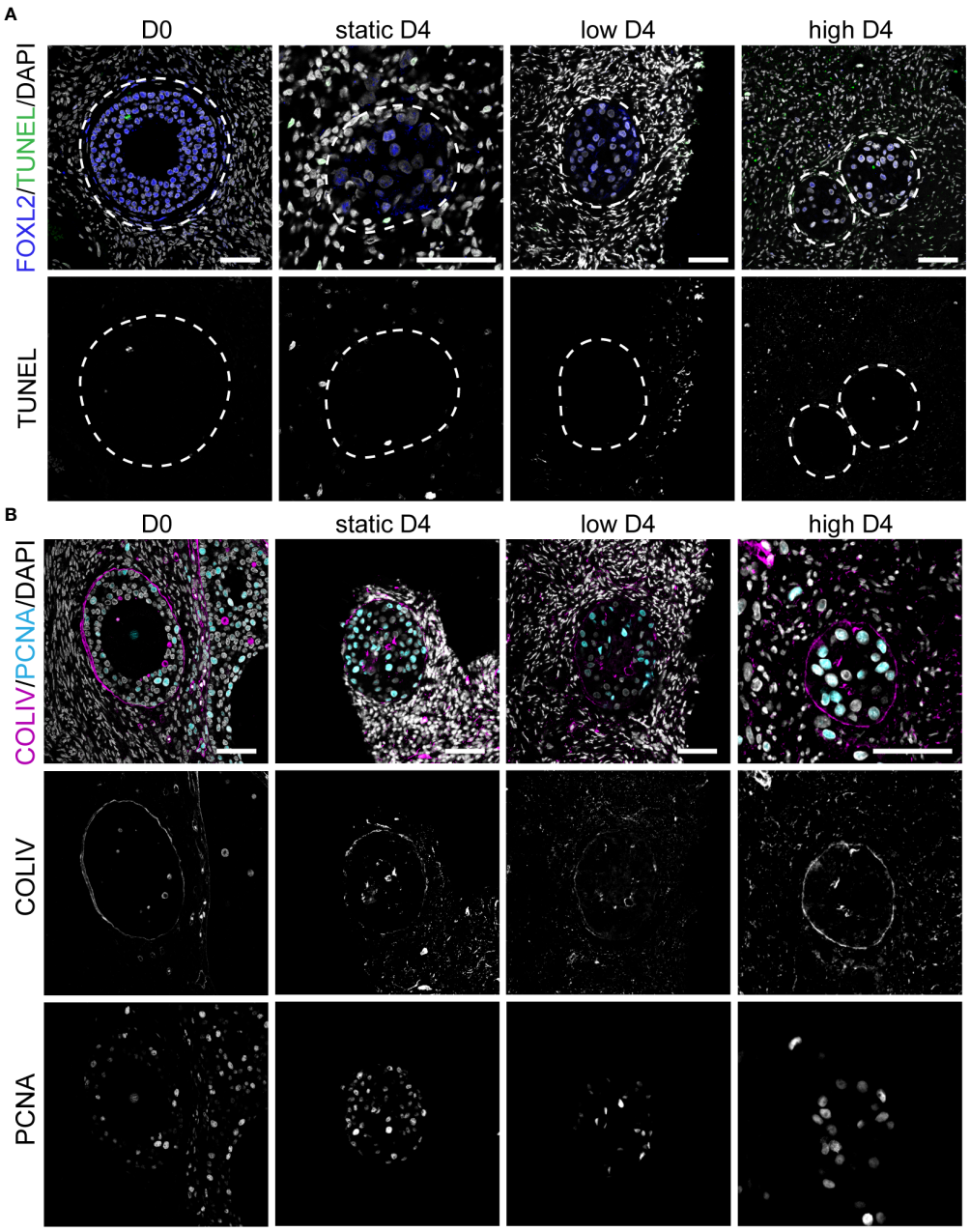

FIGURE 5
Apoptosis, proliferation and COLIV deposition in ovarian cortical cubes after four days of culture. **(A)** Immunofluorescence for FOXL2 together with TUNEL assay in secondary follicles at D0 and after four days (D4) culture in static, low and high flow rate. Scale bars= 50 µm. **(B)** Immunofluorescence for COLIV and PCNA in secondary follicles at D0 and after D4 culture in static, low and high flow rate. Scale bars= 50 µm.

transmasculine donors, a fresh age-matched control group should be considered in future experiments.

The presence of apoptotic cells in the stroma deserves special attention. Sanfilippo and colleagues reported a higher amount of TUNEL+ stromal cells on ovarian cortical tissue induced by cryopreservation-thawing (51). The correlation between stromal cell function and follicular growth and survival have been previously investigated (52). Qui and colleagues carried out an *in vitro* assay involving the co-culture of granulosa cells with stromal/theca cells from goat ovaries to evaluate the effect of factors secreted by the stromal cells in the survival and functionality of granulosa cells. It was found that stromal/theca cells promoted granulosa cells proliferation and improved their viability by triggering pro-survival BCL2 gene

10.3389/fendo.2022.936765

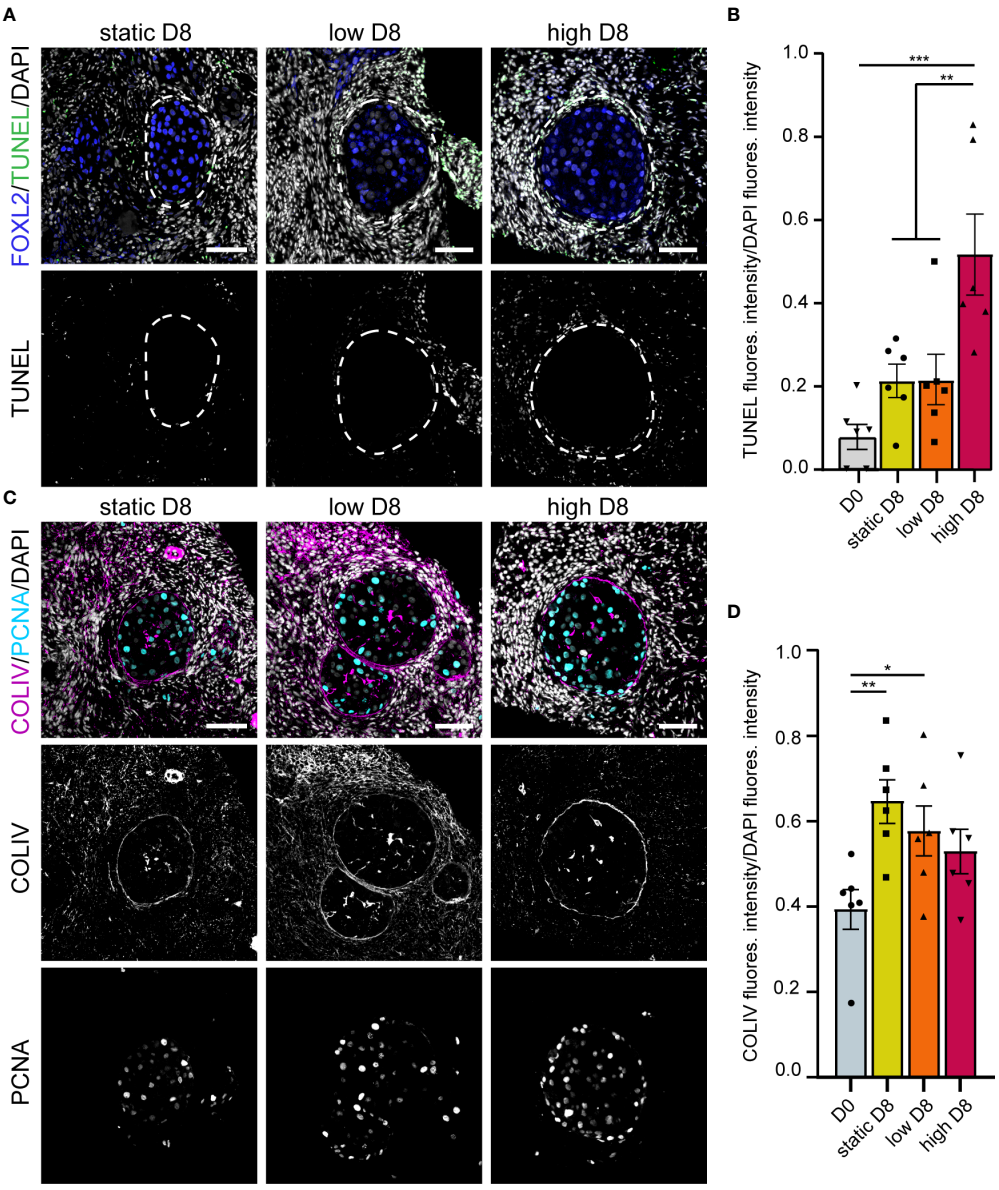

FIGURE 6
Apoptosis, proliferation and COLIV deposition in ovarian cortical cubes after eight days of culture. **(A)** Immunofluorescence for FOXL2 together with TUNEL assay in secondary follicles after eight days (D8) culture in static, low and high flow rate. Scale bars= 50 µm. **(B)** Relative TUNEL fluorescence intensity in ovarian cortical cubes at D0 and after D8 culture in static, low and high flow rate. Statistical analysis was performed using one-way ANOVA followed by Fisher test (** = p_value < 0.01; (*** = p_value < 0.001). **(C)** Immunofluorescence for COLIV and PCNA in secondary follicles after D8 culture in static, low and high flow rate. Scale bars= 50 µm. **(D)** Relative COLIV fluorescence intensity in ovarian cortical cubes at D0 and after D8 culture in static, low and high flow rate. Statistical analysis was performed using one-way ANOVA followed by Fisher test (* = p_value < 0.05; ** = p_value < 0.01).

expression and inhibiting the production of pro-apoptotic BAX gene and CASP3 activation (52). Therefore, increased levels of apoptosis in the stroma may be highly detrimental to the follicular growth and follicular quality. The fact that many stroma cells were TUNEL+ indicated that this cellular compartment showed high sensibility to the *in vitro* culture conditions tested. By contrast, the granulosa cells seemed to be proliferative and produced AMH, reflecting less sensitivity, but because they showed disorganization and retained expression of KRT19, this may reflect a defective development.

After eight days in culture, in all the conditions investigated (static, dynamic low, dynamic high) the ovarian cubes showed a strongly collagenized stroma, with high deposition of COLIV, when compared to D0. High collagenization has been reported

in aged ovaries of non-human primates, containing both lower follicular density and a higher number of atretic follicles (53). It seems unquestionable that the stroma plays a major role in the regulation of folliculogenesis, hence it is likely that both higher stromal apoptosis and collagenization may negatively affect follicular growth *in vitro* and consequently result in low number of secondary follicles. A possible reason for this is the composition of the culture medium, that may be suitable to culture fresh ovarian cortex, but not adequate to culture cryopreserved-thawed ovarian cortex, that may have an altered metabolic activity or decreased mitochondrial activity (54). Moreover, as the ovaries of transmasculine donors are exposed to an abrupt decrease in the levels of testosterone, they may not respond adequately to the culture medium used.

Although cryopreserved-thawed ovarian cortical tissue has proved viable and functional when retransplanted into the patient's body by restoring both endocrine ovarian function and fertility (3, 4), their use for *in vitro* folliculogenesis remains challenging. The culture of ovarian cortical tissue within microwells in a dynamic culture system may offer advantages compared to the traditional static culture, such as a more physiologically relevant supply of culture media and a reduction in manipulation. However, the application of a dynamic culture system to support *in vitro* folliculogenesis successfully will require several major improvements to accelerate optimization. First, the use of a higher number of ovarian cubes is desirable to obtain enough secondary follicles to allow a deeper characterization of the *in vitro* culture system. In order to do it, multiple µ-slide III 3D perfusion plates should be interconnected in series and perfused by a single pump. Secondly, thinner cortical fragments or the use of a follicular vital dye, such as Neutral Red (55) should be considered to exclude cortical fragments empty of follicles from culture.

To focus on follicular distribution rather than on the total number of follicles, we performed analysis on the percentage of follicle types per donor per condition and used the sum of follicles in all cubes per donor to eliminate the variation between cubes per condition. Nevertheless, we cannot exclude that some of the variation detected is caused by the inner variability among donors or between cubes. To overcome this aspect, it is important to use both a high number of cubes and a high number of donors.

In conclusion, we report that the culture of cryopreserved-thawed ovarian cortical tissue fragments under static condition proved to be a more efficient method to obtain secondary follicles after eight days in culture when compared to both the low and high dynamic conditions tested. Moreover, high flow rates seemed detrimental for the tissue quality. Ovarian cortical tissue cubes cultured under static condition showed low TUNEL levels in both follicular and stromal cells, displaying a higher potential for being cultured for a longer period of time. Nevertheless, the total number of secondary follicles obtained under static culture remained very low, indicating that additional studies are required to elucidate the culture conditions that can lead to efficient follicular growth *in vitro*.

Data availability statement

The raw data supporting the conclusions of this article will be made available by the authors, without undue reservation.

Author contributions

JD, VM, NM, and SC conceived the study. JD, VM, JA, XF, NM, LL, GP, and LW contributed to material collection. JM, JA, NM, and SC arranged the ethical permit. JD, VM, and ML generated data. All authors contributed to data analysis. All authors contributed to manuscript writing. All authors approved the submitted version.

Funding

This research was funded by the European Research Council (OVOGROWTH ERC-CoG-2016-725722 to JD, VM, XF and SC.

Acknowledgments

We would like to thank all patients that donated tissue for this study and the members of the Chuva de Sousa Lopes group for useful discussions.

Conflict of interest

The authors declare that the research was conducted in the absence of any commercial or financial relationships that could be construed as a potential conflict of interest.

Publisher's note

Supplementary material

The Supplementary Material for this article can be found online at: https://www.frontiersin.org/articles/10.3389/fendo.2022.936765/full#supplementary-material.

References

1. Vander Borght M, Wyns C. Fertility and infertility: Definition and epidemiology. *Clin Biochem* (2018) 62:2–10. doi: 10.1016/j.clinbiochem.2018.03.012

2. Niederberger C, Pellicer A, Cohen J, Gardner DK, Palermo GD, O'neill CL, et al. Forty years of IVF. *Fertil Steril* (2018) 110:185–324.e5. doi: 10.1016/j.fertnstert.2018.06.005

3. ESHRE Guideline Group On Female Fertility Preservation, Anderson RA, Amant F, Braat D, D'Angelo A, Chuva de Sousa Lopes SM, et al. ESHRE guideline: female fertility preservation. *Hum Reprod Open* (2020) 2020:hoaa052. doi: 10.1093/hropen/hoaa052

4. Practice Committee of the American Society for Reproductive Medicine, A. Fertility preservation in patients undergoing gonadotoxic therapy or gonadectomy: a committee opinion. *Fertil Steril* (2019) 112:1022–33. doi: 10.1016/j.fertnstert.2019.09.013

5. Bastings L, Beerendonk CC, Westphal JR, Massuger LF, Kaal SE, Van Leeuwen FE, et al. Autotransplantation of cryopreserved ovarian tissue in cancer survivors and the risk of reintroducing malignancy: a systematic review. *Hum Reprod Update* (2013) 19:483–506. doi: 10.1093/humupd/dmt020

6. Dolmans MM, Hossay C, Nguyen TYT, Poirot C. Fertility preservation: How to preserve ovarian function in children, adolescents and adults. *J Clin Med* (2021) 10(20):5247. doi: 10.3390/jcm10225247

7. Dolmans MM, Luyckx V, Donnez J, Andersen CY, Greve T. Risk of transferring malignant cells with transplanted frozen-thawed ovarian tissue. *Fertil Steril* (2013) 99:1514–22. doi: 10.1016/j.fertnstert.2013.03.027

8. Guzel Y, Oktem O. Understanding follicle growth *in vitro*: Are we getting closer to obtaining mature oocytes from *in vitro*-grown follicles in human? *Mol Reprod Dev* (2017) 84:544–59. doi: 10.1002/mrd.22822

9. Czukiewska SM, Chuva de Sousa Lopes SM. Fetal germ cell development in humans, a link with infertility. *Semin Cell Dev Biol* (2022) S1084-9521(22):00117-3. doi: 10.1016/j.semcdb.2022.03.035

10. Zhang H, Liu K. Cellular and molecular regulation of the activation of mammalian primordial follicles: somatic cells initiate follicle activation in adulthood. *Hum Reprod Update* (2015) 21:779–86. doi: 10.1093/humupd/dmv037

11. Zhang Y, Yan Z, Qin Q, Nisenblat V, Chang HM, Yu Y, et al. Transcriptome landscape of human folliculogenesis reveals oocyte and granulosa cell interactions. *Mol Cell* (2018) 72:1021–1034.e4. doi: 10.1016/j.molcel.2018.10.029

12. Baerwald AR, Adams GP, Pierson RA. Ovarian antral folliculogenesis during the human menstrual cycle: a review. *Hum Reprod Update* (2012) 18:73–91. doi: 10.1093/humupd/dmr039

13. Mcgee EA, Hsueh AJ. Initial and cyclic recruitment of ovarian follicles. *Endocr Rev* (2000) 21:200–14. doi: 10.1210/edrv.21.2.0394

14. Mihm M, Evans AC. Mechanisms for dominant follicle selection in monovulatory species: a comparison of morphological, endocrine and intraovarian events in cows, mares and women. *Reprod Domest Anim* (2008) 43 Suppl 2:48–56. doi: 10.1111/j.1439-0531.2008.01142.x

15. Matsuda F, Inoue N, Manabe N, Ohkura S. Follicular growth and atresia in mammalian ovaries: regulation by survival and death of granulosa cells. *J Reprod Dev* (2012) 58:44–50. doi: 10.1262/jrd.2011-012

16. Gougeon A. Human ovarian follicular development: from activation of resting follicles to preovulatory maturation. *Ann Endocrinol (Paris)* (2010) 71:132–43. doi: 10.1016/j.ando.2010.02.021

17. Orisaka M, Miyazaki Y, Shirafuji A, Tamamura C, Tsuyoshi H, Tsang BK, et al. The role of pituitary gonadotropins and intraovarian regulators in follicle development: a mini-review. *Reprod Med Biol* (2021) 20:169–75. doi: 10.1002/rmb2.12371

18. Telfer EE, Andersen CY. *In vitro* growth and maturation of primordial follicles and immature oocytes. *Fertil Steril* (2021) 115:1116–25. doi: 10.1016/j.fertnstert.2021.03.004

19. Fan X, Chuva de Sousa Lopes SM. Molecular makeup of the human adult ovary. *Opin Endocrine Metab Res* (2021) 18:187–93. doi: 10.1016/j.coemr.2021.03.016

20. Amorim CA, Van Langendonckt A, David A, Dolmans MM, Donnez J. Survival of human pre-antral follicles after cryopreservation of ovarian tissue, follicular isolation and *in vitro* culture in a calcium alginate matrix. *Hum Reprod* (2009) 24:92–9. doi: 10.1093/humrep/den343

21. Skory RM, Xu Y, Shea LD, Woodruff TK. Engineering the ovarian cycle using *in vitro* follicle culture. *Hum Reprod* (2015) 30:1386–95. doi: 10.1093/humrep/dev052

22. Wang TR, Yan LY, Yan J, Lu CL, Xia X, Yin TL, et al. Basic fibroblast growth factor promotes the development of human ovarian early follicles during growth *in vitro*. *Hum Reprod* (2014) 29:568–76. doi: 10.1093/humrep/det465

23. Xiao S, Zhang J, Romero MM, Smith KN, Shea LD, Woodruff TK. *In vitro* follicle growth supports human oocyte meiotic maturation. *Sci Rep* (2015) 5:17323. doi: 10.1038/srep17323

24. Xu M, Barrett SL, West-Farrell E, Kondapalli LA, Kiesewetter SE, Shea LD, et al. *In vitro* grown human ovarian follicles from cancer patients support oocyte growth. *Hum Reprod* (2009) 24:2531–40. doi: 10.1093/humrep/dep228

25. Wallace WH, Kelsey TW, Anderson RA. Fertility preservation in pre-pubertal girls with cancer: the role of ovarian tissue cryopreservation. *Fertil Steril* (2016) 105:6–12. doi: 10.1016/j.fertnstert.2015.11.041

26. Mclaughlin M, Albertini DF, Wallace WHB, Anderson RA, Telfer EE. Metaphase II oocytes from human unilaminar follicles grown in a multi-step culture system. *Mol Hum Reprod* (2018) 24:135–42. doi: 10.1093/molehr/gay002

27. Xu F, Lawson MS, Bean Y, Ting AY, Pejovic T, de Geest K, et al. Matrix-free 3D culture supports human follicular development from the unilaminar to the antral stage *in vitro* yielding morphologically normal metaphase II oocytes. *Hum Reprod* (2021) 36:1326–38. doi: 10.1093/humrep/deab003

28. Gargus ES, Rogers HB, Mckinnon KE, Edmonds ME, Woodruff TK. Engineered reproductive tissues. *Nat BioMed Eng* (2020) 4:381–93. doi: 10.1038/s41551-020-0525-x

29. Mancini V, Pensabene V. Organs-On-Chip models of the female reproductive system. *Bioeng (Basel)* (2019) 6(4):103. doi: 10.3390/bioengineering6040103

30. Xiao S, Coppeta JR, Rogers HB, Isenberg BC, Zhu J, Ollekan SA, et al. A microfluidic culture model of the human reproductive tract and 28-day menstrual cycle. *Nat Commun* (2017) 8:14584. doi: 10.1038/ncomms14584

31. Zhu J, Xu Y, Rashedi AS, Pavone ME, Kim JJ, Woodruff TK, et al. Human fallopian tube epithelium co-culture with murine ovarian follicles reveals crosstalk in the reproductive cycle. *Mol Hum Reprod* (2016) 22:756–67. doi: 10.1093/molehr/gaw041

32. Hoekman EJ, Louwe LA, Rooijers M , Westerlaken LAJ, Klijn NF, Pilgram GSK, et al. Ovarian tissue cryopreservation: Low usage rates and high live-birth rate after transplantation. *Acta Obstet Gynecol Scand* (2020) 99:213–21. doi: 10.1111/aogs.13735

33. Cheng Y, Feng Y, Jansson L, Sato Y, Deguchi M, Kawamura K, et al. Actin polymerization-enhancing drugs promote ovarian follicle growth mediated by the hippo signaling effector YAP. *FASEB J* (2015) 29:2423–30. doi: 10.1096/fj.14-267856

34. Schindelin J, Arganda-Carreras I, Frise E, Kaynig V, Longair M, Pietzsch T, et al. Fiji: an open-source platform for biological-image analysis. *Nat Methods* (2012) 9:676–82. doi: 10.1038/nmeth.2019

35. Taub RL, Ellis SA, Neal-Perry G, Magaret AS, Prager SW, Micks EA. The effect of testosterone on ovulatory function in transmasculine individuals. *Am J Obstet Gynecol* (2020) 223:229.e1–8. doi: 10.1016/j.ajog.2020.01.059

36. Lass A. Assessment of ovarian reserve - is there a role for ovarian biopsy? *Hum Reprod* (2001) 16:1055–7. doi: 10.1093/humrep/16.6.1055

37. Poirot C, Vacher-Lavenu MC, Helardot P, Guibert J, Brugieres L, Jouannet P. Human ovarian tissue cryopreservation: indications and feasibility. *Hum Reprod* (2002) 17:1447–52. doi: 10.1093/humrep/17.6.1447

38. Schmidt KL, Byskov AG, Nyboe Andersen A, Muller J, Yding Andersen C. Density and distribution of primordial follicles in single pieces of cortex from 21 patients and in individual pieces of cortex from three entire human ovaries. *Hum Reprod* (2003) 18:1158–64. doi: 10.1093/humrep/deg246

39. Weenen C, Laven JS, Von Bergh AR, Cranfield M, Groome NP, Visser JA, et al. Anti-mullerian hormone expression pattern in the human ovary: potential implications for initial and cyclic follicle recruitment. *Mol Hum Reprod* (2004) 10:77–83. doi: 10.1093/molehr/gah015

40. Heeren AM, van Iperen L, Klootwijk DB, de Melo Bernardo A, Roost MS, Gomes Fernandes MM, et al. Development of the follicular basement membrane during human gametogenesis and early folliculogenesis. *BMC Dev Biol* (2015) 15:4. doi: 10.1186/s12861-015-0054-0

41. Murray AA, Molinek MD, Baker SJ, Kojima FN, Smith MF, Hillier SG, et al. Role of ascorbic acid in promoting follicle integrity and survival in intact mouse ovarian follicles *in vitro*. *Reproduction* (2001) 121:89–96. doi: 10.1530/rep.0.1210089

42. Rose UM, Hanssen RG, Kloosterboer HJ. Development and characterization of an *in vitro* ovulation model using mouse ovarian follicles. *Biol Reprod* (1999) 61:503–11. doi: 10.1095/biolreprod61.2.503

43. van Wezel IL, Irving-Rodgers HF, Sado Y, Ninomiya Y, Rodgers RJ. Ultrastructure and composition of call-exner bodies in bovine follicles. *Cell Tissue Res* (1999) 296:385–94. doi: 10.1007/s004410051298

44. Kim MS, Bae CY, Wee G, Han YM, Park JK. A microfluidic *in vitro* cultivation system for mechanical stimulation of bovine embryos. *Electrophoresis* (2009) 30:3276–82. doi: 10.1002/elps.200900157

45. Nagashima JB, Assal R, Songsasen N, Demirci U. Evaluation of an ovary-on-a-chip in large mammalian models: Species specificity and influence of follicle isolation status. *J Tissue Eng Regener Med* (2018) 12:e1926–35. doi: 10.1002/term.2623

46. de Roo C, Lierman S, Tilleman K, de Sutter P. *In-vitro* fragmentation of ovarian tissue activates primordial follicles through the hippo pathway. *Hum Reprod Open* (2020) 2020:hoaa048. doi: 10.1093/hropen/hoaa048

47. Fan Y, Flanagan CL, Brunette MA, Jones AS, Baker BM, Silber SJ, et al. Fresh and cryopreserved ovarian tissue from deceased young donors yields viable follicles. *F S Sci* (2021) 2:248–58. doi: 10.1016/j.xfss.2021.06.003

48. Rodrigues JK, Navarro PA, Zelinski MB, Stouffer RL, Xu J. Direct actions of androgens on the survival, growth and secretion of steroids and anti-mullerian hormone by individual macaque follicles during three-dimensional culture. *Hum Reprod* (2015) 30:664–74. doi: 10.1093/humrep/deu335

49. de Roo C, Lierman S, Tilleman K, Peynshaert K, Braeckmans K, Caanen M, et al. Ovarian tissue cryopreservation in female-to-male transgender people: insights into ovarian histology and physiology after prolonged androgen treatment. *Reprod BioMed Online* (2017) 34:557–66. doi: 10.1016/j.rbmo.2017.03.008

50. Wang TR, Yan J, Lu CL, Xia X, Yin TL, Zhi X, et al. Human single follicle growth *in vitro* from cryopreserved ovarian tissue after slow freezing or vitrification. *Hum Reprod* (2016) 31:763–73. doi: 10.1093/humrep/dew005

51. Sanfilippo S, Canis M, Romero S, Sion B, Dechelotte P, Pouly JL, et al. Quality and functionality of human ovarian tissue after cryopreservation using an original slow freezing procedure. *J Assist Reprod Genet* (2013) 30:25–34. doi: 10.1007/s10815-012-9917-5

52. Qiu M, Liu J, Han C, Wu B, Yang Z, Su F, et al. The influence of ovarian stromal/theca cells during *in vitro* culture on steroidogenesis, proliferation and apoptosis of granulosa cells derived from the goat ovary. *Reprod Domest Anim* (2014) 49:170–6. doi: 10.1111/rda.12256

53. Wang S, Zheng Y, Li J, Yu Y, Zhang W, Song M, et al. Single-cell transcriptomic atlas of primate ovarian aging. *Cell* (2020) 180:585–600.e19. doi: 10.1016/j.cell.2020.01.009

54. Rodrigues AQ, Picolo VL, Goulart JT, Silva IMG, Ribeiro RB, Aguiar BA, et al. Metabolic activity in cryopreserved and grafted ovarian tissue using high-resolution respirometry. *Sci Rep* (2021) 11:21517. doi: 10.1038/s41598-021-01082-z

55. Chambers EL, Gosden RG, Yap C, Picton HM. *In situ* identification of follicles in ovarian cortex as a tool for quantifying follicle density, viability and developmental potential in strategies to preserve female fertility. *Hum Reprod* (2010) 25:2559–68. doi: 10.1093/humrep/deq192

frontiers | Frontiers in Endocrinology

TYPE Original Research
PUBLISHED 05 October 2022
DOI 10.3389/fendo.2022.903831

OPEN ACCESS

EDITED BY
Yuting Fan,
Boston IVF, United States

REVIEWED BY
David Mark Robertson,
University of New South Wales, Australia
Arup Acharjee,
Allahabad University, India
Angela Baerwald,
University of Saskatchewan, Canada

*CORRESPONDENCE
And Demir
drand@demir.net

SPECIALTY SECTION
This article was submitted to Reproduction, a section of the journal Frontiers in Endocrinology

RECEIVED 24 March 2022
ACCEPTED 19 August 2022
PUBLISHED 05 October 2022

CITATION
Demir A, Hero M, Holopainen E and Juul A (2022) Quantification of urinary total luteinizing hormone immunoreactivity may improve the prediction of ovulation time. *Front. Endocrinol.* 13:903831. doi: 10.3389/fendo.2022.903831

Quantification of urinary total luteinizing hormone immunoreactivity may improve the prediction of ovulation time

And Demir[1*], Matti Hero[1], Elina Holopainen[2] and Anders Juul[3,4]

[1]New Children's Hospital, Pediatric Research Center, University of Helsinki and Helsinki University Hospital, Helsinki, Finland, [2]Department of Obstetrics and Gynecology, University of Helsinki and Helsinki University Hospital, Helsinki, Finland, [3]Department of Growth and Reproduction, Copenhagen University – Rigshospitalet, Copenhagen, Denmark, [4]Department of Clinical Medicine, University of Copenhagen, Copenhagen, Denmark

Objectives: Most of the currently available ovulation prediction kits provide a relatively rough estimation of ovulation time with a short fertility window. This is due to their focus on the maximum probability of conception occurring one day before ovulation, with no follow-up after LH surge until ovulation nor during the subsequent days thereafter. Earlier studies have shown that urine of reproductive age women contains at least 3 different molecular forms of luteinizing hormone (LH); 1) intact LH, 2) LH beta-subunit (LHβ) and a 3) small molecular weight fragment of LHβ, LHβ core fragment (LHβcf). The proportion of these LH forms in urine varies remarkably during the menstrual cycle, particularly in relation to the mid-cycle LH surge. In this exploratory study, we studied the potential implications of determining the periovulatory course of total LH immunoreactivity in urine (U-LH-ir) and intact LH immunoreactivity in serum (S-LH-ir) in the evaluation of the fertility window from a broader aspect with emphasis on the post-surge segment.

Methods: We determined total U-LH-ir in addition to intact S-LH-ir, follicle-stimulating hormone (FSH), progesterone, and estradiol in 32 consecutive samples collected daily from 10 women at reproductive age. Inference to the non-intact U-LH-ir levels was made by calculating the proportion of total U-LH-ir to intact S-LH-ir.

Results: Total U-LH-ir increased along with LH surge and remained at statistically significantly higher levels than those in serum for 5 consecutive days after the surge in S-LH-ir. S-LH-ir returned to follicular phase levels immediately on the following day after the LH surge, whereas the same took 7 days for total U-LH-ir.

Conclusions: The current exploratory study provides preliminary evidence of the fact that U-LH-ir derived from degradation products of LH remains detectable at peak levels from the LH surge until ovulation and further during the early postovulatory period of fecundability. Thus, non-intact (or total) U-LH-ir

appears to be a promising marker in the evaluation of the post-surge segment of the fertility window. Future studies are needed to unravel if this method can improve the prediction of ovulation time and higher rates of fecundability in both natural and assisted conception.

KEYWORDS

Luteinizing hormone, LH-beta, LH core fragment, estrone-3-glucuronide, E3G, ovulation predictor kit, urine, women

Introduction

In order to optimize the probability of conception in a menstrual cycle, the appropriate timing of intercourse is of utmost importance. Randomized controlled trials show evidence that ovulation predictor kits (OPKs) may increase pregnancy rates (1).

In ovulatory cycles, ovulation usually occurs about 14 days before the onset of the next period. The length of the normal ovulatory cycle may vary considerably (26-35 days, mean 28 days), and extensive variations both in follicular (10-23 days) and luteal phases (7-19 days) have been reported (2, 3). Thus, making the prediction of ovulation and appropriate timing for intercourse or natural cycle intrauterine insemination is rather challenging (2, 4).

Since the ovulation time may vary from cycle to cycle, women are required to apply a urine test daily from the mid-follicular phase until getting a positive result, which causes undue stress in addition to financial burden (5, 6). The majority of currently commercially available OPKs accurately detect the urinary LH (U-LH) surge, which gives only a rough estimate of imminent ovulation. The LH surge occurs roughly 1 or 2 days prior to ovulation (7, 8). The maximum probability of conception in intercourse is one day before ovulation. If testing is performed after the LH peak has taken place due to various reasons, such as personal reasons or variations in the expected duration of the follicular phase, ovulation can be missed. Also, the vast majority of ejaculated spermatozoa remains viable in the female reproductive tract for 3-5 days (9), and an ovum can be fertilized usually for 24 hours after ovulation (10). Thus, there is a need to cover the early postovulatory segment of the fertility window to improve the currently available OPKs.

We recently demonstrated the occurrence of three distinct forms of LH immunoreactivity (LH-ir), i.e. intact LH and its degradation products, namely LH beta-subunit (LHβ), and a 12 kD fragment of LHβ, called core fragment (LHβcf) by a commercially available diagnostic method in urine samples obtained from fertile women (11). The proportion of these distinct forms of urinary LH-ir (U-LH-ir) varied significantly during the periovulatory period and total U-LH-ir prevailed for at least 3 days following the day of LH surge (12). Based on the findings of our recent studies (11, 12), we hypothesized that evaluation of the periovulatory course of different forms of U-LH-ir may provide valuable information about the post-surge segment of the fertility window.

In this exploratory study, we investigated the potential use of total U-LH-ir measurements along with S-LH-ir, serum estradiol and progesterone determinations for the evaluation of a broader fertility window beyond the LH surge, which may eventually improve the prediction of ovulation time and fecundability.

Materials and methods

Subjects

This study was conducted at the Department of Growth and Reproduction, Copenhagen University Rigshospitalet, Denmark and the Children's Hospital, University of Helsinki, Finland. Ten healthy women (aged 18 to 40 years) visiting the former hospital volunteered to participate in the study. Inclusion criteria included being a healthy woman in the reproductive age range. Any history of irregularity in menstrual cycles was an exclusion criterion. Exclusion criteria also required that none of the subjects had a history of endocrine or metabolic disease and none were using any medication or hormonal contraceptives known to interfere with reproductive function at the time of the study. All the subjects had regular menstrual cycles (length of cycle 29.9 ± 5.1 days, duration of menstrual flow 5.6 ± 0.8 days; both expressed as mean ± 2 SD), and they were prospectively enrolled in the study with due consent. The study protocol was approved by the ethics committee of Copenhagen University Rigshospitalet. Laboratory investigations of the samples obtained from the subjects were performed in both institutions.

Study design

Blood and urine samples were collected every morning at 8:00 am for 32 consecutive days. Every second day the subjects fasted overnight before blood sampling. The day of ovulation

was determined in reference to the day of peak serum follicle-stimulating hormone (FSH) and luteinizing hormone (LH) levels. For each participant, the 32 consecutive days were transformed into days in each individual cycle, based on the data from the 3 consecutive menstrual cycles prior to initiation of the study. The regularity of the menstrual cycles in each individual was hence confirmed by a 3-month registration of menstrual bleedings (without blood and urine sampling). Urine was collected every morning except during menstrual flow and stored at +4°C for up to 10 days (2-3 days on average) before analysis. The term "LH surge" referred to the surge in LH-ir in serum (S-LH-ir).

Assays

The immunofluorometric assays (IFMA) utilized in this study are commercially available sandwich assays using monoclonal antibodies (AutoDELFIA hFSH and hLH [the latter formerly known as LHspec], Wallac, PerkinElmer Finland Oy). One antibody is immobilized onto a microtiter strip well and the other one is labeled with a europium chelate. Both the capture and the detection antibody are directed toward the ß-subunit of LH recognizing different, distinct epitopes (13). This LH assay which has been designed specifically to detect intact LH and LHβ, but not human chorionic gonadotropin, measured also LHβcf as shown in our earlier study (11). Therefore, h-LH assay in this study measured total U-LH-ir, deriving from the intact LH, LHβ, and LHβcf. However, the serum LH (S-LH) assay measured only intact S-LH-ir, because LHβ and LHβcf concentrations were at negligible levels in serum (12). Due to the unavailability of a different assay for detecting intact U-LH-ir in this study, the non-intact LH-ir could not be determined as the arithmetic difference between total and intact LH-ir as performed in our previous studies (11, 12). Therefore, inference to the non-intact U-LH-ir levels was made by calculating the proportion of total U-LH-ir to intact S-LH-ir (Figure 2) because of the high correlation between U-LH-ir and S-LH-ir at similar absolute concentrations as shown in our earlier studies (14–16). The assays were performed according to the instructions of the manufacturer. A sample volume of 25 µL was used for serum and urine. The total assay volume was 225 µL. The assays were calibrated against the WHO Second International Standard for pituitary LH for immunoassay (80/552) and the Second International Reference Preparation of Pituitary FSH/LH (78/549), respectively. The limits of detection calculated by utilizing both the measured limits of blank and test replicates of a sample known to contain a low concentration of the analyte for the U-LH, U-FSH, S-LH, and S-FSH assays were 0.015 IU/L, 0.018 IU/L, 0.020 IU/L, and 0.035 IU/L, respectively (17). The intra- and inter-assay CVs for the U-FSH and U-LH assays ranged between 2.3% and 5.7%, and 5.2% and 6.4%, respectively (16). The intra-assay coefficients of variation for both assays were <2% at levels between 3 and 250 IU/l and about 10% at 0.3 IU/L. The inter-assay coefficient of variation was <3% at 4–18 IU/L for both FSH and LH (18). Hormone concentrations were not corrected for variations in urine excretion rate (such as urinary density or creatinine), because the correlation with serum levels was not improved but even impaired due to overcorrection in very dilute urine samples (14).

Serum samples were analyzed for progesterone and estradiol by RIA assays (Diagnostic Products Corporation, Los Angeles, USA and Immunodiagnostic System Ltd. Boldon, UK; respectively). For the progesterone assay, sensitivity was 0.23 nmol/L, and intra- and inter-assay CVs were 3.8% and 8.6%, respectively. For the estradiol assay, sensitivity was 18 pmol/L and intra- and inter-assay CVs were 7.5% and 8.4%, respectively.

Statistics

The paired-samples t-test was used to analyze differences in the concentrations of LH in urine and serum from the same subjects on the same day, whereas the Kruskal-Wallis test was chosen for the nonparametric comparison of day-to-day variations of a hormone or ratio for analyzing the significance of change between consecutive days of the menstrual cycle. Pearson correlation coefficient was used for calculating correlations. This study was designed as an exploratory study with the aim of generating new hypotheses and therefore formal power calculations were not performed.

Results

Overall changes in hormone levels during periovulatory days

Normal changes in serum estradiol and progesterone levels confirmed the ovulatory cycles in this study population (Figure 1B). Serum LH concentrations increased steadily starting from day -3 onwards, with the steepest increase representing the LH surge on day 0, which was followed by a steep drop on day +1 (Figure 1A). These changes were associated with significant increases in serum progesterone concentrations continuously from day -1 through day +1 (Figure 1B).

There was no significant difference between the mean concentrations of S-LH and U-LH on day 0 (P=.74), indicating a similar pattern of increase in the concentrations of these two parameters on the day of LH surge. Also, serum FSH levels showed a similar pattern with an abrupt increase on day 0 followed by a drop on the following day; low serum FSH and high progesterone concentrations were maintained throughout the luteal phase (Figure 1B).

Urinary LH concentrations increased significantly again between days 1 and 2. Total U-LH-ir levels remained at

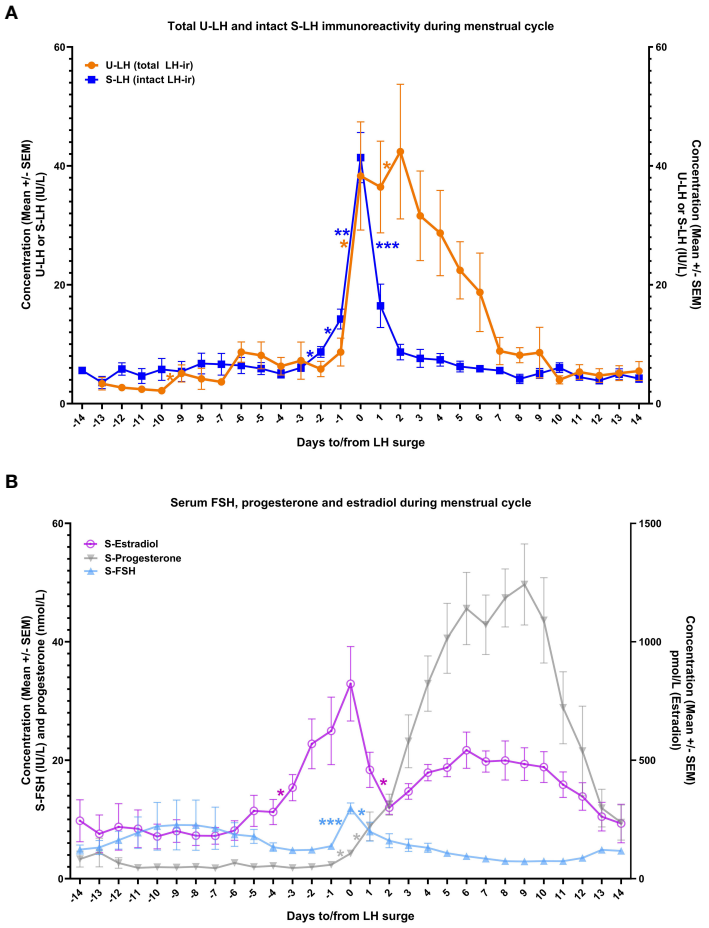

FIGURE 1
The course of total luteinizing hormone immunoreactivity (LH-ir) in urine and intact LH-ir in serum (total U-LH-ir and intact S-LH-ir, respectively) [panel **A**], and follicle-stimulating hormone (FSH), progesterone, and estradiol in serum [panel **B**] during the menstrual cycle. Symbols depict the mean values and bars represent the standard error of the mean. The statistically significant changes are denoted as follows: *P<.05, **P<.01, ***P<.001.

significantly higher levels than those of S-LH-ir for 5 consecutive days following day 0 (P<.001). Unlike the steep fall in S-LH-ir levels right after the surge in S-LH-ir, the decrease in U-LH-ir was gradual over a one-week period following the LH surge. In contrast, S-LH-ir levels returned to follicular phase levels immediately on the following day after the LH surge and remained at similarly low levels thereafter with no significant day-to-day variations for at least 14 days after LH surge (Figure 1A).

S-LH-ir levels started to increase already on day -1, causing a significant difference (P=.001) compared to U-LH-ir levels on the same day. The mean value of total U-LH-ir to S-LH-ir ratio was 1.0 on day 0 (Figure 2). Mean values of this ratio rose significantly over the next 2 days, 2 to 3-fold on day +1 and over 4 to 5-fold on day +2 (the former figure representing the fold increase shows the cautious estimate as the fold increases were calculated by considering not only the means but also the distributions of all the concentrations for each consecutive day). Likewise, the total U-LH-ir to S-LH-ir ratio did not fall below 3.0, 2.2, and 1 within 5, 6, and 9 days from the LH surge, respectively (Figure 2).

Serum estradiol concentrations measured on day -3 or -7 as well as integrated estradiol concentrations for the last 3 or 7 days before the LH surge correlated well with S-LH-ir levels on day 0 (Table 1). Serum estradiol concentrations measured on day -7 as well as integrated estradiol concentrations for the last 3 or 7 days before the LH surge correlated negatively with the U-LH-ir/S-LH-ir ratio on day 0, but not positively or negatively with that on day 1 (Table 1). Additionally, serum progesterone concentrations on day +1 (after significant increases on days 0 and +1, Figure 1B) correlated well with the U-LH-ir/S-LH-ir ratio during the period following the LH surge, very strongly during days 2-3, but not at all on day 0 (Table 2).

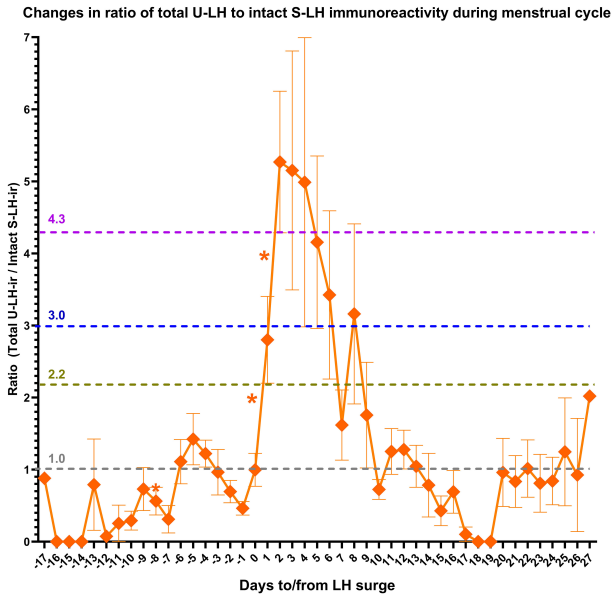

FIGURE 2
Changes in the ratio of total luteinizing hormone immunoreactivity (LH-ir) in urine to intact LH-ir in serum (representing the non-intact LH-ir in urine) during the menstrual cycle. Symbols depict the mean values and bars represent the standard error of the mean. The statistically significant changes are denoted as follows: *P<.05.

TABLE 1 Correlation between serum estradiol concentrations and S-LH concentrations or the ratio of total luteinizing hormone immunoreactivity (LH-ir) in urine to intact LH-ir in serum (representing the non-intact LH-ir in urine) around the days of LH peak.

	S-estradiol on day -3 from LH peak	S-estradiol on day -7 from LH peak	S-estradiol integrated for the last 3 days before LH peak	S-estradiol integrated for the last 7 days before LH peak
S-LH on day 0	**0.78***	**0.72***	**0.70***	**0.75***
U-LH/S-LH on day 0	0.54	**-0.70***	**-0.79***	**0.78***
U-LH/S-LH on day +1	0.02	0.06	0.44	0.34

The statistically significant correlation (r) values are marked with an asterisk; *P<.05.

TABLE 2 Correlation of serum progesterone levels on the day after LH peak with the the ratio of total luteinizing hormone immunoreactivity (LH-ir) in urine to intact LH-ir in serum (representing the nonintact LH-ir in urine) during the first week after LH peak.

	U-LH/S-LH (day 0)	U-LH/S-LH (days 1-3)	U-LH/S-LH (days 2-3)	U-LH/S-LH (days 1-7)
S-progesterone (day + 1)	0.31	**0.79***	**0.85*****	**0.76***

The statistically significant correlation (r) values are marked with an asterisk; *P<.05, ***P<.001.

Discussion

The period of high fertility prior to ovulation has previously been believed to include the five days prior to ovulation plus the day of ovulation (19–22). However, Wilcox et al. have revealed that these earlier assumptions are outdated in the light of several recent findings (23). According to this, the fertility window may extend for a much longer period, albeit with lower probabilities for conception, starting with a preovulatory period of up to 4 to 7 days and continuing with a postovulatory period of up to 2 days. Indeed, earlier studies revealed that the mean lifespans for sperm and ovum are 1.4 days and 0.7 days, respectively, and sperm would have a 5% probability of surviving more than 4.4 days and a 1% probability of surviving more than 6.8 days (9, 21, 24). Prediction of ovulation time is of crucial importance for timing the encounter of sperm and ovum within their lifespans for a conception with a reasonable probability.

Ovulation time may vary considerably even during 28-day-long regular cycles (23, 25, 26), making the prediction of LH surge and optimal fertilization time challenging. In efforts to overcome this challenge, a combination of different markers was studied (27–33). Studies published by WHO have demonstrated that the median time for a defined rise in the concentration of urinary E3G occurred on day 9 of the menstrual cycle, approximately 118 h (approximately 5 days) before the urinary LH peak in women with regular menstrual cycles (32, 33). Indeed, a rise in the concentration of E3G of 50% over the mean of the previous three values was shown to locate the start of the potentially fertile period (between day -3 and -7) in over 90% of the cycles (27, 28), thus a combination of urinary E3G and LH determinations has been used for the prediction of the optimal timing for conception (29–31, 34). On the other hand, current ovulation predictor kits (OPKs) do not detect any hormonal activity beyond LH surge for those who were "too late" and missed the day of LH surge, rather inform the ovulation time as a projection derived from the E3G and LH measurements from before the LH peak.

We recently demonstrated that urine from fertile women contains three forms of U-LH-ir, i.e. intact LH, LH beta-subunit (LHβ), and a 12 kD fragment of LHβ, called core fragment (LHβcf), the latter two forming the non-intact portion of LH-ir (11). The proportions of these forms vary remarkably during the menstrual cycle; non-intact LH-ir, particularly LHβcf is the major form of LH-ir for at least 3 days after the LH surge (11, 12). The LH-ir determined in this study was comprised of mainly intact S-LH-ir on the day of LH surge and of non-intact U-LH-ir during the post-surge days (Figure 1A), confirming the findings of earlier studies (11, 12).

The onset of the LH surge precedes ovulation by 35–44 hours, and the peak serum level of LH precedes ovulation by 10–12 hours (8, 35). This fact combined with the 24-hour fertilizability of an ovulated ovum (10) (and the 3-5 day viability of the ejaculated spermatozoa in the female reproductive tract (9)) indicates a window of fecundability for almost 3 days after the onset of the LH surge.

Findings of our earlier study had shown that the non-intact (degraded) portion of the U-LH-ir predicts the LH surge one day in advance and increases sharply after LH surge to five-fold until day +2 (hence until the day of ovulation) and remains over five-fold until day +3 and over three-fold until day +5 (12). All these phenomena were observed exactly at the same time points and magnitudes also in this study, further substantiating these findings as seen in Figure 2.

Other aspects including serum LH, FSH, progesterone, E2, inhibin A and B have previously been published (36, 37). Table 2 shows that the non-intact U-LH-ir correlated strongly with the progesterone levels immediately before and after the ovulation but not any earlier (not on day 0), and at the strongest level on days 2 and 3 (which is the highest probable postovulatory period of time for conception).

Observations from our earlier studies (11, 12) also imply the possibility of utilizing data derived from the decreasing total (or non-intact) U-LH-ir before LH surge as an add-on to E3G in the algorithm if the urine sample was taken too close to an imminent LH surge or too late after an LH surge, because the fall in non-intact U-LH-ir and increase in E3G levels herald an impending LH surge within 1-3 days and 3-7 days in advance, respectively, but neither E3G nor LH surge data provide any predictive information in regard to the postovulatory segment of the fertility window.

S-LH-ir and U-LH-ir/S-LH-ir ratio on the day of LH surge correlated at similar levels positively and negatively, respectively, with the serum estradiol concentrations measured on day -7 as well as integrated estradiol concentrations for the last 3 or 7 days before LH surge (27, 28). The negative correlation between serum estradiol levels and U-LH-ir/S-LH-ir ratio disappeared on day +1.

Also, the significant fall in non-intact U-LH-ir on day -1 (represented by the total U-LH-ir/S-LH-ir ratio in this study) confirmed the findings of our earlier study (12). The falling trend in total U-LH-ir during days -4 through -1 further supports this finding (Figure 2). These findings together indicate the build-up of an intact LH pool until day -1, after which the trend reverses in favor of the non-intact U-LH-ir during the post-surge period for at least 5 days, the peak being observed on day +3 ((12); also in Figure 2).

The current exploratory study provides preliminary evidence of the fact that U-LH-ir derived from degradation products of LH remains detectable at peak levels from the LH surge until ovulation and further during the early postovulatory period of fecundability. Thus, non-intact (or total) LH-ir appears to be a promising marker in the evaluation of the post-surge segment of the fertility window, which may improve the prediction of ovulation time and fecundability in both natural and assisted conception.

The current study design can be developed further by incorporating an assay that can detect intact U-LH-ir for assessing the total or non-intact to intact U-LH-ir ratio directly without further calculations. This limitation can be overcome by the availability of an assay to measure non-intact U-LH-ir or even better urinary LHβ and LHβcf concentrations separately. Unfortunately, non-intact U-LH-ir or its components cannot be measured directly at present due to the unavailability of antibodies specific for LHβ and LHβcf.

One other major reason behind the suboptimal functional utility of current OPKs is the variability of LH surge patterns. Park et al. and Direito et al. documented various examples of short, medium, double, and prolonged LH surges with single, double, multiple, or plateau peaks (10, 38). LH surges with several peaks were associated with statistically significant smaller

follicle sizes before rupture and lower LH levels on the day of ovulation (10). Also, premature LH surges in women with regular menstrual cycles were reported (39). These all suggest that not all detected LH surges lead to ovulation even in regularly ovulating women. Some anovulatory events may be associated with false-positive results due to rises in LH, e.g., luteinized unruptured follicles, and hemorrhagic anovulatory follicles (40). False-positive results may also occur due to some OPKs of poor specificity detecting epitopes for intact LH, LHβ or LHβcf in the form of double, multiple, or plateau peaks (10, 38) rather than the targeted intact LH only, for which the product was designed to detect at the first place. On the other hand, there may be several missed cases in which signals of imminent ovulation remained undetected by current OPKs. Such false-negative results may be due to a failure to detect different naturally occurring LH variants (13, 41). The current OPKs with some or all of the above-mentioned drawbacks predict the LH surge by E3G and the ovulation by the LH surge, with no follow-up after the LH surge until ovulation nor during the subsequent hours thereafter.

We suggest that the utilization of highly specific intact LH assays designed for different LH variants to detect the true LH peak jointly with total (or non-intact) U-LH-ir assays may be combined with pre-surge E3G determinations for covering the postsurge segment of the fertility window. The findings of this study justify further research towards a novel OPK model, which could employ a more extensive ray of predictors for attaining a more accurate interpretation of the window of fertility as well as for distinguishing the LH surges of menstrual cycles with true ovulation from those without.

These preliminary findings yet lack clinical validation, thus meriting further research in the clinical setting for validating optimal test designs and algorithms, particularly due to the findings of the current study being based on 10 volunteers only. Another limitation was the lack of some exclusion criteria like the factor of alcohol consumption and aging of subjects, which may have induced alterations in the course of menstrual cycles or LH-ir, respectively. However, irregularity in menstrual cycles was an exclusion criterion for subjects in this study, therefore this limitation may be considered a minor one. On the other hand, the absence of ultrasound to confirm structural changes consistent with ovulation/anovulation was a major limitation of this study.

We conclude that future larger studies are needed to evaluate the utility of U-LH-ir levels by employing a gold standard test of ovulation, serum LH-ir and progesterone determinations along with the ultrasonographic evidence of ovulation. Such improved studies may unravel if a broader window of fertility could be achieved through the detection of periovulatory total LH-ir or its non-intact portion (LHβ or LHβcf) along with E3G concentrations in urine. This would mean improved algorithms for OPKs and higher rates of success in predicting ovulation time and attaining fecundability in both natural and assisted conception.

Data availability statement

The raw data supporting the conclusions of this article will be made available by the authors, without undue reservation.

Ethics statement

The studies involving human participants were reviewed and approved by Department of Growth and Reproduction, Copenhagen University - Rigshospitalet Copenhagen, Denmark. The patients/participants provided their written informed consent to participate in this study.

Author contributions

All authors contributed to the article, accepted responsibility for the entire content of the manuscript and approved the submitted version.

Funding

Part of the study was financed by grants from The Finnish Medical Foundation (Suomen Lääketieteen Säätiö).

Acknowledgments

The authors would like to express their gratitude to the subjects for their cooperation in this study.

Conflict of interest

The authors declare that the research was conducted in the absence of any commercial or financial relationships that could be construed as a potential conflict of interest.

Publisher's note

References

1. Yeh PT, Kennedy CE, van der Poel S, Matsaseng T, Bernard L, Narasimhan M. Should home-based ovulation predictor kits be offered as an additional approach for fertility management for women and couples desiring pregnancy? A systematic review and meta-analysis. *BMJ Glob Health* (2019) 4:e001403. doi: 10.1136/bmjgh-2019-001403

2. Bull JR, Rowland SP, Scherwitzl EB, Scherwitzl R, Danielsson KG, Harper J. Real-world menstrual cycle characteristics of more than 600,000 menstrual cycles. *NPJ Digit Med* (2019) 2:83. doi: 10.1038/s41746-019-0152-7

3. Fehring RJ, Schneider M, Raviele K. Variability in the phases of the menstrual cycle. *J Obstet Gynecol Neonatal Nurs* (2006) 35:376–84. doi: 10.1111/j.1552-6909.2006.00051.x

4. Mihm M, Gangooly S, Muttukrishna S. The normal menstrual cycle in women. *Anim Reprod Sci* (2011) 124:229–36. doi: 10.1016/j.anireprosci.2010.08.030

5. Louis GM, Lum KJ, Sundaram R, Chen Z, Kim S, Lynch CD, et al. Stress reduces conception probabilities across the fertile window: Evidence in support of relaxation. *Fertil Steril* (2011) 95:2184–9. doi: 10.1016/j.fertnstert.2010.06.078

6. Tiplady S, Jones G, Campbell M, Johnson S, Ledger W. Home ovulation tests and stress in women trying to conceive: A randomized controlled trial. *Hum Reprod* (2013) 28:138–51. doi: 10.1093/humrep/des372

7. WHO TFI. Temporal relationships between ovulation and defined changes in the concentration of plasma estradiol-17 beta, luteinizing hormone, follicle-stimulating hormone, and progesterone. i. probit analysis. World health organization, task force on methods for the determination of the fertile period, special programme of research, development and research training in human reproduction. *Am J Obstet Gynecol* (1980) 138:383–90.

8. Hoff JD, Quigley ME, Yen SS. Hormonal dynamics at midcycle: A reevaluation. *J Clin Endocrinol Metab* (1983) 57:792–6. doi: 10.1210/jcem-57-4-792

9. Ecochard R, Marret H, Rabilloud M, Bradai R, Boehringer H, Girotto S, et al. Sensitivity and specificity of ultrasound indices of ovulation in spontaneous cycles. *Eur J Obstet Gynecol Reprod Biol* (2000) 91:59–64. doi: 10.1016/s0301-2115(99)00249-3

10. Direito A, Bailly S, Mariani A, Ecochard R. Relationships between the luteinizing hormone surge and other characteristics of the menstrual cycle in normally ovulating women. *Fertil Steril* (2013) 99:279–85. doi: 10.1016/j.fertnstert.2012.08.047

11. Demir A, Hero M, Alfthan H, Passioni A, Tapanainen JS, Stenman UH. Intact luteinizing hormone (LH), LHbeta, and LHbeta core fragment in urine of menstruating women. *Minerva Endocrinol (Torino)* (2022) 32–33. doi: 10.23736/S2724-6507.22.03565-5

12. Demir A, Hero M, Alfthan H, Passioni A, Tapanainen JS, Stenman UH. Identification of the LH surge by measuring intact and total immunoreactivity in urine for prediction of ovulation time. *Hormones (Athens)* (2022). doi: 10.1007/s42000-022-00368-9

13. Pettersson K, Ding YQ, Huhtaniemi I. An immunologically anomalous luteinizing hormone variant in a healthy woman. *J Clin Endocrinol Metab* (1992) 74:164–71. doi: 10.1210/jcem.74.1.1727817

14. Demir A, Alfthan H, Stenman UH, Voutilainen R. A clinically useful method for detecting gonadotropins in children: Assessment of luteinizing hormone and follicle-stimulating hormone from urine as an alternative to serum by ultrasensitive time-resolved immunofluorometric assays. *Pediatr Res* (1994) 36:221–6. doi: 10.1203/00006450-199408000-00014

15. Demir A, Dunkel L, Stenman UH, Voutilainen R. Age-related course of urinary gonadotropins in children. *J Clin Endocrinol Metab* (1995) 80:1457–60. doi: 10.1210/jcem.80.4.7714124

16. Demir A, Voutilainen R, Juul A, Dunkel L, Alfthan H, Skakkebaek NE, et al. Increase in first morning voided urinary luteinizing hormone levels precedes the physical onset of puberty. *J Clin Endocrinol Metab* (1996) 81:2963–7. doi: 10.1210/jcem.81.8.8768859

17. Armbruster DA, Pry T. Limit of blank, limit of detection and limit of quantitation. *Clin Biochem Rev* (2008) 29 Suppl 1:S49–52.

18. Demir A, Voutilainen R, Stenman UH, Dunkel L, Albertsson-Wikland K, Norjavaara E. First morning voided urinary gonadotropin measurements as an alternative to the GnRH test. *Horm Res Paediatr* (2016) 85:301–8. doi: 10.1159/000440955

19. Wilcox AJ, Weinberg CR, Baird DD. Timing of sexual intercourse in relation to ovulation. effects on the probability of conception, survival of the pregnancy, and sex of the baby. *N Engl J Med* (1995) 333:1517–21. doi: 10.1056/NEJM199512073332301

20. Dunson DB, Baird DD, Wilcox AJ, Weinberg CR. Day-specific probabilities of clinical pregnancy based on two studies with imperfect measures of ovulation. *Hum Reprod* (1999) 14:1835–9. doi: 10.1093/humrep/14.7.1835

21. Royston JP. Basal body temperature, ovulation and the risk of conception, with special reference to the lifetimes of sperm and egg. *Biometrics* (1982) 38:397–406.

22. Schwartz D, Macdonald PD, Heuchel V. Fecundability, coital frequency and the viability of ova. *Popul Stud (Camb)* (1980) 34:397–400. doi: 10.1080/00324728.1980.10410398

23. Wilcox AJ, Dunson D, Baird DD. The timing of the "fertile window" in the menstrual cycle: Day specific estimates from a prospective study. *BMJ* (2000) 321:1259–62. doi: 10.1136/bmj.321.7271.1259

24. Ferreira-Poblete A. The probability of conception on different days of the cycle with respect to ovulation: An overview. *Adv Contracept* (1997) 13:83–95. doi: 10.1023/a:1006527232605

25. Baird DD, McConnaughey DR, Weinberg CR, Musey PI, Collins DC, Kesner JS, et al. Application of a method for estimating day of ovulation using urinary estrogen and progesterone metabolites. *Epidemiology* (1995) 6:547–50. doi: 10.1097/00001648-199509000-00015

26. Lenton EA, Landgren BM, Sexton L. Normal variation in the length of the luteal phase of the menstrual cycle: Identification of the short luteal phase. *Br J Obstet Gynaecol* (1984) 91:685–9. doi: 10.1111/j.1471-0528.1984.tb04831.x

27. Adlercreutz H, Brown J, Collins W, Goebelsman U, Kellie A, Campbell H, et al. The measurement of urinary steroid glucuronides as indices of the fertile period in women. World health organization, task force on methods for the determination of the fertile period, special programme of research, development and research training in human reproduction. *J Steroid Biochem* (1982) 17:695–702. doi: 10.1016/0022-4731(82)90573-8

28. Branch CM, Collins PO, Collins WP. Ovulation prediction: Changes in the concentrations of urinary estrone-3-glucuronide, estradiol-17 beta-glucuronide and estriol-16 alpha-glucuronide during conceptional cycles. *J Steroid Biochem* (1982) 16:345–7. doi: 10.1016/0022-4731(82)90189-3

29. Collins WP, Collins PO, Kilpatrick MJ, Manning PA, Pike JM, Tyler JP. The concentrations of urinary oestrone-3-glucuronide, LH and pregnanediol-3alpha-glucuronide as indices of ovarian function. *Acta Endocrinol (Copenh)* (1979) 90:336–48. doi: 10.1530/acta.0.0900336

30. May K. Home monitoring with the ClearPlan easy fertility monitor for fertility awareness. *J Int Med Res* (2001) 29 Suppl 1:14A–20A. doi: 10.1177/14732300010290S103

31. Schiphorst LE, Collins WP, Royston JP. An estrogen test to determine the times of potential fertility in women. *Fertil Steril* (1985) 44:328–34. doi: 10.1016/s0015-0282(16)48856-4

32. Temporal relationships between indices of the fertile period. *Fertil Steril* (1983) 39:647–55. doi: 10.1016/s0015-0282(16)47060-3

33. A prospective multicentre study to develop universal immunochemical tests for predicting the fertile period in women. world health organisation task force on methods for the determination of the fertile period, special programme of research, development and research training in human reproduction. *Int J Fertil* (1985) 30:18–30.

34. Spieler J, Collins W. Potential fertility–defining the window of opportunity. *J Int Med Res* (2001) 29 Suppl 1:3A–13A. doi: 10.1177/14732300010290S102

35. Cahill DJ, Wardle PG, Harlow CR, Hull MG. Onset of the preovulatory luteinizing hormone surge: Diurnal timing and critical follicular prerequisites. *Fertil Steril* (1998) 70:56–9. doi: 10.1016/s0015-0282(98)00113-7

36. Sehested A, Juul AA, Andersson AM, Petersen JH, Jensen TK, Muller J, et al. Serum inhibin a and inhibin b in healthy prepubertal, pubertal, and adolescent girls and adult women: Relation to age, stage of puberty, menstrual cycle, follicle-stimulating hormone, luteinizing hormone, and estradiol levels. *J Clin Endocrinol Metab* (2000) 85:1634–40. doi: 10.1210/jcem.82.12.4449

37. Johansen ML, Anand-Ivell R, Mouritsen A, Hagen CP, Mieritz MG, Soeborg T, et al. Serum levels of insulin-like factor 3, anti-mullerian hormone, inhibin b, and testosterone during pubertal transition in healthy boys: A longitudinal pilot study. *Reproduction* (2014) 147:529–35. doi: 10.1530/REP-13-0435

38. Park SJ, Goldsmith LT, Skurnick JH, Wojtczuk A, Weiss G. Characteristics of the urinary luteinizing hormone surge in young ovulatory women. *Fertil Steril* (2007) 88:684–90. doi: 10.1016/j.fertnstert.2007.01.045

39. Krotz S, McKenzie LJ, Cisneros P, Buster J, Amato P, Carson S. Prevalence of premature urinary luteinizing hormone surges in women with regular menstrual cycles and its effect on implantation of frozen-thawed embryos. *Fertil Steril* (2005) 83:1742–4. doi: 10.1016/j.fertnstert.2004.11.078

40. Bashir ST, Baerwald AR, Gastal MO, Pierson RA, Gastal EL. Follicle growth and endocrine dynamics in women with spontaneous luteinized unruptured follicles versus ovulation. *Hum Reprod* (2018) 33:1130–40. doi: 10.1093/humrep/dey082

41. Pettersson KS, Soderholm JR. Individual differences in lutropin immunoreactivity revealed by monoclonal antibodies. *Clin Chem* (1991) 37:333–40.

Advantages of publishing in Frontiers

OPEN ACCESS
Articles are free to read for greatest visibility and readership

FAST PUBLICATION
Around 90 days from submission to decision

HIGH QUALITY PEER-REVIEW
Rigorous, collaborative, and constructive peer-review

TRANSPARENT PEER-REVIEW
Editors and reviewers acknowledged by name on published articles

Frontiers
Avenue du Tribunal-Fédéral 34
1005 Lausanne | Switzerland

Visit us: www.frontiersin.org
Contact us: frontiersin.org/about/contact

REPRODUCIBILITY OF RESEARCH
Support open data and methods to enhance research reproducibility

DIGITAL PUBLISHING
Articles designed for optimal readership across devices

FOLLOW US
@frontiersin

IMPACT METRICS
Advanced article metrics track visibility across digital media

EXTENSIVE PROMOTION
Marketing and promotion of impactful research

LOOP RESEARCH NETWORK
Our network increases your article's readership